

Assessing genetic diversity of the circulating A/H1N1pdm09 in Eastern India: Identification and characterization of synthetic small molecules as potential antiviral therapeutics

**Thesis submitted for the
Degree of Doctor of Philosophy (Science)
In Life Science & Biotechnology**

**By
Priyanka Saha
(Index no. 62/20/Life Sc./27)**



**Department of
Life Science & Biotechnology
Jadavpur University
2024**



icmr
INDIAN COUNCIL OF
MEDICAL RESEARCH

NICED
NATIONAL INSTITUTE OF
CHOLERA AND ENTERIC DISEASES

आई. सी. एम. आर. – राष्ट्रीय कॉलरा और आंत्र रोग संस्थान

ICMR - NATIONAL INSTITUTE OF CHOLERA AND ENTERIC DISEASES

स्वास्थ्य अनुसंधान विभाग, स्वास्थ्य और परिवार कल्याण मंत्रालय, भारत सरकार

Department of Health Research, Ministry of Health and Family Welfare, Govt. of India

WHO COLLABORATING CENTRE FOR RESEARCH AND TRAINING ON DIARRHOEAL DISEASES

CERTIFICATE FROM THE SUPERVISOR

This is to certify that the thesis entitled “Assessing genetic diversity of the circulating A/H1N1pdm09 in Eastern India: Identification and characterization of synthetic small molecules as potential antiviral therapeutics” Submitted by Smt. Priyanka Saha who got her name registered on 13th November, 2020 for the award of Ph. D. (Science) degree of Jadavpur University, is absolutely based upon her own work under the supervision of Dr. Mamta Chawla-Sarkar and that neither this thesis nor any part of it has been submitted for either any degree / diploma or any other academic award anywhere before.

Mamta Sarkar 24-6-24

Signature of the Supervisor (date with official seal)

Dr. Mamta Chawla Sarkar
Scientist - F (Sr. Deputy Director)
& Head - Division of Virology
ICMR-National Institute of
Cholera & Enteric Diseases
Kolkata, WB, INDIA

पी-३३, सी.आई.टी. रोड, स्किम - १०एम, बेलियाघाटा, कोलकाता - ७०००१०, भारत

P-33, C.I.T. Road, Scheme - XM, Beliaghata, Kolkata - 700010, India

निदेशक / Director : 91-33-2363 3373, 2370 1176, पि.बि.एक्स / PBX : 91-33-2353 7469 / 7470, 2370 5533 / 4478 / 0448

फैक्स / Fax : 91-33-2363 2398, 2370-5066, वेब / Website : www.niced.org.in

This Thesis is dedicated to

The 4 Pillars

of my life:

Maa, Baba, Dada & Sourav

**For their unlimited trust and
support**

THANK YOU



It is one of the happiest moments of my life while I am going to submit my thesis entitled "Assessing genetic diversity of the circulating A/H1N1pdm09 in Eastern India: Identification and characterization of synthetic small molecules as potential antiviral therapeutics" which contains solely my research activities performed in the Division of Virology, ICMR-National Institute of Cholera and Enteric Diseases (ICMR-NICED), Kolkata-700010, India. It is a great pleasure to convey my deepest gratitude to all who have contributed towards the successful completion of this research work and had inspired, timely supported and guided during my Ph.D. study.

Firstly, I would like to express my sincere gratitude to my supervisor Dr. Mamta Chawla-Sarkar for the continuous support during my Ph.D. study and related research, for her patience, motivation and immense knowledge. Her guidance helped me in conducting research and writing this thesis. I could not have imagined having a better supervisor and mentor for my Ph.D. study.

I am thankful to be part of such a wonderful lab, where I have not only studied science but also enjoyed. I can't think of a better place to work in or better colleagues to work with. I thank my lab seniors - Dr. Anupam Mukherjee, Dr. Anindita Banerjee, Dr. Arpita Mukherjee, Dr. Rakesh Sarkar, Dr. Upayan Patra, Dr. Urbi Mukhopadhyay, Dr. Mahadeb Lo and Suvroto Mitra for teaching me cell biology, lab techniques and having immensely useful discussions. Special mention to Dr. Rakesh Sarkar and Suvroto Mitra for helping me to keep my focus and confidence intact during my tough times. I thank my junior labmates - Pritam, Shreya, Ritubrita, Ranjana, Srija and Saswata for maintaining a healthy and joyful work culture. I wish to acknowledge the support that our staff members- Malay da, Papiya di, Musharaff da, Gopal da and Ashish da for their constant support in our day-to-day activities in the lab.

I thank all my teachers at:

Acknowledgement

Department of Life Science and Biotechnology, Jadavpur University, where I completed M.Sc. I would like to acknowledge Prof. Supriya Chakraborty, JNU for the support and guidance in my 2nd year summer project during the M.Sc program. Department of Microbiology, Asutosh College, Calcutta University, where I completed B.Sc. Welland Gouldsmith and Our Lady Queen of the Missions Schools that had made such a strong foundation for me upon which I could build a strong career.

I thank my friends Shraya and Mou, who were always there in my tough times and support me to achieve my life goals.

I thank all my teachers, family and friends for giving me the support and strength to achieve my dreams. I thank my husband, Sourav Sarkar, for being by my side and guiding me academically since 2012, showing me my true merit and supporting me during my struggles. I thank him for being a true partner in all sense. I am also thankful to my mother-in-law Mrs. Ratna Sarkar for being a source of inspiration during my struggles. I am grateful to my father-in-law Mr. Swapan Kumar Sarkar for always encouraging me to give my best in whatever I do.

And finally, my parents (Late) Mrs. Sipra Saha and Mr. Dulal Chandra Saha. It was my parent's hard efforts which has brought me here. They have lived their dreams with me earning the degree. Earning the degree was my mother's last wish, which will be fulfilled. Just hope if I could have my mother watch me getting the degree. Another person needs special mention is my brother Mr. Suvojit Saha, who is actually a genie in disguise. From fulfilling my demands to convincing our parents on my behalf for pursuing Ph.D., as they had no knowledge regarding its scope. He is always there to pull me back when I am at the edge and confused. It's hard to describe what they mean to me. I would go an extra mile to make them proud always.

Finally, I would like to thank the Department of Science and Technology (DST-INSPIRE), New Delhi, India for providing financial assistance during my research work in ICMR-National Institute of Cholera and Enteric Diseases, Kolkata.

Thanking the Almighty for this opportunity.

Priyanka Saha

Title of the Thesis: Assessing genetic diversity of the circulating A/H1N1pdm09 in Eastern India: Identification and characterization of synthetic small molecules as potential antiviral therapeutics

Submitted by: Priyanka Saha (Index no.: 62/20/Life Sc./27)

Influenza viruses are more closely associated with winter; the local climate/habitat and geography sometimes differentiate this tendency. The symptoms include fever, sore throat, headache, dry cough, nasal discharge depending on the nature of the infection, and may end up in severe complications, particularly in those who are at risk like pregnant women, infants, elderly and immunocompromised individuals. The antigenic variation is rapid and occurs through antigenic drift and shift where new strain emerges with pandemic causing potential. Even with improvised vaccination and widespread use of antivirals, influenza continues to challenge the global health community. The genus Orthomyxoviridae includes the virus which is of 4 types (A, B, C and D) with only types A and B cause epidemics. The virus has eight single-stranded RNA fragments coding for eleven proteins.

A retrospective analysis of A/H1N1pdm09 positivity rates in eastern India during April' 2017- March' 2019 showed a remarkable reduction compared to prior influenza outbreaks. In contrast to high incidence of influenza activity in winter and spring, we noted no seasonality pattern of virus activity possibly of passive surveillance where only severe cases are referred to laboratories for testing. Sequencing data revealed novel glycosylation sites and amino acid substitution in hemagglutinin (HA). In contrast, no classical mutations implicated in antiviral resistance was observed in neuraminidase (NA). Phylogenetic studies revealed that majority of circulating strains were similar to the currently used vaccine strains. The study led to the conclusion that influenza vaccination policy for whole nation is necessary, especially for groups which are exceptionally high-risk due to recurring outbreaks in the country.

The continuous evolution of influenza viruses due to antigenic shift and presence of large number of HA and NA subtypes have made developing effective antivirals a challenging task. Introduction of mutations have reduced the efficacy of NA inhibitors and M2-ion channel blockers. Thus, there is continuous need to develop new antivirals. Currently the focus is on drug repurposing and on developing active phytochemical from natural resources. This study has tried to exploit both avenues. Minocycline, which is a tetracycline analogue, was studied for its anti-influenza activity. Minocycline showed potent anti-influenza activity both in vitro and in vivo at non-toxic doses. Minocycline exerted its antiviral activity by integrating both inhibition of late-stage apoptosis and suppressing the phosphorylation of ERK which inhibited the export of viral ribonucleoproteins (vRNPs) from the nucleus, which is an essential process for viral assembly and release. It may thus be proposed that minocycline may act as an antiviral drug. Using FDA approved drug minocycline in a new way brings an exciting prospect for influenza therapy.

Priyanka Saha
24/6/24

Mamta Chawla Sarkar
24/6/24
Dr. Mamta Chawla Sarkar
Scientist - F (Sr. Deputy Director)
& Head - Division of Virology
ICMR-National Institute of
Cholera & Enteric Diseases
Kolkata, WB, INDIA

Abbreviations

A	Adenosine	IgM	Immunoglobulin M
aa	Amino acid	IgG	Immunoglobulin G
ADP	Adenosine diphosphate	K2	Kimura 2-parameter
AMP	Adenosine monophosphate	kb	Kilobase
ATP	Adenosine 5'-triphosphate	KCl	Potassium chloride
BIC	Bayesian Information Criterion bp Base pair	kDa	Kilodalton
BrU	Bromouridine	ltr	litre
cDNA	Complementary deoxyribonucleic acid	M	Molar
CDC	Centre for Disease Control	Ma	Milliamperes
DNA	Deoxyribonucleic acid	mAb	Monoclonal antibody
DTT	Dithiothreitol	MDCK	Madin-Darby canine kidney
dNTPs	Deoxynucleoside triphosphates	MHC	Major Histocompatibility Complex
EDTA	Ethylenediamine tetra-acetic acid	mRNA	Messenger RNA
EIA	Enzyme immunosorbent assay	mM	Millimolar
ELISA	Enzyme linked immunosorbent assay	ml	Milliliter
EM	Electron microscopy	ML	Maximum likelihood
ER	Endoplasmic reticulum	min	Minute
EtBr	Ethidium Bromide	mg	Milligram
E-type	Electropherotype	mw	Molecular weight
et al.,	Latin phrase means “and others”	MgCl ₂	Magnesium chloride
GDP	Guanosine diphosphate	NaCl	Sodium chloride
GTP	Guanosine-5'-triphosphate	NaOH	Sodium hydroxide
i.e.	That is	NJ	Neighbour joining
IAV	Influenza A Virus	ng	Nanogram
IgA	Immunoglobulin A	NIP	National Immunization Program
nm	Nanometer	Secs	Seconds
nM	Nanomolar	ssRNA	Single stranded RNA
no.	Number	T92	Tamura 3-parameter

Abbreviations and Symbols

NP	Nucleoprotein	TAE	Tris-acetate EDTA buffer
nt.	Nucleotide	TBE	Tris-boric acid EDTA buffer
NTP	Nucleotide triphosphate	Taq	Thermus aquaticus (DNA polymerase)
NTPase	Nucleotide tri-phosphatase	TBS-T	Tris-buffered saline with 0.1% Tween
OPD	Outpatient department	TLPs	Triple layered particles
ORF	Open reading frame	TN93	Tamura-Nei
PAGE	Poly acrylamide gel electrophoresis	Tris	Tris (hydroxymethyl) amino methane
pH	Negative logarithm of Hydrogen ion concentration	tRNA	Transfer RNA
pdm09	pandemic 2009	ts	Temperature sensitive
PBS	Phosphate buffered saline	U	Uracil
pmol	Picomole	U	Unit
PCR	Polymerase chain reaction	UIP	Universal Immunization Program
PFU	Plaque forming unit	V	Volts
rRNA	Ribosomal RNA	WHO	World Health Organization
RNA	Ribonucleic acid	μl	Microliter
RPM	Revolution per minute	μm	Micrometer
RT-PCR	Reverse transcription-polymerase chain reaction	μM	Micromolar
SDS	Sodium dodecyl sulphate		

Symbols

%	Percent	Å	Ångström
<	Less than	α	Alpha
>	Greater than	β	Beta
±	Plus-minus	γ	Gamma
~	Equivalent	δ	Delta
≤	Less than or equal to	ε	Epsilon
≥	Greater than or equal to	χ	Chi
°C	Degree Celsius	ω	Omega

Table of Contents

DEDICATION	I
ACKNOWLEDGMENT	II
ABSTRACT	IV
LIST OF ABBREVIATIONS	V
TABLE OF CONTENTS	VII
FIGURES AND TABLES	XI
 Chapter 1. Review of Literature	 1
1.1. Introduction	2
1.1.1. Taxonomy and nomenclature	2
1.1.2. Symptoms	3
1.1.3. Diagnosis	4
1.1.3.1. Identification of Influenza isolates by Hemagglutination Inhibition (HAI)	4
1.1.3.2. Enzyme immunoassay	5
1.1.3.3. Rapid diagnostic kits	5
1.1.3.4. Molecular testing methods	6
1.1.3.4.1. Reverse transcription-polymerase chain reaction (RT-PCR)	6
1.1.3.4.2. Sequence analysis	7
1.2. Influenza A virus (IAV)	8
1.2.1. History of Influenza A virus	8
1.2.2. Epidemiology	9
1.2.3. Morphology of Influenza A virus	9
1.3. Influenza A virus proteins	10
1.3.1. Structural proteins	10
1.3.1.1. Segment 1 [Basic Polymerase Protein 2 (PB2)]	10
1.3.1.2. Segment 2 [Basic Polymerase Protein 1 (PB1)]	11
1.3.1.3. Segment 3 [Acidic Polymerase Protein (PA)]	12
1.3.1.4. Segment 4 [Hemagglutinin (HA)]	13
1.3.1.5. Segment 5 [Nucleoprotein (NP)]	14
1.3.1.6. Segment 6 [Neuraminidase (NA)]	15
1.3.1.7. Segment 7 [Matrix Protein-M1 and M2]	16
1.3.2. Non-structural proteins	18
1.3.2.1. Segment 8 [Non-structural proteins-NS1 and NS2]	18
1.3.2.2. PB1-F2 Protein	20
1.4. Virus life cycle	21
1.4.1. IAV Cell Binding and Fusion	21
1.4.2. IAV Genome Trafficking to the Host Cell Nucleus	22
1.4.3. Replication of the vRNAs	23
1.4.4. Viral mRNA Transcription	24
1.4.5. Assembly and Trafficking of vRNPs	25
1.4.6. ER Targeting and Maturation of the IAV Membrane Proteins	27
1.4.7. HA Proteolytic Activation at the Golgi or Plasma Membrane	28
1.4.8. IAV Assembly and Budding	29
1.4.9. IAV Cell Release and Movement	30
1.5. Genetic diversity and antigenic variation of Influenza A viruses	32
1.6. Transmission	33

1.7. Pathogenesis	33
1.8. Treatment strategy	34
1.8.1. Vaccination	34
1.8.2. Drug-based therapy	37
1.8.3. Immuno-therapy	39
1.9. Host-virus interaction	39
1.9.1. Double-stranded RNA (dsRNA)- activated protein kinase R (PKR) and downstream signalling	41
1.9.2. Toll-like receptors (TLRs) and downstream signalling	41
1.9.3. Retinoic acid-inducible gene-I-like receptors (RLRs) and downstream signalling	42
1.9.4. Protein kinase C (PKC) and Influenza virus entry	42
1.9.5. Raf/MEK/ERK pathway and ribonucleoprotein (RNP) export	42
1.9.6. Eukaryotic translation initiation factor 4e (eIF4E) and viral protein translation	43
1.9.7. Phosphatidylinositol-3-kinase (PI3K)/Akt signalling pathway and viral infection	43
1.9.8. Evasion of innate immune response by Influenza virus	44
1.9.9. Influenza virus induced apoptosis	45
1.10. Host-targeted antivirals	45
1.10.1. Antivirals targeting host cytokine signalling pathway	45
1.10.2. Antivirals targeting host glycosylation pathway	46
1.10.3. Antivirals targeting host nucleoside synthesis pathway	47
1.10.4. Antivirals against heat shock proteins (Hsp)	48
1.11. Minocycline: antiviral potential of an antibiotic	48
1.11.1. Antiviral potential of minocycline against viruses of public health importance	48
Chapter 2. Materials and methods	50
2.1. Collection of clinical nasal and throat swab samples	51
2.2. Cell line maintenance and isolation of influenza virus	51
2.2.1. Maintenance of MDCK and A549 cell lines	51
2.2.2. Influenza virus infection and harvesting	51
2.2.3. Cryopreservation of MDCK and A549 cells	51
2.2.4. Influenza virus infection in vivo and Ethics statement	52
2.3. Extraction of RNA by QIAamp method	52
2.4. Reverse transcription-Polymerase Chain Reaction (RT-PCR)	53
2.4.1. Reverse transcription reaction	54
2.4.2. Amplification of viral genes by polymerase chain reaction	54
2.4.3. Agarose gel electrophoresis	55
2.5. Real-time Polymerase Chain Reaction (Real-time PCR)	55
2.6. Sequencing PCR and precipitation of sequencing PCR product	55
2.7. GenBank accession numbers for nucleotide sequences	56
2.8. Bioinformatics tools for sequence data annotation	57
2.8.1. Sequence analysis	57
2.8.2. Construction of Phylogenetic tree and its analysis	57
2.9. Cytotoxicity assay	57
2.9.1. Crystal Violet (CV) assay	57
2.9.2. MTT assay	58
2.10. Hemagglutination test (HA)	58

2.11. Cytopathic effect inhibition (CPE) assay	59
2.12. Enzyme based Neuraminidase inhibition assay	59
2.13. Enzyme kinetics studies	59
2.14. Gel electrophoresis and immunoblot analyses	60
2.15. Nuclear and cytoplasmic protein extraction	60
2.16. Immunofluorescence	60
2.18. Apoptosis assay	61
Chapter 3. Molecular and phylogenetic characterization of Influenza A pandemic H1N1 strains in eastern India	62
3.1. Introduction	63
3.2. Results	64
3.2.1. Proportion of A/H1N1pdm09 strains	64
3.2.2. Phylogenetic analyses of HA and NA genes of A/H1N1pdm09 strains	65
3.2.2.1. HA gene	66
3.2.2.2. NA gene	68
3.2.3. Comparative antigenic analyses of HA and NA proteins of A/H1N1pdm09 strains	70
3.2.3.1. HA protein	70
3.2.3.2. NA protein	72
3.3. Discussion	75
Chapter 4. Studying drug repurposing of antimicrobial agents: Minocycline	77
4.1. Introduction	78
4.2. Results	79
4.2.1 Minocycline treatment showed potent anti-IAV activity in vitro	79
4.2.2 Minocycline impedes IAV infection without triggering interferon (IFN) signalling	82
4.2.3 Minocycline prevents the shuttling of vRNPs from the nucleus to cytosol by inhibiting ERK pathway	84
4.2.4 Minocycline impedes IAV-induced late-stage apoptosis	87
4.2.5 Minocycline treatment attenuates IAV infection in vivo	89
4.3. Discussion	93
Chapter 5. Assessing antiviral property of small synthetic molecules and its mechanism of action	96
5.1. Introduction	97
5.2. Results: Evaluation of anti-influenza activity of the designed molecules	98
5.2.1. Cytotoxicity studies of the designed molecules	99
5.2.2. Estimation of cytopathic effect (CPE) inhibition of the molecules	101
5.2.3. Determination of viral titer reduction by Hemagglutination inhibition (HAI) assay	102
5.2.4. Quantification of effective concentration of molecules by cell-based crystal violet (CV) assay	103
5.2.5. Determination of inhibitory concentration of molecules by enzyme-based NA inhibition	103
5.2.6. Enzyme kinetics studies to evaluate the mechanism of inhibition of molecules	105
5.3. Discussion	107

Chapter 6. Epilogue	108
Chapter 7. References	113
List of Publications	145

Figures

Figure 1.1: Symptoms and treatment measures of flu

Figure 1.2: Hemagglutination Inhibition assay

Figure 1.3: Rapid diagnostic kit: steps from sample collection to interpretation of results.

Figure 1.4: Real-time PCR: step by step procedure of DNA/RNA amplification.

Figure 1.5: (A) Ribbon structure of PB2 cap binding domain bound with m⁷GTP (Guilligay et al., 2008). (B) Ribbon diagram of the 627-NLS-double domain (627-domain shown in red and yellow while core NLS-domain in cyan and blue and the truncated nuclear localization peptide marked in purple), showing the position of lysine 627

Figure 1.6: Ribbon structure showing the interaction of helices of PB1 (depicted in red) and PB2 (depicted in blue)

Figure 1.7: Ribbon structure of C-terminal domain of PA (helices colored in red) bound to N-terminal peptide of PB1 (dark blue)

Figure 1.8: (A) Schematic illustration of cleavage of HA0 into HA1 and HA2, which are disulphide linked. The cleavage site is marked with an arrow. (B) ribbon structure of H3 HA0 trimer. Cleavage site R329 indicated with an arrow

Figure 1.9: Crystal structure of IAV Nucleoprotein. (A & B) Side and top view of IAV H1N1 NP trimer (PDB: 2IQH). (C) Monomer of IAV H1N1 NP (PDB: 2IQH)

Figure 1.10: Ribbon structure of NA monomer consisting of 4 distinct domains- catalytic head, stalk, transmembrane region and the cytoplasmic tail

Figure 1.11: Crystal structure of Matrix protein M1 (3DPX-009473)

Figure 1.12: Domain of IAV M2 protein showing the ectodomain (ED), transmembrane domain (TMD) and C-terminal domain (CTD)

Figure 1.13: 3D crystal structure of H6N6 NS1 protein containing the RNA binding domain (comprising of 3 helices) and an effector domain (consisting of α -helices and β -strands) connected by a linker region [PDB ID: 4OPH]

Figure 1.14: Synthesis of PB1-F2 protein from PB1 mRNA by translation from an AUG codon downstream of the PB1 start site

Figure 1.15: Life cycle of Influenza virus

Figure 1.16: Antigenic drift and antigenic shift.

Figure 1.17: Host cellular responses activated during influenza infection.

Figure 3.1: Distribution of IAV H1N1pdm09 according to age circulating during April 2017-March 2019

Figure 3.2: Distribution of IAV H1N1pdm09 according to season circulating during April 2017-March 2019

Figure 3.3: Phylogenetic dendrogram of HA protein of eastern Indian IAV H1N1pdm09 strains circulating during April 2017- March 2019

Figure 3.4: Phylogenetic dendrogram of NA protein of eastern Indian IAV H1N1pdm09 strains circulating during April 2017- March 2019

Figure 4.1: (A) chemical structure of minocycline; (B) evaluation of viral titre from supernatant extracted from IAV/PR8-infected MDCK cells treated with DMSO or 500 nM Minocycline (at 24, 48 and 72 hpi), cells treated with 100 μ M Ribavirin is treated as positive control; (C) cell viability of MDCK cells when treated with different concentrations of minocycline (1nM - 1mM) for 72 hrs, was measured using MTT assay to calculate CC50; (D) infectious IAV particles produced from IAV/PR8 MDCK cells subjected to varying concentrations of minocycline (0.1 nM-1 mM) for 72 hrs were used to calculate IC50; (E) IAV/PR8-infected MDCK cells were treated with DMSO or minocycline (500 nM) 1 hour prior to infection (pre-treatment), at the time of virus addition (co-treatment) and 1 hour after viral addition (post-treatment) to assess its effect on viral protein expression; (F) post-treatment of DMSO or minocycline (500 nM) at 0-24 hpi, 6-24 hpi and 12-24 hpi to IAV/PR8-infected cells to assess the stage of viral life cycle inhibited by minocycline.

Figure 4.2: (A-D) relative expressions of vRNA, cRNA and mRNA extracted from IAV/PR8-infected MDCK cells treated with DMSO or 500 nM Minocycline (at 6, 12 and 24 hpi) was estimated by quantitative RT-PCR. Relative fold change in M1 mRNA transcript was also estimated at 48 and 72 hpi. Cells treated with 100 μ M Ribavirin is treated as positive control; (E-F) IAV/CAL or IAV/H3N2 infected MDCK cells were treated with minocycline (500 nM) or ribavirin (100 μ M) for 24, 48 and 72 hpi, cell supernatant was collected and viral titre was estimated by hemagglutination assay and represented as TCID50/ml; (G-H) IAV/PR8 and IAV/CAL infected MDCK cells were treated with different concentrations of minocycline (100 nM - 1 μ M), viral protein estimated by western blotting after 24hrs.

Figure 4.3: Minocycline does not trigger the IFN signalling pathway in MDCK or A549 cells with/without IAV/PR8 infection. Cellular phosphorylation of the JAK1/STAT1 proteins were not observed in Minocycline-treated MDCK and A549 cells (A). IFN α -2 β in the current study served as the positive control. Minocycline treatment has no effect on activation of IFN signaling activation by IAV/PR8 in the MDCK or A549 cells (B). Antiviral role of minocycline was found to IFN-independent as reduction in viral titre and NS1 protein expression was observed in minocycline treated IFN signalling deficient vero cells (C).

Figure 4.4: (A-B) IAV/PR8 infected MDCK cells treated with minocycline (500 nM) or PD98059 (30 μ M) and incubated for 18 and 24 hpi. Cells were then fixed, permeabilized and stained with anti-NP antibody (raised in mouse). Cells were then secondary stained with DyLight488 labelled anti-mouse secondary antibody. Cells were mounted using DAPI and visualized under confocal microscope (63X oil immersion). Scale bar: 20 μ m. NP positive cells

were quantified and randomly 100 cells from different fields were selected and analysed. Data was represented as percentage of infected cells; (C) HEK293 cells were transfected with only pcDNA3 vector and pcDNA3-HA plasmid and treated with 500 nM of minocycline for 24 hrs, cells were lysed and western blot was performed to detect the level of phospho-ERK

Figure 4.5: Minocycline suppresses ERK signalling pathway in both MDCK cells and A549 cells. (A-D) IAV/PR8 activates ERK cascade, leading to phosphorylation of ERK. Treatment with minocycline reduces the phosphorylation of ERK in PMA-induced cells and IAV/PR8 infected cells; (E) Whole cell lysate and Cytosol-nucleus is extracted and NP protein was shown to be located in the nucleus of the minocycline-treated IAV/PR8 infected cells in 24hpi. Densitometric analysis of blots for NP, Lamin and β -actin was done as represented as fold change in total NP protein and fold change in nuclear/cytosol ratio of NP protein (E).

Figure 4.6: (A-B) Annexin V Apoptosis assay confirmed the inhibition of apoptosis in presence of minocycline. Caspase 3 cleavage is inhibited in both minocycline treated IAV/PR8-infected cells and Staurosporine-induced cells (C-D)

Figure 4.7: (A) BALB/c mice (5 mice/group) were treated with 5, 15 and 30mg/Kg/day of minocycline for 5d to test the toxicity level. Weight of mice were weighed daily for 5d. (B) Intranasal infection with the IAV/PR8 (4 x 50% Lethal doses, MLD50) to BALB/c mice (5 mice per group). On day 2, mice received treatment with 30 mg/kg/day of Minocycline or DMSO till 15th day. Body weight and survivability were measured for every mouse over 15d. (C-E) Viral RNA from lungs tissue at 5dpi and viral proteins were detected. The viral titre was measured in lungs in terms of TCID50/ml.

Figure 4.8: (A) BALB/c mice (5 mice/group) received treatment with 30 mg/kg/day of Minocycline or DMSO. The HE staining was performed on vital organs- lung, heart, kidney and liver tissues. (B) The HE staining was performed on lung tissues, and tissue integrity was viewed at 10X and 40X magnifications in microscope.

Figure 4.9: Illustration of the role of minocycline in hindering the export of vRNPs from the nucleus leading to inhibition of viral assembly and dissemination.

Figure 5.1: Histogram showing percentage of HA titer reduction of virus treated with candidate molecules

Figure 5.2: Effects of candidate molecules, standard inhibitors i.e. oseltamivir carboxylate (OMVC) and quercetin (QR) on H1N1-NA for hydrolysis of substrate.

Figure 5.3: Lineweaver–Burk plots of inhibition of oseltamivir carboxylate (OMVC), quercetin (QR) and candidate molecules on H1N1-NA.

Tables

Table 3.1. Amino acid substitutions in the HA gene (antigenic epitopes) among IAV H1N1pdm09 isolates in comparison to previously reported eastern Indian strains and vaccine strains A/human/California/07/2009(H1N1), A/human/Michigan/45/2015(H1N1) and A/human/Brisbane/02/2018(H1N1)

Table 3.2: Amino acid substitutions in NA gene (antigenic epitopes) among IAV H1N1pdm09 isolates in comparison to previously reported eastern Indian strains and vaccine strains- A/human/California/07/2009(H1N1), A/human/Michigan/45/2015(H1N1), A/human/Brisbane/02/2018(H1N1)

Table 3.3: Amino acid substitutions in the NA gene (antigenic epitopes) among the IAV H1N1pdm09 isolates in comparison to eastern Indian strains and vaccine strains- A/human/California/07/2009(H1N1), A/human/Michigan/45/2015(H1N1), A/human/Brisbane/02/2018(H1N1).

Table 3.4: Amino acid substitutions in the NA gene (non-antigenic domains) of IAV H1N1pdm09 isolates in comparison to eastern Indian strains and vaccine strains- A/human/California/07/2009(H1N1), A/human/Michigan/45/2015(H1N1), A/human/Brisbane/02/2018(H1N1).

Table 5.1: Cell-based EC₅₀, Enzyme-based IC₅₀ and K_i values of synthesized molecules obtained by crystal violet, NA-inhibition and enzyme kinetics assays.

Table 5.2: Degree of inhibition on CPE of pandemic H1N1 on MDCK cells by all the designed molecules at a concentration of 100 µM obtained by qualitative CPE inhibition assay



Chapter 1

Review of Literature

1.1.Introduction

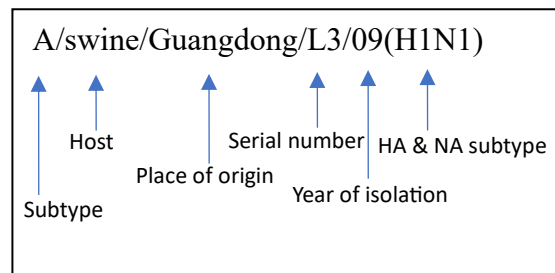
Seasonal epidemics caused by influenza virus typically occur in the winter depending on the local climate and geography (Weinstein et al., 2003; Babazadeh et al., 2019; Ebrahimipour et al., 2019; Morens and Taubenberger, 2019). It causes an acute febrile illness with varying degrees of respiratory and systemic symptoms. In high-risk people, complications due to influenza infection have the potential to be severe or even fatal (Clohisey and Baillie, 2019). Fever, chills, headache, red eyes, sore throat, dry cough and nasal discharge are the signs and symptoms of influenza infection (Nakagawa et al., 2017). Rapid antigenic variation leads to evolution of the virus. Viruses undergo mutation and give rise to new strains by processes referred to as antigenic drift and shift. Antigenic shift is a rare phenomenon but has the potential to cause a pandemic (Morens and Taubenberger, 2019). Antigenic drift involves drastic modification in viral genome leading to development of novel hemagglutinin (HA) and neuraminidase (NA) proteins (Kim et al., 2018). Despite notable advancements in the prevention, control, and management of cases, influenza infection remains a significant global communicable illness. The influenza viruses belonging to "Orthomyxoviridae" family, is an RNA-type virus. They are of four types: A, B, C and D. Flu types A and B typically cause epidemics and outbreaks (Mosnier et al., 2015).

1.1.1. Taxonomy and nomenclature

According to the proposal of WHO in 1971, the complete designation of the viral strains includes:

- type
- host organism
- place of origin
- its serial number
- year of its isolation
- antigenic subtypes of
- HA and NA

Generally, for human isolates, the host of origin is not indicated. For example: A/swine/Guangdong/L3/09(H1N1).



Influenza viruses are classified into 4 types: A, B, C and D.

Influenza A virus (IAV): It targets the different species including humans, swine, avians, equine and others. The subtypes of this virus depend on serotypes of HA and NA. There are 16 subtypes including H1N1, H1N2, H2N2, H3N1, H3N2, H3N8, H5N2, H5N3, H5N8, H5N9, H7N1, H7N2, H7N3, H9N2, H10N7. IAV evolves within the genome either by antigenic drift (the mutation within the genome) or antigenic shift (genetic re-shuffling through co-infection with different subtypes leading to emergence of new subtypes). H2N2 Asian flu (1957), H3N2 Hong Kong flu (1968) and H1N1 Swine flu (2009) are the prominent ones.

Influenza B virus: It has 2 lineages namely Victoria and Yamagata. They are more prone to genetic re-assortments causing epidemics and seasonal flu.

Influenza C virus: They are antigenically stable, having no subtypes or lineage. They are capable of infecting humans and pigs. They do not cause epidemics but cause mild respiratory disease.

Influenza D virus: They were initially isolated from infected swine in Oklahoma in 2011. It has four lineages: D/OK, D/Yama2016, D/660, and D/Yama2019 and is less prevalent.

1.1.2. Symptoms

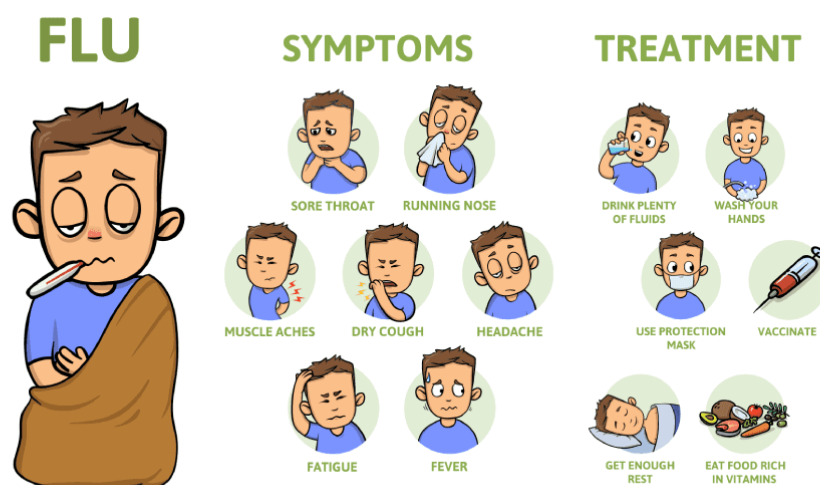


Figure 1.1: Symptoms and treatment measures of flu

Symptoms of Influenza develop quite rapidly, within 1-2 days after infection. Initial symptom includes chills along with fever (temperature ranging from 100-103°F) (Nayak, 2014). Other symptoms include cough, body ache primarily in joints and throat, nasal congestion, headache, watery eyes and fatigue as shown in **fig. 1.1** (Nakagawa et al., 2017). In case of children, incidence of diarrhea and abdominal pain along with flu symptoms was also observed (Dilantika et al., 2010).

1.1.3. Diagnosis

The diagnosis of the infection is mostly done through virus isolation, its antigen or nucleic acid detection, or both. The sample should be collected after disease manifestation. The viral samples are then cultured in either cell lines or chicken embryos. The hemagglutination and neuraminidase inhibition assays as well as the RT-PCR analytic method or ELISA are just some of the diagnostic tools that could aid in the detection of the virus. Eventually, antigens may be detected either by using a direct method like immunofluorescence or by using enzyme-linked immunosorbent assay (ELISA) in respiratory secretions (Couch, 1996). Within 30 minutes, commercial rapid diagnostic test kits can offer a diagnosis, however they are not highly sensitive (Control and Prevention, 2009). Serological assays such as complement fixation and immunodiffusion can also be used to diagnose infections (Couch, 1996; Acha, 2001; Szyfres, 2001; Control and Prevention, 2009). The most popular diagnostic assays today are ELISA or real-time RT-PCR because of its sensitivity, specificity and less time involving.

1.1.3.1. Identification of Influenza isolates by Hemagglutination Inhibition (HAI)

Red blood cells (RBCs) have the potential to bind to HA protein of influenza virus, thereby causing the RBCs to agglutinate (referred as hemagglutination). This characteristic property of RBCs is used in the conventional detection of influenza viruses. This hemagglutination is inhibited when antibodies against HA bind to the antigenic sites of HA, thereby blocking these sites from RBC binding. This type of inhibition is referred to as HAI (**Fig. 1.2**).

Hemagglutination Test

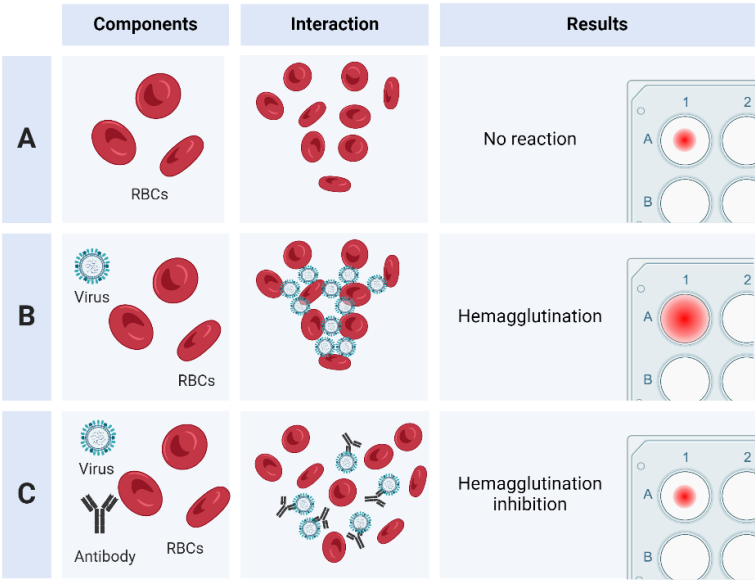


Figure 1.2: Hemagglutination Inhibition assay

1.1.3.2. Enzyme immunoassay

Commercially available enzyme immunoassays can quickly detect influenza viruses in clinical samples. Therefore, they are widely used. Nasopharyngeal aspirates, nasal washes and nasopharyngeal and/or throat swabs serve as good specimens for the testing. The sensitivity and specificity of the test varies based on the type of specimen. It is crucial to combine these tests with virus isolation during outbreaks and after the peak influenza activity in order to verify the results of the test kit.

1.1.3.3. Rapid diagnostic kits

Rapid diagnostic kits including the Directigen Flu A & B Kit, Flu Optical Immuno Assay, QuickVue Influenza Test, and ZstatFlu Test can rapidly determine whether influenza viruses are present in the suspected clinical sample (Fig. 1.3). While some of these tests are based on the extraction and detection of influenza A or B nucleoprotein or the detection of influenza-specific neuraminidase activity, the others are based on the interaction between enzyme-labelled monoclonal antibodies specific to influenza virus and viral antigen.

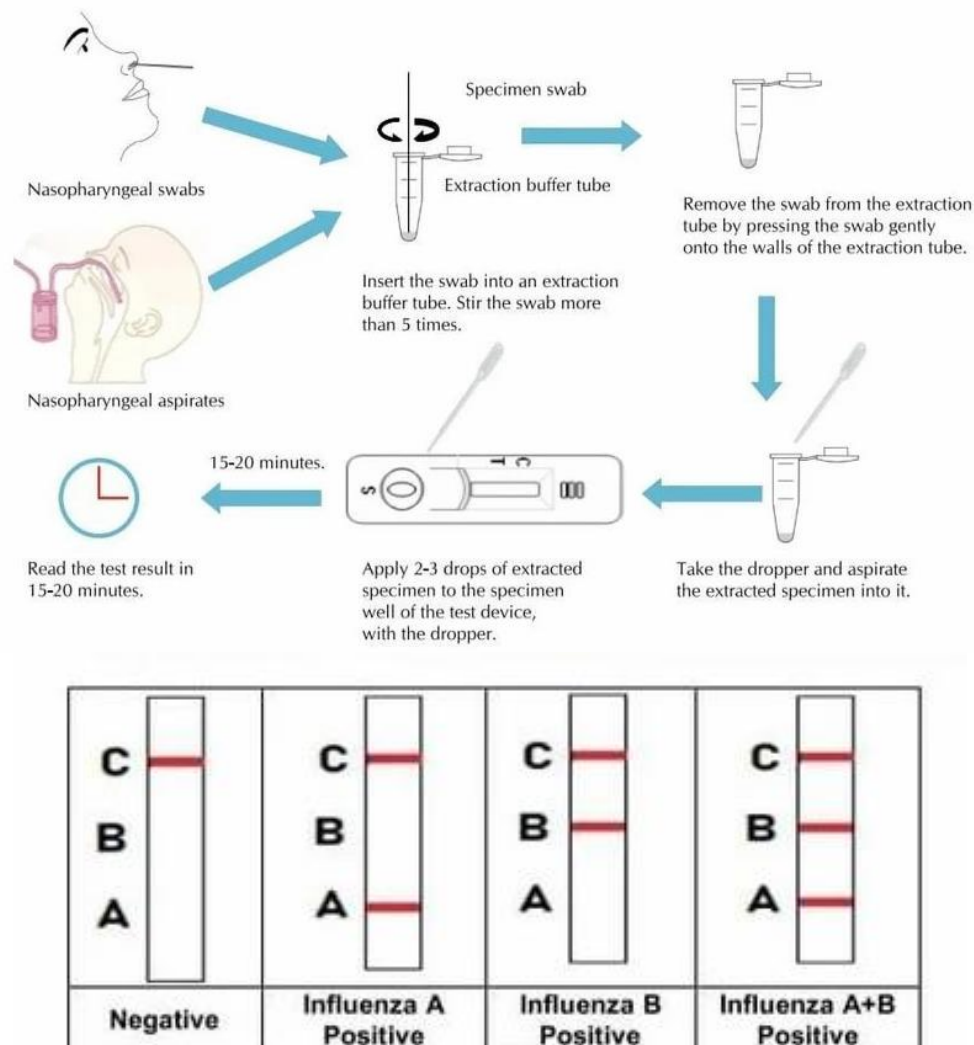


Figure 1.3: Rapid diagnostic kit: steps from sample collection to interpretation of results.

1.1.3.4. Molecular testing methods

1.1.3.4.1. Reverse transcription-polymerase chain reaction (RT-PCR)

Polymerase chain reaction (PCR) is capable of detecting very low quantities of viral genome. Since Influenza viruses have single-stranded RNA genome, a DNA copy (cDNA) which is complementary to the viral RNA is synthesised before PCR takes place. A polymerase called reverse transcriptase (RT) is used to synthesise this cDNA from viral RNA, this cDNA is then amplified. This process is known as RT-PCR and is a strong approach for the detection of Influenza virus. "Quantitative" or "real-time" RT-PCR techniques use fluorescently labelled molecules or oligonucleotides to identify target DNA amplification at each cycle of the PCR thermocycling procedure. There are several benefits of real-time RT-PCR systems over

conventional RT-PCR experiments. Unlike conventional RT-PCR, for real-time systems that save data electronically, post-amplification processing is not necessary. So, without the use of gel electrophoresis and photographic documentation, the results can be viewed, examined, and archived (**Fig. 1.4**). Additionally, more samples can be analysed at once while the danger of carry-over contamination is diminished.

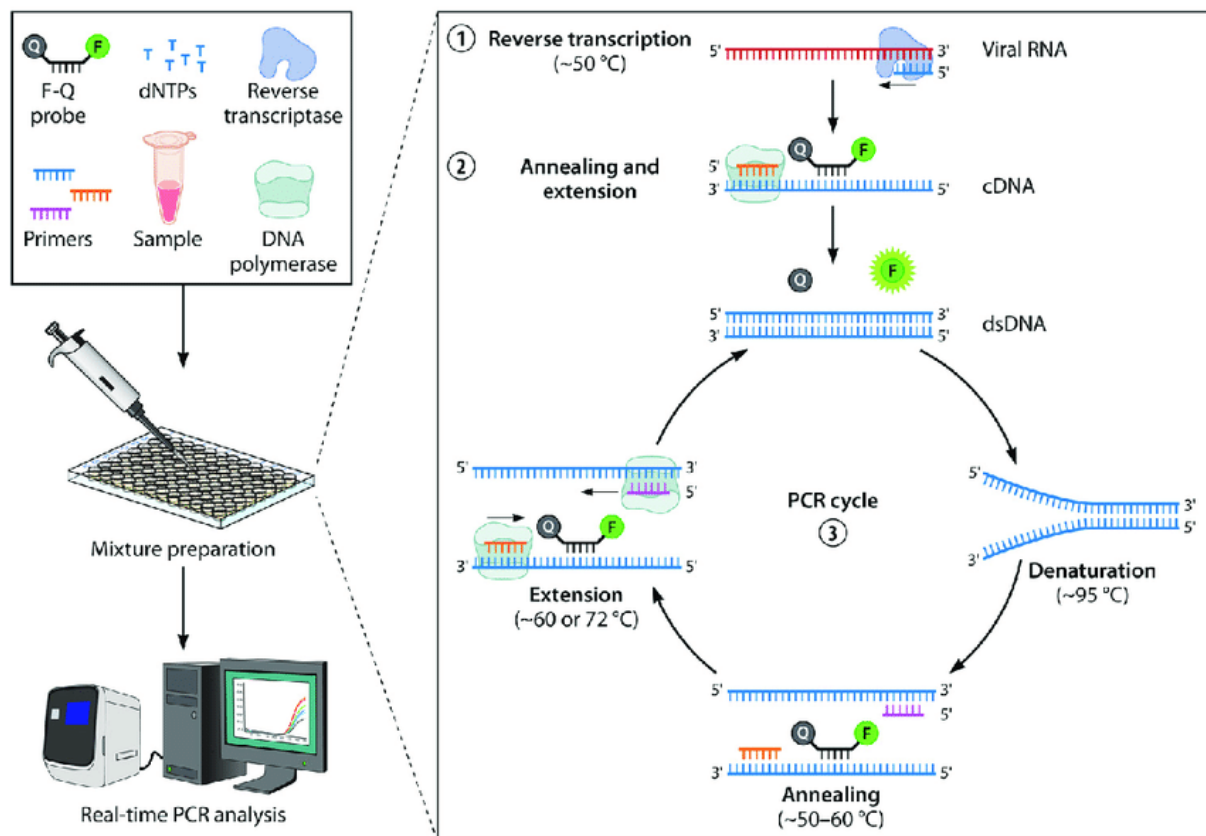


Figure 1.4: Real-time PCR: step by step procedure of DNA/RNA amplification.

1.1.3.4.2. Sequence analysis

By comparing sequence data from isolates collected during an influenza season, the worldwide spread of a virus variant can be followed closely, and genetic analysis of the virus genes aids in monitoring the evolution of influenza viruses and determining the degree of relatedness between viruses isolated in different geographical areas and during different times of the year. The aforementioned analysis results can go into the development of the influenza virus vaccine.

1.2. Influenza A virus (IAV)

The first documented account of the flu-like outbreak dates to 1173-74, while the first detailed epidemic report dates back to 1694 (Molineux, 1694;Hirsch, 1883). The epidemic of 1918 is the greatest epidemic ever recorded in history which accounted for more than 21 million human lives all over the world (Johnson and Mueller, 2002). A total of 4 subtypes of flu strains caused worldwide pandemics and outbreaks in the 20th and 21st century: 1957 (H2N2), 1968 (H3N2), 2009 (H1N1), 2015 (H1N1), 2017 (H1N1), 2023 (H3N2). HA and NA are the two surface proteins of IAV which are used to categorize them into different subtypes. There are currently 18 HA subtypes and 11 NA subtypes. Any of these HA and NA subtypes have the potential to combine to form a new virus. In order for the virus to complete its life cycle, HA functions to fuse the virus to cell membranes after attaching the virus to host cells. When NA cleaves sialic acid from cell surface and progeny virions at the end of infection, it facilitates the release of the virus from infected cells (Air and Laver, 1989;Skehel and Wiley, 2000).

1.2.1. History of Influenza A virus

Flu is a common disease since last 1500 years. Hippocrates, in 5th century BC, was the first person to describe the spread of an influenza-like illness from northern Greece to southern islands and elsewhere. As viruses weren't discovered until 1892, the flu epidemic experienced in Florence and Italy during 1300s was known as "influenza di freddo" (cold influence), as per their belief in the source of the disease. Numerous flu outbreaks were reported worldwide, one such originated in 1918, referred as the 'Spanish flu' affecting one-third of the world's population and claiming 21 million lives. It was the deadliest epidemic ever. More number of American troops perished from this flu during World War I than from the battle.

Another outbreak took place in China during 1997, where highly pathogenic avian Influenza A (H5N1) virus infected humans. The infection spread to Europe and Africa, infecting hundreds and killing a large percentage of them during 2005 (Wang et al., 2008). The 2009 influenza A (H1N1) pandemic affecting primarily children and young people, began circulating from North America and spread globally (Patient, 2009). Several elderly people were protected by their antibodies since they had previously been exposed to a similar H1N1 strain. Yet it resulted in 2,00,000 deaths globally.

1.2.2. Epidemiology

Every year, it is common to hear of flu outbreaks that differ greatly in terms of severity. This epidemiologic pattern of influenza is based on a plethora of factors which directly impinge the contagion feature of the virus, and indirectly the probability of new cases appearing among relatively big population masses. The susceptibility of the society influences to a greater extent the magnitude and seriousness of epidemics, leading to more instances of death or disease than would have otherwise been the case. For example, during a recent spread of an epidemic, the people of Iran had baseline infection that prevented a high mortality rate in the nation (Moghadami et al., 2010).

Antigenic epitopes of surface glycoproteins, HA and NA undergo modification. "Antigenic shifts" give rise to pandemics and epidemics, while "antigenic drifts" cause outbreaks of varying size and intensity. Outbreaks caused due to antigenic drifts are less severe and widespread than pandemics or epidemics. The virus continues mutating, adapting to the new immune systems of the susceptible population. This type of mutation is called antigenic drift that occurs consecutively among the HA or NA genes (Webster et al., 1979). It is the young people who are often hospitalized due to influenza while the elderly population has higher mortality. It is also noted that people with certain immuno-compromised health conditions are at a higher risk of death and complications such as lung dystrophy, dementia, elderly people with cardiovascular disorders and diabetic patients are high up on this list. During the pandemic of 2009, pregnant women were at high risk of infection leading to morbidity and mortality, specially the second and third trimesters (Freeman and Barno, 1959; Siston et al., 2010).

1.2.3. Morphology of Influenza A virus

Influenza A viruses are spherical or filamentous in shape. The spherical ones are of 100 nm in diameter while the filamentous ones measure 300 nm in length. The envelope of the virion is studded with glycoprotein -HA and NA, in the ratio four to one (Palese and Shaw, 2007). Matrix ion channels M2 (fewer in number) traverse the lipid envelope in the ratio of one M2 channel per 101-102 HA molecules (Zebedee and Lamb, 1988). The virion core is enclosed by a matrix M1 protein, which lies under the overlay of the envelop embedded with the integral proteins HA, NA, and M2. The viral core comprises of nuclear export protein (NEP or NS2) and the ribonucleoprotein (RNP) complex. The RNP complex consists of nucleoprotein (NP) and RNA-dependent RNA polymerase (PB1, PB2, and PA) coated viral RNA segments in helical symmetry.

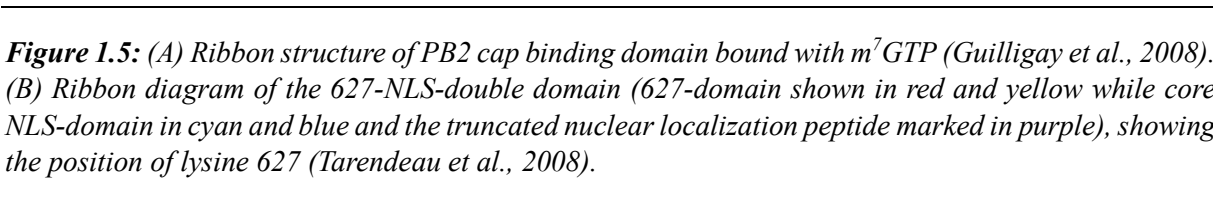
1.3. Influenza A virus proteins

The eight negative-sense RNA segments codes for eleven proteins. Segments 1, 3, 4, 5 and 6 encode a single protein: the PB2, PA, HA, NP and NA proteins, respectively. Segment 2 codes for polymerase subunit PB1 and an accessory protein PB1-F2. RNA splicing leads to segment 7 encoding Matrix protein M1 and M2 ion channel. Colinear transcription of segment 8 results in the NS1 protein while spliced mRNA of segment 8 encodes for NS2.

1.3.1. Structural proteins

1.3.1.1. Segment 1 [Basic Polymerase Protein 2 (PB2)]

The segment 1 (2,341 nucleotides long) of the influenza genome codes for PB2 protein. It comprises of 759 amino acids (aa). It is an important subunit of the RNA-dependent RNA polymerase (RdRp) complex and a major determinant of viral pathogenicity. Position 627 is responsible for the pathogenicity (Hatta et al., 2001). PB2 is responsible for cap binding (Blass et al., 1982). The C terminal of PB2 (PB2_C) has a bipartite nuclear localization signal (NLS) sequence [K736RKR739X (12) K752RIR] which guides its import into the nucleus from the cytoplasm (**Fig. 1.5B**) (Fontes et al., 2003). The cap binding domain (residues 318-483) of PB2 bound to a 5' cap analog (m⁷GTP) (**Fig. 5A**), share structural similarity with other cap-binding proteins like eIF4E (Marcotrigiano et al., 1997;Guilligay et al., 2008). A guanine base is sandwiched between positions 357(His) and 404(Phe) of PB2_{cap}, where the N1 and N2 of guanine are involved in salt bridge formation with the 361(Glu). It has higher affinity towards m⁷GTP than GTP due to the 7-methyl group present in the cap (Guilligay et al., 2008). Adjacent to PB2_C lies an RNA binding domain (residues 535-684). Lysine at position 627 is crucial for viral replication in mammals (**Fig. 1.5A**). PB2 is reported to have endonuclease activity where it generates cap primers from host mRNA, for viral mRNA synthesis (Bouloy et al., 1980;Plotch et al., 1981;Shi et al., 1995). Cells expressing PA, PB1, NP but not PB2, synthesizes transcripts lacking the 5' cap, further proving role of PB2 in cap-snatching (Nakagawa et al., 1995). PB2 along with PB1 and PA subunits form the RdRp complex responsible for viral replication and transcription. PB2 has binding sites for PB1 and NP proteins (Poole et al., 2004). PB2 is imported into the mitochondria where it is localized in the matrix. It inhibits the expression of interferon by associating with mitochondrial antiviral signaling (MAVS) protein, which acts downstream of RIG-1 and MDA-5 in the interferon induction pathway thereby regulating the innate immune responses. It also has a role in regulating apoptosis (Long and Fodor, 2016).



PB1 is a component of RdRp encoded by segment 2. It harbors the polymerase activity (González and Ortín, 1999). Positions 444 to 446 of the S-D-D motif make up the active site for the polymerization activity (Biswas and Nayak, 1994). The RdRp active site is located in the PB1 subunit, which also interacts with the PA and PB2. The amino- and carboxyl-termini of PB1 are thought to be the binding sites for the PA and PB2 polymerase subunits, respectively, according to deletion mutant analysis of PB1 (González et al., 1996; Toyoda et al., 1996). A PB1_C (residues 678–757)-PB2_N (residues 1-35) complex structure shows that three helices from each of the domains are clubbed together to form a "revolver-shaped structure" (Sugiyama et al., 2009a) (**Fig. 1.6**). The amino terminus of PB1 was identified as the location of the nuclear localization signal (Ilyushina et al., 2006). Both the assembly of the three polymerase protein subunits and its catalytic activity of RNA polymerization depend heavily on the PB1 subunit. The catalytic activity of the PB1 subunit is modified to transcriptase when interacting with PB2 or replicase when interacting with PA (Honda et al., 2002).

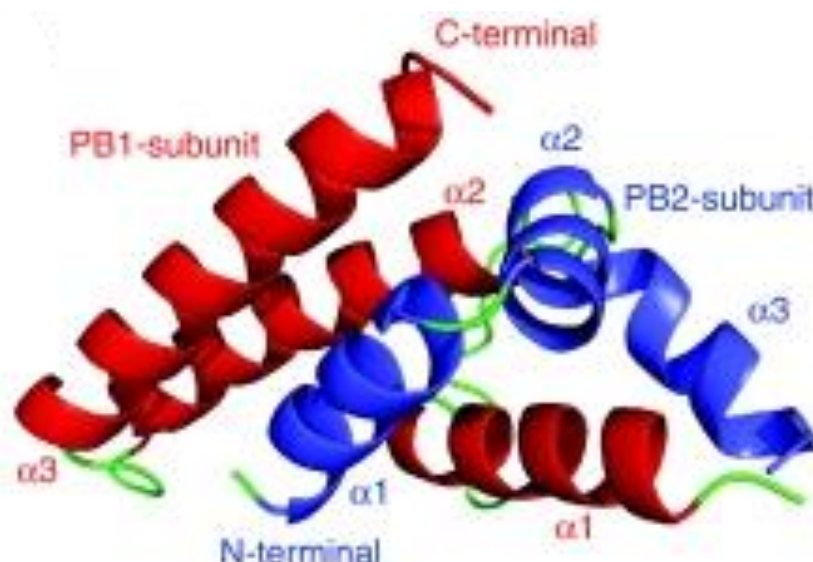


Figure 1.6: Ribbon structure showing the interaction of helices of PB1 (depicted in red) and PB2 (depicted in blue) (Sugiyama et al., 2009b)

1.3.1.3. Segment 3 [Acidic Polymerase Protein (PA)]

Segment 3 encodes the PA protein, which is the smallest component of the RdRp complex. PA is reported to have endonuclease and protease activity, it participates in viral RNA (vRNA)/complementary RNA (cRNA) promoter binding and interacts with the PB1 subunit (Richardson and Akkina, 1991). A cation-dependent endonuclease active-site is present in the N-terminal of PA (PA_N) where aa residues His41, Glu80, Asp108, and Glu119 is conserved among influenza A subtypes and strains. In order to synthesize viral mRNAs, cleavage of host pre-mRNA by PA_N is crucial. The crystal structure analysis reveals the first 14 residues (2-15) of N-terminal of PB1 (PB1_N) interacts with PA_C domain (He et al., 2008;Obayashi et al., 2008). The interaction is between the sequence PTLLFLK of PB1_N located in a small 310-helix and a cleft bounded by four almost-parallel α -helices ($\alpha 8$, $\alpha 10$, $\alpha 11$ and $\alpha 13$) and a β -hairpin ($\beta 8$ - $\beta 9$). Different IAV subtypes share a number of highly conserved residues from PA_C and PB1_N at the interface. Any mutations in the interacting residues or use of a PB1_N peptide inhibits viral replication and transcription, establishing the importance of PA_C-PB1_N interaction in polymerase activity and/or heterotrimer formation (Obayashi et al., 2008). Additionally, it has nuclear localization signals necessary for transit into the nucleus, just like the other influenza virus polymerase subunits (Nieto et al., 1994) (**Fig. 1.7**).

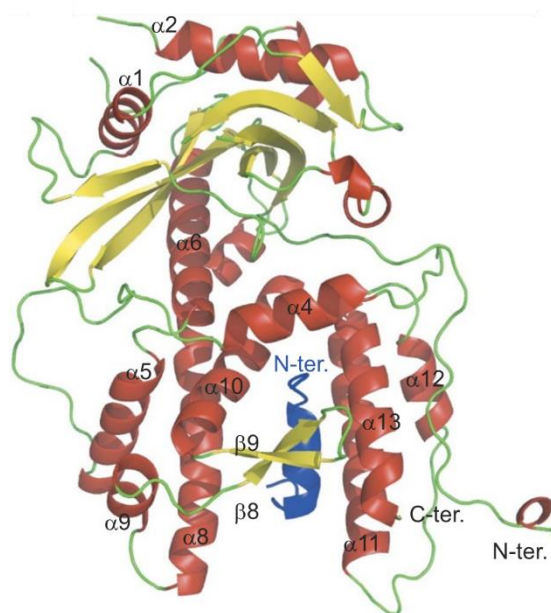


Figure 1.7: Ribbon structure of C-terminal domain of PA (helices colored in red) bound to N-terminal peptide of PB1 (dark blue) (Obayashi et al., 2008).

1.3.1.4. Segment 4 [Hemagglutinin (HA)]

Segment 4 of the influenza virus forms homotrimers to bind to sialic acid receptors on the cell surface, thereby helps the virus to attach to the cell. The HA proteins are located on the envelop of the viral particle. It controls the release of vRNPs into the cytoplasm. It is the primary target for neutralizing antibodies (Staudt and Gerhard, 1983). The newly synthesized precursor polypeptide HA0 is cleaved into HA1 and HA2 by trypsin-like protease, essential for viral infectivity (**Fig. 1.8A**). The HA1 and HA2 are linked by disulphide bond. Cleavage of HA0 at position R329 releases HA2 with the 'fusion peptide' at its amino terminus while leaving behind HA1 (**Fig. 1.8B**). The globular head domain of HA1 has the sialic acid binding site. The "fusion peptide" at the amino terminus of HA2 is made available for membrane fusion. Additionally, this cleavage enables the native HA0 molecule to experience a conformational change, which is facilitated by an acidic environment and is necessary for membrane fusion (Skehel et al., 1982). Upon cleavage, HA1 is dissociated from the endosomal membrane, a loop-to-helix transition in HA2 occurs thereby allowing the fusion peptide at the N terminus of HA2 to attach to the endosomal membrane and promote the fusion of the viral and endosomal membranes, which causes the release of the vRNPs into the cytoplasm (Skehel and Wiley, 2000).

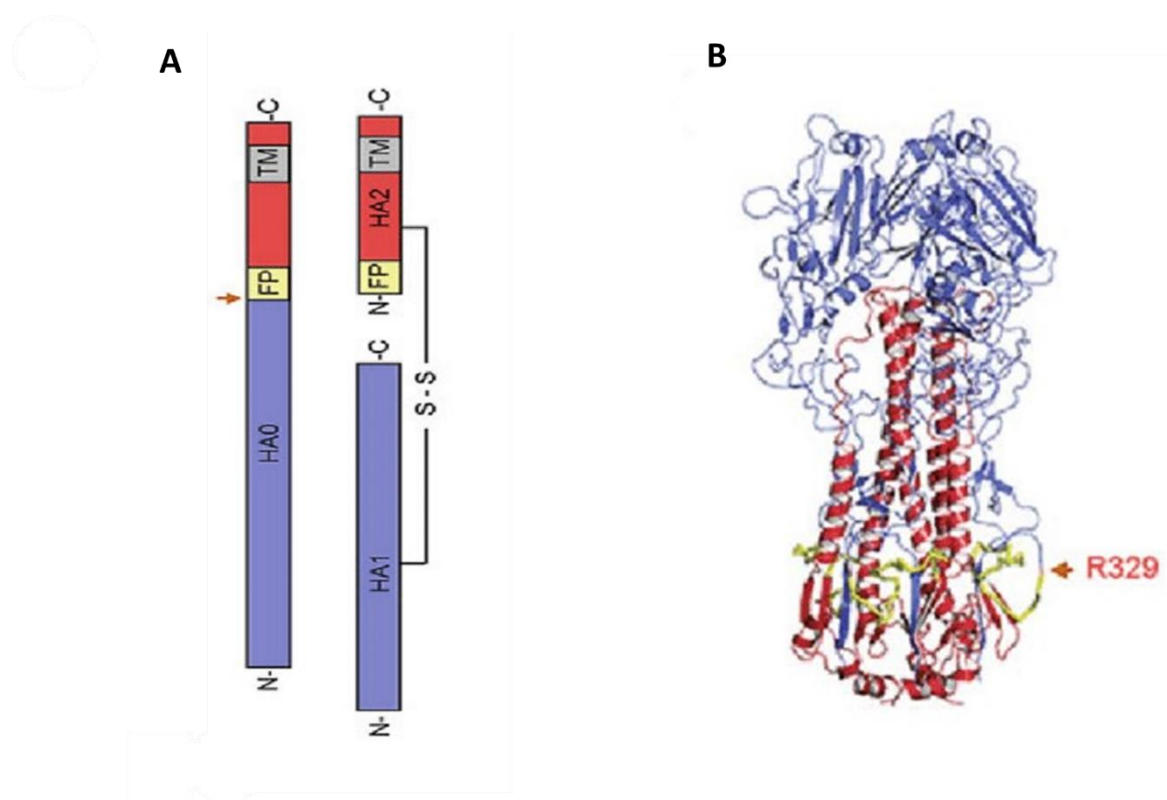


Figure 1.8: (A) Schematic illustration of cleavage of HA0 into HA1 and HA2, which are disulphide linked. The cleavage site is marked with an arrow. (B) ribbon structure of H3 HA0 trimer. Cleavage site R329 indicated with an arrow (Galloway et al., 2013).

1.3.1.5. Segment 5 [Nucleoprotein (NP)]

Segment 5 encodes the NP protein. It has a net positive charge at neutral pH and is a phosphorylated basic protein (Winter and Fields, 1981; Kistner et al., 1989). It plays a crucial role in viral replication and transcription (Huang et al., 1990). The ssRNA binding groove is situated on the external surface of a nucleoprotein molecule that folds into a crescent shape with a head and a body domain (Fig. 1.9C). The oligomerization of nucleoprotein, which is necessary for vRNP production, takes place when the tail loop of each nucleoprotein is inserted into a neighboring nucleoprotein molecule (Fig. 1.9A & 1.9B). The 12-residue tip (residues 408-419) of the tail loop is firmly grasped in a loop-binding cavity that measures 16 x 16 x 10 at the back of a nearby nucleoprotein molecule (Garten et al., 2009). Both hydrophilic and hydrophobic interactions take place at this contact. Site-directed mutagenesis investigations revealed that this nucleoprotein-nucleoprotein interaction is specifically dependent on an intersubunit salt bridge between Arg416 in the tail loop and Glu339 in the neighboring nucleoprotein molecule. The hydrophobic side chains of Ile408, Pro410, Phe412, Val414 and

Pro419 in the tail loop interact with hydrophobic regions in the cavity. Small-molecules mimicking the structural elements of the tail loop could be designed to prevent the oligomerization of nucleoprotein molecules. Additionally, NP is necessary for viral RNA replication, it interacts with the viral polymerase to mediate the transition from capped-primed viral mRNA synthesis to unprimed viral RNA replication (Newcomb et al., 2009).

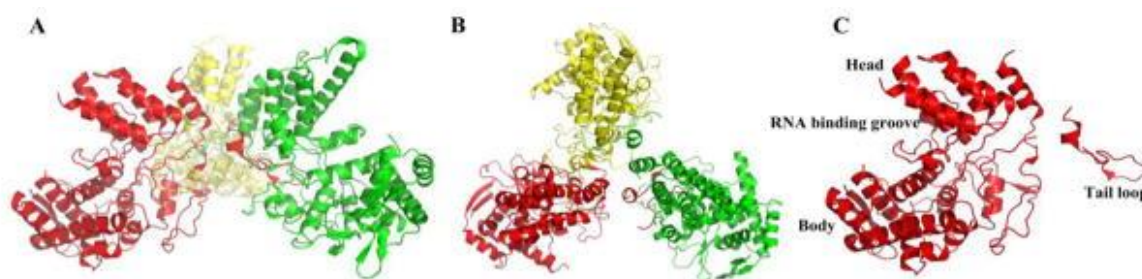


Figure 1.9: Crystal structure of IAV Nucleoprotein. (A & B) Side and top view of IAV H1N1 NP trimer (PDB: 2IQH). (C) Monomer of IAV H1N1 NP (PDB: 2IQH) (Hu et al., 2017).

1.3.1.6. Segment 6 [Neuraminidase (NA)]

NA encoded by segment 6 has 4 domains- a thin stalk, a box-shaped globular head, a transmembrane domain and a cytoplasmic domain (**Fig. 1.10**) (Varghese and Colman, 1991). Due to the glycosylation of the surface glycoprotein NA, the pathogenicity of the virus increases (Li et al., 1993). NA being a homotetramer performs receptor-destroying activity by cleaving α -ketosidic bond between terminal sialic and an adjacent D-galactose or galactosamine (Colman, 1994; Hausmann et al., 1997). A NA-deficient virus was shown to be infectious *in vitro* and *in vivo*, indicating that the NA molecule is not necessary for viral entrance, replication, and assembly (Liu et al., 1995). However, progeny virus particles adhere to one another and/or the cell surface to form huge aggregates when NA activity is blocked (Palese et al., 1974; Palese and Compans, 1976). Therefore, NA plays a vital role in the release of the progeny virions from the infected cells. According to research, the conserved cytoplasmic tail of NA may regulate the morphology and pathogenicity of virion (Bilsel et al., 1993; Jin et al., 1997).

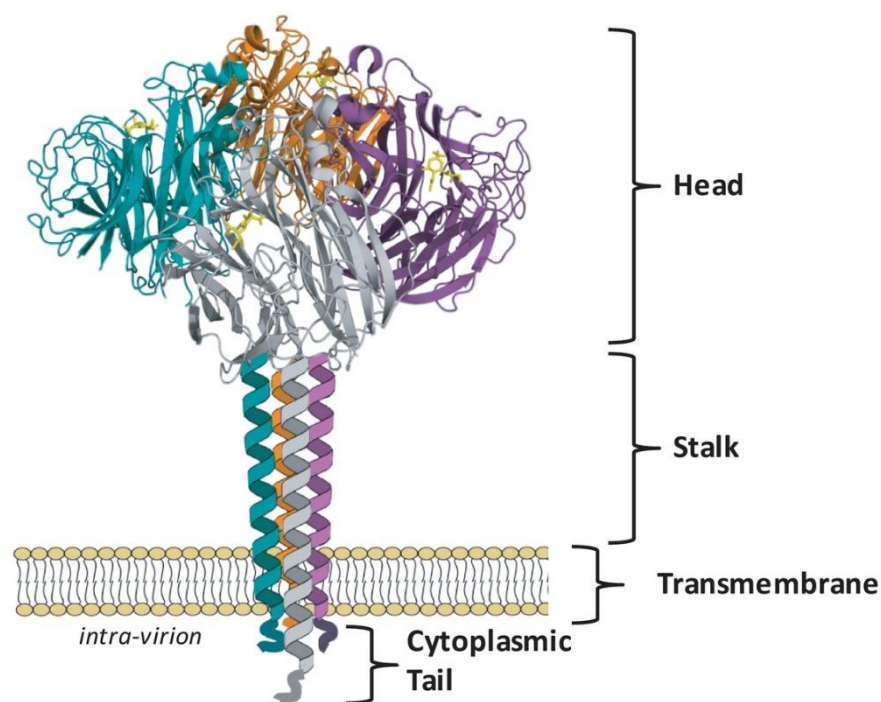


Figure 1.10: Ribbon structure of NA monomer consisting of 4 distinct domains- catalytic head, stalk, transmembrane region and the cytoplasmic tail (McAuley et al., 2019).

1.3.1.7. Segment 7 [Matrix Protein-M1 and M2]

Segment 7 of influenza virus encodes two proteins namely M1 and M2. M1 is the transcription product of segment 7 while M2 is the spliced mRNA transcription product of segment 7.

Matrix protein M1: It is the most abundant protein lying beneath the envelop. It connects the cytoplasmic tails of the glycoproteins with the vRNPs, thus bridging the gap between the membrane proteins and the inner core components (**Fig. 1.11**) (Nayak et al., 2004; Schmitt and Lamb, 2005). According to structural studies, the M1 protein is made up of two globular helical domains connected by a protease-sensitive region. M1 protein monomers are rod-shaped structures observed under electron microscopy of virions with one end in contact with the membrane and the other end pointing toward the interior of the particle (Ruigrok et al., 2000). The rods (M1) are positioned so that the positively and negatively charged residues are on either side of the oligomer (Arzt et al., 2001). Several studies have shown that M1 can interact with lipid membranes and with both NEP/NS2 and vRNP (Zhang and Lamb, 1996). As a result, it is claimed that M1 plays a crucial role in viral assembly by guiding the viral components to the plasma membrane. Additionally, it has been demonstrated that M1 is required for the

formation of virus-like particles, demonstrating its crucial role in the budding process (Latham and Galarza, 2001).

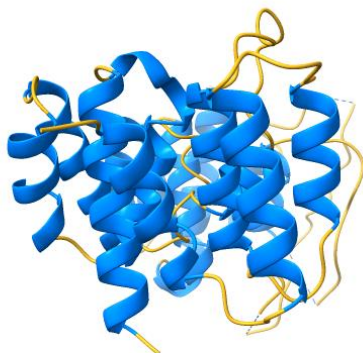


Figure 1.11: *Crystal structure of Matrix protein M1 (3DPX-009473)*

Matrix protein M2: The M2 protein is a type III integral membrane protein. This tetramer lacks a signal peptide sequence but has a short ectodomain, a transmembrane domain and a palmitate and phosphate modified endodomain (**Fig. 1.12**) (Hay, 1992). It plays a role as an ion channel in the viral uncoating process where it conducts protons from the acidic endosomes into the virus in order to dissociate the RNP complex from the other components. In case of highly acid-sensitive HAs, M2 protects the HAs in the trans-Golgi network against premature low pH transitions (Ciampor et al., 1992). M2 proteins have a role in viral assembly and its budding (Hughey et al., 1995). According to models, there is a transmembrane area and an amphipathic helix that runs parallel to the membrane (Tian et al., 2003). This transmembrane region has four helices that are positioned at an angle in the lipid bilayer to create a pore that can accept the drug amantadine and block the ion channel. The highly conserved exterior region of M2 serve as the basis of an influenza virus vaccination and therapeutic strategy. Viral resistance to M2 ion channel inhibitors like amantadine and rimantadine have restricted their use.

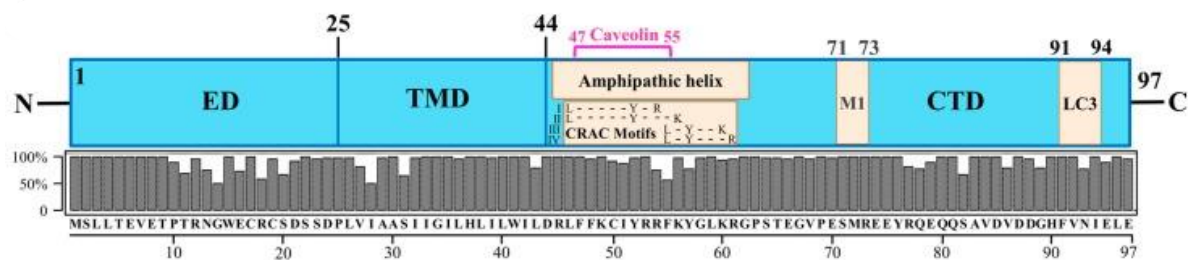


Figure 1.12: Domain of IAV M2 protein showing the ectodomain (ED), transmembrane domain (TMD) and C-terminal domain (CTD) (Manzoor et al., 2017).

1.3.2. Non-structural proteins

1.3.2.1. Segment 8 [Non-structural proteins-NS1 and NS2]

Segment 8 of the influenza virus codes for two proteins: NS1 and NS2. Colinear transcription of segment 8 results in the NS1 protein while spliced mRNA of segment 8 encodes the NS2.

NS1 protein: NS1 has three distinct domains: an N-terminal RNA-binding domain, which *in vitro* binds with low affinity to several RNAs in a sequence independent manner and an effector domain which predominantly mediates interactions with host-cell proteins, but also functionally stabilizes the RNA-binding domain and a C-terminal tail (**Fig. 1.13**) (Wang et al., 2002;Chien et al., 2004). It has a molecular weight of 26 kDa. The RNA binding and effector domains of full-length NS1 are homodimers that contribute to multimerization (Nemeroff et al., 1995). Each monomer of the symmetrical homodimer RNA-binding domain has three α -helices (Chien et al., 1997;Liu et al., 1997). Dimerization of NS1 is required for the binding of dsRNA, and the stoichiometry of dimer to dsRNA is 1:1 (Wang et al., 1999). Each NS1 monomer has two identical helices that form antiparallel 'tracks' on either side of a deep cleft, which aid in the binding of dsRNA (Liu et al., 1997). The 'tracks' are made up of conserved basic and hydrophilic residues that make complementary interactions with the polyphosphate backbone of dsRNA (Yin et al., 2007). Thr-5, Pro-31, Asp-34, Arg-35, Arg-38, Lys-41, Gly-45, Arg-46, and Thr-49 are residues in NS1 that facilitate this interaction, either directly or by enhancing complex stability (Wang et al., 1999;Yin et al., 2007). NS1 is known to decrease host innate immunological responses, restrict host cell mRNA polyadenylation, interact with different cellular signaling pathways, and regulate viral RNA synthesis and splicing as its principal functions.

According to the reports, the main purpose of RNA binding by NS1 is to sequester dsRNA away from 2'-5' oligo synthetase, hence inhibiting the interferon (IFN)- α/β -induced 2'-5' oligo A synthetase/RNase L (OAS/RNase L) pathway (Min and Krug, 2006). The C-terminal effector domain of human and avian NS1 proteins (residues 74–230/237) can independently homodimerize, with each monomer consisting of seven β -strands and three α -helices (Bornholdt and Prasad, 2006;Hale et al., 2008a;Das et al., 2010). This was discovered by crystallographic investigations. Around a long, central α -helix, the β -sheets in each monomer twist while the β -strands twists to form a crescent-like structure. For the NS1 effector domain, two dimer conformations have been suggested: strand-strand and helix-helix (Bornholdt and Prasad, 2006;Hale et al., 2008a). The amino acids that are present at both dimer surfaces seem to be quite well conserved. It should be noted that the structure of an avian influenza virus' effector domain was reported with an allele B NS1 protein, but the structure of a human effector domain was reported with an allele A NS1 protein (Bornholdt and Prasad, 2006). A third dimeric state of the NS1 effector domain may also exist, according to intriguingly recent data [PDB ID: 2RHK]. The effector domain of NS1 is reported to bind several cellular proteins, thereby is involved in cellular pathways. It interacts with p853 subunit of phosphatidylinositol-3 kinase (PI3K), thus activating the PI3K signaling (Hale et al., 2006). Binding of NS1 to protein kinase R (PKR) inhibits the PKR activation which would otherwise inhibit protein synthesis and viral replication (Min et al., 2007). NS1 inhibits the 3'-end processing of cellular pre-mRNAs, including IFN- β pre-mRNA by interacting with the 30-kDa subunit of cleavage and polyadenylation specificity factor (CPSF30) (Nemeroff et al., 1998).

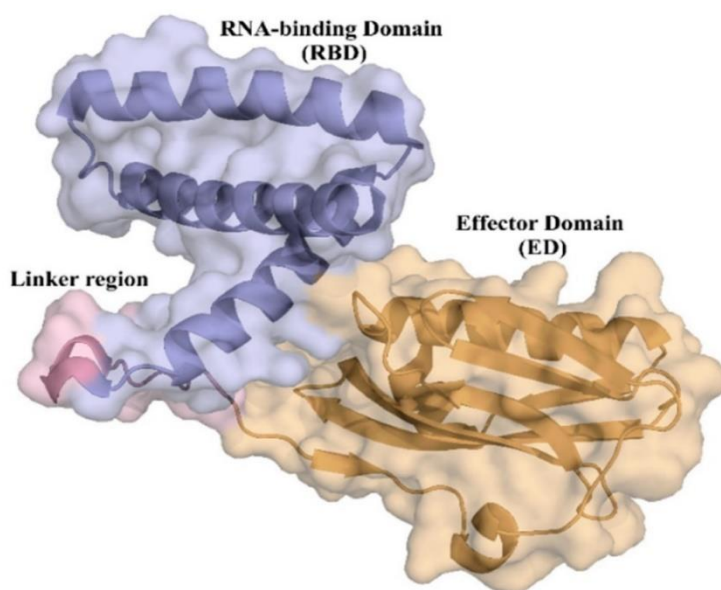


Figure 1.13: 3D crystal structure of H6N6 NS1 protein containing the RNA binding domain (comprising of 3 helices) and an effector domain (consisting of α -helices and β -strands) connected by a linker region [PDB ID: 4OPH] (Cunha et al., 2023).

NS2 protein: From the spliced mRNA of the NS gene, a 15 kDa nuclear export protein (NEP, officially known as NS2) is translated. The NS2 protein was first thought to be a nonstructural protein. It participates in an independent interaction with the human chromosomal region maintenance protein Crm1 and mediates the export of viral ribonucleoproteins (vRNPs) from the nucleus to the cytoplasm through nuclear export signals (O'Neill et al., 1998; Neumann et al., 2000). The M1 protein can attach to the carboxyl-terminal region of NS2 (Ward et al., 1995), indicating that NS2 may regulate viral assembly through its interaction with the M1 protein (Schmitt and Lamb, 2005).

1.3.2.2. PB1-F2 Protein

A small nonstructural protein called PB1-F2 with 87 residues is also encoded by the PB1 RNA segment. Leaky ribosomal scanning causes translation from an AUG codon downstream of the PB1 start site (**Fig. 1.14**) (McAuley et al., 2010). PB1-F2 is encoded in the +1 reading frame of the PB1 gene. According to studies on overexpression, PB1-F2 has been demonstrated to cause cell death, trigger inflammation by recruiting inflammatory cells *in vivo* (Chen et al., 2001; Gibbs et al., 2003; McAuley et al., 2007).

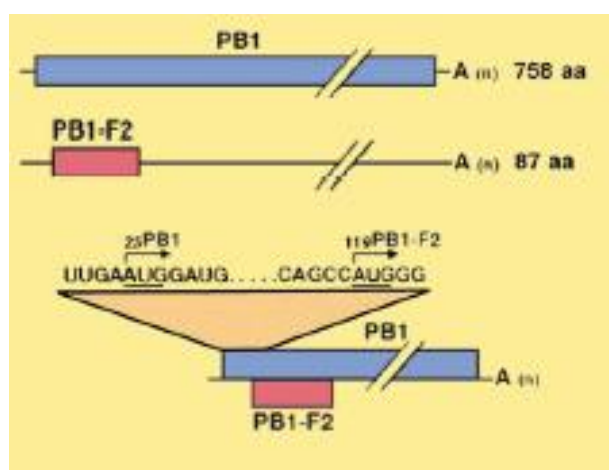


Figure 1.14: Synthesis of PB1-F2 protein from PB1 mRNA by translation from an AUG codon downstream of the PB1 start site.

1.4. Virus life cycle

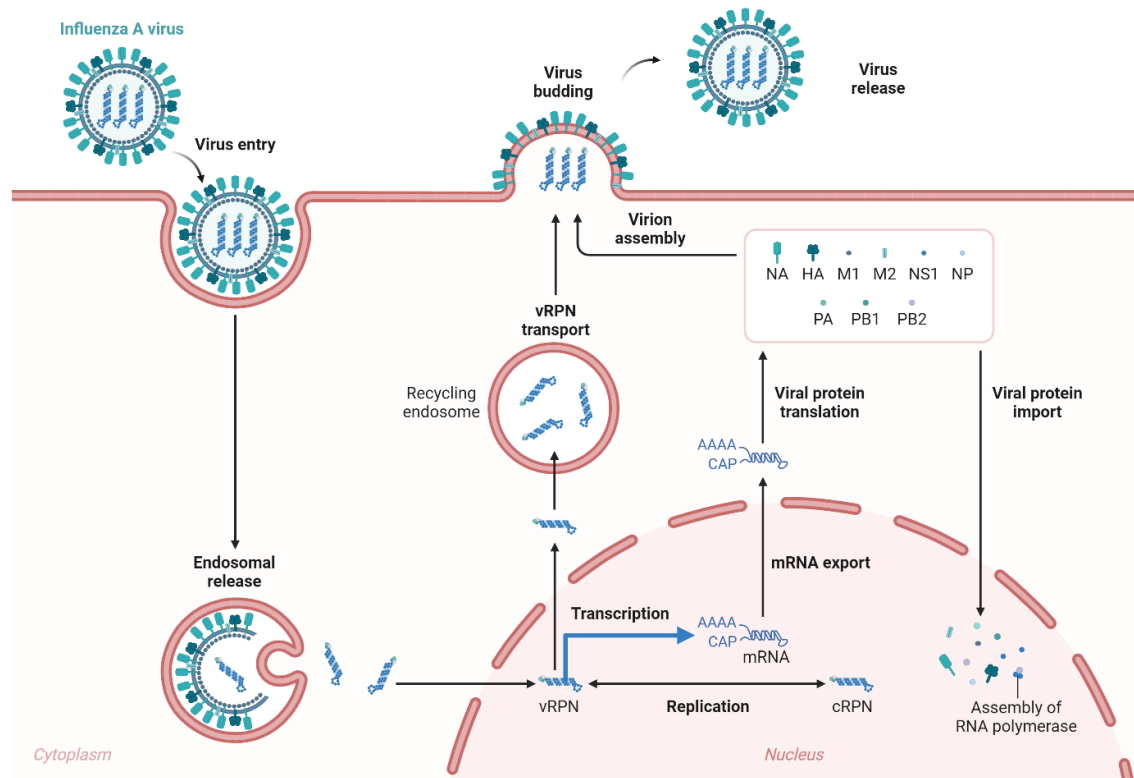


Figure 1.15: Life cycle of Influenza virus (Created with BioRender.com).

1.4.1. IAVCell Binding and Fusion

IAVs use the HA molecules on the viral envelope to start the infection process. The HA receptor-binding site connects the virus to surface glycoconjugates that include terminal SA residues once it has made contact with a potential host cell (Weis et al., 1988; Gamblin and Skehel, 2010; Hamilton et al., 2012). IAVs then use the sialidase function of NA to eliminate local SAs and release non-productive HA interactions before scanning the cell surface for the appropriate sialylated "receptor" (Sakai et al., 2017). The "receptor's" species is unknown at this time, but it is generally accepted that HAs from avian IAVs have higher specificity for receptors with $\alpha 2,3$ -linked SAs that have a "linear" presentation (Rogers and Paulson, 1983; Nobusawa et al., 1991), whereas HAs from human IAVs prefer a $\alpha 2,6$ -linkage, which results in a more "bent" presentation (Gambaryan et al., 1997; Matrosovich et al., 2000). HAs from swine recognize both the linkages (Skehel and Wiley, 2000). Although these preferences

are associated with the SA links in the relevant hosts (Böttcher-Friebertshäuser et al., 2014), numerous studies have demonstrated that matching HA receptor binding preferences with the SA linkages in a specific host is more important for transmission than infection (Tumpey et al., 2007;Herfst et al., 2012;Imai et al., 2012;Linster et al., 2014). This suggests that IAVs may use more than one receptor, or that the IAV "receptor" exhibits strong cell tropism in the airways.

Despite the fact that the receptor's identity is unknown, it is evident that HA-mediated binding to the sialic acid residues on host cell causes the virion to be endocytosed (**Fig. 1.15**). Endocytosis can either take place via macropinocytosis or a clathrin-dependent mechanism involving dynamin and the adaptor protein Epsin-1 (Roy et al., 2000;Chen and Zhuang, 2008). When the virus has entered the cell, it is transported to the endosome, where the low pH (5 to 6) activates the M2 ion channel (Lakadamyali et al., 2003;Rust et al., 2004;Pinto and Lamb, 2006) and leads to a significant conformational shift in HA that exposes the fusion peptide on the N-terminus of the HA2 while maintaining the HA1 receptor-binding domain (White et al., 1982;Yoshimura and Ohnishi, 1984;Bullough et al., 1994). The C-terminal transmembrane domain (TMD) fixes HA2 in the viral membrane, forming a pre-hairpin conformation, while the fusion peptide, once exposed, inserts into the endosomal membrane. After that, the HA2 trimers fold back on themselves to form a hairpin that starts to bring the two membranes together. The two membranes then fuse together as a result of the creation of the lipid stalk, which was made possible by the further collapse of the hairpin bundles into a six-helix bundle. A proton-selective ion channel is formed by the tetrameric type III transmembrane protein M2 (Holsinger and Alams, 1991;Pinto et al., 1992). The viral core becomes acidic when the M2 ion channels are opened. This virion's acidic environment frees the vRNP from M1, allowing it to enter the host cell's cytoplasm (**Fig. 15**) (Pinto and Lamb, 2006). The packaged vRNPs are released from M1 when the M2 ion channel opens, which permits the transport of the vRNPs to the host cytoplasm after HA-mediated fusion (Martin and Heleniust, 1991;Bui et al., 1996).

1.4.2. IAV Genome Trafficking to the Host Cell Nucleus

The transcription and replication of influenza virus take place in nucleus, so the vRNP must enter the nucleus after being released into the cytoplasm. Contrary to the first stages of IAV entry, vRNP trafficking to the nucleus after the fusion event is heavily reliant on the transport systems and machinery of the host cell (Eisfeld et al., 2015). Numerous investigations have supported the current theory, which states that the freshly released cytoplasmic vRNPs enter the host cell nucleoplasm via the importin- α -importin- β nuclear import pathway (**Fig. 1.15**)

(Martin and Heleniust, 1991;Kemler et al., 1994;O'Neill et al., 1995;Wang et al., 1997;Cros et al., 2005;Wu et al., 2007;Chou et al., 2013). The vRNPs are made of viral proteins namely NP, PA, PB1 and PB2, all of which have nuclear localization signals (NLSs). It is believed that the vRNPs initially activate this pathway by recruiting the adaptor protein importin- α by using the surface-exposed nuclear localization sequences from the NP molecules (Wang et al., 1997;Cros et al., 2005;Wu et al., 2007). The importin- β transport receptor detects importin- α after it binds to the vRNP and sends the vRNP to the nuclear pore complex, where it is transported into the nucleoplasm.

The complete entrance process can now be observed in single cells thanks to recent advancements in imaging and RNA labelling techniques (Rust et al., 2004;Chen and Zhuang, 2008;Chou et al., 2013;Lakdawala et al., 2014;Dou et al., 2017). According to the combined findings of these investigations, IAVs can transport their vRNPs from the cell surface to the nucleus in around 1 h, with entry and fusion taking place relatively quickly (10 min), and nuclear import taking up the majority of the time (Dou et al., 2017). The efficiency with which the eight vRNAs reach the nucleus, which demonstrates how successfully vRNPs recruit the host nuclear import factors, is a startling finding from these investigations. This discovery was supported by the finding that productive IAV infections need NP adaptation to the importin-isoforms of a specific species (Gabriel et al., 2011). Although the majority of the research on vRNP trafficking has been done on a variety of immortalized cell lines, the potential species-related variations and the crucial part vRNP trafficking plays in reassortment highlight the need for additional methodology development to look into the specifics of IAV entry in primary cells and tissue explants.

1.4.3. Replication of the vRNAs

In order to transcribe the negative sense influenza viral RNA genome, it has to be first converted into positive sense RNA, which will serve as a template for transcription. The transcription and replication of the vRNAs are carried out inside the nucleus by the heterotrimeric viral RNA-dependent RNA polymerase (RdRp) (**Fig. 1.15**) (Fodor, 2013;Pflug et al., 2017). RdRp doesn't require a primer here, it can initiate RNA synthesis on the viral RNA. The partial inverse complementary sequences exhibited at the 5' and 3' ends of the viral RNA makes it possible, thereby they base pair with one another in corkscrew configurations (Flick et al., 1996;Azzeh et al., 2001;Crow et al., 2004;Deng et al., 2006). The transcription of complementary RNA (cRNA), followed by the transcription of new vRNA copies utilizing the

cRNAs as templates, are the two stages involved in the replication of the influenza genome. The proper complementation of free rNTPs (often GTP and ATP) with the 3' end of the vRNA template is required for the production of the cRNAs in an unprimed process (Newcomb et al., 2009; York and Fodor, 2013). The vRNA template is locked onto the PB1 subunit's polymerase active site by nucleotide complementation, which also causes the creation of an A-G dinucleotide from which the cRNA is extended (Robb et al., 2016). After leaving the polymerase, the cRNA joins forces with freshly created NP molecules, one copy of the viral polymerase, and a cRNP to form (York and Fodor, 2013).

According to current theories, the newly created viral polymerases that are incorporated into the cRNPs produce numerous copies of vRNA similarly to how cRNA is translated. There is one peculiarity, though, that has to do with where the longer 3' end of the positive-sense cRNA is located. The cRNA is positioned in the polymerase due to its length increase in such a way that the rNTP annealing and dinucleotide production are most likely to take place at the bases 4 and 5 bases from the cRNA 3' end (Deng et al., 2006; Jorba et al., 2009; Zhang et al., 2010; York and Fodor, 2013). Prior to elongation, the dinucleotide primer must then dissociate and reanneal to the nucleotides at the 3' end. Another possibility is that the cRNA 3' end could move within the polymerase as a result of rNTP binding, directly producing full-length vRNA transcripts. It is theoretically difficult to rule out either hypothesis because the rNTP annealing and dinucleotide synthesis are both temporary processes. The final step in vRNP construction is comparable to cRNP production.

1.4.4. Viral mRNA Transcription

In comparison to cRNA and vRNA transcription, viral mRNA transcription from the vRNA templates is primed, which greatly increases its efficiency (Reich et al., 2014). Through a process known as cap snatching, the viral polymerase acquires the primers with the help of the association with the cellular RNA polymerase II C-terminal domain (Plotch et al., 1981; Engelhardt et al., 2005; Martínez-Alonso et al., 2016; Lukarska et al., 2017). Phosphorylation at serine 5 on the c-terminal domain of cellular RNA pol II activates the cellular cap synthesis complex. Viral RdRp preferentially binds to this form of cellular Pol II (Engelhardt et al., 2005). The PB2 subunit of nascent host transcripts is bound by the viral polymerase for cap snatching, and the PA subunit's endonuclease domain cleaves 10–13 nucleotides downstream of the 5' cap (Guilligay et al., 2008; Dias et al., 2009; Yuan et al., 2009; Rialdi et al., 2017). The newly acquired capped primer is subsequently positioned into

the PB1 catalytic centre by rotation of the PB2 cap-binding domain, where it is expanded utilising the vRNA as a template (Reich et al., 2014). The short poly-U region at the 5' end of the vRNA triggers a reiterative stuttering process, which leads to the final polyadenylation step for each transcript (**Fig. 1.15**) (Robertson et al., 1981; Poon et al., 1999). To achieve polyadenylation, this procedure probably entails several cycles of mRNA dissociation, relocation, and reannealing to this template region of the vRNA.

Because the introduction of primers greatly improves the initiation effectiveness, mRNA transcription is considerably more common over the course of infection and occurs before cRNA and vRNA transcription (Reich et al., 2014). The vRNP-associated polymerases synthesise the first mRNAs, which are then exported from the nucleus to be translated by cytoplasmic ribosomes (Reich et al., 2014). However, the donor and acceptor splice sites in the M and NS transcripts likewise closely resemble those in human transcripts (Dubois et al., 2014). Both M2 and NS2 proteins are encoded via spliced transcripts from segment 7 and 8 that are created by the cell spliceosome as a result of these sites' recruitment (Lamb et al., 1980; Lamb and Lai, 1980; Inglis and Brown, 1981; Lamb et al., 1981; Mor et al., 2016). While the ratio of spliced M transcripts (encoding M2) has been demonstrated to grow throughout infection, the NS transcript has been reported to maintain a similar ratio of non-spliced and spliced transcripts during infection (Inglis and Brown, 1981; Valcárcel et al., 1991). These findings suggest that while M2 expression is more biased towards the later phases of infection, NS1 and NS2 expression are always equal. The NS and M transcripts' splicing effectiveness most likely varies between IAV strains (Robb and Fodor, 2012; Winkvist et al., 2012).

1.4.5. Assembly and Trafficking of vRNPs

IAV protein synthesis is wholly dependent on the host cell's translational apparatus. The translation of the viral mRNAs is split between cytosolic ribosomes (for PB1, PB2, PA, NP, NS1, NS2, and M1) and endoplasmic reticulum (ER)-associated ribosomes (for the membrane proteins HA, NA, and M2) after nuclear export (York and Fodor, 2013). The newly synthesized NP proteins and polymerase subunits (PB1, PB2, and PA) contain nuclear localization sequences that direct these proteins to the nucleus by enlisting the importin- α -importin- β -pathway, which is used for vRNP nuclear import (**Fig. 1.15**). While the PB1 and PA proteins are imported as a heterodimer, the NP and PB2 proteins are imported separately (Cros et al., 2005; Huet et al., 2010). These recently created proteins help in viral mRNA transcription and vRNA replication in the nucleus. In order to build vRNPs and cRNPs, NP monomers attach to

12 nucleotide sequences in vRNAs and likely cRNAs that have a partial G bias. This process may be controlled by NP phosphorylation (Mondal et al., 2015; Lee et al., 2017; Williams et al., 2018). In Figure 15, the heterotrimeric polymerase assembles and binds to the newly formed cRNPs to transcribe vRNAs, which, once assembled into vRNPs, can produce more viral mRNA or cRNA transcripts (Jorba et al., 2009; York and Fodor, 2013).

Early RNA-binding protein synthesis and nuclear import both enable the viral NS1 protein to suppress interferon signaling (Ayllon and García-Sastre, 2014). By connecting the viral transcripts to the cellular nuclear export factors TAP/NXF1, p15, Rae1, E1B-AP5, and the nucleoporin NUP98, NS1 may also aid in the export of viral mRNA from the nucleus (Satterly et al., 2007). M1 and NS2, also referred to as the nuclear export protein, are transported into the nucleus. These two proteins have been linked to the nuclear export of vRNPs in numerous studies (Martin and Helenius, 1991; Bui et al., 1996; O'Neill et al., 1998; Neumann et al., 2000; Cao et al., 2012; Huang et al., 2013). Current findings suggest a concept where M1 functions as an adapter protein connecting NS2 to vRNPs, even if the exact process is yet unknown (Akarsu et al., 2003; Shimizu et al., 2011). The vRNP complex is subsequently directed by NS2 to the CRM1 nuclear export pathway for transport to the cytoplasm through pre-existing connections with CRM1 (Huang et al., 2013), where M1 might inhibit the re-import of vRNPs by obstructing access to the NP nuclear localization sequences (**Fig. 1.15**) (Bui et al., 1996).

The vRNPs are transported by Rab11 from the cytoplasm to the plasma membrane for viral assembly. Rab11 interacts with viral polymerase PB2 component, thereby ensures that progeny virions including vRNPs contain a polymerase (Amorim et al., 2011). According to earlier research, endosomes use microtubules to transport towards the cell surface, and vRNPs preferentially bind with Rab11 on these endosomes (Amorim et al., 2011; Eisfeld et al., 2011; Momose et al., 2011). In a different scenario recently put forth, infection tubulates the ER membrane network, and the vRNPs attach to Rab11 molecules that have gathered in this network to be transported to the plasma membrane (de Castro Martin et al., 2017). It is currently unknown how IAVs include all eight of the distinct vRNPs in a "1 + 7" structure, or how vRNPs are transported to the plasma membrane in either paradigm. The underlying mechanisms are still unknown, despite the fact that various investigations have suggested that particular vRNP associations probably contribute to the packing of the eight vRNPs (Elton et al., 2001; Gavazzi et al., 2013; Moreira et al., 2016).

1.4.6. ER Targeting and Maturation of the IAV Membrane Proteins

Ribosomes attached to the ER membrane synthesize the IAV membrane proteins, which are ultimately destined for the viral envelope. Similar to cellular secretory proteins, interactions between the hydrophobic targeting regions of ribosome-nascent chain complexes containing NA, HA, or M2 and the signal recognition particle (SRP) co-translationally route the complexes to the ER (Bos et al., 1984; Hull et al., 1988; Daniels et al., 2003; Dou et al., 2014). In contrast to NA and M2, which employ their respective TMD as an ER targeting sequence, HA has a cleavable signal sequence that makes it easier for it to engage with SRP. SRP binds to the ribosome-nascent chain complexes and directs them to the SRP receptor in the ER membrane, where they are transferred to the translocon, a Sec61 protein-conducting channel (Gilmore et al., 1982; Deshaies and Schekman, 1987; Görlich et al., 1992). Mutations that change the targeting sequence hydrophobicity of cellular secretory proteins have been demonstrated to reduce their ER targeting and subsequent production (Kang et al., 2006; Karamyshev et al., 2014), which is related to their reliance on SRP. IAVs may use this technique to titrate NA and HA production, even though this feature has not been thoroughly studied for the IAV membrane proteins. Evidence shows this is the case because the hydrophobicity of their ER-targeting sequences changes (Nordholm et al., 2013; Dou et al., 2014).

Additionally, many N-linked glycans are added to HA and NA. The oligosaccharyltransferase transfers the glycans to Asn-X-Ser/Thr sequences, and the number and placement of the glycans change depending on the strain or subtype (Mandon et al., 2013). The calnexin and calreticulin (lectin chaperons) and oxidoreductase ERp57, which facilitates in the creation of disulphide bonds, are recruited by the glycans to boost the folding efficiency of NA and HA (Hebert et al., 1997; Daniels et al., 2003; Daniels et al., 2004; Wang et al., 2008). This is necessary for all proteins, but it is crucial for HA and NA as they have intramolecular disulphide bonds (e.g. six in HAs, eight in N1 and nine in N2) (Wilson et al., 1981; Varghese et al., 1983; Li et al., 2010). M2 has two intermolecular disulphide bonds in contrast when it is in its tetrameric conformation (Holsinger and Alams, 1991). NA tetramers may also have two or more intermolecular disulfide linkages, depending on the subtype.

Despite all of the information available, there are still some questions regarding the synthesis and assembly of the IAV membrane proteins. Obtaining full-length atomic structures of HA and NA in a membrane is one of them; this should become simpler with advancements in cryo-

electron microscopy structure determination. figuring out whether the NA protein directly removes SA residues from substrates inside the Golgi, as this would reduce the potency of nonmembrane permeable NA inhibitors. Since viral mRNA transcription exhibits little temporal variation, it is also unknown how IAVs govern the timing and quantities of viral protein expression (Vester et al., 2010; Kawakami et al., 2011). M2 is probably partially regulated by splicing, although HA and NA are not affected by this (Valcárcel et al., 1991; Mor et al., 2016). The nucleotide profile of the 5' coding sections for NA and HA's ER-targeting sequences, which significantly differs from that of the comparable areas in human secretory protein mRNAs, has recently been related to their regulation (Palazzo et al., 2007; Nordholm et al., 2017). The viral RNA-binding protein NS1 is a clear candidate for post-transcriptional regulation. In fact, numerous studies have demonstrated that NS1 can speed up the translation of certain mRNAs, possibly by increasing the rate of translation initiation by attracting eIF-4G to the 5' region of viral mRNAs (Enami et al., 1994; De La Luna et al., 1995; Aragón et al., 2000; Nordholm et al., 2017; Panthu et al., 2017; Trapp et al., 2018). However, the control of influenza protein lacks a clear mechanistic understanding.

1.4.7. HA Proteolytic Activation at the Golgi or Plasma Membrane

HA0, a fusion-incompetent precursor, is the form in which HA traffics from the ER. HA must be split into the subunits HA1 and HA2 in order to acquire its fusion function (Klenk et al., 1975; Huang et al., 1981; Maeda et al., 1981). Either a monobasic or a multibasic cleavage site is where the cleavage takes place (Böttcher-Friebertshäuser et al., 2014). Highly pathogenic avian IAVs frequently contain multibasic sites that furin, a trans-Golgi network-based calcium-dependent serine endoprotease, can cleave (Stieneke-Gröber et al., 1992). One of the key factors contributing to the pathogenicity of avian IAVs with multibasic cleavage sites is the ubiquitous expression of furin (Schalken et al., 1987).

Contrarily, it has been demonstrated that several proteases are used in human respiratory epithelial cells to process HAs with a monobasic cleavage site, which are encoded by human (and low pathogenic avian) IAVs. These include the human airway trypsin-like protease (HAT), the transmembrane protease serine S-1 member 2 (TMPRSS2), and perhaps the TMPRSS4 (Böttcher et al., 2006; Chaipan et al., 2009). HAT is located in the plasma membrane, where it can cleave either freshly synthesised HA or the HA present in virions that are attached to cells (Zhirnov et al., 2002; Böttcher-Friebertshäuser et al., 2010). TMPRSS2, like furin, is a member of the trans-Golgi network and cleaves HA on its way to the plasma membrane. By balancing

the somewhat acidic pH of the Golgi, the M2 ion channel is suggested to stop the early activation of HA after cleavage (Steinhauer et al., 1991; Takeuchi and Lamb, 1994). While HAT was primarily observed to be expressed in the upper respiratory tract, TMPRSS2 expression has been discovered to be more confined to the upper and lower respiratory tracts than furin (Bertram et al., 2012). These cell tropisms imply that lower respiratory infections are probably mediated by TMPRSS2, which may be one of the main causes of human IAVs being restricted to the respiratory tract's epithelial layer.

1.4.8. IAV Assembly and Budding

IAV envelopes are richer in cholesterol and sphingolipids compared to the bulk lipid profile of the plasma membrane (Gerl et al., 2012), indicating that they originate from unique apical plasma membrane areas frequently referred to as "rafts" (Lingwood and Simons, 2010). To target the eight vRNPs, M1, HA, NA, and M2, to these membrane locations, infectious IAVs must have mechanisms (Rossman and Lamb, 2013). Based on fatty acid changes of the C-terminal cysteine that take place in the Golgi (Zurcher et al., 1994; Takeda et al., 2003; Wagner et al., 2005; Kordyukova et al., 2008), it is thought that HA localises to these unique areas, whereas NA enrichment has previously been linked to a feature in the C-terminus of the TMD (Barman et al., 2004). The cytosolic protein M1 has been postulated to localise to the budding region by interacting with the brief cytoplasmic tails of HA and NA (Ali et al., 2000). In contrast, M2 has been demonstrated to accumulate at the limits of these budding regions (Rossman et al., 2010). It is equally likely, nevertheless, that NA and HA produce membrane domains with a distinct lipid composition and a strong affinity for M1. Finally, it is believed that the vRNPs that Rab11 delivers to the cell periphery localise to the budding site by binding to M1 (Zhang et al., 2000; Noton et al., 2007).

IAVs must alter the membrane to promote bud formation and ultimately scission of the viral envelope from the plasma membrane in addition to directing the assembly of the appropriate viral components at the apical budding location. The virus must first cause a sizable membrane curvature, and then it must constrict the two opposing membranes of the viral envelope to aid in membrane scission and promote bud development. One leaflet of a bilayer can become curved as a result of (i) protein or "molecular" crowding, (ii) curved or "bending" proteins joining the bilayer, (iii) biased accumulation of cone-shaped lipids, (iv) the cytoskeleton, and (v) other factors (Jarsch et al., 2016). IAVs seem to cause membrane curvature by a mix of these processes, according to accumulating data about budding. Multiple investigations have

shown that the expression of HA and NA is sufficient to cause budding and that the presence of M1 improves efficiency and shape uniformity, which is indicative of the use of molecular crowding and bending proteins (Chen et al., 2007; Lai et al., 2010; Yondola et al., 2011; Chlanda et al., 2015). These findings suggest that curvature of the membrane can be influenced by the concentration of HA and NA on one side. As NA is frequently observed clustering in the viral membrane (Chlanda et al., 2015), it is intriguing to hypothesise that its asymmetric structure plays a role in this process (Varghese et al., 1983). While M1 is attracted to the cytosolic side of the membrane budding site, oligomerizes once it reaches the membrane, and these oligomers have been modelled to form curved shapes, M1 appears to be akin to a membrane-bending protein (Harris and Johnson, 2001; Hilsch et al., 2014; Shtykova et al., 2017). These characteristics suggest that M1 has a major influence on the membrane curvature at the budding site, which could account for how it controls whether IAVs form spheres or filaments (Elleman and Barclay, 2004).

The amphiphilic α -helix where M2's membrane-bending ability is located is able to insert the amino acid side chains from its hydrophobic face into a leaflet of the bilayer. It has been suggested that intercalation, with this domain located in the cytosol, causes negative membrane curvature, which shortens the distance between the two opposing membranes of the viral envelope, so facilitating the development and scission of the viral bud neck (Rossman and Lamb, 2013). The IAV budding framework has been established in large part, but it has been challenging to pinpoint the specifics of the budding process, in part because of the mobility and variability of the plasma membrane. It's also possible that IAVs have incorporated redundancy into the budding process given the absence of robust phenotypes from domains that have been suggested to contribute to budding (Jin et al., 1994; Stewart and Pekosz, 2011). Given that IAVs include all the elements required for a combination of lipid recruitment, molecular crowding, and a membrane-bending protein, the prospect of redundancy is unquestionably conceivable.

1.4.9. IAV Cell Release and Movement

The newly formed IAVs' ability to be released once they bud heavily depends on NA's sialidase activity. NA is a homotetramer, and each subunit has a globular enzymatic head domain, a TMD, a length-variable stalk, and a short N-terminal cytoplasmic tail (six amino acids) at the end (Air, 2012). Each blade of the six-bladed propeller structure the globular head domain creates is made up of four antiparallel β -sheets that are supported by disulfide linkages

(Burmeister et al., 1992;Colman, 1994;Li et al., 2010). The active site, which forms a deep pocket in the middle of each monomer and contains the catalytic Tyr residue, is well conserved (Kim et al., 2013). It is difficult to understand why NA evolved to act as a tetramer because each monomer contains all of the residues required for catalysis (Colman et al., 1983;Paterson and Lamb, 1990;Air, 2012). NA tetramers have been demonstrated to bind up to five calcium ions, according to the structures of the enzymatic head domain (Li et al., 2010;Air, 2012). Calcium has also been proven to influence NA activity. The reason influenza NA developed to place a calcium ion at the tetrameric interface is still a mystery.

By catalysing the hydrolysis of the glycosidic bond that connects SA to the underlying sugar molecules, NA facilitates viral release (Burnet et al., 1947;Burnet, 1948). In order to prevent HA from adhering to the cell surface and facilitating the release of the virus during budding, NA eliminates local SA residues (Webster and Laver, 1967;Palese and Compans, 1976). By eliminating SA residues from the N-linked glycans on the HA and NA molecules in the viral envelope, NA has also been demonstrated to aid in the separation of IAVs (Palese et al., 1974). As opposed to HA, human IAV NAs have a general predilection for 2,3-linked SA with varying propensities to cleave 2,6-linked SA residues (Gulati et al., 2005;Mochalova et al., 2007;Air, 2012). However, there is a lack of a comprehensive analysis of SA preference of NA. The topic of whether an ineffective NA enzyme could contribute to or take the place of the HA receptor-binding function has been raised by more recent research that have discovered that some strains contain NAs that are inefficient enzymes but still capable of binding SA (Lin et al., 2010;Zhu et al., 2012).

Due to the existence of many cell types and a mucus layer, the transfer of IAVs from cell to cell in the respiratory epithelium differs dramatically from that in immortalised cell lines cultured in liquid culture. The mucus layer acts as a barrier of defence for the epithelium and is abundant in mucins that have been extensively glycosylated. These mucins can interact with IAVs to reduce cell binding (Burnet, 1951;Cohen et al., 2013). Studies examining the movement of viruses through mucus and respiratory epithelial cells have demonstrated that IAV movement through the mucus layer and infectivity are both improved by NA-mediated cleavage of SAs from mucins (Matrosovich et al., 2004;Cohen et al., 2013;Yang et al., 2014). The lack of aerosol and contact transmission by IAVs with low NA activity and mucus inhibition in recent research demonstrated that this function may also apply to transmission (Zanin et al., 2015).

1.5. Genetic diversity and antigenic variation of Influenza A viruses

Influenza is the archetype of a viral disease in which the virus's continual evolution is crucial for yearly epidemics and sporadic human pandemics. The influenza A viruses exhibit both antigenic drift and genetic change in humans, pigs, and horses. Both the HA and NA of influenza A viruses exhibit antigenic drift. By comparing sequences, five antigenic domains (A-E) on the HA1 have been identified. Genetic diversity arises due to accumulation of molecular alterations in the RNA segments, which occurs by point mutation (antigenic drift), gene reassortment (genetic shift), defective-interfering particles and RNA recombination (**Fig. 1.16**).

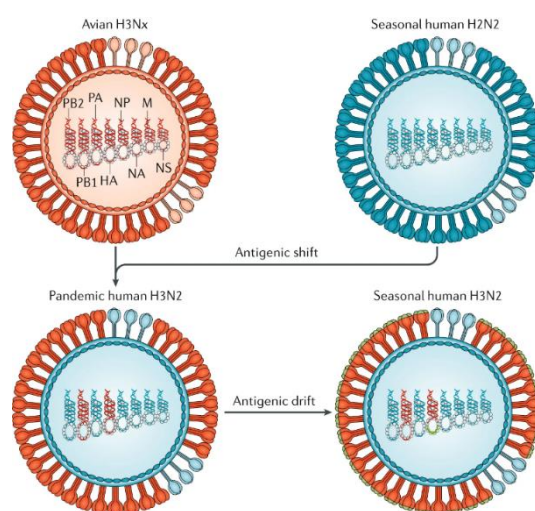


Figure 1.16: Antigenic drift and antigenic shift.

One of the most significant methods for causing variety in influenza viruses is mutation, which includes substitutions, deletions, and insertions. Replication mistakes on the order of 1 in 10⁴ bases are caused by RNA polymerases' lack of proofreading (Holland et al., 1982; Steinhauer and Holland, 1987). In contrast, DNA polymerases exhibit substantially better replication fidelity, with mistakes of the order of 1 in 10⁹ bases per replication cycle. Every time an RNA virus replicates, it creates a mixed population of variants; the majority of these are not viable, but some of them include mutations that may be favourable and may become dominant in the correct selection circumstances.

Reassortment is a crucial process for developing variation quickly because influenza viruses contain segmented genomes. It happens naturally among Influenza A viruses and plays a crucial role in the emergence of pandemics in human populations. Intermolecular recombination and defective-interfering particle mediated interference are two additional processes that result in

genetic diversity. Although defective-interfering particles can affect evolution by lowering the yields of non-defective particles and altering pathogenicity (Steinhauer and Holland, 1987), little attention has been paid to their involvement in influenza virus evolution. Intermolecular recombination in negative-stranded viruses is uncommon, but research has shown that it does happen occasionally (Khatchikian et al., 1989). This offers an additional method for delivering quick evolutionary changes.

1.6. Transmission

Large viral loads are frequently seen in the respiratory secretions of influenza patients, making it possible for each infected person to spread infection to others by sneezing and coughing. It has been suggested that big particle droplets ($>5\mu\text{m}$) are the main means of disease transmission (Bhat et al., 2005). As infectious droplets are so big, intimate contact is necessary for the disease to spread. These huge particles typically only go a short distance and don't hang around in the air for very long. Therefore, airborne transmission is not frequently considered for the spread of disease (Brankston et al., 2007). A short report indicates that the tiny aerosolic respiratory droplets which linger in the air for longer time, carry influenza virus and contributes to the transmission of the illness (Fiore et al., 2011). This implies that efforts to stop the spread of the influenza A virus through touch or big droplets might not be sufficient to do so in homes or communities (Cowling et al., 2013). Therefore, additional re-evaluation of the preventative techniques used often in hospitals is necessary.

Furthermore, coming into contact with contaminated surfaces that have respiratory droplets on them might also spread disease. According to the majority of research and some other investigations, viral shedding in persons without other underlying disorders begins 24 to 48 hours before disease manifestation and ends 6 to 7 days or 10 days afterwards (Wong et al., 2010). Patients with chronic illness, elderly individuals, immunocompromised individuals and youngsters have longer periods of shedding and infectiousness (Boivin et al., 2002; Carrat et al., 2008).

1.7. Pathogenesis

Influenza viruses are transmitted from one person to another via aerosols and droplets. The virus then exploits the respiratory system in order to infiltrate the host. Despite the fact that the entire respiratory system is infected by the virus, the most affected region is the lower respiratory tract. The respiratory tract's columnar epithelial cells are the primary targets of the virus. The receptor binding site of HA is necessary for viral attachment to galactose-bound

sialic acid on host cell surface (Weis et al., 1988). This site is highly conserved among viral subtypes (Daniels et al., 1987). Within a few hours of successful infection in pulmonary epithelial cells, the virus begins to replicate itself and give rise to a large number of virions. By a process known as budding, infectious particles (virions) are selectively released from the apical plasma membrane of epithelial cells into the respiratory airways. Rapid infection of the nearby cells facilitates the virus in spreading throughout the lungs. Infection with influenza is frequently accompanied by hyperreactivity of the bronchial system, blockage of small airways, and decreased diffusion ability (Horner and Gray Jr, 1973; Hall et al., 1976; Little et al., 1978). Particularly in allergic disease, hyperreactivity and broncho-obstruction may last for a long time and may be caused by pro-inflammatory cytokines that prevents the induction of tolerance to aerosolic allergens (Tsitoura et al., 2000). Viral infection and replication halts host cell protein synthesis and induces apoptosis, thereby damaging the pulmonary epithelial cells (Katze et al., 1986; Sanz-Ezquerro et al., 1996).

Rarely viral pneumonia due to a severe form of alveolar inflammation occurs in human influenza infections. On the other hand, bacterial superinfection is more common in patients with human influenza, affecting elderly persons and is responsible for the deaths of the infected people. Damaged columnar epithelial cells caused by disruption of epithelial cell barrier, reduced mucociliary clearance, adhesion of bacteria and function change of neutrophils, increase the chance for bacterial infections of the respiratory tract (Levandowski et al., 1985; Mori et al., 1995).

1.8. Treatment strategy

1.8.1. Vaccination

World Health Organisation (WHO) suggests vaccination strains for the best regional efficacy in the northern (NH) and southern (SH) hemispheres based on the prevalent IAV subtypes (World Health Organisation, 2018a, 2018b). Despite the fact that India has access to both the NH and SH influenza vaccines, WHO has classified India as being in the tropical Asia (SH) southern hemisphere (Thakre and Patil, 2019) vaccination zone. The A/human/Michigan/45/2015 (H1N1)pdm09 strain replaced the A/California/07/2009 (H1N1)pdm09-like virus strain in the IAV vaccine from 2010 to 2016 to 2017 to 2019 in both hemispheres. The World Health Organisation has recommended A/human/Brisbane/02/2018 (H1N1)pdm09 for both hemispheres in 2020, replacing A/human/Michigan/45/ 2015 (H1N1)pdm09-like strain only for the northern hemisphere in 2019 (WHO, 2015a, 2015b,

2016a, 2016b, 2017a, 2017b, 2018a, 2018b, 2019a, 2019b). Additionally, Sanofi Pasteur introduced their first quadrivalent influenza vaccine (FluQuadri) in India in 2018. This vaccine has been found to offer those over three years of age widespread protection against IAV. It consists of the virus strains B/Colorado/06/2017 (B/ Victoria/2/87 lineage), B/Phuket/3073/2013 (B/ Yamagata/16/88 lineage), A/human/Michigan/45/2015 (H1N1) pdm09, A/Switzerland/8060/2017 (H3N2), and B/Colorado/06/2017 (B/ Victoria/2/87 lineage). Despite both live attenuated and recombinant vaccines being available in India, they have not been incorporated into the national immunization programme. The influenza vaccine has been recommended by the Ministry of Health and Family Welfare (MOHF&W) for the elderly (> 65 years), children (0.5-8 years), pregnant women, and healthcare professionals (Kant and Guleria, 2018);Dang and Sharma, 2020). Additionally, the Indian Academy of Paediatrics has advised influenza vaccination for all newborns in 2018–19. However, altogether, there is very little ($\approx 1\%$) influenza vaccination coverage in the low- and middle-income nations of Asia and Africa (Hirve and Organization, 2015;Palache et al., 2017).

The annual vaccine against seasonal influenza is the most crucial measure for preventing influenza and its serious consequences. Since the influenza virus has a high rate of mutation and is resistant to the immune system's ability to recognize new variants, new vaccines are created every year to keep up with the strains that are currently in circulation (Kilbourne, 2006;Glezen, 2008). Based on the global surveillance of influenza viruses in circulation and the global transmission of novel strains of the influenza virus, the influenza antigens to be included in the vaccines are chosen (Ang et al., 2016). The World Health Organization (WHO) suggested that the following virus antigens be included in quadrivalent influenza vaccinations for use during the 2023 southern hemisphere influenza season (Organization, 2008):

Egg-based vaccines

- an A/Sydney/5/2021 (H1N1)pdm09-like virus;
- an A/Darwin/9/2021 (H3N2)-like virus;
- a B/Austria/1359417/2021 (B/Victoria lineage)-like virus;
- a B/Phuket/3073/2013 (B/Yamagata lineage)-like virus.

Cell culture- or recombinant-based vaccines

- an A/Sydney/5/2021 (H1N1)pdm09-like virus;

- an A/Darwin/6/2021 (H3N2)-like virus;
- a B/Austria/1359417/2021 (B/Victoria lineage)-like virus;
- a B/Phuket/3073/2013 (B/Yamagata lineage)-like virus.

Recommended influenza strains for trivalent vaccines to be used in the 2023 southern hemisphere influenza season contain the following:

Egg-based vaccines

- an A/Sydney/5/2021 (H1N1)pdm09-like virus;
- an A/Darwin/9/2021 (H3N2)-like virus;
- a B/Austria/1359417/2021 (B/Victoria lineage)-like virus.

Cell culture- or recombinant-based vaccines

- an A/Sydney/5/2021 (H1N1)pdm09-like virus;
- an A/Darwin/6/2021 (H3N2)-like virus;
- a B/Austria/1359417/2021 (B/Victoria lineage)-like virus

The WHO emphasizes that vaccination is crucial for those who are at higher risk of serious influenza complications, with pregnant women receiving the highest priority, followed by children between the ages of 6 and 59 months, the elderly, people with certain chronic medical conditions (such as renal failure and diabetes mellitus), and then those at high risk (such as members of the medical profession) (Meerhoff et al., 2015). In contrast, the Advisory Committee on Immunization Practices (ACIP) of the United States expanded the recommendation for a yearly influenza vaccination in 2010 to include everyone 6 months of age and older who did not have any contraindications (Grohskopf et al., 2015).

How well the seasonal influenza vaccination can prevent influenza virus infections in a given population during an influenza season depends on the vaccine effectiveness of influenza vaccines (Ohmit et al., 2015). Recent evidence of antigenic drift from the vaccine strain in the majority of isolates taken into consideration has sparked worries that vaccine effectiveness may not be as good as it may be, particularly in older people or other high-risk populations. The 2022–2023 influenza season's preliminary findings from six European studies show that those who received the influenza vaccine for all ages experienced 27% and 50% and greater reductions for influenza A and B, respectively (Kissling et al., 2023). Thus, it was concluded

that influenza vaccinations are crucial for preventing serious illness in select high-risk populations. In light of this, the WHO advises seasonal influenza vaccines for the aforementioned populations each year, as vaccine can protect against multiple subtypes of Influenza virus.

1.8.2. Drug-based therapy

The recommended medications for the prevention of influenza are oseltamivir and zanamivir due to their proven efficacy and low rates of resistance compared to adamantanes (Li et al., 2015). This antiviral work well to prevent influenza in healthy people, people who are at high risk of influenza complications, and people who are residents of long-term care institutions. Oseltamivir and zanamivir have not yet been compared for effectiveness (Merritt et al., 2016). Some factors, such as preventing problems in patients at high risk and lowering the danger of increasing antiviral drug resistance, are taken into account when adopting an antiviral chemoprophylaxis strategy (Fiore et al., 2011). These factors include:

- Regardless of prior influenza vaccinations, senior residents in long-term care facilities should receive influenza prophylaxis during influenza epidemics.
- Unvaccinated people who have recently been exposed to someone who has the flu are at a high risk of developing complications.
- When there is a poor match between the vaccination and the viruses circulating in a particular year, antiviral prophylaxis should be used for vaccinated high risk individuals who have had close contact with an infected person during the past 48 hours.
- Antiviral chemoprophylaxis is advised for pregnant women and postpartum women who have close contact with people who are either suspected or proven to have influenza A. Due to its low systemic absorption, zanamivir may be the best medication for prophylaxis (Louie et al., 2015).

For the treatment and prevention of influenza, at least four antiviral medications are now available. The ability of the influenza virus to spread quickly in healthy immunocompetent people with intact immunity is noteworthy; as a result, the antiviral medications' ability to prevent viral replication is limited and has no practical impact. Additionally, no research has yet shown that antiviral medications that are started more than 48 hours after the onset of symptoms are useful. The first 24 hours of therapy are traditionally when the greatest impact is observed. For those who meet the following criteria and have influenza virus infection, treatment is advised for both adults and children (Harper et al., 2009):

- Within 48 hours of the onset of symptoms, those in high-risk groups with laboratory-confirmed or strongly suspected influenza virus infection.
- Regardless of underlying conditions, patients needing hospitalization for laboratory-confirmed or highly suspected influenza disease if treatment may start within 48 hours of symptom onset.
- Outpatients with a high risk of complications and a persistent illness, as well as outpatients who received a positive influenza test result from a sample collected more than 48 hours after the onset of symptoms.

Neuraminidase inhibitors (NAIs), especially oseltamivir and zanamivir, were frequently administered for patients with confirmed or suspected A H1N1pdm09 infection during the previous pandemic wave (Gasparini et al., 2014; Muthuri et al., 2014). Prior to the 2009-2010 pandemic, evidence of their usefulness in reducing mild symptoms of seasonal influenza was robust, but less so for lowering the incidence of pneumonia or improving its prognosis (Kaiser et al., 2003; Doshi et al., 2012; Hsu et al., 2012). Recent research showed that individuals with influenza-related pneumonia treated early (within 48 hours of disease onset) with an NAI had a roughly one-third lower risk of passing away or needing ventilator support than those treated later in the day (Muthuri et al., 2014). Influenza viruses are evolving quickly, as are the antiviral drugs that are now in the market. Oseltamivir-resistant infections that are sporadic as well as infrequent bouts of restricted transmission have been found. These drugs are not advised for use against influenza A virus-induced infections caused by the H3N2 and 2009 H1N1 strains of influenza A, which have developed adamantane resistance. However, neuraminidases like oseltamivir and zanamivir are still effective against the majority of influenza A and B virus strains, hence these medications are chosen for use in treating affected individuals. A recent study found that seasonal influenza A (H1N1) virus infections experienced the development of oseltamivir resistance 27% more frequently than seasonal influenza A (H3N2) virus infections or seasonal influenza B virus infections (Chen et al., 2011).

The majority of research have found that corticosteroid medication has a negative impact on outcomes associated to influenza. 37% to 55% of the patients admitted to ICUs in Europe during the 2009 influenza pandemic were treated with corticosteroids (Brun-Buisson et al., 2011; Linko et al., 2011; Diaz et al., 2012). However, despite significant limitations, a recent meta-analysis research found evidence from observational studies that corticosteroid medication for alleged influenza-related sequelae was linked to higher mortality (Rodrigo et al., 2015).

1.8.3. Immuno-therapy

Additional therapeutic options with a different mechanism of action have also been explored as treatment for people with severe influenza virus disease. For instance, a few mAbs directed against influenza virus proteins are now being tested for the prevention of human infections (Ramos et al., 2015). These monoclonal antibodies (mAbs) specifically target the M2 protein's (M2e) ectodomain. The highly conserved amino acid sequences of the M2e's domains among isolates from various subtypes of influenza A viruses make it an appealing target for influenza vaccines and therapeutic antibodies (Schotsaert et al., 2009).

Anti-M2e Ab-mediated protection's exact mechanisms are not yet known. Hemagglutination inhibition or in vitro viral neutralization abilities are not present in anti-M2 Abs (Jegerlehner et al., 2004). Human cells infected by viruses are thought to be the major target for the anti-M2e antibody since these cells highly express M2e on their surfaces (Mair-Jenkins et al., 2015).

1.9. Host-virus interaction

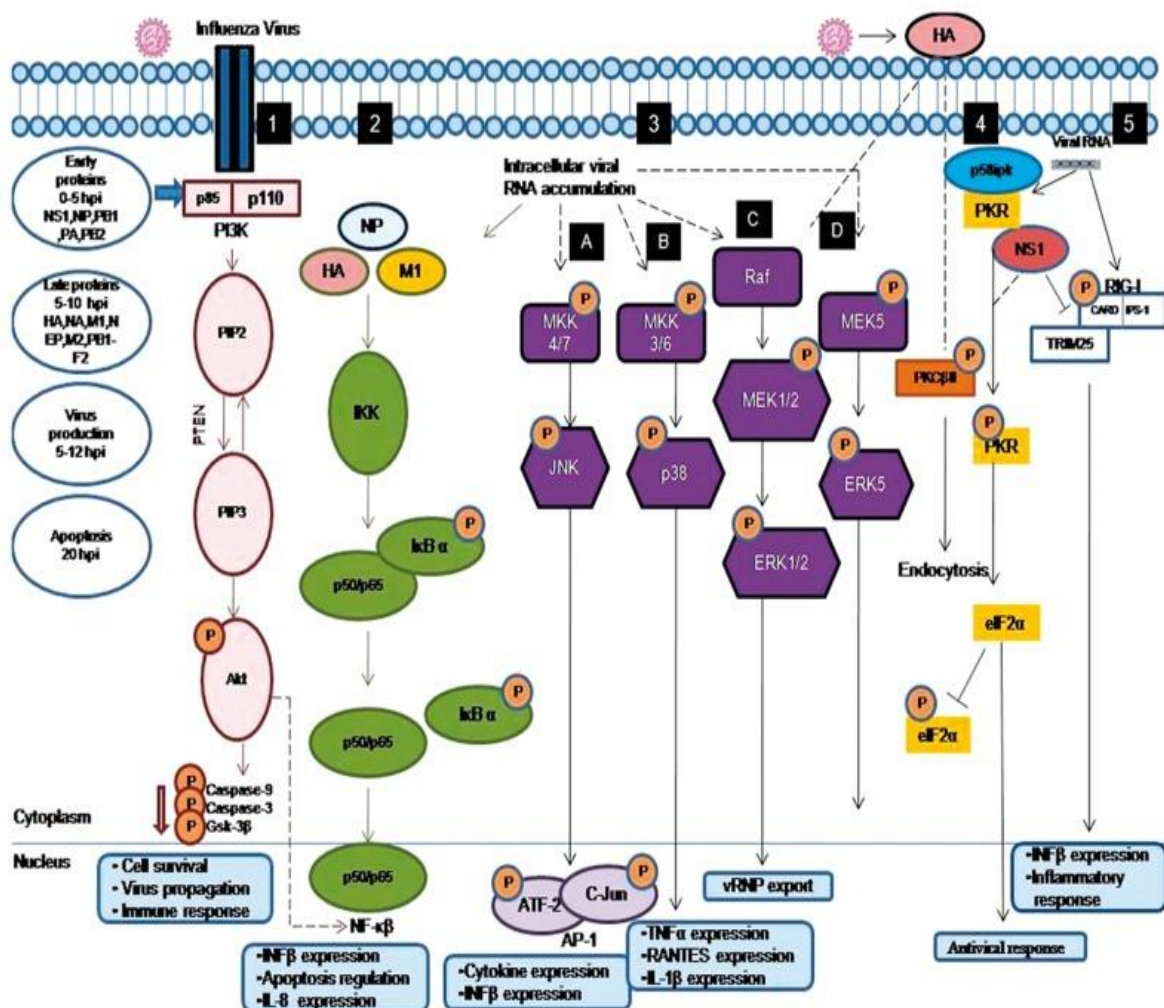


Figure 1.17: *Host cellular responses activated during influenza infection. Early proteins, including NS1, NP, PB1, and PB2, are synthesized within 0-5 hours post infection (hpi), whereas late proteins such as HA, NA, M1, NEP, M2, and PB1-F2 are produced between 5-10 hpi. This sequential protein synthesis process results in virus production occurring between 5-12 hpi, followed by cell apoptosis at 20 hpi. Throughout these processes, several pathways are known to be induced, including the PI3K-Akt pathway, NFκB/IκB pathway, MAPK pathways (A. JNK pathway, B. p38 pathway, C. ERK1/2 pathway, D. ERK5 pathway), protein kinase C (PKC)/PKR signaling, and TLR/RIG-I signaling (Gaur et al., 2011).*

All living things have created a variety of defence mechanisms to keep viruses and other foreign germs out. Although other host cells also have some immune defences against viral infection, the creation of neutralising antibodies and activation of cytotoxic T lymphocytes (CTL) or natural killer (NK) cells are necessary for a focused and efficient antiviral immune response. Type I IFNs are the main cytokines implicated in the antiviral response, despite the fact that other cytokines and chemokines are produced by various types of host cells during viral infection. Multiple IFN-isoforms, a single IFN- β , and additional members like IFN- ϵ , - κ , and so forth are all types of IFNs (Stetson and Medzhitov, 2006). In contrast to type II IFN (IFN- γ), which can only be produced by T cells and NK cells in response to viral infection, type I IFNs can be produced by all nucleated cells. IFN- λ 1, λ 2, and λ 3—type III IFNs—have also just lately been discovered (Kotenko et al., 2003). These IFNs share downstream signalling molecules and regulate the same genes despite having various receptors. IFNs perform a variety of tasks. In addition to inducing apoptosis in virus-infected cells and cellular resistance to viral infection, they also increase the expression of intrinsic proteins such TRIM5a, Fv, Mx, eIF20, and 2'-5' OAS (Samuel, 2001). Additionally, they cause the activation of the adaptive immune system and the activation of NK cells and dendritic cells (DC) (Le Bon and Tough, 2002). A germline-encoded PRR system that controls intracellular signalling controls the production of type I IFN and cytokine genes. These receptors identify microorganism-specific molecular patterns, such as the nucleic acids found in viral genomes. All living things contain nucleic acids like DNA and RNA, so being able to distinguish between self- and non-self nucleic acids is crucial, particularly in cases of virus infection. Recent advancements in the study of innate immunity have shown that PRRs, such as Toll-like receptors (TLRs), retinoic acid-inducible gene I (RIG-I)-like receptors (RLRs), and nucleotide-binding oligomerization domain (NOD)-like receptors (NLRs), are crucial for this discrimination (**Fig. 1.17**).

During viral infections such as influenza, host cells activate multiple signalling pathways. Some pathways trigger the host's innate immune response, while others facilitate virus

replication. These pathways include PRR-related signalling, protein kinase C (PKC), Raf/MEK/ERK, and phosphatidylinositol-3-kinase (PI3K)/Akt signalling. Understanding these interactions improves knowledge of influenza virus-host dynamics and aids in discovering new antiviral strategies. In summary, living organisms employ diverse defense mechanisms against viruses, including IFNs and innate immune receptors. Understanding the interplay between viruses and host cells enhances insights into viral infections like influenza, facilitating the development of novel antiviral approaches.

1.9.1. Double-stranded RNA (dsRNA)- activated protein kinase R (PKR) and downstream signalling

Activated PKR phosphorylates eukaryotic translation initiation factor 2 (eIF2) at the beginning of viral infection, inhibiting both cellular and viral protein synthesis (Balachandran et al., 2000; Garcia et al., 2007). PKR is a crucial element of innate immunity that functions in the early stages of host defence before IFN counteraction and the acquired immune response begin. Additionally, PKR has a role in the apoptosis that the influenza virus causes (Balachandran et al., 2000; Dai et al., 2011). In order to prevent PKR from activating and circumventing the cellular antiviral effects it causes, the influenza virus NS1 protein can directly attach to dsRNA or PKR (**Fig. 1.17**) (Lu et al., 1995; Li et al., 2006).

1.9.3. Toll-like receptors (TLRs) and downstream signalling

Type I integral membrane glycoproteins known as toll-like receptors (TLRs) are essential for early host defence against encroaching infections. There are now 11 TLR family members known to exist in mammals. The downstream molecules involved in the TLR family signalling cascades include MyD88, TAK1, TAB1, TAB2, TRAF6, and NF κ B (**Fig. 17**) (Diebold et al., 2004; Lund et al., 2004). Influenza A virus and dsRNA have been shown to positively influence TLR3 expression in lung epithelial cells (Guillot et al., 2005). The dsRNA and influenza A virus-induced activation of NF κ B and IRF/ISRE depend on the TLR/TRIF pathway (Guillot et al., 2005). For effective antiviral immunity in influenza-infected cells, mitogen-activated protein kinase (MAPK) family members, particularly Jun-N-terminal kinase (JNK) and p38 MAPK, play a critical role.

It has been established that the expression of numerous pro-inflammatory cytokines as well as the control of apoptosis depend on p38 MAPK and/or JNK (Kujime et al., 2000; Maruoka et al., 2003; Ludwig et al., 2006). Influenza Extracellular signal-regulated kinase (ERK) 1/2, JNK, and p38 are three members of the MAPK family whose phosphorylation is highly upregulated

by viral infection, which also increases interleukin (IL)-8 and RANTES production (Kujime et al., 2000). Recent research has revealed that the RSK2 MAPK-activated kinase also contributes to cellular antiviral responses. Viral RNA has been demonstrated to activate p38 MAPK and/or JNK, although it is yet unclear whether and how TLR interacts with these proteins. TLR2 expression is increased by influenza virus infection, according to certain *in vivo* tests, although its purpose is still unknown (Lee et al., 2006; Kajiya et al., 2008).

1.9.4. Retinoic acid-inducible gene-I-like receptors (RLRs) and downstream signalling

Another important receptor system for identifying RNA viruses is the retinoic acid-inducible gene-1-like receptors (RLRs). RLRs are made up of three people: LGP2, MDA5, and RIG-1. Important cytoplasmic viral RNA sensors like RIG-1 and MDA5 are crucial for antiviral innate defence. Different viral RNAs are recognised by RIG-1 and MDA5. They trigger the activation of IRF-3/7 and NF κ B, which results in the generation of IFNs and proinflammatory cytokines, together with the adaptor protein MAVS (Yoneyama and Fujita, 2007; Takeuchi and Akira, 2008; Barral et al., 2009). RIG-1 is regarded as the primary influenza regulator. In human lung epithelial cells, a virus promoted the expression of antiviral cytokines (Le Goffic et al., 2007) (**Fig. 1.17**). In influenza A virus-infected epithelial cells, overexpression of RIG-1 gene constructs dramatically increases IFN- β promoter-driven transcription.

1.9.5. Protein kinase C (PKC) and Influenza virus entry

A sizable family of serine/threonine kinases that are activated by a variety of extracellular cues includes Protein Kinase C (PKC). Receptor-mediated endocytosis has been demonstrated to be essential for the entrance of enveloped viruses (Constantinescu et al., 1991). When the influenza virus infects a cell, the hemagglutinin quickly activates PKC to aid entry into the host cell since PKC is crucial for maintaining the low pH in the endosome (Arora and Gasse, 1998).

1.9.6. Raf/MEK/ERK pathway and ribonucleoprotein (RNP) export

The MAPK cascade family includes the Raf/MEK/ERK signal transduction cascade. The development of ribonucleoproteins (RNPs) and nuclear export are critical phases in the life cycle of the influenza virus. Numerous investigations have shown that the Raf/MEK/ERK cascade is necessary for a successful nuclear RNP export (Pleschka et al., 2001). According to reports, the buildup of influenza virus hemagglutinin (HA) membrane and its close connection with the lipid-raft domain cause MAPK cascades to be activated by PKC- α activation and RNP export (Marjuki et al., 2006). The greater polymerase activity of influenza virus promotes HA

membrane accumulation, upregulating the MAPK cascade, and improving nuclear RNP-export along with viral generation (Marjuki et al., 2007) (Fig. 1.17).

1.9.7. Eukaryotic translation initiation factor 4e (eIF4E) and viral protein translation

The influenza virus has the ability to efficiently stop host cell protein production and translate viral RNA only in certain cells. The NS1 protein interacts with the 5'-terminal conserved regions of viral mRNAs to improve the start rate of translation of viral mRNAs (Park and Katze, 1995). The identification of poly (A) binding protein 1 (PABPI), eukaryotic translation initiation factor (eIF)4GI, and a component of the cap-binding complex eIF4F as cellular targets of NS1 supports the involvement of NS1 in protein translation (Burgui et al., 2003). eIF4F is attracted to the 5' UTR of viral mRNA by NS1's binding to eIF4GI, which also starts the translation of viral mRNA. During an influenza infection, eIF4E, a subunit of eIF4F, is dephosphorylated. The dephosphorylation of eIF4E, which may result in a reduction in its cap-binding ability, may be a factor in the suppression of cellular mRNA translation brought on by influenza viruses (Feigenblum and Schneider, 1993). A widespread suppression of translation initiation in virus-infected cells may result from activation of the interferon-induced kinase PKR, which phosphorylates the eIF2 α . The viral protein NS1 and cellular p58IPK (Protein Kinase Inhibitor p58) are both used by influenza viruses to limit PKR function in order to maintain a specific level of cellular protein translation (Katze, 1995; Goodman et al., 2007). The expression of the viral genes within influenza viruses is temporally regulated (Shapiro et al., 1987; Hatada et al., 1989). While HA, neuraminidase, and matrix protein (M1) are largely expressed in the late stages of infection, nucleoprotein (NP) and NS1 protein are extensively abundant in the early stages. The 5' UTR of influenza virus mRNAs may be crucial for this translation control, according to the theory that viral mRNA translation efficiency is controlled. But the precise mechanisms are still unknown (Yamanaka et al., 1991).

1.9.8. Phosphatidylinositol-3-kinase (PI3K)/Akt signalling pathway and viral infection

During acute and persistent infections, viruses exploit PI3K/Akt signalling to delay apoptosis and extend viral replication. The viral NS1 protein directly binds to the p85 β regulatory subunit in influenza A virus-infected cells, activating PI3K and causing the PI3K-dependent phosphorylation of Akt (Hale et al., 2006; Hale and Randall, 2007; Shin et al., 2007a; Shin et al., 2007b; Hale et al., 2008a). Caspase 9 is phosphorylated by Akt directly. Akt additionally phosphorylates and inactivates the apoptosis modulator Glycogen Synthase Kinase (GSK)-3 β . As a result, increased Akt signalling prevents virally-induced apoptosis (Ehrhardt et al.,

2007;Shin et al., 2007a). Through the p53-dependent pathway, Akt signalling furthermore prevents influenza-infected cells from undergoing rapid apoptosis. According to a recent study, the PI3K/Akt pathway inhibits JNK-dependent, Bax-mediated apoptosis during influenza A virus infection by negatively regulating the JNK pathway through ASK1 (Lu et al., 2010). Before influenza A virus NS1 protein was revealed to stimulate PI3K/Akt signalling and facilitate effective viral multiplication by blocking apoptotic signalling. Reports reveal that dsRNA activates PI3K, which activates transcription factor IRF3. On inhibiting PI3K signalling, IRF3 dependent promoter activity is reduced and IRF3 dimerization is hindered (Ehrhardt et al., 2006).

1.9.9. Evasion of innate immune response by Influenza virus

IFN gene expression and other innate immune responses are induced by influenza infection, but influenza viruses have developed a variety of ways to circumvent host defences. Non-structural proteins are crucial to these procedures. The most significant non-structural protein of the influenza virus is non-structural protein 1 (NS1), a viral antagonist of IFN production and its downstream effects (Hale et al., 2008b). In order to prevent pattern recognition receptors (PRRs) from recognising dsRNA, NS1 binds to it (Lu et al., 1995;Talon et al., 2000;Li et al., 2006). Additionally, NS1 disrupts viral ssRNA that has free 5' triphosphate groups, a pattern that PRRs can detect (Ehrhardt et al., 2010). Additionally, it was noted that NS1 directly binds to RIG-1 to impact viral RNA recognition, which in turn inhibits the generation of IFN- β (Guo et al., 2007;Mibayashi et al., 2007;Opitz et al., 2007). According to reports, NS1 can also specifically inhibit TRIM25-mediated RIG-1 ubiquitination and decrease RIG-1 signalling (Gack et al., 2009). Additionally, type I IFN production can be suppressed by NS1's interaction with molecules involved in type I IFN transcription and translation (Nemeroff et al., 1998).

Another influenza virus non-structural protein, the PB1-F2, serves a number of purposes in influenza virus infection. Apoptosis brought on by the flu virus can be impacted by PB1-F2. According to reports, PB1-F2 causes increased sensitivity to influenza virus-induced apoptosis by localising in the inner and outer mitochondrial membranes (Conenello and Palese, 2007). According to reports PKC-mediated PB1-F2 phosphorylation boosts the induction of apoptosis in monocytes and may be brought on by PB1-F2's interaction with the mitochondrial membrane proteins ANT3 and VDAC1 (Mitzner et al., 2009). Through perforations in the mitochondrial membrane, this contact causes the release of cytochrome C (Zamarin et al., 2005). The results of earlier reported animal tests suggest that PB1-F2 is crucial for the pathogenicity of influenza

virus (McAuley et al., 2007). In infected lungs, PB1-F2 can increase the expression of cytokines. The interaction between PB1 and PB1-F2, which results in increased viral polymerase activity and viral RNA accumulation in the infected cells may have caused this upregulation (Mazur et al., 2008).

1.9.10. Influenza virus induced apoptosis

A case of the flu Both Fas-mediated processes and Fas-independent signals, such as the creation of the FADD/caspase-8 complex by protein kinase R (PKR), which starts a caspase cascade, mediate a virus-induced apoptosis. IFN induces and dsDNA activates PKR, a crucial regulatory element in numerous apoptotic pathways (Brydon et al., 2005). Influenza promotes transforming growth factor (TGF)- β via viral neuraminidase as a third pathway to apoptosis. NA helps TGF- β cleave into its active form, which activates latent TGF- β on the cell surface. TGF- β triggers a signalling cascade that activates the c-Jun N-terminal kinase (JNK) or stress activated protein kinase (SAPK), which in turn activates transcription factors and increases the production of genes that promote apoptosis. This route, together with the effects of PB1-F2 on the stability of the mitochondrial membrane (Chen et al., 2001), has been linked to the death of lymphocytes and may be the cause of the lymphopenia seen after acute infection. According to Influenza reports 2006 (Kamps et al. 2006), cellular oxidative stress, the production of reactive oxygen species (ROS), and the induction of nitric oxide synthetase-2 which results in the formation of toxic reactive nitrogen intermediates have all been linked to lung tissue injury after infection with the influenza virus.

1.10. Host-targeted antivirals

1.10.1. Antivirals targeting host cytokine signalling pathway

The Type I IFN system serving the vertebrates class is a welcome solution that stands the breeding of various viruses across diverse taxons. In reverse order, viruses have been working out within humans, discovering various tricks to vanish behind an immune defense and breaking a plan produced by IFN of the host.

Inhibitor	Target	Virus
Quercetin (Johari et al., 2012; Rojas et al., 2016)	TNF- α -mediated activity	JEV, HCV
Intron A, Rebeton, Rebetol, pegintron/Sylatron, and Pegasys (Patel et al., 2014)	IFN-mediated activity	HCV
Azithromycin (Bagheri et al., 2021)	Upregulation of IFN type I Signalling	JKV, SARS-CoV2
PF-04878691 or 852A (Patel et al., 2014)	Agonist of TLR7/8	HCV
Mycophenolic Acid (Bagheri et al., 2021)	Upregulation of ISGs	MERS
Gefitinib (Bagheri et al., 2021)	NF κ B pathway	DENV
Ribavirin (Bagheri et al., 2021)	Enhances IFN- α -JAK/STAT signalling pathway	HCV
Berberine (Bagheri et al., 2021)	Enhances the production of IFN- γ by stimulating IL-12 secretion and inhibiting IL-6 production	CHIKV, SARS-CoV, HCV

1.10.2. Antivirals targeting host glycosylation pathway

Glycosylation, a widespread post-translational modification, plays essential roles in biology. Viruses exploit the host's glycosylation machinery during replication, utilizing the endoplasmic reticulum (ER) for various life cycle stages (Frabutt and Zheng, 2016; Ravindran et al., 2016). N-linked glycosylation begins at the ER membrane, where precursor tetradecasaccharides assemble and attach to nascent polypeptides (Watanabe et al., 2019). Enzymes in the ER and Golgi modify these precursors to form diverse glycans (Ravindran et al., 2016). Some viruses, such as HCV, bypass Golgi glycan maturation, leading to early budding and translocation to the plasma membrane. Others may deviate from the secretion pathway due to unique viral glycoprotein glycans (Bayer et al., 2016). Host glycans serve as receptors, co-receptors, or

attachment factors depending on the virus (Inoue and Tsai, 2013). This intricate interplay between viruses and host glycosylation pathways underscores the importance of glycosylation in viral replication and pathogenesis.

Virus	Target	Inhibitors
SARS-CoV-2 (Yang et al., 2020; Yao et al., 2020)	N-Glycans ER α -glucosidase I α -mannosidase inhibitors α -glucosidase inhibitors	Peptide-N-Glycosidase F (PNGase-F) Iminosugars Miglustat, Celgosivir and NN-DNJ Deoxymannojirimycin, mannostatin A N-butyl deoxynojirimycin, N-nonyl deoxynojirimycin, castanospermine, celgosivir
ZIKV (Mohd Ropidi et al., 2020)	Sec61 α translocon	Myolactone treatment
DENV (Courageot et al., 2000)	α - Glycosidase	Castanospermine (CST) and deoxynojirimycin (DNJ)

1.10.3. Antivirals targeting host nucleoside synthesis pathway

Viruses take advantage of host nucleosides for replication through host machinery to produce new virus particles. Targeting the host enzymes for nucleoside synthesis is a promising tactic for antiviral agents. Inosine monophosphate dehydrogenase (IMPDH) and dihydroorotate dehydrogenase (DHODH) are the key enzymes involved in this process. Ribavirin, a broad-spectrum antiviral, prevents guanine synthesis, and is usually combined with PEGylated interferon- α for chronic HCV treatment (Cornberg et al., 2002). Immunosuppressant mycophenolic acid suppresses CHIKV replication by depleting intracellular GTP reservoirs which strongly support the idea of nucleotide pool depletion as a possible antiviral approach, especially against flaviviruses (Khan et al., 2011). DHODH inhibition with immunosuppressant brequinar inhibits DENV serotypes (Madak et al., 2017). DHODH inhibition by NITD-982 analogue, nevertheless, is cells affected by dietary pyrimidines. Such compounds as 6-azauridine provide for the suppression of virus replication through the

depletion of UTP pools due to competitive inhibition of OMP (orotidine monophosphate decarboxylase) (Levine et al., 1980). Atovaquone, which is an antiparasitic drug, stops *de novo* pyrimidine synthesis and displays dose-dependent chikungunya virus (CHIKV) replication inhibition. These results outlined the possibility of the nucleotide synthesis as a broad-spectrum anti-viral strategy (Abdelnabi and Delang, 2020).

1.10.4. Antivirals against heat shock proteins (Hsp)

Another broad-spectrum antiviral drug target of great interest is the native cellular protein homeostasis (stress response) pathway controlled by various molecular chaperone, which control many cellular processes like protein translation, correct folding, degradation, apoptosis, cell cycle regulation and intracellular trafficking (Lahaye et al., 2012;Taguwa et al., 2015). Chaperones proteins like Hsp70 and Hsp90 are reported to play pivotal roles in life cycle of viruses like IAV, DENV, HCV, CHIKV, etc. Hsp inhibitor, quercetin, attenuates HCV and IAV replication, geldanamycin and SNX-2112 reduces CHIKV viral titres and HS-72 inhibits DENV entry (Cabrera-Hernandez et al., 2007;Gonzalez et al., 2009;Manzoor et al., 2014;Rathore et al., 2014;Howe et al., 2016).

1.11. Minocycline: antiviral potential of an antibiotic

As a second-generation, semi-synthetic tetracycline with antibacterial activity against both gram-positive and gram-negative bacteria, minocycline has been used therapeutically for more than 30 years. It is primarily used to treat various sexually transmitted infections including acne vulgaris. This tetracycline derivative interacts with the 30S ribosomal subunit, thereby preventing the synthesis of bacterial proteins. Side effects related to long term use include yellow to gray-brown discoloration of teeth, skeletal growth retardation, renal toxicity, photosensitivity and hyperpigmentation of nose, hands and feet, epigastric burning, nausea, vomiting, anorexia, diarrhea, hearing loss, visual disturbances, lightheadedness, dizziness. Rare but fatal hepatotoxic effects are present.

1.11.1. Antiviral potential of minocycline against viruses of public health importance

Minocycline has an antiviral impact on all four of the virus' serotypes of Dengue Virus (DENV). It reduces DENV infection by inhibiting infectious virus generation, intracellular viral protein synthesis, and viral RNA synthesis. The phosphorylation of ERK1/2 is linked to increased pathogenesis and organ damage in DENV infection. Treatment with minocycline decreases the phosphorylation (Sreekanth et al., 2014). Similar to Hepatitis C virus (HCV)

infection where ERK signalling has been reported to suppress the expression of antiviral genes, reduction of DENV-induced ERK1/2 phosphorylation by minocycline increased the mRNA expression of antiviral genes such 2'-5'-oligoadenylate synthetase 1 (OAS1), OAS3, and interferon (IFN α) (Zhang et al., 2012; Leela et al., 2016).

Minocycline plays a role in down-regulating proinflammatory cytokines (Nikodemova et al., 2006). Recent studies show that in Japanese Encephalitis Virus (JEV) infection, active microglia release proinflammatory mediators that cause neuronal death (Ghoshal et al., 2007). Therefore, minocycline is a very effective neuroprotective drug against JEV. This neuroprotective property is associated with reduction in (i) viral titre, (ii) active caspase 3 activity, (iii) proinflammatory cytokines, (iv) neuronal death and (v) microgliosis (Mishra and Basu, 2008). Thus, minocycline serves as a potential new therapeutic for preventing the neurological impediment of JEV.

Minocycline has been shown to significantly reduce viral titre in the cerebrospinal fluid, diminish viral RNA in the brain and reduces the extremity of the disease caused by Human Immunodeficiency virus (HIV). In primary human lymphocytes, minocycline also reduced p38 activation and HIV replication, suggesting that it functions through influencing CD4⁺ T cells, the main host cell for HIV infection (Szeto et al., 2010). In-vivo studies reveal that minocycline alters cell signalling in order to modulate cellular activation and proliferation. It is hypothesized that treatment with minocycline might inhibit HIV replication by modulating the activation state of the host (McDougal et al., 1985; Copeland, 2005). It is also noted that minocycline alters activation of T cell resulting in change of expression of T cell activation (CD25)/proliferation (Ki-67) markers and cytokine secretion (IL2, IFN γ , TNF α), which are critical for activation pathways that regulate HIV replication (Szeto et al., 2010).

Minocycline has been proved to be antiviral against West Nile Virus (WNV). Minocycline not only inhibits replication of WNV but also inhibits activation of caspase-3 and PARP cleavage (markers of apoptosis) (Michaelis et al., 2007). WNV is known to induce apoptosis in infected neuronal cells (Harris and Johnson, 2001; Whitfield et al., 2001). Inhibition of WNV-induced apoptosis, protects the neuronal cells. Minocycline exhibits neuroprotective property by suppressing JNK signalling, thereby stalling the pro-apoptotic role of JNK signalling in neurons (Michaelis et al., 2007).



Chapter 2

Materials and methods

2.1. Collection of clinical nasal and throat swab samples

Nasopharyngeal and/or throat swab samples were collected from patients hospitalized with severe acute respiratory illness (SARI) in eastern India, during the period from April 2017 to March 2019. The sample collection vials containing viral transport media (VTM) were accordingly labelled with sample number and date. A cotton swab was inserted in the nose and/or throat of patient and withdrawn in a circular motion. Swabs were dipped in VTM and transported to the laboratory maintaining cold chain (Agrawal et al., 2009).

2.2. Cell line maintenance and isolation of influenza virus

2.2.1. Maintenance of MDCK and A549 cell lines

The Madin-Darby canine kidney (MDCK) and African green monkey fibroblasts (Vero) were cultured in minimal essential medium (MEM) and human epithelial (A549) and Human embryonic kidney (HEK293) cell lines were maintained in Dulbecco modified Eagle medium (DMEM) supplemented with 10% fetal bovine serum (FBS) and 1% antibiotic-antimycotic solution (Gibco, Life Technologies). Cells were maintained in 5% CO₂ at 37°C in humidified incubator.

2.2.2. Influenza virus infection and harvesting

The prototype human Influenza A/H1N1 strain [A/Puerto Rico/8/1934 (H1N1)], Influenza A H3N2 strain (gifted by ICMR- NIV, Pune) and A/California/04/2009 (H1N1)pdm09 denoted as IAV/PR8, IAV/H3N2 and IAV/CAL, respectively, were used in this study. Prior to infection, viruses are activated using TPCK-treated trypsin (500µg/ml) at 37°C for 1 hr. Viruses are added to cells and allowed to adsorb for 1 hr at 37°C. Cells are washed with media thrice to remove the unbound viruses. The time of removal of virus is considered as 0 hours post infection (hpi) for all the experiments. At various time-points cells are freeze-thawed for cell lysis, supernatant containing the virus are harvested and titrated by hemagglutination (HA) assay. In all experiments, DMSO (≤0.25%) was added to the mock infected control to rule out any effect of DMSO.

2.2.3. Cryopreservation of MDCK and A549 cells

Cells were trypsinized and resuspended in complete media, centrifuged at 300g for 5 mins. The pellet was resuspended in freezing medium comprising of MEM, 10% DMSO, % FBS at 5-10 X 10⁶ cells/ml. Cryovials are labelled with the cell line, date of storage and passage number and the cells are aliquoted into each vial. Cells are allowed to freeze at 1°C/min in programmable coolers in a -80°C freezer. After 24-48 hrs they are shifted to liquid nitrogen storage.

2.2.4. Influenza virus infection *in vivo* and Ethics statement

BALB/c mice aged 4-6 weeks were orally administered with minocycline (5, 15, and 30 mg/kg/day) for 5 days to assess toxicity. Survivability, body weight changes, and histological alterations in vital organs were monitored. Non-toxic dose of minocycline (30 mg/kg/day) was administered from day 2 to 15 after intranasal inoculation with IAV/PR8 (4 x 50% mouse lethal dose) and body weights were measured. Another group was infected with IAV/PR8 and treated with minocycline (30 mg/kg/day) or DMSO (vehicle control), or ribavirin (70 mg/kg/day) from day 2 to day 4. On day 5, mice were sacrificed, and viral titers were determined by HA assay. Expression of viral protein NS1 and RNA (M1 gene) in lung homogenates was quantified by western blot and quantitative Real-time PCR, respectively. Lung samples were fixed, sectioned, and stained with haematoxylin and eosin (H&E). Images were captured using an EVOSTM XL Core microscope (magnification, x10 & x40; Invitrogen, Thermo Fisher Scientific). Each experimental condition involved three-five mice per group. All the experiments were performed according to national regulations and approved by the institutional animal ethics committee (PRO/200/June 2023-26).

2.3. Extraction of RNA by QIAamp method

Viral RNA was extracted from clinical samples using commercially available QIAamp viral RNA Mini Kit (Qiagen, GmbH, Hilden, Germany) according to manufacturer's protocol with minor modifications.

250µl of clinical sample was added to 560µl of AVL buffer containing carrier RNA in a micro centrifuge tube (MCT) and incubated at room temperature (RT) for 10mins. 560µl of absolute ethanol was added to the above mixture. The mixture was then added to QIAamp spin columns and centrifuged at 8000rpm for 1 min. The filtrate in the collection tubes is discarded, collection tubes were replaced with the fresh ones, 500µl of AW1 buffer was added to the spin columns. Columns were centrifuged at 8000rpm for 1 min, collection tubes were discarded and replaced with new ones, 500µl of AW2 was added to each column. The spin columns were centrifuged at 14000rpm for 3 mins and placed into new collection tube. Columns were further centrifuged at 14000rpm for an additional 1min to remove the residual buffer. Columns are finally placed in new 1.5µl MCTs, 50µl of EB buffer was added directly to the column membrane and allowed to incubate for 5 mins at RT. Columns are centrifuged at 8000rpm for 1 min to collect the eluted RNA. They are stored at -80°C for future use.

2.4. Reverse Transcription-Polymerase Chain Reaction (RT-PCR)

Since Influenza virus is a ssRNA virus, complementary DNA (cDNA) from ssRNA was prepared by reverse transcription reaction prior to PCR amplification. Only positive samples were processed further.

Materials

1. Isolated ssRNA
2. 5X RT buffer
3. Random Hexamer (Invitrogen™, CA)
4. dNTP mix
5. RNase inhibitor/ Ribolock
6. Revertaid
7. Nuclease-free water (Promega, WI)
8. DTT (Dithiothretol) (Invitrogen, USA)
9. Dream Taq Polymerase
10. Dream Taq Buffer
11. Agarose (Sigma-Aldrich®)
12. 5X DNA loading buffer (BIO-RAD Laboratories, CA)
13. Ethidium bromide (10mg/ml; Sigma-Aldrich®) [EtBr]
14. 1kb DNA ladder (BIO-RAD Laboratories, CA)
15. Primers for HA and NA genes amplification as listed below

Name of the gene	Name of the primer	Sequence of the primer
NA	NA1F	5'-ATG AAT CCA AAC CAA AAG-3'
	NA1R	5'-CTG ATT TGA CTA TCT TTC CC-3'
	NA2F	5'-TGT AAA ACG ACG GCC AGT AAT GGR CAR GCC TCR TAC AA-3'
	NA2R	5'-CAG GAA ACA GCT ATG ACC AGT AGA AAC AAG GAG TTT-3'
HA	HA1F	5'-AGC AAA AGC AGG GGA AAA TAA AAG C-3'

	HA1R	5'-ACA TGC TGC CGT TAC ACC TTG GTT-3'
	HA2F	5'-TTC CCC AAG ACA AGT TCA TGG CC-3'
	HA2R	5'-TAA CCG TAC CAT CCA TCT ACC AT-3'
	HA3F	5'-AGA GGC CTA TTT GGG GCC AT-3'
	HA3R	5'-CTC ATG CTT CTG AAA TCC TAA TG-3'

2.4.1. Reverse transcription reaction

- Template mixture was prepared with 500ng of isolated viral ssRNA, 1µl of random hexamer (300ng/µl) and volume made up to 13µl with nuclease-free water.
- The prepared template mixture was denatured at 65°C for 5 mins in a thermal cycler (StepOnePlus™ Real-Time PCR System), followed by snap chilling on ice for 5 mins, thereby enabling the primers to anneal to the RNA.
- The reaction mixture for reverse transcription was prepared in a micro-centrifuge tube which consisted of 4µl of 5X RT buffer, 1µl of dNTP mix, 1µl of DTT, 0.5µl each of Ribolock and Revertaid.
- The reaction mixture was added to the template mixture, briefly vortexed and centrifuged. The tubes were then placed in thermal cycler and the program was set as following:
 - 25 °C for 10 minutes
 - 42 °C for 45 minutes
 - 60 °C for 15 minutes
 - Hold at 4 °C
- The cDNAs recovered after the cycle were immediately used for PCR amplification or stored at -20 °C until further needed.

2.4.2. Amplification of viral genes by polymerase chain reaction

Viral genes like HA, NA or M1 were amplified by PCR assays using the specific consensus primers. The PCR reaction includes a brief denaturation step at 95°C, followed by cooling to 45-65°C for the primers to anneal to its complementary sequences. This is followed by heating

at 72°C for the polymerisation activity of Taq DNA polymerase. This cycle is repeated for another 34 cycles, where the PCR products accumulate exponentially with each round of amplification.

2.4.3. Agarose gel electrophoresis

1.5µl of loading dye (Bromophenol Blue) was mixed with 10µl of PCR amplified product and loaded onto 1.5% agarose gel containing EtBr. 2µl of 1kb ladder was loaded in parallel with the samples, in order to compare and estimate the length of the PCR products. Gels were run in submarine gel apparatus (BIO-RAD Laboratories, USA), immersed in 1X TAE buffer at 100V for approximately 90 minutes. Amplification was confirmed when gels were placed in Gel Doc XR system using Quantity One[®] software version 4.6.3 (BIO-RAD, USA).

2.5. Real-time Polymerase Chain Reaction (Real-time PCR)

One-step RT-PCR was conducted using CDC approved primer set in Influenza detection kit (Applied Biosystems). For RT-PCR using cDNA, PowerUp[™] SYBR[™] Green Master mix, nuclease-free water, and gene specific forward and reverse

Primers were subjected to the following cycle for amplification in StepOnePlus[™] Real-Time PCR System: 50°C for 2 minutes, 95°C for 10 minutes, 40 cycles of 95°C for 15 seconds and 60°C for 30 seconds, and 72°C for 10 minutes). The relative gene expressions were normalized to 18s rRNA using the formula $2^{-\Delta\Delta CT}$ ($\Delta\Delta CT = \Delta CT_{\text{Sample}} - \Delta CT_{\text{Untreated control}}$), where CT is the threshold cycle. Relative change in expression of viral RNA in inhibitor treated cells was represented as “Relative expression of viral RNA (%)” considering expression of viral RNA in DMSO treated control cells as 100%.

2.6. Sequencing PCR and precipitation of sequencing PCR product

Applied Biosystem's ABI Prism 3100 Genetic Analyzer and Big Dye Terminator Cycle Sequencing Kit version 3.1, Foster City, CA, USA were used to sequence purified PCR products of influenza virus strains using the chain termination method. The sequencing reactions used a slightly modified version of Sanger's dideoxy chain termination technique. The dNTP, thermostable DNA polymerase, dye terminators, MgCl₂, and buffer were combined together and placed in a single tube. The four terminators can be identified in a single tube and one lane of the polyacrylamide gel since they are marked with four separate acceptor dyes. Ethanol precipitation is used to eliminate unincorporated dye terminators from the sequencing reaction. Using electrokinetic injection at 320 volts/cm samples were electrophoretically separated as they passed through the polymer POP-6 (Performance Optimized Polymer-6, Perkin Elmer, Applied Biosystems, CA, USA) in capillaries and using the seq POP6 RAPID E run module with the DTPOP6 (BD Set-any primer) mobility file. Using the ABI prism 3100

data collection software, base sequence data were created from the sample fluorescence spectra (PE, Applied Biosystems, USA). The ABI prism DNA sequencing analysis software (Perkin Elmer, Applied Biosystems, California, USA) was used to examine the raw sequencing data. To approximately 50-100ng of sample DNA 2 µl of sequencing reaction mix, 1 µl of sequencing buffer, 3.5 pmoles of primer and 10 µl final volume was made with double distilled water. The reaction mixture was subjected to the following program was used for the sequencing PCR: 96°C for 2 mins, 96°C for 15 secs, 50°C for 5 secs, 60°C for 4 mins and storage at 4°C in a thermal cycler (Applied Biosystems 7600, USA).

Ethanol precipitation of sequenced PCR products

Before the precipitation step, the sequence PCR products were kept on ice.

- To 10µl of the sequencing PCR product, 5µl of 3 M sodium acetate buffer (pH 4.6), 50µl water, 2µl of 125 mM EDTA (Sigma, USA), and 125µl of 100% ethanol (Sigma, USA) were added.
- The mixture was pulsed down in a micro-centrifuge at room temperature after being vortexed for 30 seconds followed by snap chill on ice for 15 minutes.
- The samples were centrifuged at 13,000 rpm for 20 min at 4°C and the supernatant was discarded.
- The pellet was resuspended in 200µl of pre-chilled 70% ethanol and centrifuged at 13,000 rpm for 20 min at 4°C following which the supernatant was aspirated.
- The tubes were placed in a desiccator under vacuum for five minutes at 45°C after the leftover fluid was aspirated out of them (Eppendorf concentrator 5301, Germany).
- After the tubes had dried completely, they were refrigerated at -20°C until they were added into an automated sequencer.
- 19µl of Hi-Di formamide was added to the precipitated DNA at room temperature, and the dry pellets were vortexed.
- The DNA was first denaturized at 95°C for two minutes, and then it was quickly snap-chilled on ice. Utilizing the ABI PRISM® DNA Sequence Analysis Software, raw sequencing data was analysed (PE Applied Biosystems, CA, USA)

2.7. GenBank accession numbers for nucleotide sequences

The HA and NA genes sequences were submitted to NCBI GenBank under accession numbers MN508837 to MN508844, MN508846 and MN508847, MN508849 to MN508863, MN508971 to MN508995.

2.8. Bioinformatics tools for sequence data annotation

2.8.1. Sequence analysis

The National Centre for Biological Information's (NCBI) public domain nucleotide database was searched with the Basic Local Alignment Search Tool (BLASTN version 2.8.1+) (Altschul et al., 1997). Gapped setting, non-redundant databases, expectation value of 10, SEG algorithm filtering of low-complexity regions, and BLOSUM62 (gap existence cost = 11, per residue gap cost = 1, lambda ratio = 0.85) substitution matrix were the default parameters utilised for the sequence alignment.

2.8.2. Construction of Phylogenetic tree and its analysis

MEGA (Molecular Evolutionary Genetics Analysis, version 7) was used to conduct evolutionary analyses where the phylogenetic trees were deduced using the maximum-likelihood statistical technique (Saitou and Nei, 1987). The standard software NCBI (National Institutes of Health, Bethesda, MD) and BLAST (Basic Local Alignment Search Tool) was used to perform the nucleotide and protein sequence BLAST analyses. Using the TRANSEQ software (Transeq Nucleotide to Protein Sequence Conversion Tool, EMBL-EBI, Cambridgeshire, UK), amino acid sequences were derived from nucleotide sequences and LALIGN (EMBnet, Swiss Institute of Bioinformatics, Switzerland), DDBJ, and CLUSTAL Omega tools were used to align the DNA sequences. Each operational taxonomic unit (OTU) was examined at each nucleotide or amino acid location to create the phylogenetic trees.

In the current work, the p-distance was employed to calculate the distance needed to build phylogenetic trees. It is the proportion of nucleotide sites where the two nucleotide sequences under comparison continue to differ. To determine this, the total number of nucleotides differences was divided by the total number of nucleotides compared. Therefore, when the distances between the compared nucleotide sequences were small, p-distance yields results were similar to those estimated by other methods (Kumar et al., 2004). To verify accuracy, the discrete character approach and the distance method were both used. Prior to constructing phylogenetic tree, model testing was performed and suitable model was used to calculate the evolutionary distances.

2.9. Cytotoxicity assay

2.9.1. Crystal Violet (CV) assay

Seeding of MDCK cells was done into 48-well tissue culture plates, and then allowed to incubate for 24 hours at 37°C in CO₂ at 5%. Following this, the media was removed. Controls were established, including a cell-only control (CC), virus control (VC), and drug control (DC). Except for CC and DC, 30µl of 256 HA units/ml virus was added to each well and incubated for 1 hour. Various dilutions of drug compounds were added to treatment cells and to control

cells (CC, DC, and VC) serum-free media were added. The plates were then further incubated for 1-2 days until cytopathic effects (CPE) were observed. After incubation, the media was aspirated, and cells were washed with 1X PBS. 0.5% crystal violet staining solution, added to each well, and incubated at room temperature on a bench rocker for 20 minutes. After incubation, the plates were rinsed using tap water to get away with the unbound dye and air dried at room temperature. Subsequently, 300µl of absolute methanol was added to each well and incubated at room temperature in shaking condition for 20 minutes. Optical density was measured at 570 nm. The percentage inhibition ratio in wells corresponding to treated cells was calculated and compared with CC. the results were plotted against the concentration of the molecule. EC₅₀ values determination was carried out with the help of linear regression in Microsoft Excel software. The experiment was conducted in triplicates for each candidate molecule.

2.9.2. MTT assay

To determine the cytotoxic effects of chemical inhibitors and small molecules, MTT assay was conducted. Cells were infected with IAV and/or treated with DMSO or inhibitors and incubated for 72 hours, following which approximately 200µl each of MTT reagent (5mg/ml) and media were added to each well of the 24-well plate. The cells were incubated at 37°C for 3 hours in dark. Purple formazan crystals were formed by the enzymatic reduction of MTT via mitochondrial dehydrogenases in actively replicating cells. Following incubation, these purple crystals were dissolved in 600µl MTT solvent (4 mM HCl, 0.1% NP-40 in isopropanol). Optical density (OD) of the solution was measured at 570 nm and cell viability was calculated using the formula $(OD_{\text{Sample}} - OD_{\text{Blank}}) \times 100 / (OD_{\text{Control}} - OD_{\text{Blank}})$. Cell viability was represented as “% viability” considering cellular viability of control cells as 100%.

2.10. Hemagglutination test (HA)

Hemagglutination test is a type of immunoassay, done to estimate the presence and titre of Influenza virus present. Here erythrocytes are used as carrier particles. 50µl of PBS (pH 7.2) was added to each well, except the first column, of a labelled U-bottom 96 well microtitre plate. 100µl of viral supernatant (antigen) was added to the first well of row and serially ½ dilution was done across each row till the 11th column of each row. Remaining 50µl was discarded from the 11th column. 50µl of 1% chicken RBCs was added to each well and gradually mixed by agitating the plate. The plate was left undisturbed at room temperature for 60 minutes. The RBCs will either form a ring/button or will show agglutination (hemagglutination) at the bottom of the well. The ring or button formation was denoted as “O” and well where agglutination occurs, RBCs will remain in suspension, it is denoted as “+”. The highest dilution

of the virus at which it causes hemagglutination is considered the end point of the titration. Reciprocal of this dilution of the virus gives the HA titre.

2.11. Cytopathic effect inhibition (CPE) assay

The modifications in host cell morphology by virus are referred to as the cytotoxic impact. CPE happens when the invading virus causes the host cell to lyse (dissolve), or when the cell dies without lysing because it is incapable of reproducing. Test articles' capacity to suppress CPE can be evaluated using a CPE inhibition assay. After removing the medium from almost confluent MDCK cells cultured at 37°C in a 5% CO₂ incubator, the cells were infected with IAV for 1 hour to allow viral adsorption. In the designated wells, various dilutions of molecules were added and incubated for three to four days at 37°C in 5% CO₂ incubator, with daily checks to see if CPE developed. If there was no viral CPE, the candidate molecule was said to exhibit antiviral action.

2.12. Enzyme based Neuraminidase inhibition assay

The neuraminidase inhibitory activity was evaluated utilizing the NA-Star influenza neuraminidase inhibitor resistance detection kit by Applied Biosystem. In a 96-well microtiter plate, various concentrations of drug molecules (25µl) were added. Following this, each well received 25µl of diluted virus and was then incubated at 37°C for 20 minutes. Subsequently, 10µl of the diluted substrate was added to each well, and the reaction mixtures were allowed to incubate at room temperature for 15 minutes before activation with 60µl of accelerator. The resulting chemiluminescent signal was promptly quantified using a microplate reader. To determine the inhibitory activity of the test molecules, the 50% inhibitory concentration (IC₅₀) was calculated relative to the activity observed in the positive control well, which contained the virus but no test molecule. Analysis of the data was performed using GraphPad Prism software.

2.13. Enzyme kinetics studies

To 96-well microtiter plate, 25µl of diluted virus was incubated with same volume of drug molecules (taking concentrations higher and lower than IC₅₀ value) at 37 °C for 20 min, followed by addition of different concentrations of substrate. A control experiment without the drug molecules was parallelly performed. Measuring the chemiluminescent signal of the hydrolysed product provides the kinetic characterization for the hydrolysis of substrate catalysed by H1N1-NA. Analysis of the data was performed using GraphPad Prism software.

2.14. Gel electrophoresis and immunoblot analyses

After experimentation, cells were washed with prechilled PBS and lysed in 1X cell lysis buffer under ice-cold condition. Protein concentration was measured using Bradford reagent (SigmaAldrich). Whole cell lysates, cytosolic and nuclear fractions were mixed with 6X Laemmli buffer (protein sample buffer) and boiled for 15 minutes (Bhowmick et al., 2015). Samples were run on SDS-PAGE, transferred onto Polyvinylidene Fluoride (PVDF) membrane and immunoblotted with specific antibodies as described previously (Bagchi et al., 2010). These Primary antibodies were detected using secondary antibody conjugated with horseradish peroxidase (HRP) (ThermoFisher Scientific™) and developed using chemiluminescent substrate (Millipore) within ChemiDoc Imaging System (Bio-Rad).

2.15. Nuclear and cytoplasmic protein extraction

IAV or mock-infected cells were harvested using trypsin-EDTA, centrifuged at 500g for 5 minutes. The supernatant was discarded and the pellet was washed with 1X ice-cold PBS. The cells were vigorously vortexed for 15 seconds. The cells were resuspended in Cytoplasmic Extraction Reagent I (CER I) and incubated in ice for 15 minutes. CER II was added to the cells, vigorously vortexed, centrifuged at 16000g for 5 minutes. The cytoplasmic fraction i.e. supernatant was immediately collected in fresh MCTs and stored at -80°C until further use. Nuclear Extraction Buffer (NER) was used to resuspend the insoluble pellet before it was incubated on ice for 40 minutes with vigorous vortexing occurring every 10 minutes. The tube was then centrifuged at 16000 x g for 10 minutes, and the nuclear extract was collected and kept at -80°C until further use.

2.16. Immunofluorescence

MDCK cells grown on glass coverslips (30-50% confluency) were either treated with minocycline or only DMSO and/or infected with IAV/PR8 strain. MEK/ERK inhibitor PD98059-treated cells served as positive control. Cells were fixed in 4% (W/V) paraformaldehyde for 20 min, followed by 3–4 washes with PBS. Cells were then permeabilized using PBS supplemented with 0.1% Triton X-100 (v/v) for 30 min followed by blocking in blocking buffer (PBS supplemented with 2% bovine serum albumin [w/v]) for 1 hr. After blocking, cells were treated with primary antibodies specific for NP in blocking buffer. After 4–5 washes with PBS supplemented with 0.05% Triton X-100, cells were incubated with DyLight488-labelled goat anti-mouse secondary antibodies (ThermoFisher Scientific™, USA) in blocking buffer at room temperature for 1 hr. After 3-4 washes with PBS supplemented with 0.05% Triton X-100, cells were mounted with 4', 6'-diamidino-2-phenylindole (DAPI), covered with a coverslip, to visualise the nuclei. Imaging was done in Zeiss Axioplan LSM

710, 63×/N.A. 1.4 Oil immersion DICIII. Acquired images were analysed using Zen Blue software. Scattergram of colocalized pixels and Pearson's correlation coefficient were generated from Zen Blue software.

2.18. Apoptosis assay

MDCK cells grown on glass coverslips (70% confluency) were minocycline treated and/or infected with IAV/PR8. Staurosporine-treated cells served as positive control while mock infected cells were treated as negative control. After 24 hours of infection, supernatant was discarded and cells were washed thrice with PBS and were allowed to equilibrate with 1X annexin buffer (V13241; Thermo Scientific™) for 2 minutes at 37°C. As per manufacturer's protocol, cells on coverslips were prepared and visualised under Zeiss Axioplan LSM 710, 63×/N.A. 1.4 Oil immersion DICIII. Acquired images were analysed using Zen Blue software. Scattergram of colocalized pixels and Pearson's correlation coefficient were generated from Zen Blue software.



Chapter 3.

Molecular and phylogenetic characterization of pandemic H1N1 strains in eastern India

3.1. Introduction

Influenza A virus (IAV) is one of the most common respiratory viruses. yearly death toll of almost 650,000 from infection among humans globally (<http://www.who.int/mediacentre/news/releases/2017/seasonal-flu>). IAV is an Orthomyxoviridae family member and has a single-stranded, segmented negative-sense RNA genome. Hemagglutinin (HA) and neuraminidase (NA), the two surface proteins, are in charge of creating a high level of genetic diversity among the co-circulating IAV strains. Due to the accumulation of point mutations in the antibody-binding sites and gene-segment reassortments (various combinations of HA and/or NA types), co-infection of numerous strains may cause IAV to evolve quickly (Webster et al., 1992; Rambaut et al., 2008; Domingo, 2010). As a result, antigenic drift eventually occurs, causing the formation of novel subtypes that cannot be effectively neutralized by antibodies prevailing against the prior IAV strains (Treanor, 2015). The novel recombinant A/H1N1 pandemic strain appeared in Mexico in 2009. It caused 18,449 deaths worldwide, of which 3.6% ($n = 981/27,236$) were recorded only from India (Girard et al., 2010).

According to studies, triple reassortant pandemic A/H1N1pdm09 viruses have gradually replaced pre-pandemic seasonal influenza A/H1N1, A/H3N2, and influenza B viruses as the predominant form of the virus since 2009, infecting nearly 24% of the global population (Broor et al., 2012; Majanja et al., 2013; Mishra, 2015; Mudhigeti et al., 2018). The 2009 pandemic had a substantial impact on Indian states including Maharashtra, Delhi, Rajasthan, Gujarat, Tamil Nadu, Madhya Pradesh, Karnataka, Haryana, Kerala, and Andhra Pradesh (Gurav et al., 2010; Choudhry et al., 2012; Mudhigeti et al., 2018). However, in the 2015 and 2017 outbreaks, 42,592 and 38,811 cases, respectively, were reported, compared to the following years in India (5000 cases annually) with deaths totaling 5.8% ($n = 2266/38,811$) and 7.02 % ($n = 2990/42,592$), respectively (Kulkarni et al., 2019) (State/UT-wise, 2020). In comparison to 2009–10, the 2017–18 flu season showed significantly higher rates of influenza-like illness and hospitalization worldwide (CDC, 2019). Due to the restricted testing capability, the percentage of A/H1N1pdm09-related mortality in India in 2017–18 was approximately 5.6% ($n = 4511/81,115$); however, this figure may be underestimated (Kulkarni et al., 2019) (State/UT-wise, 2020). It is yet unknown whether any genetic changes to the surface antigens caused the repeated A/H1N1pdm09 epidemics in India.

The yearly case fatality ratio (CFR) estimates of A/H1N1pdm09 (3.6-7.02%) in India from 2009 to 2017 are higher than those reported from a number of other nations, highlighting the severity of the disease among the population (Nishiura, 2010). There are a few places in India where small scale IAV epidemiology data is available (Agrawal et al., 2009;Agrawal et al., 2010;Mukherjee et al., 2010;Sarkar et al., 2011;Mukherjee et al., 2012;Mukherjee et al., 2016) (Pandey et al., 2018;Jagadesh et al., 2019;Jones et al., 2019). This study examined the prevalence of Influenza A/H1N1pdm09, the affected age group, antiviral resistance, and the phylodynamics of circulating strains among patients needing hospitalization for severe acute respiratory illness (SARI). Future epidemics can be effectively controlled by ongoing surveillance of the circulating IAV subtypes and the appearance of novel reassortant strains. Estimating the efficiency of the vaccine in the area may be aided by the pertinent dataset produced by comparing the antigenic epitopes of the circulating A/H1N1pdm09 strains with the strains that are advised for vaccination.

3.2. Results

3.2.1. Proportion of A/H1N1pdm09 strains

16.5% (n = 677/4106) of the 4106 nasopharyngeal and/or throat swab samples were reported to be positive for A/H1N1pdm09. The positive rates in the age groups of 5 to 20 years, 40 to 60 years, and above 60 years were found to be nearly identical (19.1%, 18.9%, and 19.1%, respectively), while the higher age group (> 60 years) had a substantially reduced positivity rate of 12.7% (Chi-square value = 24.35, p-value.0001) (**Fig. 3.1**). According to the information from the referring hospitals, 1% of the patients admitted with SARI had received any vaccinations. Although there was no clear seasonal pattern, the proportion of hospitalizations attributable to A/H1N1pdm09 infection was substantially greater throughout the summer and monsoon months (April to July and June to October, respectively, in 2017 and 2018) (**Fig. 3.2**). A/H1N1pdm09 virus was detected in 15.4% (n=347/2260) of the males and 17.9% (n=330/1846) of the females.

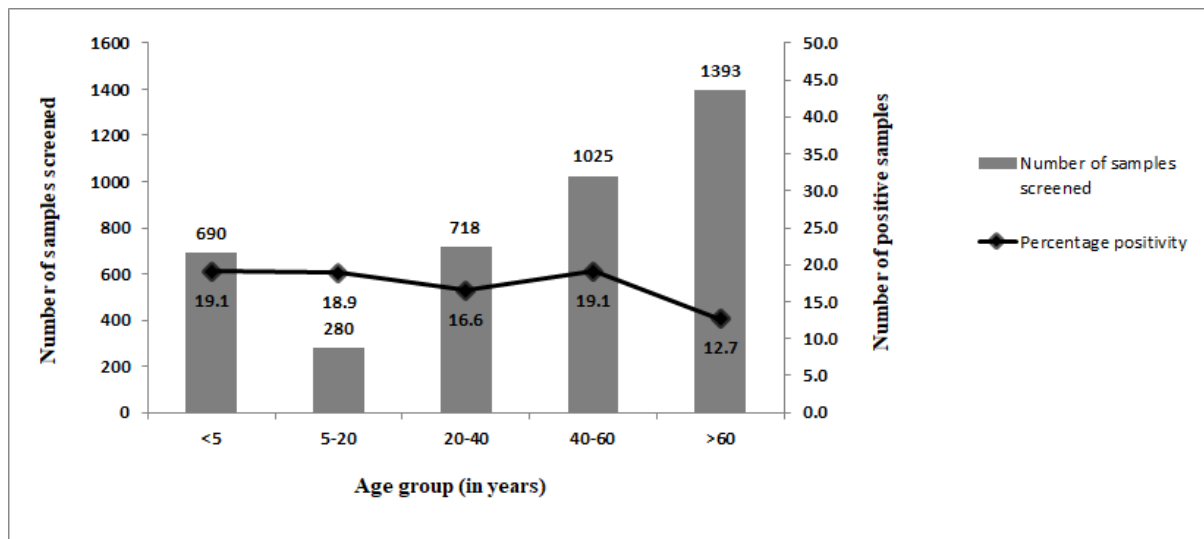


Figure 3.1: Distribution of IAV H1N1pdm09 according to age circulating during April 2017-March 2019.

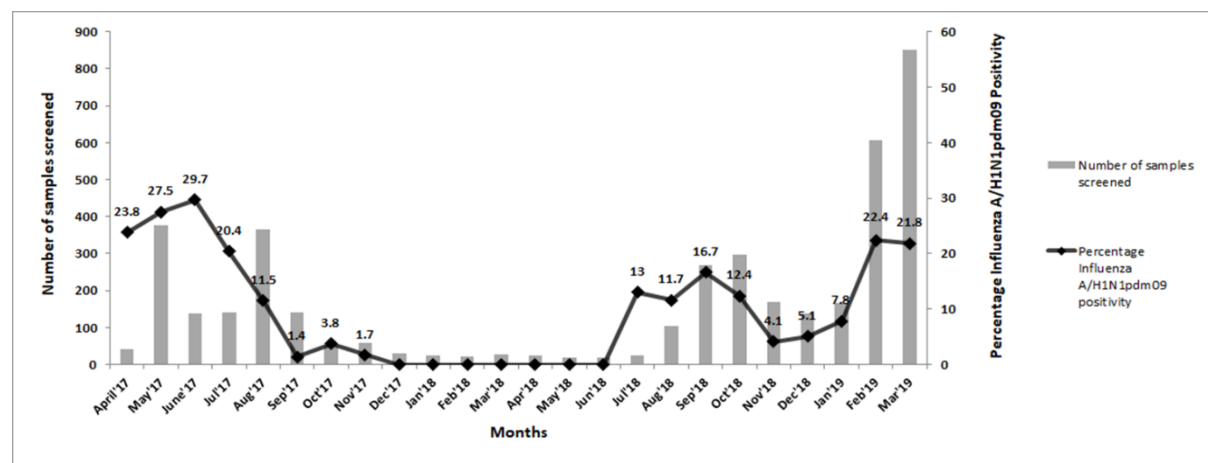


Figure 3.2: Distribution of IAV H1N1pdm09 according to season circulating during April 2017-March 2019.

3.2.2. Phylogenetic analyses of HA and NA genes of A/H1N1pdm09 strains

The phylogenetic dendrogram of circulating A/H1N1pdm09 strains was examined in relation to other circulating IAV H1N1 and H3N2 (outgroup) strains using the aa sequences of the HA and NA genes. Based on their aa sequence homology, the typical eastern Indian A/H1N1pdm09 strains that were represented in the dendrogram were selected. From each subset of related strains (with more than 98% DNA sequence homology), one representative strain was chosen.

3.2.2.1. HA gene

The representative A/H1N1pdm09 strains (n = 25) from eastern India established a distinct cluster among themselves within lineage-6b.1 (98.4–99.4% DNA homology), according to the analysis of the dendrogram. These strains shared a high degree of similarity with lineage-6b.1 strains from the USA (California, Wisconsin, Arizona, Washington; 98.1%); Africa (Nigeria, Ghana; 98.7%); and India (A/human/India/1706/2017; A/human/India/3196/2018; 98.6%). A/human/India/Kol-3846/3959/3828/2015(H1N1)] grouped at a distance and belonged to a distinct sub-lineage 6b.2 within the same lineage (94.8–95.8% DNA sequence homology) than previously reported A/H1N1pdm09 strains from the 2015 epidemic from the same location. It was discovered that the strain A/Human/ California/07/2009(H1N1), which was used as the vaccination strain in both NH and SH between 2010 and 2016, clustered within lineage-1, far from the typical strains of the current investigation (96.1–96.9% nucleotide identity). In lineage 6b.1, our representative strains clustered with A/Human/Michigan/45/2015(H1N1) and A/Human/Brisbane/02/2018(H1N1) strains that were later included in IAV vaccines (in SH and NH, respectively, for the 2019–20 flu season). This revealed >98% DNA homology. In the phylogenetic dendrogram (**Fig. 3.3**), the IAV seasonal H1N1 strains formed a distinct clade and clustered farthest away from the study's representative A/H1N1pdm09 strains.

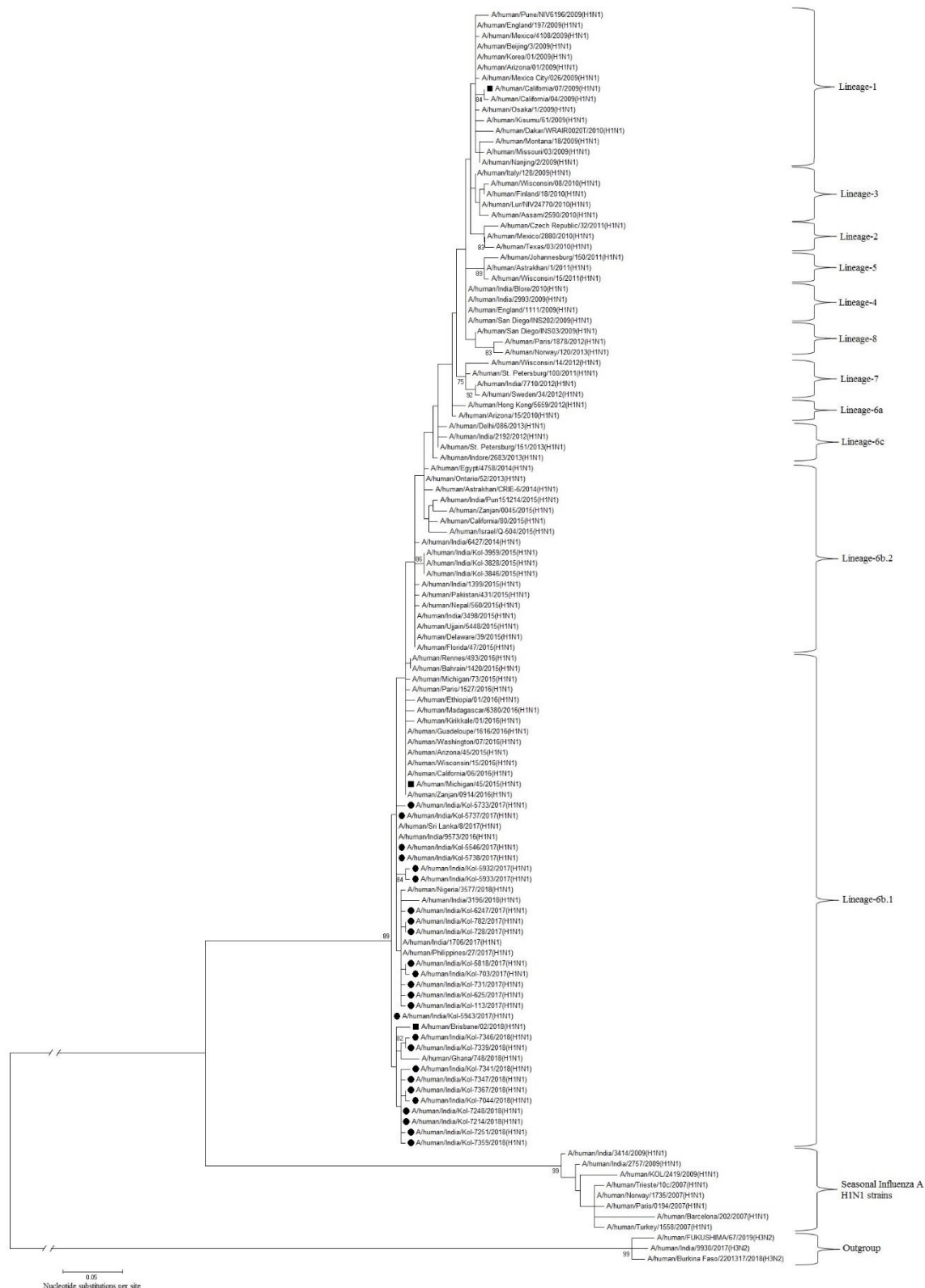


Figure 3.3: Phylogenetic dendrogram of HA protein of eastern Indian IAV H1N1pdm09 strains circulating during April 2017- March 2019. Bootstrap values < 70% are not shown here and scale bar here is 0.05 nucleotide substitutions per site.

3.2.2.2. NA gene

The phylogenetic analysis demonstrated the presence of a sub-population within lineage-6b (99.6% DNA similarity amongst themselves), 99%, 97.4% and 98.5% homology with strains of Africa, USA and Asia, respectively. In this study, the current strains and 2015 pandemic A/H1N1 strains from eastern India [A/India/Kol-3846/3959/3828/2015(H1N1)] segregated at a distance from each other within the same lineage 6b (DNA homology: 97.7-98.4%). The vaccine strain, A/Human/California/07/2009(H1N1), recommended for both NH and SH during 2010-16, was found to be almost 96.8-97.5% similar to circulating strains but clustered in lineage-1. A/Human/Michigan/45/2015(H1N1) (98.4–99.2% homology) appeared to cluster at a distance in the same lineage while the representative strains from eastern India shared the same lineage with A/Human/Brisbane/02/2018(H1N1) (99.2-99.8%) in the dendrogram. The seasonal H1N1 strains were observed to have separated from the representative A/H1N1pdm09 strains (**Fig. 3.4**).

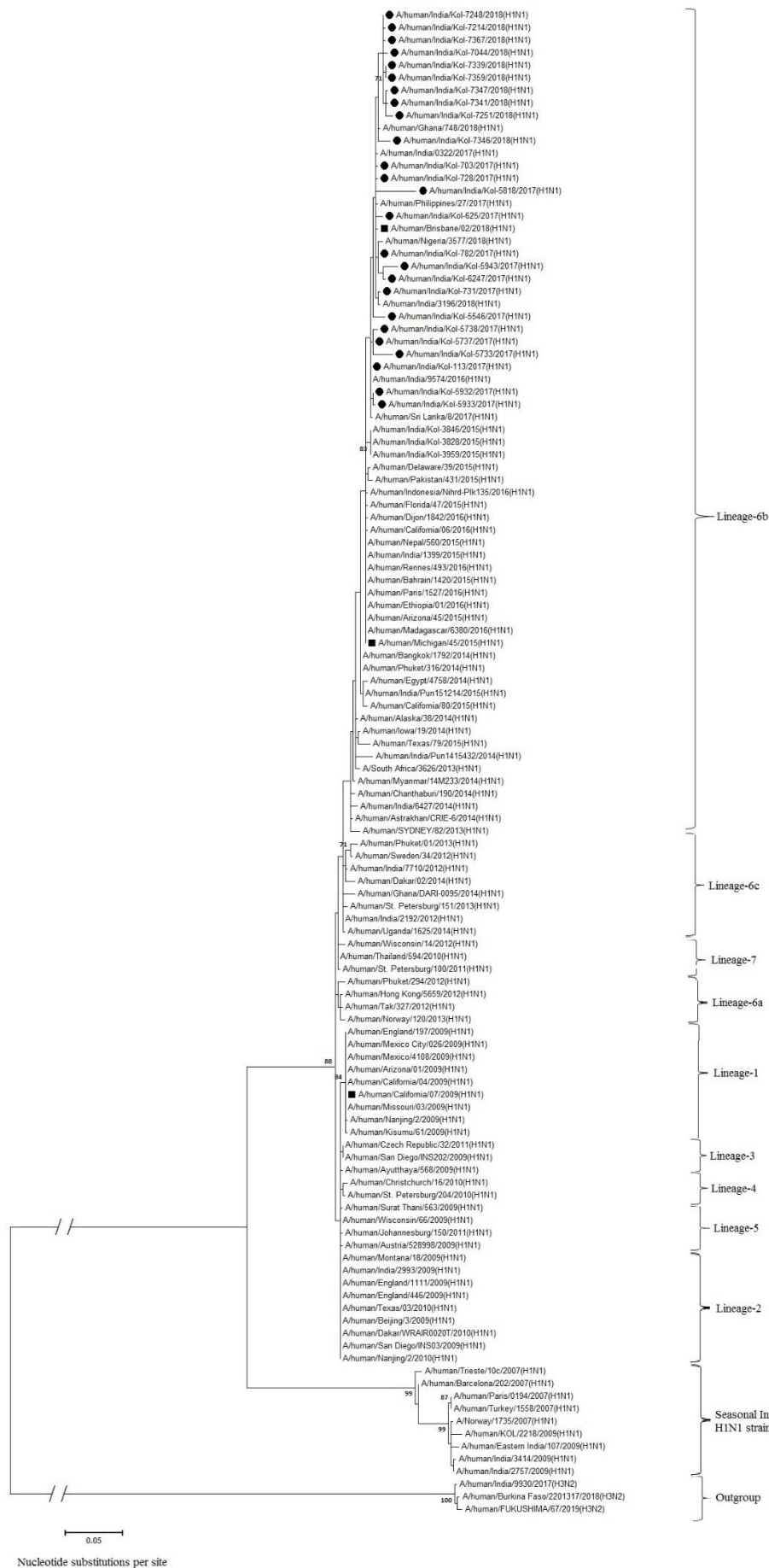


Figure 3.4: Phylogenetic dendrogram of NA protein of eastern Indian IAV H1N1pdm09 strains circulating during April 2017- March 2019. Bootstrap values < 70% are not shown here and scale bar here is 0.05 nucleotide substitutions per site.

3.2.3. Comparative antigenic analyses of HA and NA proteins of A/H1N1pdm09 strains

In order to identify any potential differences between the IAV H1N1 vaccine strains and the representative eastern Indian A/H1N1pdm09 strains, antigenic epitopes of the HA and NA proteins of the three IAV H1N1 vaccine strains—A/Human/Michigan/45/2015(H1N1) and A/Human/Brisbane/02/2018(H1N1)—were compared.

3.2.3.1. HA protein

The Cb, Ca2, Sa, Ca1 and Sb domains of the HA protein, which are highly conserved antigenic epitopes, contain 49 aa residues that are necessary for antibody recognition (Caton et al., 1982; Liu et al., 2018). With the exception of three strains [A/human/India/Kol-7346/2018(H1N1), A/human/India/Kol-7339/2018(H1N1), and A/human/India/Kol-6247/2017(H1N1)], the representative eastern Indian strains clustered into one broad group (group A).

At the same aa locations, these three strains differed significantly. Six incompatibilities between group A strains and A/Human/California/07/2009(H1N1) were found [1, 0, 3, 1, 1 in domains Cb, Ca2, Sa, Ca1 and Sb, respectively]. A/Human/Michigan/45/2015(H1N1) had three mismatches [1, 0, 1, 1, 0 in domains Cb, Ca2, Sa, Ca1 and Sb, respectively], whereas A/Human/Brisbane/02/2018(H1N1) had only one [0, 0, 1, 0, 0 in domains Cb, Ca2, Sa, Ca1 and Sb, respectively] (**Table 3.1**).

DOMAINS	Cb DOMAIN					Sa DOMAIN					Ca2 DOMAIN					Sa DOMAIN					Ca1 DOMAIN					Sb DOMAIN					Ca1 DOMAIN																			
	87	88	89	90	91	92	143		154	155	156	157	158	159	170	171	172	173	174	176	177	178	179	180	181	183	184	185	186	187	201	202	203	204	205	206	207	208	209	210	211	212	220	221	222	239	252	253	254	
Amino acid positions	L	S	T	A	S	S	P	N	P	H	A	G	A	K	K	K	G	N	S	P	K	L	S	K	S	I	N	D	K	G	T	S	A	D	Q	Q	S	L	Y	Q	N	A	S	S	R	D	E	P	G	
A/human/California/07/2009(H1N1)	L	S	T	A	S	S	P	N	P	H	A	G	A	K	K	K	G	N	S	P	K	L	N	Q	S	T	I	N	D	K	G	T	T	A	D	Q	Q	S	L	Y	Q	N	A	T	S	R	D	E	P	G
A/human/Michigan/45/2015(H1N1)	L	S	T	A	R	S	P	N	P	H	A	G	A	K	K	K	G	N	S	P	K	L	N	Q	S	T	I	N	D	K	G	T	T	A	D	Q	Q	S	L	Y	Q	N	A	T	S	R	D	E	P	G
A/human/Brisbane/02/2018(H1N1)	L	I	S	K	E	S	N	H	S	H	N	G	E	R	G	K	G	N	S	P	L	N	S	K	S	S	A	N	N	K	E	S	I	S	D	Q	Q	S	L	Y	H	T	E	S	S	H	D	E	P	G
A/human/KOL/241/9/2009	L	S	T	A	S	S	N	H	P	H	A	G	A	K	K	K	G	N	S	P	K	L	S	Q	S	T	I	N	D	K	G	T	T	A	D	Q	Q	S	L	Y	Q	N	A	T	S	R	D	E	P	G
A/human/India/Ko-1-3959/2015 Group A	L	S	T	A	R	S	P	N	P	H	A	G	A	K	K	K	G	N	S	P	K	L	N	Q	T/S	T	I	N	D	K	G	T	T	A	D	Q	Q	S	L	Y	Q	N	A	T	S	R	D	E	P	G
A/human/India/Ko-1-7346/2018(H1N1)	L	S	T	A	R	S	P	N	P	H	A	G	A	K	K	K	G	N	S	P	K	L	N	Q	T	T	I	N	D	K	G	T	I	A	D	Q	Q	S	L	Y	Q	N	A	T	S	R	D	E	P	G
A/human/India/Ko-1-7389/2018(H1N1)	L	S	T	A	R	S	P	N	P	H	A	G	A	K	K	K	G	N	S	P	K	L	N	Q	T	T	I	N	D	K	G	T	I	A	D	Q	Q	S	L	Y	Q	N	A	T	S	R	D	E	P	G
A/human/India/Ko-1-6247/2017(H1N1)	L	S	T	A	R	S	P	N	P	H	A	G	A	K	K	K	G	N	S	P	K	L	N	Q	T	T	I	N	D	K	G	T	T	A	D	Q	Q	S	L	Y	Q	N	A	T	S	R	D	E	P	G

Table 3.1. Amino acid substitutions in the HA gene (antigenic epitopes) among IAV H1N1pdm09 isolates in comparison to previously reported eastern Indian strains and vaccine strains A/human/California/07/2009(H1N1), A/human/Michigan/45/2015(H1N1) and A/human/Brisbane/02/2018(H1N1).

The highly conserved residues (Y108, W167, 197H, and 209Y) that comprise the base of the receptor binding pocket, aside from the antigenic epitopes, have not changed in any of the representative strains in this study (Mir et al., 2012). All of the isolates of the virus had the substitution I233T at the receptor binding site as a common trait. the research. All of the aa of the 130-loop and 220-loop of the receptor binding site in all of the current isolates were determined to be largely conserved, whereas S202T and T214A aa modifications in the 190-helix region were identified (Fukuzawa et al., 2011). All of the isolates also showed some additional alterations (as seen in **Table 3.2**).

Amino acid positions	13	101	108	114	167	197	209	214	233	312
A/human/California/07/2009(H1N1)	A	S	Y	D	W	H	Y	A	I	I
A/human/Michigan/45/2015(H1N1)	T	N	Y	N	W	H	Y	A	T	I
A/human/Brisbane/02/2018(H1N1)	T	N	Y	N	W	H	Y	A	T	V
A/human/KOL/2419/2009	T	N	Y	N	W	H	Y	S	K	V
A/human/India/Kol-3959/2015	T	N	Y	N	W	H	Y	A	I	I
Group A	T	N	Y	N	W	H	Y	A/T	T	V
A/human/India/Kol-7346/2018(H1N1)	T	N	Y	N	W	H	Y	A	T	V
A/human/India/Kol-7339/2018(H1N1)	T	N	Y	N	W	H	Y	A	T	V
A/human/India/Kol-6247/2017(H1N1)	T	N	Y	N	W	H	Y	A	T	V

Table 3.2: Amino acid substitutions in NA gene (antigenic epitopes) among IAV H1N1pdm09 isolates in comparison to previously reported eastern Indian strains and vaccine strains- A/human/California/07/2009(H1N1), A/human/Michigan/45/2015(H1N1), A/human/Brisbane/02/2018(H1N1).

3.2.3.2. NA protein

The typical strains' modifications to the aa residues surrounding the antigenic sites (83-143, 156-190, 252-303, 330, 332, 340-345, 368, 370, 387-395, 400, 431-435, and 448-468) were compared to the Influenza. Along with previously known strains from eastern India, A H1N1 vaccine strains include A/Human/California/07/2009(H1N1), A/Human/Michigan/45/2015(H1N1), and A/Human/Brisbane/02/2018(H1N1) (Maurer-Stroh et al., 2010; Graham et al., 2011). Except for nine strains (A/human/India/Kol-5546/2017(H1N1), A/human/India/Kol-625/2017(H1N1), A/human/India/Kol-5733/2017(H1N1), A/human/India/Kol-5943/2017(H1N1), A/human/India/Kol-6247/2017(H1N1), A/human/India/Kol-7341/2017 which, as a result of certain aa

modifications, did not cluster under any of the three groupings. With respect to the vaccination strains A/Human/California/07/2009(H1N1), A/Human/Michigan/45/2015(H1N1), and A/Human/Brisbane/02/2018(H1N1), the group A strains had 4, 1, and 0 mismatches, respectively.

In contrast to the strains of group C, which showed 5, 3 and 1 changes with A/Human/California/07/2009(H1N1), A/Human/Michigan/45/2015(H1N1), and A/Human/Brisbane/02/2018(H1N1), respectively, the group B strains had 5, 2 and 1 aa variations with each of those strains, respectively (Table 3.3).

Amino acid positions	93	117	143	188	264	267	270	292	294	301	389	394	432	451	452	455	458	460
A/human/California/07/2009(H1N1)	P	I	K	I	V	V	N	C	D	R	I	V	K	D	T	W	P	G
A/human/Michigan/45/2015(H1N1)	P	I	K	I	I	V	K	C	D	R	I	V	E	D	T	W	P	G
A/human/Brisbane/02/2018(H1N1)	P	I	K	T	I	V	K	C	D	R	I	V	E	D	T	W	P	G
A/human/India/Kol-3959/2015	P	I	K	I	I	V	K	C	D	R	I	V	E	D	T	W	P	G
Group A	P	I	K	T	I	V	K	C	D	R	I	V	E	D	T	W	P	G
Group B	P	M	K	T	I	V	K	C	D	R	I	V	E	D	T	W	P	G
Group C	P	I	R	T	I	V	K	C	D	R	I	V	E	D	T	W	P	G
A/human/India/Kol-5546/2017(H1N1)	P	I	K	T	I	I	K	C	D	P	I	V	E	D	T	W	P	G
A/human/India/Kol-625/2017(H1N1)	P	I	K	T	I	V	K	W	E	R	I	V	E	D	T	W	P	G
A/human/India/Kol-5733/2017(H1N1)	P	I	K	T	I	V	K	C	D	R	M	V	E	D	T	W	R	D
A/human/India/Kol-5943/2017(H1N1)	P	I	K	T	I	V	K	C	D	R	I	G	E	D	T	C	P	A
A/human/India/Kol-6247/2017(H1N1)	H	I	K	T	I	V	K	C	D	R	I	V	E	A	T	C	P	A
A/human/India/Kol-7341/2017(H1N1)	P	I	K	T	I	V	E	C	D	R	I	V	E	D	T	W	P	G
A/human/India/Kol-7346/2017(H1N1)	P	I	K	T	I	V	K	C	D	R	I	I	E	D	I	W	P	G
A/human/India/Kol-731/2017(H1N1)	P	I	K	I	V	V	K	C	D	R	I	V	E	D	T	W	P	G
A/human/India/Kol-7367/2017(H1N1)	P	I	K	T	I	V	K	C	D	R	I	V	G	D	T	W	P	G

Table 3.3: Amino acid substitutions in the NA gene (antigenic epitopes) among the IAV H1N1pdm09 isolates in comparison to eastern Indian strains and vaccine strains- A/human/California/07/2009(H1N1), A/human/Michigan/45/2015(H1N1), A/human/Brisbane/02/2018(H1N1).

None of the isolates included in the study had the Tamiflu (Oseltamivir) resistance mutation H275Y. All of the NA protein's catalytic sites (118R, 119E, 151D, 152R, 179W, 223I, 225R, 277E, 368R, and 402Y) as well as the framework residues (156R, 180S, 228E, 247S, 278E, and 295N) supporting the catalytic sites were found to be conserved in the isolates used in this study (data not shown). Some additional mutations were observed in the non-antigenic domains in the study isolates (Table 3.4).

Amino acid positions	13	19	34	200	223	232	241	248	275	295	313	314	369	386	427	436
A/human/California/07/2009(H1N1)	V	M	I	N	I	A	V	N	H	N	Q	I	N	N	I	I
A/human/Michigan/45/2015(H1N1)	I	M	V	S	I	A	I	D	H	N	Q	M	K	K	I	I
A/human/Brisbane/02/2018(H1N1)	T	M	V	S	I	A	I	D	H	N	Q	M	K	K	I	I
A/human/KOI/2419/2009	I	I	A	N	I	V	I	N	Y	N	Q	I	K	D	V	T
A/human/India/Kol-3959/2015	I	M	V	S	I	A	I	N	H	N	Q	M	K	K	I	I
Group A	I	M/V	V	S	I	A	I/V	D	H	N	Q	M	K	K	I	I
Group B	I	M	V	S	I	A	I	D	H	N	Q	M	K	K	I	I
Group C	I	M	V	S	I	A	I	D	H	N	Q	M	K	K	I	I
A/human/India/Kol-5546/2017(H1N1)	I	M	V	S	I	A	I	D	H	N	Q	M	K	K	I	I
A/human/India/Kol-625/2017(H1N1)	I	M	V	S	I	A	I	D	H	N	Q	M	K	K	I	I
A/human/India/Kol-5733/2017(H1N1)	I	M	V	S	I	A	I	D	H	N	Q	M	K	K	I	I
A/human/India/Kol-5943/2017(H1N1)	I	M	V	S	I	A	I	D	H	N	Q	M	K	K	I	I
A/human/India/Kol-6247/2017(H1N1)	I	M	V	S	I	A	I	D	H	N	Q	M	K	K	I	I
A/human/India/Kol-7341/2017(H1N1)	I	M	V	S	I	A	I	D	H	N	Q	M	K	K	I	I
A/human/India/Kol-7346/2017(H1N1)	I	M	V	S	I	A	I	D	H	N	Q	M	K	K	I	I
A/human/India/Kol-7331/2017(H1N1)	I	M	V	S	I	A	I	D	H	N	Q	M	K	K	I	I
A/human/India/Kol-7367/2017(H1N1)	I	M	V	S	I	A	I	D	H	N	Q	M	K	K	I	I

Table 3.4: Amino acid substitutions in the NA gene (non-antigenic domains) of IAV H1N1pdm09 isolates in comparison to eastern Indian strains and vaccine strains- A/human/California/07/2009(H1N1), A/human/Michigan/45/2015(H1N1), A/human/Brisbane/02/2018(H1N1).

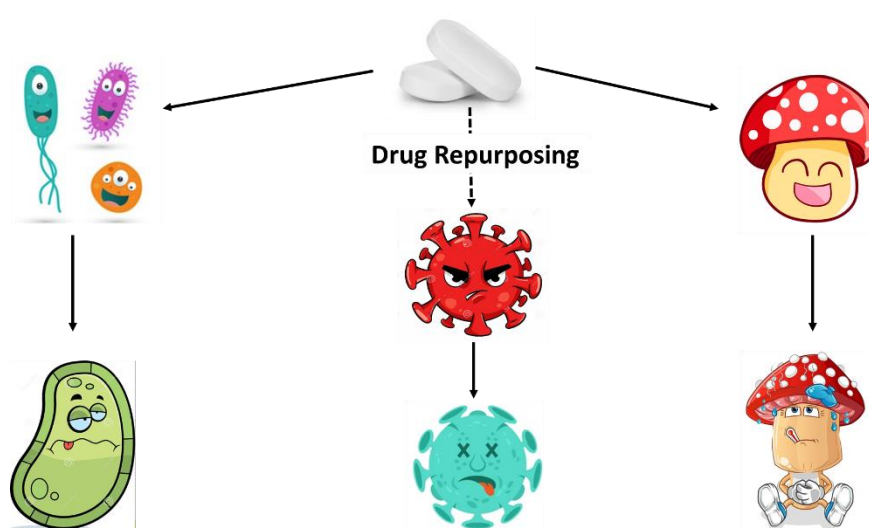
3.3. Discussion

The 2015 A/H1N1pdm09 outbreak was widespread than the pandemic of 2009 as the infection spread into 22 Indian states, increasing by almost 10% (Cousins, 2015; Murhekar and Mehendale, 2016). It is worth noting that the period between the two peaks of the infection (2011-2014), Indian population exhibited a lower level of viral activity. The A/H1N1pdm09 positivity rates in eastern India during 2017-19 (16.5%) was much lower than the 2015 outbreak (23.3%) and the Andhra Pradesh outbreak during 2017-18 (27.68%) (Mukherjee et al., 2016; Mudhigeti et al., 2018). Cases in Vietnam and England reveal dual peaks of seasonal and pandemic strains during summer and winter months (Lofgren et al., 2007; Elliot et al., 2009; Nguyen et al., 2015). India experiences influenza activity all year long (Chadha et al., 2015). Two resurgence patterns of seasonal infection have been noted: monsoon peak in a tropical region and winter peak in temperate regions (Koul et al., 2013; Chadha et al., 2015; Mudhigeti et al., 2018; Jagadesh et al., 2019). Nevertheless, the ongoing investigation of trends in A/H1N1pdm09 did not provide clear evidence of seasonality associated with an increase in viral activity during the summer and monsoon months which corresponds with those in previous reports (Agrawal et al., 2009; Mukherjee et al., 2010; Chadha et al., 2015; Mudhigeti et al., 2018). This lack of seasonal variation found in this study may in fact be due to the non-retrospective data as only referred hospital samples were enrolled instead of a system surveillance.

While the immunization rate ($1 \pm 0.5\%$) of the records from the referring hospitals is considered to be low, two possible reasons could explain it: First, the community members may be unaware of the benefits of immunization; and second, some of them may find the vaccine to be too expensive for them (Hirve and Organization, 2015). Indigenous research based in healthcare professionals in India have equally depicted lower vaccination coverage ($\approx 5\%$) despite the awareness and affordability. Causes for non-acceptance are often due to the skepticism of efficacy, fears of side effects, lack of time, and a perception of low personal risk (Bali et al., 2013; Gambhir et al., 2016; Kant and Guleria, 2018).

The investigation was based on sequencing Influenza A/H1N1pdm09 strains, discovering a new glycosylation site and amino acids in HA, which were conserved and associated with the enzymatic activity (Mukherjee et al., 2016; Al Khatib et al., 2019). Circulating viral strains showed no mutations in neuraminidase which trigger multidrug resistance (McKimm-Breschkin, 2013). For population, especially the high-risk patients, Tamiflu, an antiviral

therapy, was effective. The evolving A/H1N1pdm09 viruses raise concerns for vaccine effectiveness in an epidemic setting. The process of phylogenetic analysis comparing sequences of circulating strains on a global scale with vaccine strains that are recommended by WHO reveal the presence of a number of drastic variations. A higher DNA homology was found with the vaccine strains A/human/Michigan/45/2015 (98.8%) and A/human/Brisbane/02/2018 (99%) compared to A/human/California/07/2009 (96.9%). Recurring epidemics, high lethality percentages partly due to the limited knowledge of vaccine benefits in India, all on the one hand emphasize the need for a national influenza vaccination policy which covers the high-risk groups. The limitations of the study include the absence of active monitoring, thus underestimating the disease burden of Influenza A/H1N1 in the population and lack of detailed data on vaccination history, co-morbidities, and outcomes.



Chapter 4

Studying drug repurposing of antimicrobial agents: Minocycline

4.1. Introduction

Certain communities, for instance newborns, old people, those with weak immune system, and chronically ill people, are more prone to develop severe complications from bacterial and viral respiratory infections, including influenza viruses (Trucchi et al., 2019). Pandemics in the past century start from the Spanish flu that began in 1918, with 40 million estimated global death toll (Gatherer, 2009). IAV genome consists of 8 negative-sense single-stranded RNA segments that encode 2 proteins. Each of these segments consists of nucleoprotein (NP) and RNA-dependent RNA polymerase (RdRp), forming ribonucleoprotein complexes (vRNPs). The life cycle of IAV starts from virus entrance into the cell, import of vRNPs into the nucleus, replication and transcription of the vRNAs in the nucleus, release of vRNPs into the cytoplasm, and formation and release of progeny viruses (Cros and Palese, 2003;Nayak et al., 2004). Bidirectional transport of the vRNAs is important during the viral replication while nuclear exporting of vRNPs in the last phase of infection takes place under the influence of the envelope glycoprotein named hemagglutinin (Shaw and Palese, 2007) ;Ra, 1995).

Due to its enormous genetic variety and capacity for mutation, the influenza virus is a source of major public health risk. Vaccines and antivirals have the power to effectively prevent, limit, and manage viral epidemics. Nevertheless, new subtypes arise due to point mutations and reassortment of gene fragments, disabling existing treatments and vaccines. Hence, the creation of new drugs and vaccines becomes necessary for newly emerging strains. Hence, the global monitoring of the influenza strains circulating is the fundamental for improving the vaccine effectiveness (Agrawal et al., 2009;Agrawal et al., 2010;Mukherjee et al., 2010;Mukherjee et al., 2012;Mukherjee et al., 2016).

At present, influenza management relies on two categories of drugs: Much like the neuraminidase (NA) inhibition oseltamivir, peramivir, and zanamivir are; and the M2 ion channel blockers like amantadine and rimantadine (Shen et al., 2015;Yen, 2016). The depletion of M2 inhibitors due to the point mutations (like L26F or S31N) allows the drugs to overcome the action whereas the mutation in NA (H274Y) reduces the drug sensitivity of IAV to oseltamivir inhibitors resulting in the failure of drug therapy (Wang et al., 2003;Dong et al., 2015). Therefore, there is continuous need for research or developing new antiviral drugs which can control IAV infection.

A second-generation tetracycline's chemically analogue, minocycline, contains the additional therapeutic effects of 7-dimethylamino-6-dimethyl-6-deoxytetracycline. The drug has a

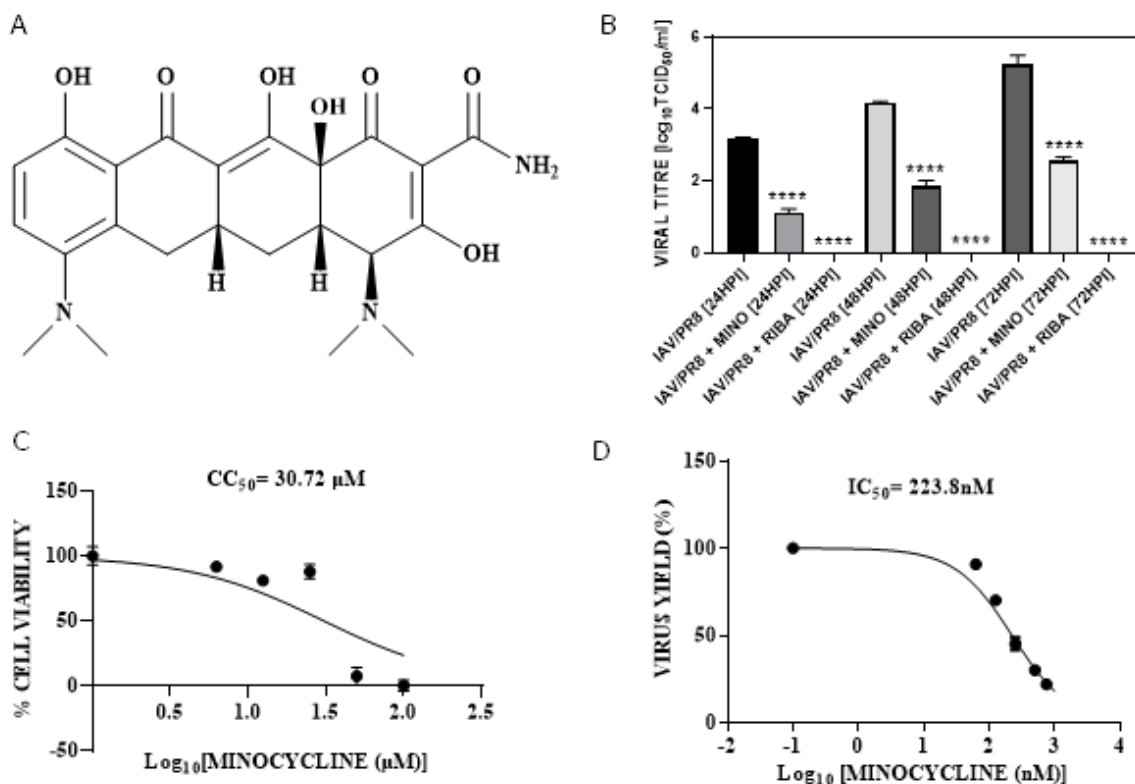
favourable pharmacokinetic profile and easily reaches the central nervous system (Chopra and Roberts, 2001). Although tolerated fairly well, minocycline abuse may lead to liver damage, pigmentation problems and lupus erythematosus-like symptoms (Garner et al., 2012). Besides the anti-inflammatory, anti-apoptotic, neuroprotective and immune-modulating properties, minocycline was described also to have antiviral effect against HIV, dengue, JEV, RSV, etc though mechanisms are not well studied (Popovic et al., 2002; Song et al., 2004; Giuliani et al., 2005) (Darman et al., 2004; Richardson-Burns and Tyler, 2005; Irani and Prow, 2007; Michaelis et al., 2007; Mishra and Basu, 2008; Dutta et al., 2010; Szeto et al., 2010; Enose-Akahata et al., 2012; Leela et al., 2016; Bawage et al., 2019). The present study showed that minocycline, the FDA approved antibiotic, degrades the viral maturation and release process by inhibiting both ERK-induced nuclear export of vRNP and apoptosis at late stage, establishing its antiviral properties against IAV.

4.2. Results

4.2.1 Minocycline treatment showed potent anti-IAV activity *in vitro*

A dose-response effect of minocycline (**Fig. 4.1A**) on the viability of MDCK cells over a 72-hour period following varying concentrations (from 1nM to 1mM) of the compound using the MTT assay was observed. A fifty percent cell death (CC_{50}) of the 50% cell compared to the control (DMSO-treated) cells was observed at 30.72 μ M minocycline (**Fig. 4.1C**). MDCK cells infected with the virus were treated with ranging concentrations of minocycline from 0.1nM to 1mM for 72 hours post infection (hpi). The supernatant at 72hpi was used to measure HA titre to determine the virus yield. The IC_{50} for minocycline treated IAV-infected cells was found to be 224 nM and the SI of minocycline was calculated as approximately 137.1 for IAV infection (**Fig. 4.1D**). To understand which stage of the viral life cycle was affected by minocycline treatment, infected cells were either pre-treated with minocycline (1 hour prior to infection) or co-treated along with infection or post-treated (at the time of virus removal) at 0 hpi. Results revealed that post-treatment of infected cells with minocycline had the maximum antiviral effect, while pre- and co-treatment had no significant effect on viral production and viral transcript synthesis (**Fig. 4.1E**), signifying no role of minocycline during viral adsorption and entry. A time- of- addition study was conducted to corroborate its effect on stages of viral life cycle. Treatment with minocycline at 0 hpi, 6 hpi and 12 hpi followed by cell lysis at 24 hpi, revealed antiviral activity of minocycline was high in cells when drug was added at 6 hpi or 12

hpi (**Fig. 4.1F**). This suggests that minocycline modulates viral replication during the last stage of life cycle. In order to provide conclusive evidence of the anti-IAV action of minocycline, the experimental design included the temporal analysis of viral mRNA synthesis and viral production in samples treated with minocycline. For further experiments 500nM dose of minocycline was used. IAV/PR8-infected MDCK cells that were treated with 500nM minocycline showed about 50 percent of decrease in the vRNA, cRNA and mRNA transcript level (M1 gene) and virus production (HA titre) at the time intervals of 6-, 12-, 24-, 48-, and 72-hpi (**Fig. 4.2A-D, 4.1B**). 50% reduction in viral titre was observed in IAV/H3N2 and IAV/CAL-infected minocycline treated cells (**Fig. 4.2E, F**). At early stage of infection (6 hpi), minocycline treatment did not show any significant effect. MDCK cells subjected to IAV/PR8 virus and ribavirin treatment (100 μ M) was used as a positive control. Minocycline dose-dependent treatment to both influenza pandemic strain IAV/CAL and prototypical influenza strain IAV/PR8 strain infected MDCK cells showed progressive decrease in IAV protein (NS1) expression as depicted in **Figure 4.2G, H**. Collectively, these results thereby give an insight on cell line and viral strain independent anti-influenza activity of minocycline *in vitro*.



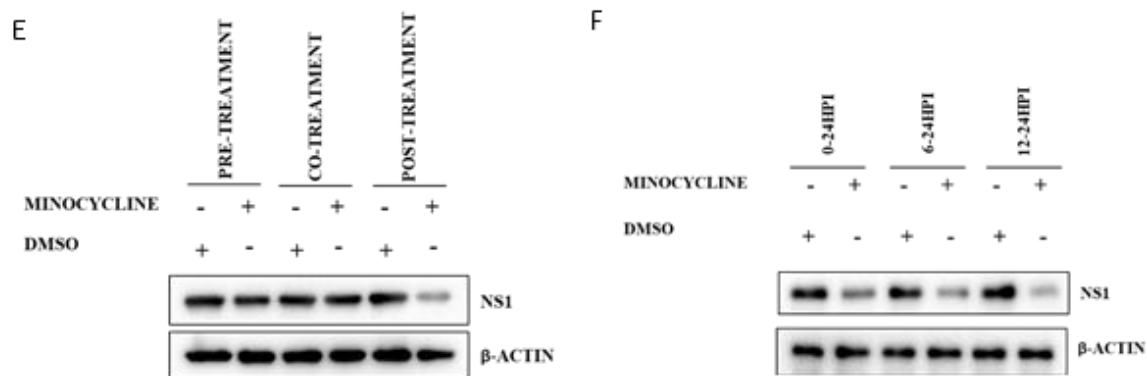
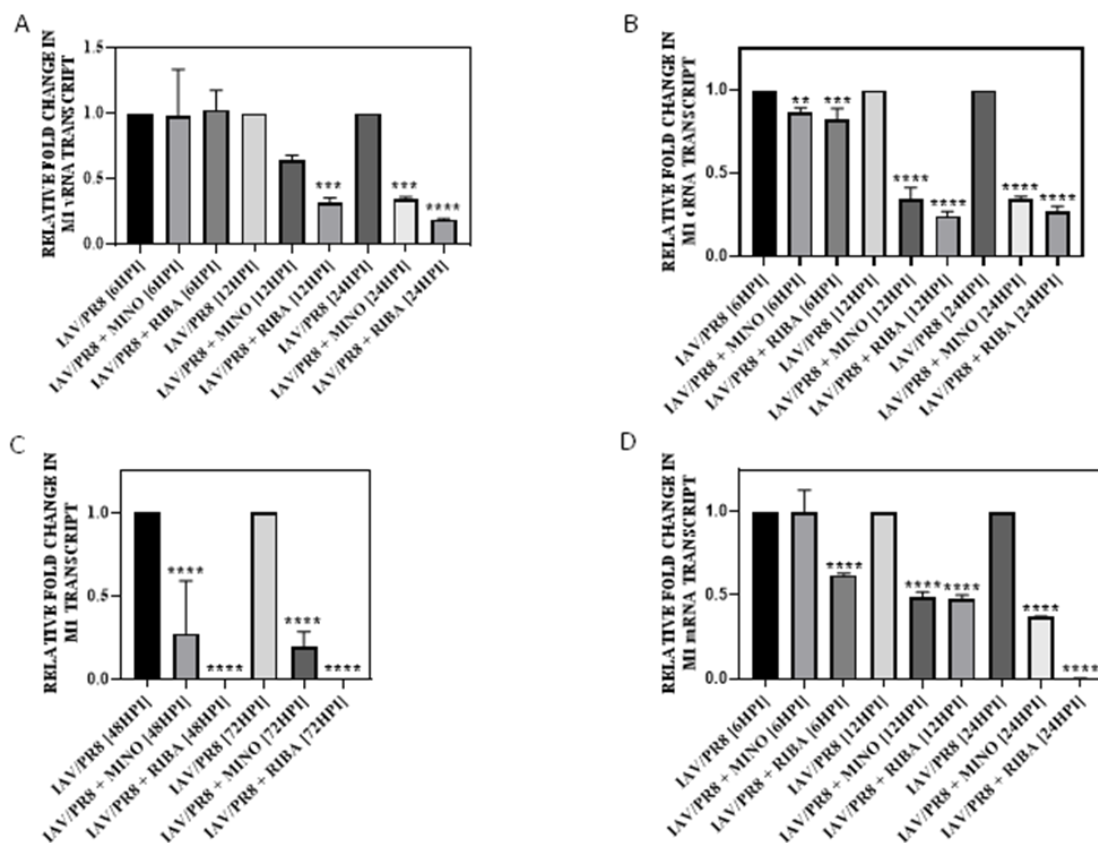


Figure 4.1: (A) chemical structure of minocycline; (B) evaluation of viral titre from supernatant extracted from IAV/PR8-infected MDCK cells treated with DMSO or 500 nM Minocycline (at 24, 48 and 72 hpi), cells treated with 100 μ M Ribavirin is treated as positive control; (C) cell viability of MDCK cells when treated with different concentrations of minocycline (1nM - 1mM) for 72 hrs, was measured using MTT assay to calculate CC_{50} ; (D) infectious IAV particles produced from IAV/PR8 MDCK cells subjected to varying concentrations of minocycline (0.1 nM-1 mM) for 72 hrs were used to calculate IC_{50} ; (E) IAV/PR8-infected MDCK cells were treated with DMSO or minocycline (500 nM) 1 hour prior to infection (pre-treatment), at the time of virus addition (co-treatment) and 1 hour after viral addition (post-treatment) to assess its effect on viral protein expression; (F) post-treatment of DMSO or minocycline (500 nM) at 0-24 hpi, 6-24 hpi and 12-24 hpi to IAV/PR8-infected cells to assess the stage of viral life cycle inhibited by minocycline.



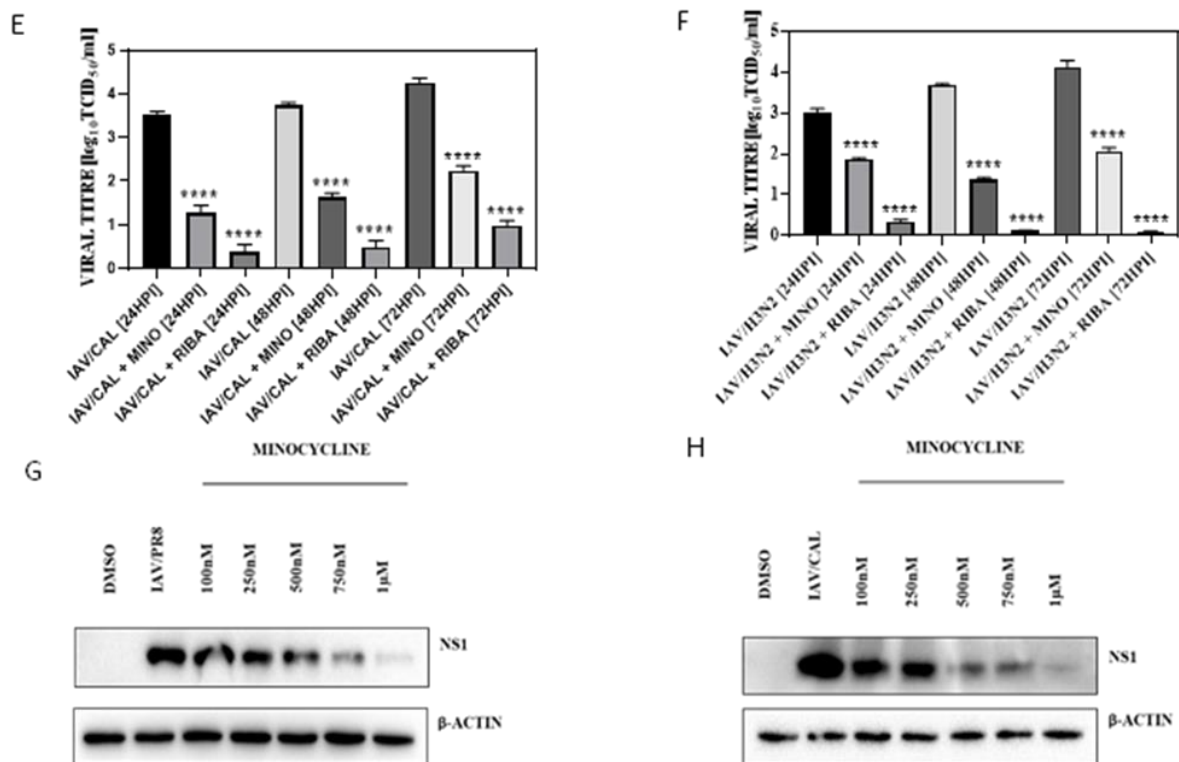


Figure 4.2: (A-D) relative expressions of vRNA, cRNA and mRNA extracted from IAV/PR8-infected MDCK cells treated with DMSO or 500 nM Minocycline (at 6, 12 and 24 hpi) was estimated by quantitative RT-PCR. Relative fold change in M1 mRNA transcript was also estimated at 48 and 72 hpi. Cells treated with 100 μM Ribavirin is treated as positive control; (E-F) IAV/CAL or IAV/H3N2 infected MDCK cells were treated with minocycline (500 nM) or ribavirin (100 μM) for 24, 48 and 72 hpi, cell supernatant was collected and viral titre was estimated by hemagglutination assay and represented as TCID₅₀/ml; (G-H) IAV/PR8 and IAV/CAL infected MDCK cells were treated with different concentrations of minocycline (100 nM - 1 μM), viral protein estimated by western blotting after 24hrs.

4.2.2 Minocycline impedes IAV infection without triggering interferon (IFN) signalling

The gene expression of JAK1-STAT1 of IFN signalling pathway was evaluated to check the effectiveness of minocycline at a dose of 500nM against MDCK and A549 cells at 12hpi. In parallel, cells concurrently treated with IFN α-2β were taken as a positive control. Under contrast to the phosphorylation of JAK1 and STAT1 following administration of interferon (IFN) α-2β, the minocycline failed to do the same suggesting that it does not trigger IFN signalling (**Fig. 4.3A, B**). JAK1 and STAT1, the two main proteins of the IFN signalling pathway, underwent phosphorylation in IAV-infected MDCK cells (**Fig. 4.3C, D**). Minocycline also showed anti-IAV effect in the IFN-deficient Vero cells as shown by reduction in virus titre and viral protein (NS1) (**Fig. 4.3E, F**). Overall, the results confirmed that the anti-IAV action of minocycline is independent of IFN signalling.

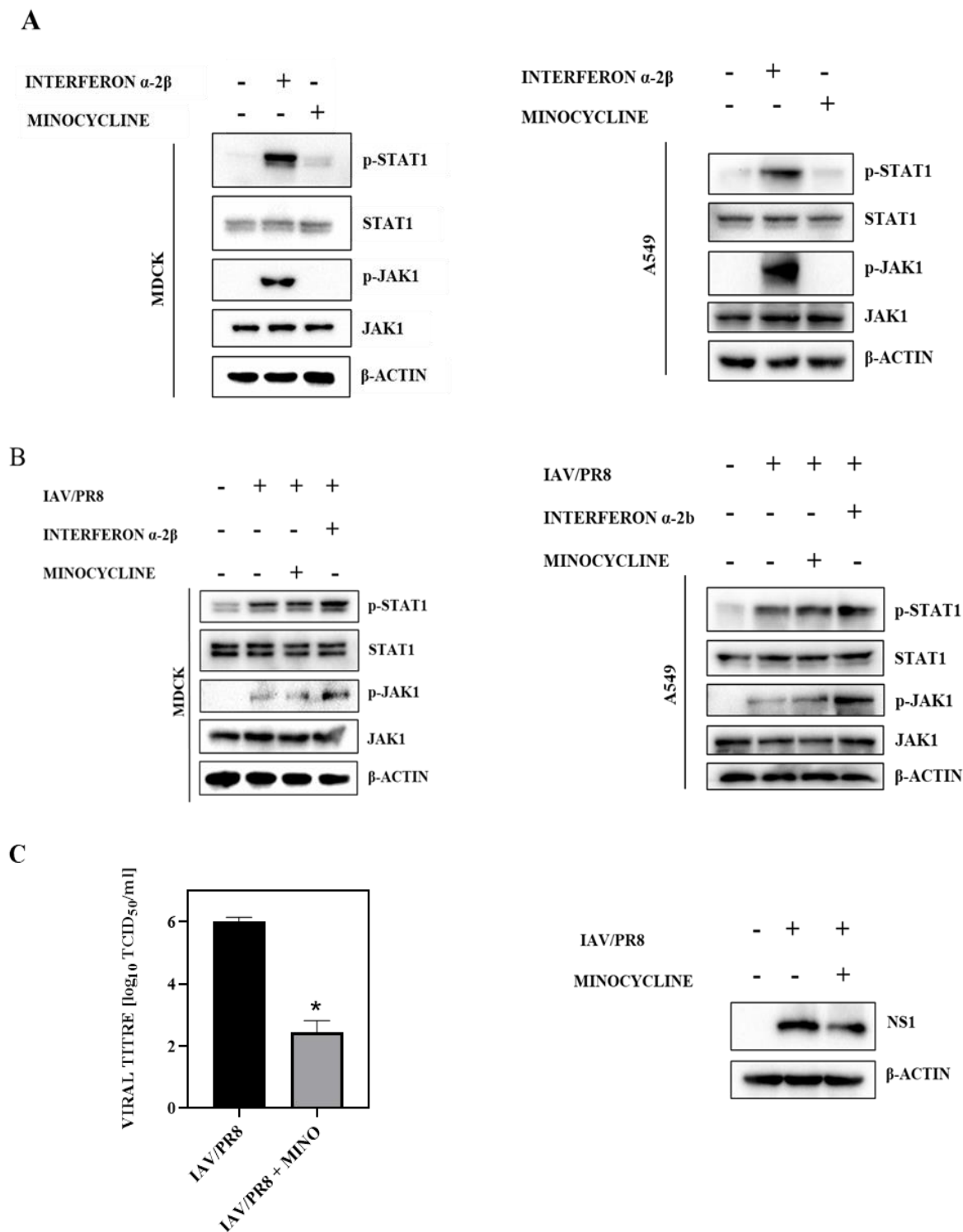
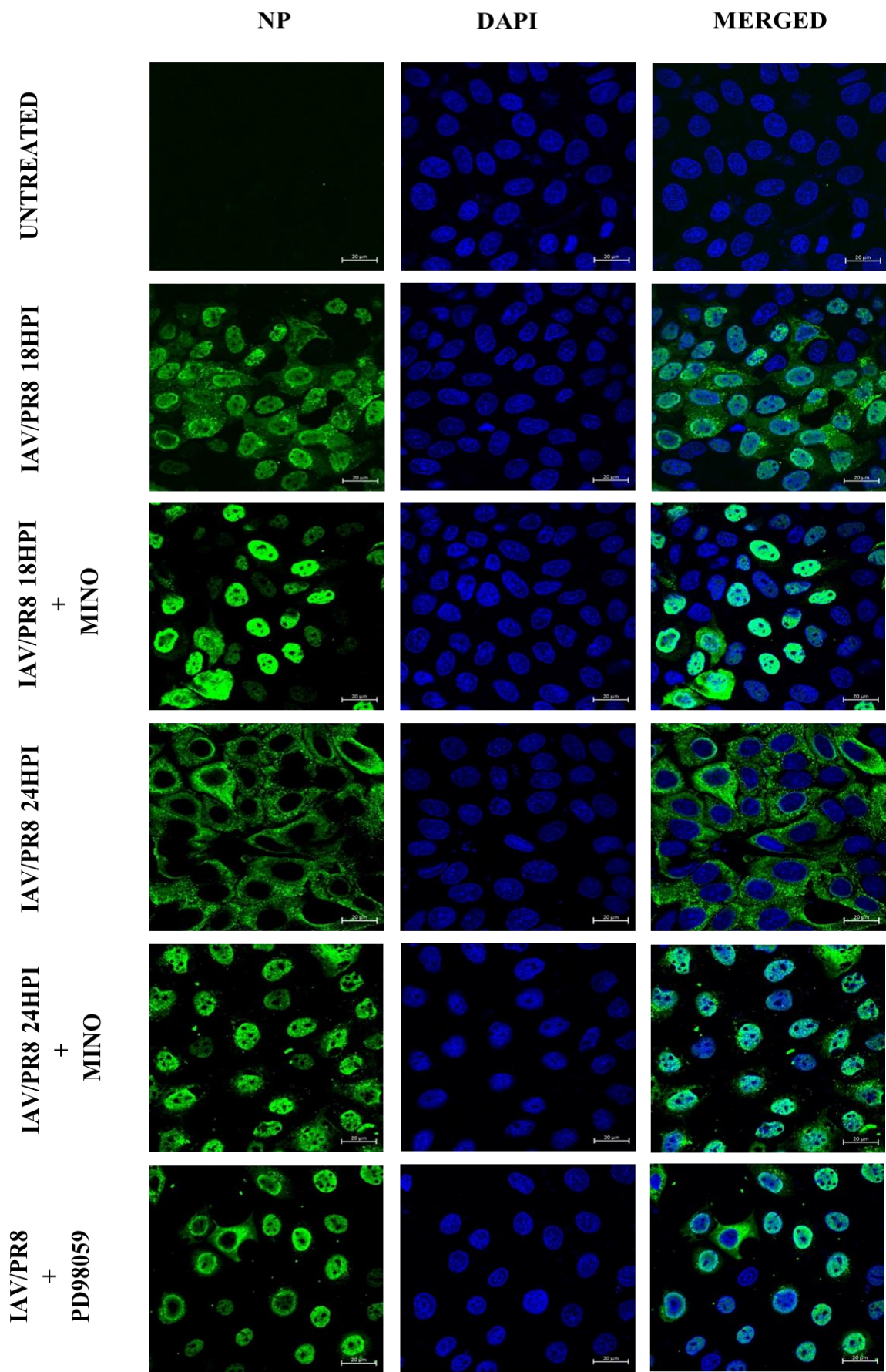


Figure 4.3: Minocycline does not trigger the IFN signalling pathway in MDCK or A549 cells with/without IAV/PR8 infection. Cellular phosphorylation of the JAK1/STAT1 proteins were not observed in Minocycline-treated MDCK and A549 cells (A). IFN α -2 β in the current study served as the positive control. Minocycline treatment has no effect on activation of IFN signaling activation by IAV/PR8 in the MDCK or A549 cells (B). Antiviral role of minocycline was found to IFN-independent as reduction in viral titre and NS1 protein expression was observed in minocycline treated IFN signalling deficient vero cells (C).

4.2.3 Minocycline prevents the shuttling of vRNPs from the nucleus to cytosol by inhibiting ERK pathway

The processes of vRNPs import and export are obligatory phases of influenza virus cycle (Bui and Helenius, 1996). The host cellular localization of vRNPs at 18 and 24 hpi was assessed, after treatment with either DMSO or minocycline (500nM) to IAV/PR8-infected MDCK cells by immunolabelling viral nucleoprotein NP, key component of viral RNP complex. Nuclear accumulation of NP proteins in minocycline treated IAV/PR8 infected cells at 18 and 24 hpi was observed in immunofluorescence microscopy compared to those of DMSO-treated cells (**Fig. 4.4A, B**). As revealed by western blotting using the whole cell, nuclear and cytoplasmic fractions of minocycline-treated IAV infected cells, NP protein showed accumulation in the nucleus at 24-hour time point but not in early time point 6hpi (**Fig. 4.4E**), implying the role of minocycline in modulating the export of vRNP from the nucleus. Previous reports have shown nuclear export of vRNPs is regulated by the cellular kinase ERK (Pleschka et al., 2001; Ludwig et al., 2004). Consistent with the findings, immunofluorescence and western blot data also substantiated the nuclear accumulation of NP following treatment with ERK inhibitor (**Fig. 4.4A, 4.5E**). To demonstrate the effect of minocycline on the ERK signalling, cells were treated with either minocycline or ERK inducer PMA alone or in the combination for 18-hours to assess the effect on phosphorylation of ERK1/2 using western blotting. Effect of minocycline as illustrated in **fig. 4.5A-D** were monitored in both MDCK and A549 cells, which resulted in reduction of PMA-induced phosphorylation of ERK1/2 and also in IAV-induced phosphorylation of ERK1/2 at 24hpi. Induction of ERK pathway by IAV HA protein has already been reported (Marjuki et al., 2006). Therefore, we further assessed the ERK inhibition potential of minocycline in HEK293T cells transiently overexpressed with pcDNA3-HA. As expected, minocycline treatment caused a decrease in ERK-induced phosphorylation in HA overexpressing cells (**Fig 4.4C**), thereby confirming that inhibitory action of minocycline on ERK signalling.

A



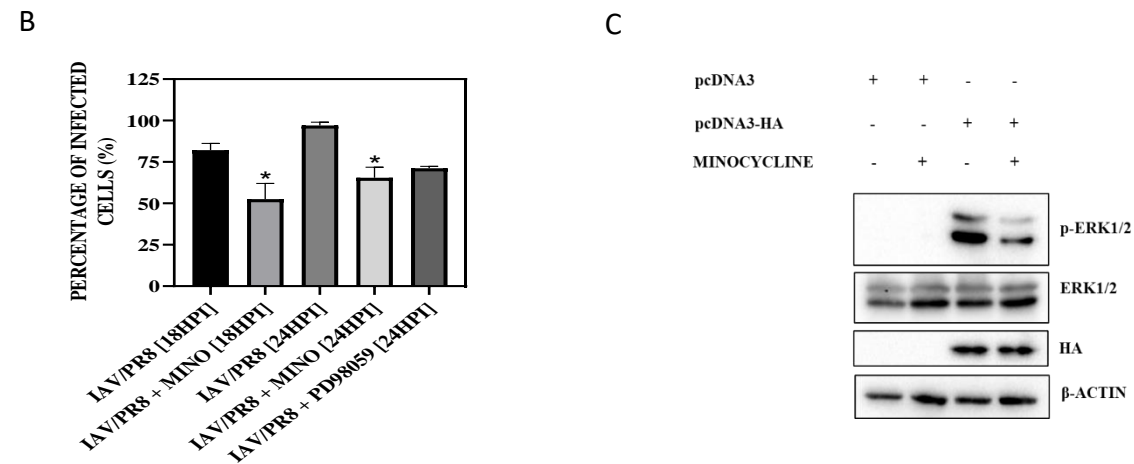
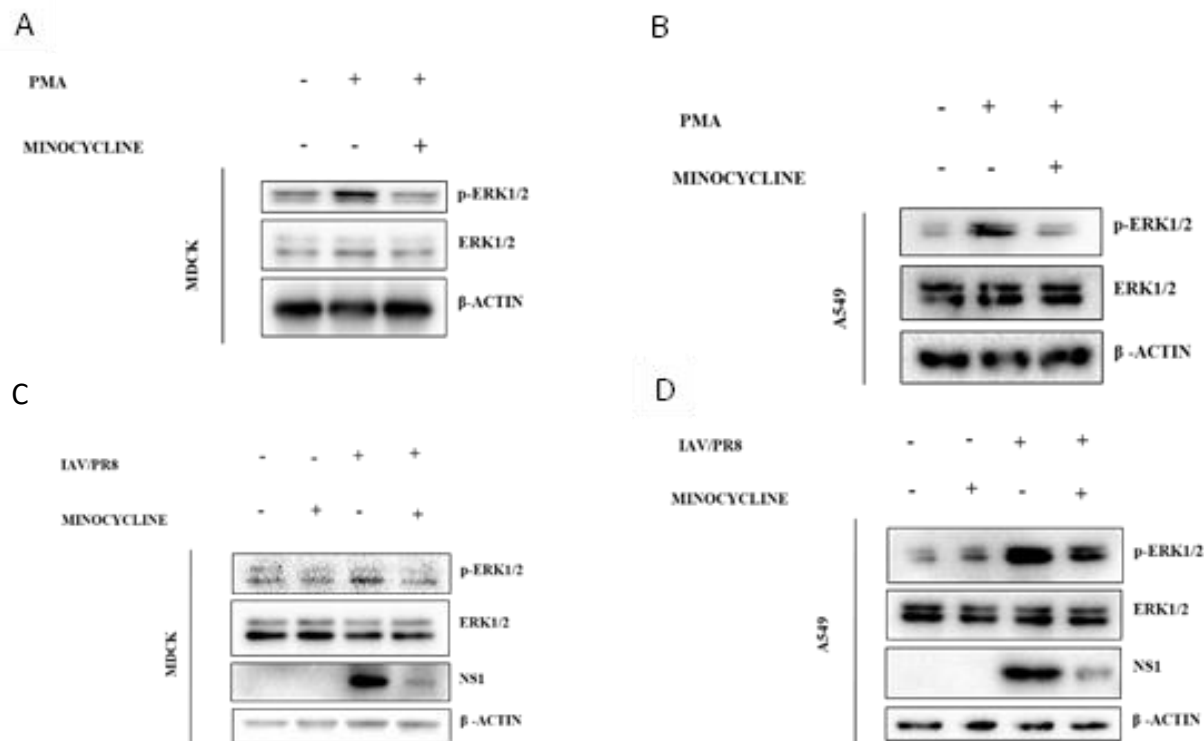


Figure 4.4: (A-B) IAV/PR8 infected MDCK cells treated with minocycline (500 nM) or PD98059 (30 μ M) and incubated for 18 and 24 hpi. Cells were then fixed, permeabilized and stained with anti-NP antibody (raised in mouse). Cells were then secondary stained with DyLight488 labelled anti-mouse secondary antibody. Cells were mounted using DAPI and visualized under confocal microscope (63X oil immersion). Scale bar: 20 μ m. NP positive cells were quantified and randomly 100 cells from different fields were selected and analysed. Data was represented as percentage of infected cells; (C) HEK293 cells were transfected with only pcDNA3 vector and pcDNA3-HA plasmid and treated with 500 nM of minocycline for 24 hrs, cells were lysed and western blot was performed to detect the level of phospho-ERK



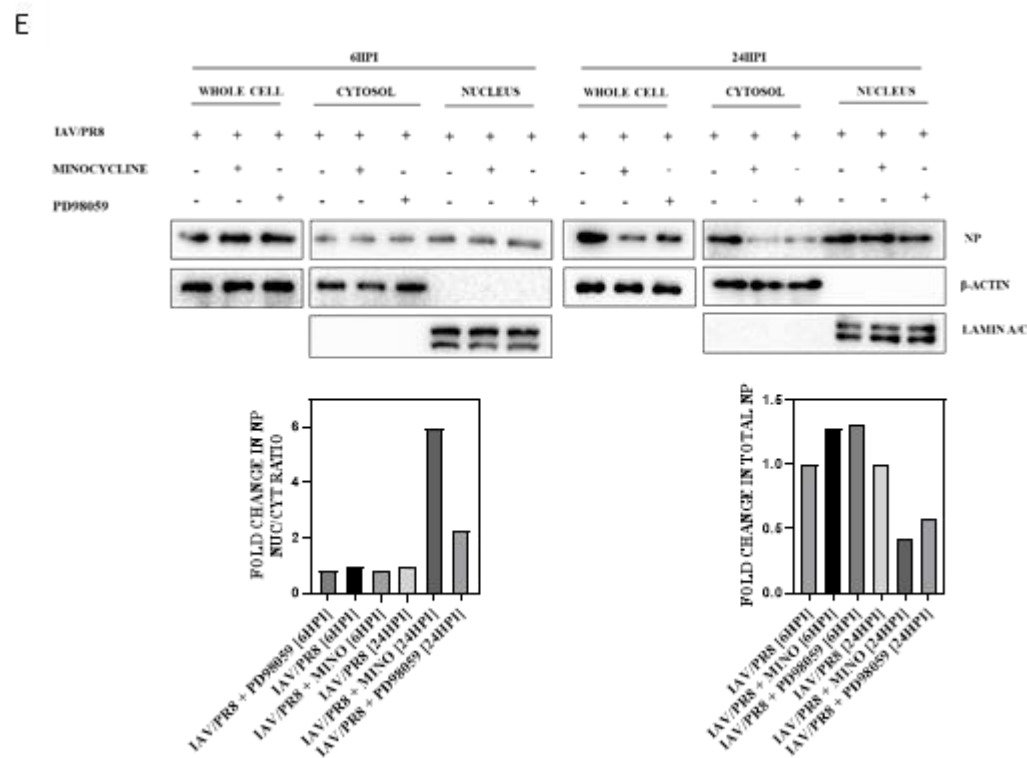
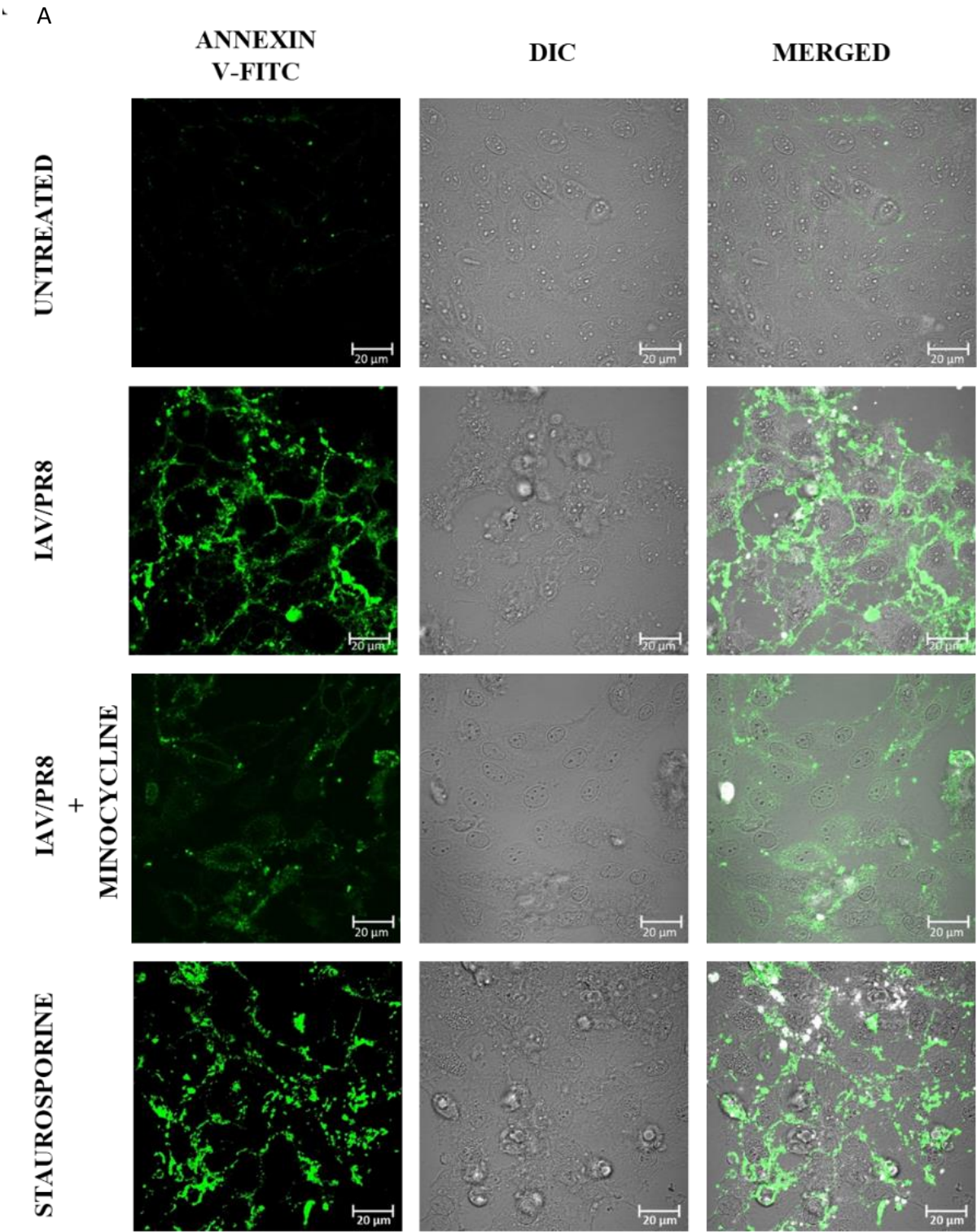


Figure 4.5: Minocycline suppresses ERK signalling pathway in both MDCK cells and A549 cells. (A-D) IAV/PR8 activates ERK cascade, leading to phosphorylation of ERK. Treatment with minocycline reduces the phosphorylation of ERK in PMA-induced cells and IAV/PR8 infected cells; (E) Whole cell lysate and Cytosol-nucleus is extracted and NP protein was shown to be located in the nucleus of the minocycline-treated IAV/PR8 infected cells in 24hpi. Densitometric analysis of blots for NP, Lamin and β -actin was done as represented as fold change in total NP protein and fold change in nuclear/cytoplasmic ratio of NP protein (E).

4.2.4 Minocycline impedes IAV-induced late-stage apoptosis

The induction of apoptosis during IAV life cycle at later stages has been observed to be crucial in releasing progeny viruses and spreading the virus (Lowy, 2003). Previous reports state anti-apoptotic role of minocycline (Wang et al., 2003; Kelly et al., 2004; Zhang et al., 2017; He et al., 2021). Therefore, to confirm its anti-apoptotic role, MDCK cells were subjected to treatment with an apoptosis inducer staurosporine in presence or absence of minocycline for 6 hours followed by assessment of caspase-3 level cleavage. The minocycline treatment attenuated staurosporine-elicited caspase-3 cleavage (Fig. 4.6C). The cleavage of caspase-3 was inhibited in minocycline-treated IAV-infected cells but not in DMSO-treated cells at both the 24-hpi and 48-hpi time points (Fig. 4.6D). Cleaved caspase 3/pro-caspase 3 ratio reveals reduction in caspase cleavage in minocycline-treated staurosporine-induced or IAV-infected cells at 24 and

48 hpi. Labeling of apoptotic cells by Annexin V-FITC revealed significant reduction of apoptotic cell number in minocycline treated IAV-infected cells (**Fig. 4.6A, B**). Finally, these results suggest that minocycline also modulates IAV-induced late-stage apoptosis which is required by virus for dissemination.



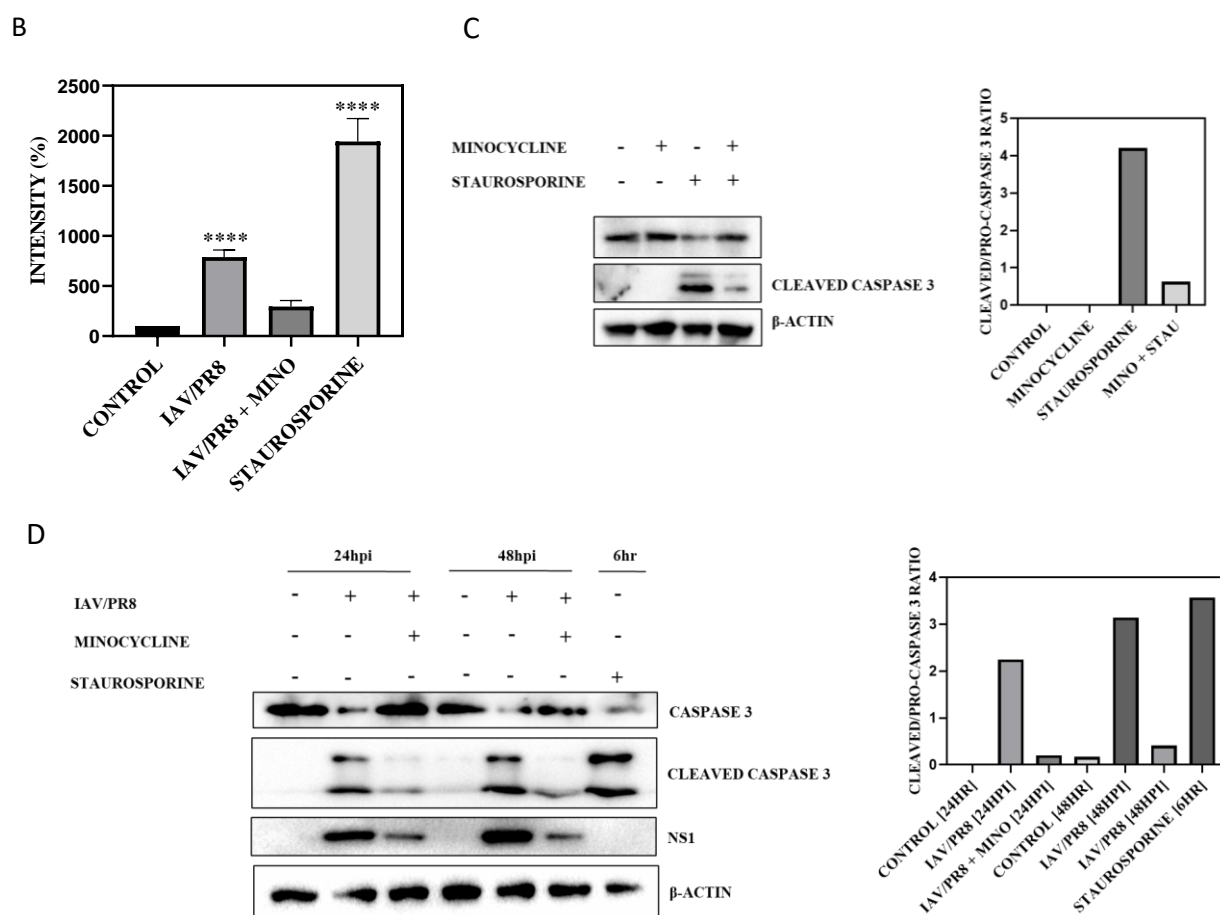


Figure 4.6: (A-B) Annexin V Apoptosis assay confirmed the inhibition of apoptosis in presence of minocycline. Caspase 3 cleavage is inhibited in both minocycline treated IAV/PR8-infected cells and Staurosporine-induced cells (C-D).

4.2.5 Minocycline treatment attenuates IAV infection *in vivo*

Once *in vitro* activity of minocycline against IAV was established, therefore its antiviral potential was assessed in mice model. Initially, minocycline was orally given to BALB/c mice (4-6 weeks, n=3) with the doses ranging from 5 mg/kg/day to the maximum of 30 mg/kg/day and the control group was given only vehicle (DMSO). Then, body weight was monitored throughout the treatment cycle of 5 days. No significant change in body weight at all doses of minocycline and time points was observed when compared with the vehicle control (DMSO) (Fig. 4.7A), indicating that dose up to 30mg/Kg/day was well tolerated. HE staining of vital organs (lung, liver, kidney and heart) of mice treated with high dose of minocycline (30 mg/kg/day) along with the control group treated with the DMSO vehicle demonstrated that minocycline had no noticeable cytotoxicity (Fig. 4.8A).

Mice ($n = 3$) were exposed intranasally to IAV/PR8 on day 1, from the next day they were given oral minocycline therapy (30 mg/kg/day) till day 15. Change in the body weight and the survival was noted **Fig. 4.7C**. The data illustrates a protective effect manifested by this compound, which ascend the survival rate to 67% in the minocycline-treated mice. The DMSO-treated IAV infected mice did not survive over 10 days. Though the body weight of vehicle-treated IAV-infected mice reduced rapidly with almost 75% achieved by day 8-9. In contrast, IAV infected mice treated with minocycline or ribavirin showed loss of body weight till day 6, followed by gain in weight (**Fig. 4.7C**). Additionally, to observe whether or not minocycline has anti-IAV potency, viral titre in the lungs of infected mice were estimated ($n=5$). A lower viral titre was noted in the lungs of IAV/PR8 viral infected mice treated with minocycline in comparison to the infected mice which were treated with DMSO (**Fig. 4.7D**). Additionally, diminished levels of both IAV transcript and NS1 protein in the lungs of IAV-infected mice and minocycline treated mice was observed (**Fig. 4.7E, F**) compared to those of DMSO-treated mice. Cytological analysis (HE staining) showed the majority of the infected mice had lesions (Influenza-induced lung pathology), while the majority of the minocycline-treated mice IAV infected but minocycline-treated mice showed little lesions. Pulmonary pleura invagination, significantly thickened pulmonary septa and inflammatory cells infiltration (pointed with the red arrow) were seen in the lungs of mice infected with PR8 subtype of influenza virus. These effects were significantly decreased in mice that were given minocycline (**Fig. 4.8B**). Only minocycline or DMSO treatment had no effect on lung pathology.

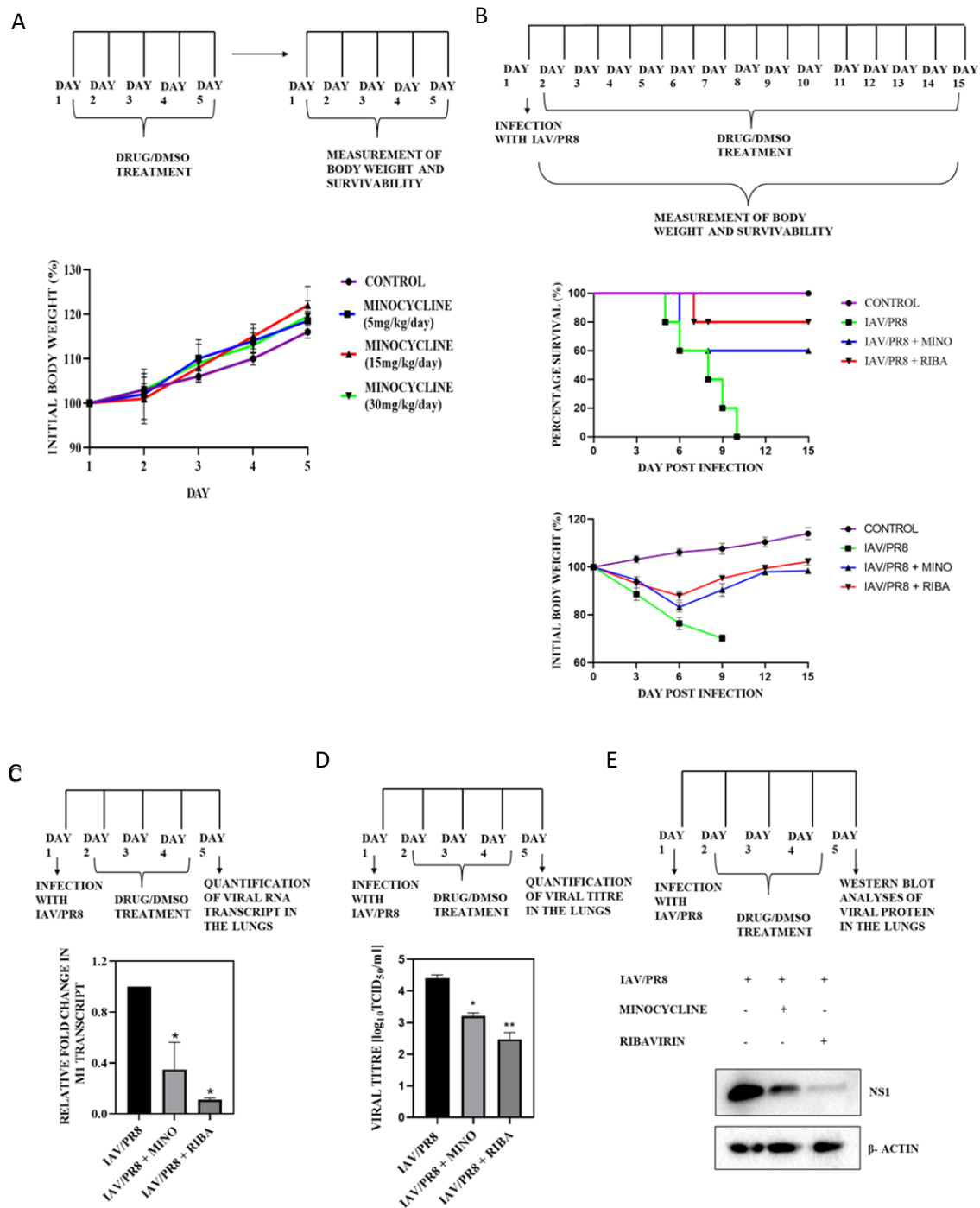


Figure 4.7: (A) BALB/c mice (5 mice/group) were treated with 5, 15 and 30mg/Kg/day of minocycline for 5d to test the toxicity level. Weight of mice were weighed daily for 5d. (B) Intranasal infection with the IAV/PR8 (4 x 50% Lethal doses, MLD₅₀) to BALB/c mice (5 mice per group). On day 2, mice received treatment with 30 mg/kg/day of Minocycline or DMSO till 15th day. Body weight and survivability were measured for every mouse over 15d. (C-E) Viral RNA from lungs tissue at 5dpi and viral proteins were detected. The viral titre was measured in lungs in terms of TCID₅₀/ml.

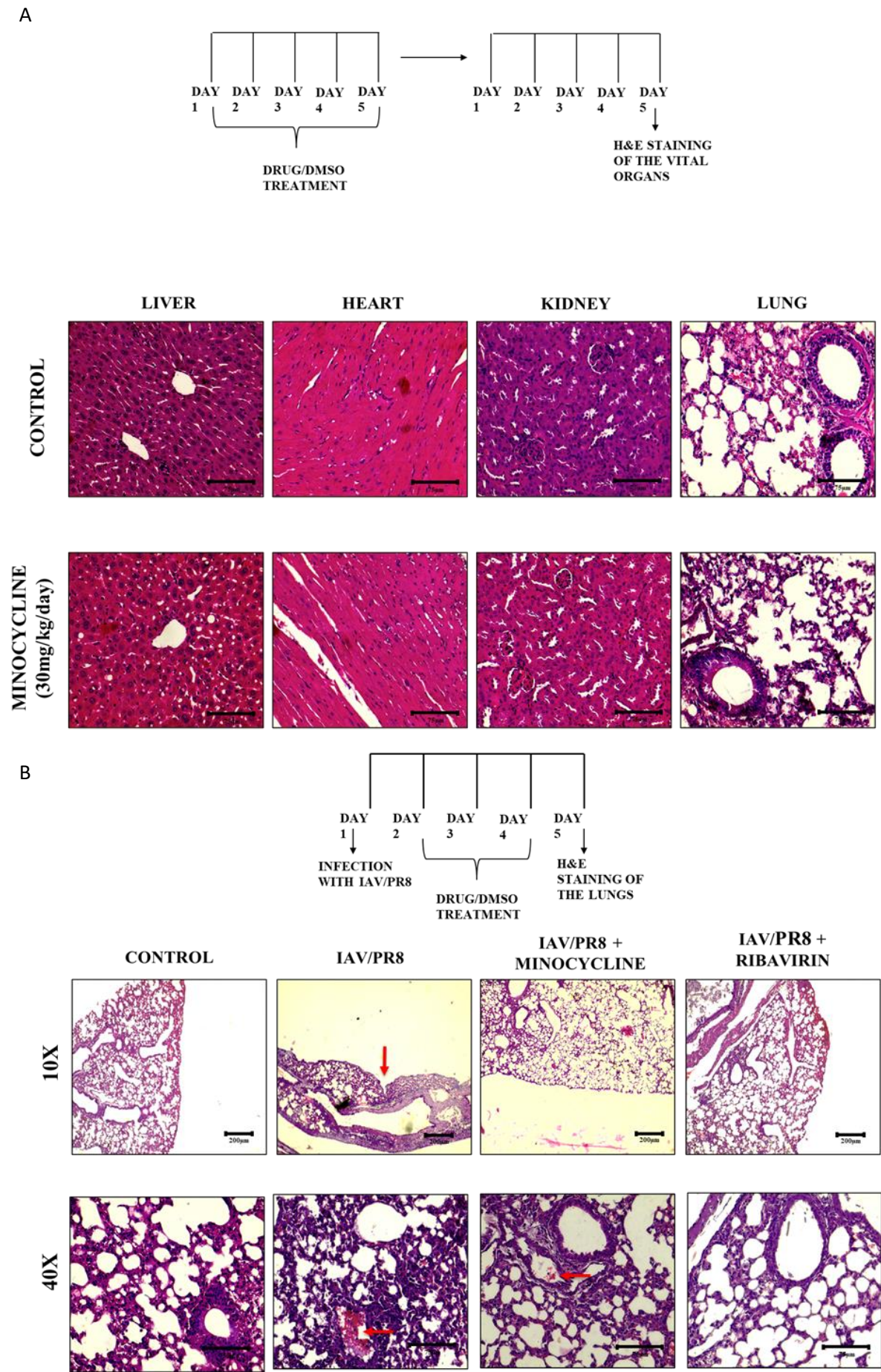


Figure 4.8. (A) BALB/c mice (5 mice/group) received treatment with 30 mg/kg/day of Minocycline or DMSO. The HE staining was performed on vital organs- lung, heart, kidney and liver tissues. (B) The HE staining was performed on lung tissues, and tissue integrity was viewed at 10X and 40X magnifications in microscope.

4.3. Discussion

The continuous antigenic drift in influenza virus is a major determinant in long term efficacy of antivirals against viral protein. The alteration of epitopes and the emerging recombinant genetic viruses prevent the antivirals, have prevented NA inhibitors and M2-ion channel blockers to work at optimum efficiency. Thus, in pursuit of developing newer alternatives, focus has shifted towards host directed antivirals (HDAs) or drug repurposing. Drug repurposing allows one to test antiviral potential of available drugs which were developed for other diseases such as antibacterials, anticancer etc (TAKATSUKI and TAMURA, 1971; Kaptein et al., 2010; Abdulaziz et al., 2022; Raymonda et al., 2022). The tetracycline analogue minocycline, which was brought to market in 1967, has been used for control and management of rickettsial infections, syphilis, pimples, etc (Shutter and Akhondi, 2023). According to the Infectious Diseases Society of America (IDSA) in 2022, minocycline therapy was proposed as treatment against carbapenem-resistant *Acinetobacter baumannii* and *Stenotrophomonas maltophilia* (Tamma et al., 2022).

Double-stranded DNA and RNA viruses including Influenza viruses involve MAPK pathway for viral gene expression (Daum et al., 1994; Benn et al., 1996; Rodems and Spector, 1998; Kujime et al., 2000; Ludwig et al., 2001; Planz et al., 2001; Terstegen et al., 2001; Barber et al., 2002). The MAPK signaling pathway involves the phosphorylation of kinase Raf via MEK followed by ERK that results in its transport into the nucleus to the phosphorylation of a number of substrates (Treisman, 1996; Robinson and Cobb, 1997). Replication of IAV takes place in the nucleus after this, it translates, and assembles in the cytosol. Post translation, viral proteins (PA, PB1, PB2 and NP) are shuttled into the nucleus where it interacts with the newly produced vRNPs, which were then exported from the nucleus for the purposes of viral assembly and dissemination. It is postulated that the presence of HA protein in the membrane results in ERK1/2 phosphorylation which stimulates the process of vRNP export from the nucleus (Ludwig et al., 2006). Mode of action of minocycline is its suppression of ERK phosphorylation, this occurs even in cells overexpressing HA, and as a result vRNPs do not

translocate into the nucleus (**Fig. 4.9**). ERK cascade, which is responsible for the dispersion of IAV, was blocked by antagonist PD9089. Hence, the discharge of vRNPs was terminated.

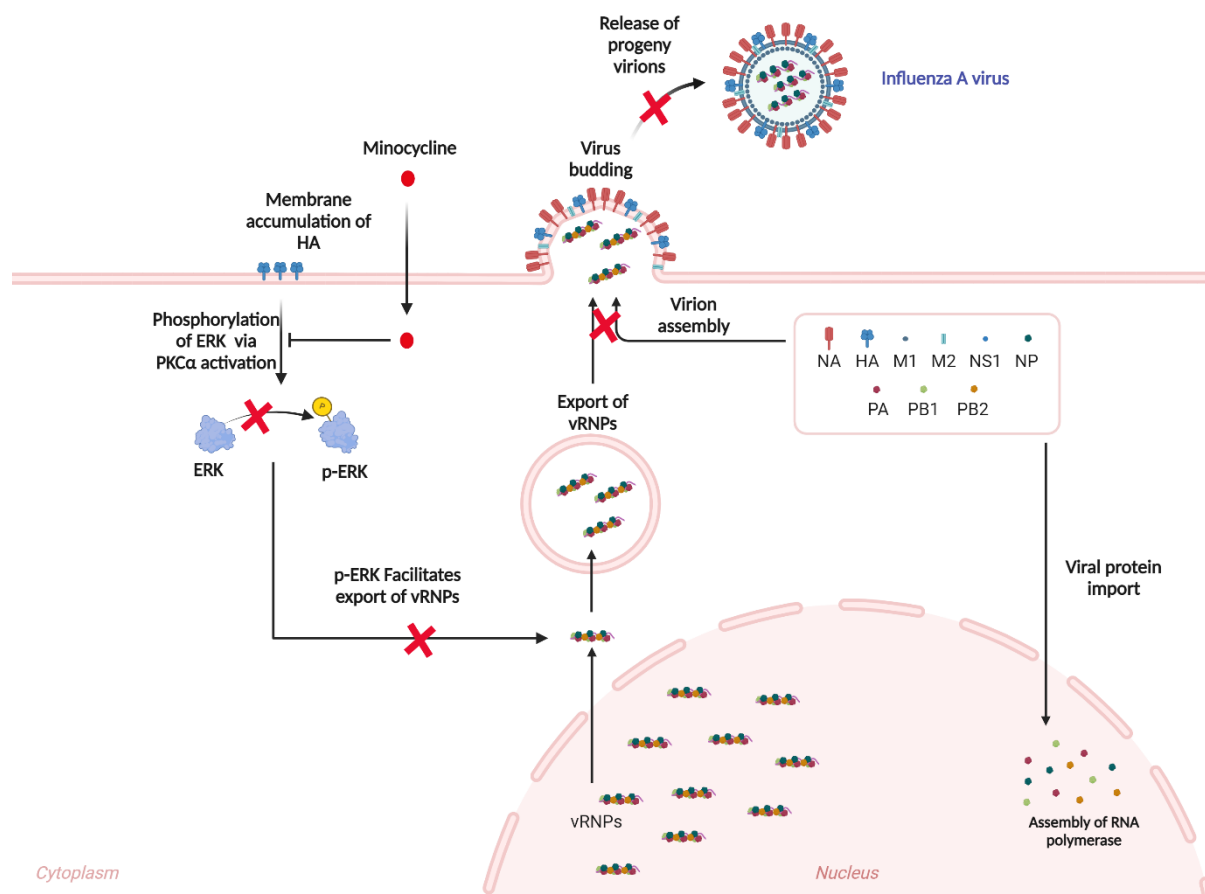


Figure 4.9: Illustration of the role of minocycline in hindering the export of vRNPs from the nucleus leading to inhibition of viral assembly and dissemination.

The induction of apoptosis of the host cell in the last stage of life cycle by IAV is essential for the release of progeny virions (Ludwig et al., 2001; Lowy, 2003; Brydon et al., 2005). The pro-apoptotic and anti-inflammatory functions of minocycline are already established but it has been found that it inhibits apoptosis in JEV infection (Garrido-Mesa et al., 2013) (Dutta et al., 2010). This research also proved that staurosporine (an inducer of apoptosis) and IAV-induced apoptosis were blocked by minocycline. Altogether, it has been revealed in the study that minocycline exerts antiviral activity against IAV by integrating both inhibition of apoptosis and

blockage of nuclear export of vRNP. It may have additional indirect impact on the virus replication cycle which needs to be studied indepth. The study results suggest that minocycline, an FDA-approved drug and widely used as a broad-spectrum antibiotic can be repurposed into an antiviral therapy.



Chapter 5

Assessing antiviral property of small synthetic molecules and its mechanism of action

5.1. Introduction

Influenza A viruses continue to pose a serious threat to public health in terms of death and morbidity. Additionally, with currently circulating high pathogenic avian influenza strains as H5N1 and H9N2, future inter genotypic reassortment events cannot be ruled out (Gerloff et al., 2014;Shanmuganatham et al., 2014;Bergervoet et al., 2019). Hemagglutinin (HA) and Neuraminidase (NA), two viral surface glycoproteins, must work in precise harmony for the influenza life cycle to occur. As a fusion protein, HA aids in the fusing of the endocytosed virus particle with the endosomal membrane of the host cell after attaching to the sialic acid (SA)-containing surface receptors. The internalization of the virus is caused by this. The α -ketosidic connection between SA and the nearby sugar residue is broken by NA, an exosialidase (Liu et al., 1995;Sheng et al., 2011).

Oseltamivir (OMV) and zanamivir (ZMV), two currently prescribed anti-influenza medications, are structurally identical to SA and, as a result, have a comparable pattern of binding to the NA enzyme. However, because of NA gene alterations, their effectiveness as competitive inhibitors is limited (Kim et al., 1999;Yen et al., 2006). This confirms the need for a different strategy in the design and synthesis of novel compounds that will be created as possible anti-influenza medicines. This might be accomplished through the identification of fresh scaffolds with alternative binding patterns in the enzyme cavity and structural differences from OMV/ZMV. By creating non-competitive inhibitors that inhibit the enzyme by binding allosterically to the target enzyme, the resistance issue towards competitive inhibitors of NA, i.e., OMV and ZMV, could be avoided. The SA/OMV binding site in NA has two cavities nearby: the 150-cavity and the 430-cavity. These two cavities might be thought of as potential additional binding sites for NA.

Numerous NA subtypes have been potently inhibited by compounds that bind to 150-cavity and 430-cavity receptors (Feng et al., 2013;Xie et al., 2014). In fact, in recent years, our lab team's discovery of various molecules led us to a series of chalcones that showed noncompetitive inhibition mechanism towards H1N1-NA and H5N1-NA as well as specific other scaffolds that showed anti-influenza activities against H1N1-NA (S Chintakrindi et al., 2016;Chintakrindi et al., 2018;Malbari et al., 2019). We chose chalcones, which are distinguished by α , β -unsaturated carbonyl functional groups, among a number of documented antiviral phytoconstituents. But chalcones have also been shown to exhibit cytotoxicity and poorer anti-influenza efficacy (Dao et al., 2010;Ryu et al., 2010;Dao et al., 2011;Nguyen et al.,

2011). This scaffold can be altered to create a variety of cyclized derivatives, including aurones, flavones, 3-indolinones, and 4-quinolones, as cyclized rigidification has been shown to increase a lead molecule's activity (Patrick, 2013). The chosen parent scaffold, chalcones, can be appropriately compared to other phytoconstituents possessing α , β -unsaturated carbonyl functional groups that have antiviral action, such as cinnamic acid derivatives (Stankyavichyus et al., 1988; Gravina et al., 2011; 天野稜大, 2019). Additionally, the piperazine moiety was chosen and connected to the cinnamic acid scaffold by molecular hybridization method since it has a wide range of activities and is a frequent scaffold in many medications (Martin, 1997; Viegas-Junior et al., 2007). The design, synthesis, and assessment of a series of four scaffolds, including aurones, 3-indolinones, 4-quinolones, and cinnamic acid-piperazine (CAPI) hybrids, against the influenza A/H1N1pdm09 virus are therefore reported here in light of the aforementioned facts and changes. The transition state of sialo-glycoconjugate being hydrolyzed by viral NA, the substrate for NA, is structurally distinct from the scaffolds that have already been chosen and stated. They were created by adding substituents with various functional groups, giving the molecules' electronic, steric, and volume effects.

The molecules that were chosen based on docking results and cytotoxicity were subjected to cytopathic effect (CPE) inhibition and hemagglutination inhibition (HAI) assays in order to screen them for further in-depth evaluation studies based on % CPE inhibition and % HA titer reduction of virus with candidate molecules. All of the compounds that passed the screening process had their EC₅₀ values determined using a cell-based assay, and then their IC₅₀ values were determined using an enzyme-based assay. Additionally, the compounds' mechanism of inhibition was discovered by Investigations on the kinetics of enzymes revealed non-competitive inhibition when compared to OMV, a competitive inhibitor. This supports our theory about creating future anti-influenza agents and suggests more effective therapeutic and preventative outcomes than what we can get from anti-influenza medications right now.

5.2. Results: Evaluation of anti-influenza activity of the designed molecules

Oseltamivir phosphate (OMVP) was used for the cellular assays such as the MTT, CPE, HAI, and CV because cells contain the esterase enzyme that converts the drug to its active metabolite, oseltamivir. Oseltamivir carboxylate was employed directly as the standard for enzymatic experiments, such as the NA inhibition assay and enzyme kinetics investigations. The benchmarks for reflecting the competitive and non-competitive inhibition, OMVP/OMVC and

quercetin [QR, the reported natural non-competitive inhibitor], were chosen, respectively (Jeong et al., 2009).

5.2.1. Cytotoxicity studies of the designed molecules

The concentration of synthetic compounds that causes a 50% reduction in cell viability (CC50) was identified by cytotoxicity tests. Except for molecule 4d, which had a CC50 of 40M, the findings of the MTT-Formazan test for cytotoxicity analysis of 27 synthesized compounds showed that they had no significant impact on MDCK cells (**Table 5.1**). Further testing of the anti-influenza action of these non-cytotoxic compounds looked at how much the presence of the molecules reduced the influenza A/H1N1pdm09 strain's cytotoxic effect (CPE) in MDCK cells.

Code	Molecules	CC ₅₀ (μM)	EC ₅₀ (μM)	SI (μM)	IC ₅₀ (μM)	KI (μM)
C2	4-amino-4-methoxy-chalcone	51.6	0.99 ± 1.07	51.12	15.67 ± 1.16	-
C7	4-amino-3-hydroxy-chalcone	116.0	2.84 ± 0.83	40.84	14.28 ± 1.04	2.05 ± 1.73
C8	4-amino-4-hydroxy-chalcone	111.2	>100	-	-	-
C9	3-hydroxy-4-methoxy-chalcone	112.6	1.8 ± 0.99	62.55	3.85 ± 1.19	11.23 ± 2.83
A1	3-methoxy-aurone	193.0	>100	-	-	-
A2	4-methoxy-aurone	170.6	1.46 ± 0.87	116.84	9.27 ± 1.41	10.52 ± 0.66
A3	3-chloro-aurone	120.1	1.02 ± 1.3	117.74	14.97 ± 1.19	-
A4	4-chloro-aurone	112.6	0.0388 ± 2.03	2902.06	1.82 ± 1.26	-
A5	4-nitro-aurone	110.7	>100	-	-	-
I1	2-methoxy-indolone	263.4	5.10 ± 0.94	51.64	20.95 ± 1.27	-
I2	3-methoxy-indolone	292.4	0.0246 ± 1.24	11886.18	22.38 ± 1.26	-
I3	4-methoxy-indolone	286.6	11.94 ± 1.33	24.00	0.516 ± 1.32	2.57 ± 1.2
I4	3,4,5-trimethoxy-indolone	127.9	0.17 ± 0.55	752.35	19.78 ± 1.27	-
I5	2-chloro-indolone	269.1	3.06 ± 1.22	87.94	19.38 ± 1.20	-
I6	3-chloro-indolone	272.4	0.00402 ± 1.42	67761.19	17.62 ± 1.44	2.79 ± 2.13
I7	4-chloro-indolone	191.8	0.00672 ± 1.34	28541.67	8.73 ± 1.36	1.98 ± 2.95
I8	3-hydroxy-indolone	115.4	0.25 ± 1.26	461.6	15.70 ± 1.21	33.72 ± 2.25
Q1	2-methoxy-quinolone	286.1	0.00496 ± 1.03	57681.54	10.53 ± 1.16	-
Q2	3-methoxy-quinolone	234.6	>100	-	24.33 ± 1.27	-
Q3	4-methoxy-quinolone	276.9	>100	-	3.80 ± 1.41	53.59 ± 8.9
Q4	3,4,5-trimethoxy-quinolone	199.9	>100	-	12.16 ± 1.14	2.79 ± 0.99
Q5	2-chloro-quinolone	180.5	>100	-	18.36 ± 1.22	-
Q6	3-chloro-quinolone	163.2	>100	-	16.98 ± 1.39	-
Q7	4-chloro-quinolone	163.3	0.22 ± 1.18	742.27	3.46 ± 1.28	7.12 ± 1.94
Q8	3-nitro-quinolone	116.9	78.94 ± 1.07	1.48	6.36 ± 1.15	8.44 ± 1.34
Q9	4-nitro-quinolone	118.4	>100	-	16.46 ± 1.18	-
CA4	4-methoxy-cinnamic acid	294.6	>100	-	-	-
CA11	4-hydroxy-cinnamic acid	264.7	>100	-	-	-
CAPI1	Unsubstituted-cinnamic acid-piperazine derivative	154.5	3.58 ± 1.47	43.16	15.39 ± 1.75	-
CAPI2	2-methoxy-cinnamic acid-piperazine derivative	106.2	5.1 ± 1.28	20.82	24.55 ± 1.29	-
CAPI3	4-methoxy-cinnamic acid-piperazine derivative	137.4	7.75 ± 1.31	17.73	18.35 ± 1.24	-
CAPI4	3,4-dimethoxy-cinnamic acid-piperazine derivative	40	>100	-	12.49 ± 1.87	-
CAPI5	4-chloro-cinnamic acid-piperazine derivative	189.4	6.71 ± 0.92	28.23	11.18 ± 1.71	-
BZ1	Benzyl-benzimidazole	123.7	>100	-	-	-
BZ2	Benzyl-sulfanyl-benzimidazole	154.8	>100	-	-	-
BZ3	Phenyl-sulfanyl-methyl-benzimidazole	148.3	>100	-	-	-
BZ4	6-Chloro-methyl-benzimidazole	172.5	>100	-	-	-
BZ5	6-Chloro-benzyl-sulfanyl-benzimidazole	109.2	0.013 ± 1.15	8400	1.31 ± 1.57	-
BZ6	6-Chloro-phenyl-sulfanyl-methyl-benzimidazole	119.0	57.8 ± 1.19	2.06	17.40 ± 1.69	-
BZ7	6-Nitro-methyl-benzimidazole	164.9	>100	-	-	-
BZ8	6-Nitro-benzyl-sulfanyl-benzimidazole	176.9	>100	-	-	-
QR	Quercetin	253.8	0.56 ± 1.22	453.21	8.72 ± 1.13	5.12 ± 1.18
OMV	Osetamivir	713.4	0.0127 ± 0.34	56173.23	0.00197 ± 1.36	0.00028 ± 0.03

Table 5.1: Cell-based EC₅₀, Enzyme-based IC₅₀ and K_i values of synthesized molecules obtained by crystal violet, NA-inhibition and enzyme kinetics assays.

5.2.2. Estimation of cytopathic effect (CPE) inhibition of the molecules

To determine the level of viral inhibitory activity of the molecules following comparison with OMVP as the reference medication, a qualitative evaluation study using the CPE inhibition assay of all twenty-seven synthesised molecules was conducted. It is interesting to note that infected cells treated with our synthetic molecules showed a significant reduction in CPEs, which are loss of cell adhesion-related symptoms of influenza A/H1N1pdm09 virus infection. This finding further supports the strong cyto-protective and anti-influenza properties of these molecules. **Table 5.2** shows how much each assessed chemical inhibited viral CPE. All of the compounds demonstrated at least a 50% CPE inhibition, indicating that they have a significant capacity to lower viral load. They were then carried forward for additional tests.

Code	Degree of Inhibition	Code	Degree of Inhibition	Code	Degree of Inhibition
C1	+	I7	+++	CA8	+
C2	+++	I8	+++	CA9	-
C3	++	Q1	+++	CA10	+
C4	+++	Q2	++	CA11	++
C5	+++	Q3	++	Lik-1	-
C6	+++	Q4	++	Lik-2	-
C7	+++	Q5	++	Lik-3	-
C8	++	Q6	++	CApi1	++
C9	+++	Q7	+++	CApi2	++
A1	++	Q8	++	CApi3	++
A2	+++	Q9	++	CApi4	++
A3	+++	P1	-	CApi5	++
A4	+++	P2	+	BZ1	++
A5	++	CA1	-	BZ2	++
I1	+++	CA2	-	BZ3	++
I2	+++	CA3	+	BZ4	++
I3	+++	CA4	++	BZ5	+++
I4	+++	CA5	+	BZ6	+++
I5	+++	CA6	+	BZ7	++
I6	+++	CA7	+	BZ8	++

Table 5.2: Degree of inhibition on CPE of pandemic H1N1 on MDCK cells by all the designed molecules at a concentration of 100 μ M obtained by qualitative CPE inhibition assay. Experiment performed in duplicates. ‘++++’ indicates 100% CPE inhibition, ‘+++’ indicates 75% CPE inhibition, ‘++’ indicates 50% CPE inhibition, ‘+’ indicates less than 50% CPE inhibition and ‘–’ indicates no CPE inhibition.

5.2.3. Determination of viral titer reduction by Hemagglutination inhibition (HAI) assay

By contrasting the virus HA titer in virus control wells with the virus HA titer in molecule-treated wells, the CPE inhibition was further evaluated. Relative viral load, or the HA titer of the molecule-treated infected cells, was expressed as a percentage (% HA titer reduction) in triplicate tests where the vehicle-treated infected control had 100% HA titer infectivity. Standards OMVP and QR were employed, and results on % HA virus titer reduction for all compounds are compiled in **Fig. 5.1**. Data clearly demonstrate that most compounds reduced viral titer by at least 50%, as shown in **Fig. 5.1**, in a robust and lasting manner. The HAI assay results showed that the molecules effectively suppressed the viral titer, with weak-to moderate-to-high potencies as compared to standards (OMVP = 85.4% and QR = 79.4%, at 100 M), further pointing to the anti-influenza action of the molecules. Due to the hazy boundaries between these compounds and the rates of % HA titer decline, it was challenging to determine the link between structure and activity. The compounds were then given more attention so that their anti-influenza activity could be quantitatively assessed.

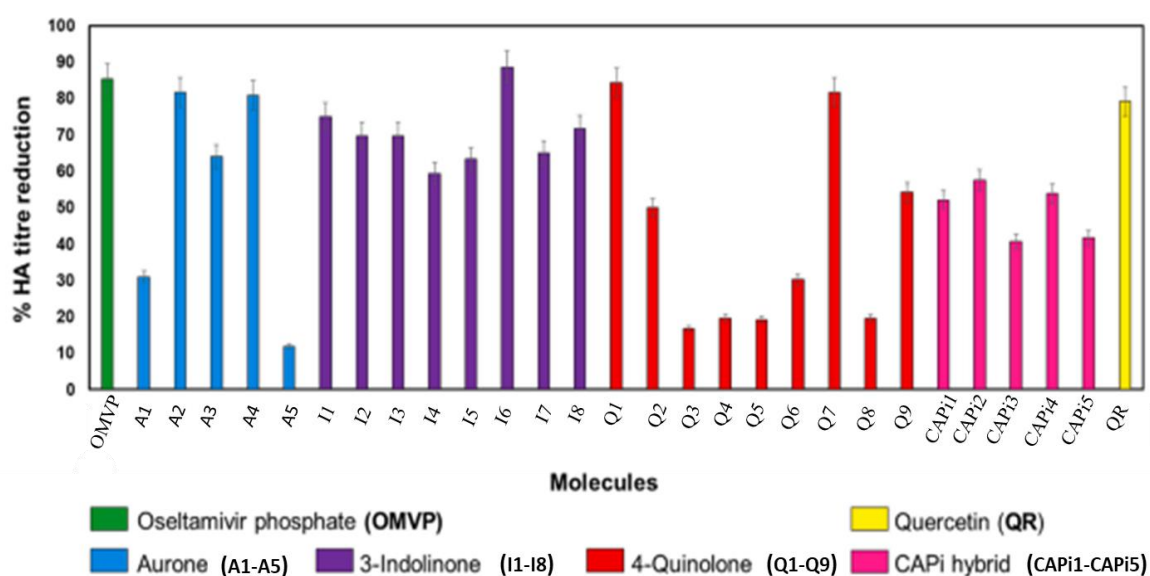


Figure 5.1: Histogram showing percentage of HA titer reduction of virus treated with candidate molecules

5.2.4. Quantification of effective concentration of molecules by cell-based crystal violet (CV) assay

The effective concentration of the investigated compounds (EC_{50}) required to achieve 50% cell survival was quantified using the CV assay. The investigated molecules notably displayed considerable levels of cell survival in the CV assay, which was consistent with the clearly decreased viral HA titer (**Table 5.1**). The most active molecules were I6 (3-indolinone with m-chloro group on benzyl ring), I7 (3-indolinone with p-chloro group on benzyl ring), and Q1 (4-quinolone with o-methoxy group on phenyl ring), which had EC_{50} values better than OMVP ($EC_{50} = 12.7 \pm 0.3$ nM) and QR ($EC_{50} = 0.56$). Although molecules A4 (aurone with a p-chloro group on the benzyl ring) and I2 (3-indolinone with an m-methoxy group on the benzyl ring) had EC_{50} values that were slightly lower than those of OMVP but higher than those of QR, they may still be considered to have exceptional anti-influenza properties. **Fig. 5.1** displays the impact of representative powerful compounds and benchmarks on the percentage of pdmH1N1 virus-infected cells that survive. These findings suggested that these compounds might prevent viral multiplication in MDCK cells as a whole. These chemicals' high selectivity index values showed that they reduced virus replication while having no negative effects on the host cells that were still alive.

5.2.5. Determination of inhibitory concentration of molecules by enzyme-based NA inhibition

The number of molecules needed to block 50% of the enzyme activity (IC_{50}) in H1N1-NA was calculated to be 25, based on the CV assay. **Figure 5.2** displays dose response curves that indicate how our compounds affect the H1N1-NA enzyme. The analysed compounds' IC_{50} values ranged from 0.52 ± 0.01 M to 24.6 ± 1.3 M. The standards used in the enzyme-based assay, OMVC and QR, had IC_{50} values of 1.9 nM and 8.7 nM, respectively (**Table 5.2**). Even while the powerful compounds mentioned in the CV assay had IC_{50} values that were lower than OMVC, they consistently display outstanding activity with IC_{50} values that are, intriguingly, superior to QR. The potent molecules 2f ($IC_{50} = 0.52 \pm 0.01$ M), 2g ($IC_{50} = 3.5 \pm 0.1$ M), and 3a ($IC_{50} = 1.3 \pm 0.2$ M) had lower IC_{50} values than other compounds in the series, continuing the trend of the effectiveness of molecules shown in the CV assay. It's interesting to note that the combined outcomes of the CV assay and NA inhibition assay revealed that the examined compounds inhibit overall viral replication instead of specifically inhibiting NA. These

findings suggested that our examined compounds may regulate virus replication via an additional mechanism, as suggested by their efficacy in vitro.

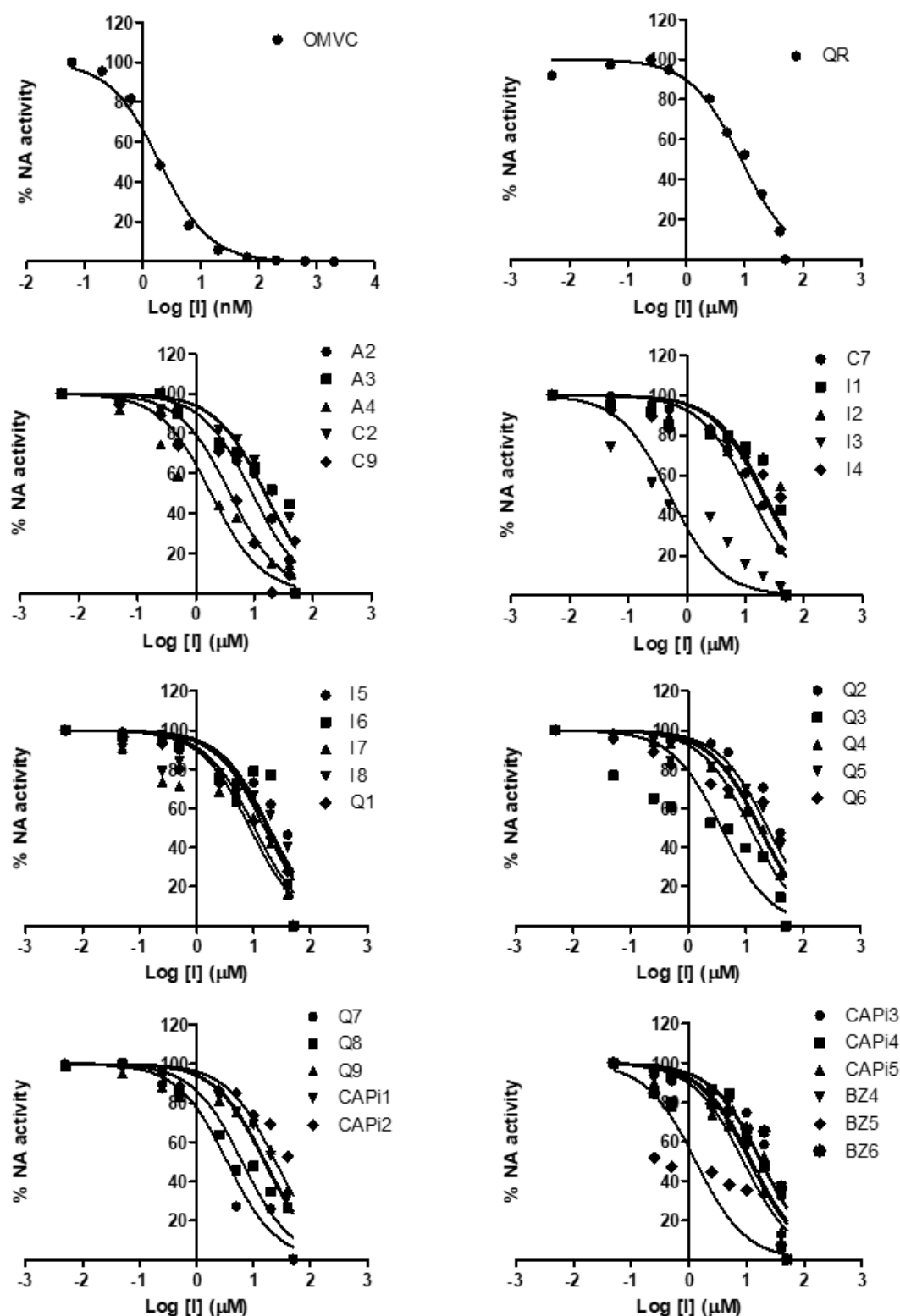


Figure 5.2: Effects of candidate molecules, standard inhibitors i.e. oseltamivir carboxylate (OMVC) and quercetin (QR) on H1N1-NA for hydrolysis of substrate.

5.2.6. Enzyme kinetics studies to evaluate the mechanism of inhibition of molecules

To confirm the noncompetitive inhibition of proposed compounds as shown by docking studies, enzyme kinetics experiments were carried out on the eleven most active molecules (based on CV and NA inhibition assay). In this investigation, the metrics for competitive and non-competitive inhibition were OMVC and QR, respectively. Due to its structural similarity to SA and analogue of its transition state, OMVC naturally exhibited competitive inhibition, as shown by the plots in **Fig. 5.3**'s Lineweaver-Burk plot of $1/V$ vs $1/[S]$. The plots were created by taking into account both the absence of the inhibitor molecule (i.e., at 0 nM concentration) and the two concentrations that fall within its IC_{50} range. Increased OMVC concentrations ($K_i = 2.8$ 10⁻⁴ M) had higher K_m values while leaving the V_{max} unaltered, meaning that their y-axis intercepts were equal but their x-axis intercepts were greater. This demonstrated its inhibition of competition.

Although the K_m remained unaffected, V_{max} showed lowering as the QR concentration increased ($K_i = 5.1$ M), resulting in collections of lines with similar x-axis intercepts and rising y-axis intercept values. This proved the non-competitive mode of inhibition. The Lineweaver-Burk plot of $1/V$ vs $1/[S]$ for our evaluated compounds, however, produced a group of lines as seen in QR, indicating that their method of enzyme inhibition is noncompetitive. In **Fig. 5.3**, the plot for the representative potent molecules.

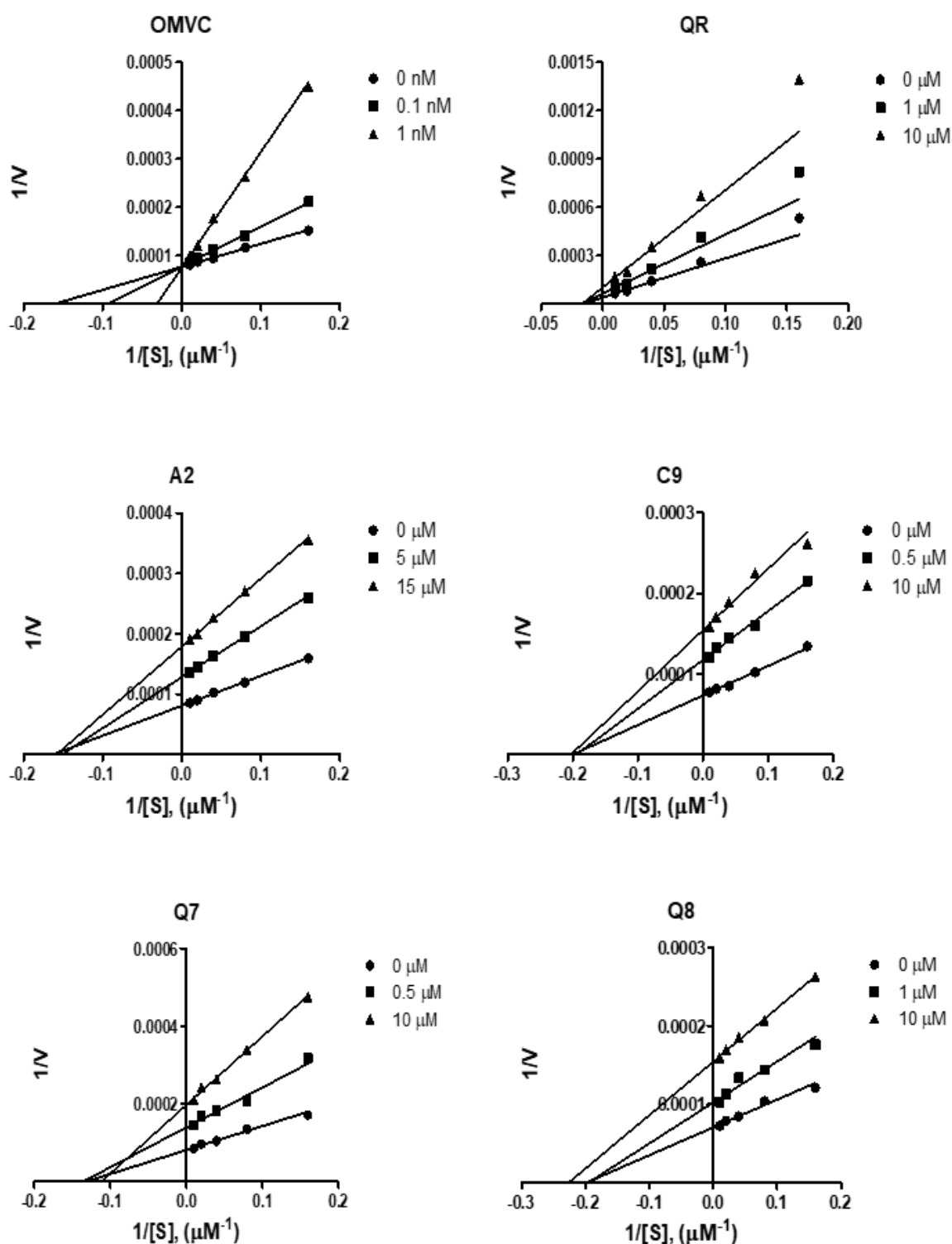


Figure 5.3: Lineweaver–Burk plots of inhibition of oseltamivir carboxylate (OMVC), quercetin (QR) and candidate molecules on H1N1-NA.

Discussion

Widely recognized is the emergence into the pharmaceutical market of relatively new agents against influenza, agents that gradually develop resistance to the classical medication means. Hence, the ensuing table advocates that some of the molecules with antiviral activity demonstrated considerable values against pandemic H1N1 virus. The outcomes of the crystal violet assay as well as NA inhibition experiments support the claim that the compounds of this study, which suppress the viral replication, are more active than their ability to inhibit the NA enzyme alone. CV potency and NA activity of I6, I7 and Q1 molecules were comparable with that of OMVP, with less activity of NA inhibition. These data suggest that in addition to the already known mechanism of virus replication control the current screening molecules might have unknown biological activity as well. Enzyme kinetics suggested that the way of regulatory mechanism of our molecules was the non-competitive one which also well accommodated the predictions made by in-silico studies. The molecules weren't competing for the sialic acid-binding area with sialic acid; rather, they were found in a neighboring and non-competitive elite site in the same active pocket. Hence the potential of these compounds as anti-influenza drugs in the future can be exploited as there is very low possibility of developing resistance. The strategy employed in this study is completely different to the approach used currently for designing antiviral molecules.



Chapter 6

Epilogue

Influenza viruses are known to cause seasonal outbreaks, epidemics and occasional pandemics. That are characterized by widespread acute febrile respiratory illness affecting all age groups, primarily infants, elderly individuals, pregnant women and immune-compromised patients. IAV belongs to the family of Orthomyxoviridae, having eight single-stranded negative sense RNA genome encoding for eleven viral proteins. There are four types of Influenza viruses namely A, B, C and D, out of which type A and B cause pandemic and epidemics. There are 18 types of HA and 11 types of NA subtypes which combine to give rise to 16 subtypes of IAV. IAV are capable of infecting multiple hosts like birds, swine, human, horse and marine mammals. Annually 650,000 deaths due to the viral infection take place globally. Genetic recombination and transmission of IAV between hosts result in its continuous evolution.

Every year WHO modifies the influenza vaccines composition for both the Northern and the Southern Hemispheres based on the data regarding predominant circulating strains. Since the vaccines need to be modified annually to account for mutant virus strains, resulting in overall increased expenditures and restricted coverage especially in low middle income countries. Moreover, without having the statistics on disease load, seasonality, and subtype variations, vaccine policy cannot be formulated. Hence, detection of the virus subtype and vaccine strain selection is only possible through the integrated genetic and antigenic analysis as well as epidemiological survey. One of the objectives of this study was to assess epidemiology of influenza virus in the region.

The positivity rates for A/H1N1pdm09 in Eastern India (16.5%) were significantly lower during 2017 to 2019 than the flu outbreak in 2015 (23.3%) and the outbreak (2017-18) in the Andhra Pradesh (27.68%). India experiences influenza activity year-round, with two distinct patterns of seasonal infection: In hot tropical humid areas, they reach their peak during the monsoon while during winter in areas with a temperate mild climate. Moreover, no seasonality was observed for A/H1N1pdm09 infection in eastern India during 2017-19. Previous studies on seasonal Influenza strain A/H1N1 and A/H3N2 had correlated Influenza positivity with rainfall. Lack of seasonality could be due to passive surveillance in this study where only severe ARI cases were referred from hospitals. The study aimed to analyze sequence variations in Influenza A/H1N1pdm09 strains that circulated during the said time period, which included a new-found glycosylation site in HA along with some specific amino acid residues that were conserved and evolutionarily active. The 130-loop and 220-loop of the receptor binding site of HA protein, remained conserved while S202T and T214A mutations in the 190-helix region were identified in this study. Circulating strains of the virus did not harbor H274Y mutation in

NA protein which causes Oseltamivir resistance. Sequence aligning of isolates from all over the world, showed a sizeable difference on biologically significant positions. It was identified that the vaccine strains A/human/Michigan/45/2015 and A/human/Brisbane/02/2018 has higher degree of homology with strains from Eastern India (98.8% and 99% respectively) while A/human/California/07/2009 showed only 96.9% of homology. Lack of knowledge about vaccine benefits and high cost of the vaccines in India has resulted in low vaccination cover (~1%) leading to seasonal outbreaks and substantially elevated mortality risks. Therefore, the introduction of national influenza vaccination policy tailored to high-risk segments of population.

Vaccines and antivirals against Influenza viruses effectively prevent disease severity and mortality. However, evolution of new subtypes due to point mutations and reassortment of gene fragments, constantly challenge existing treatments and vaccines. Therefore, the need of new drugs and vaccines becomes necessary for the newly emerging strains. Prevention of the influenza virus by the M2 ion channel blockers- amantadine, rimantadine and neuraminidase inhibitors- zanamivir, and oseltamivir, has been established. However, strains resistant to M2 ion channel blockers and/or neuraminidase inhibitors, have emerged following indiscriminate use of antivirals.

To control Influenza virus and associated mortality, alternative antiviral drugs are needed. Drug repurposing and screening of small molecules for its antiviral property are the two possible therapeutic approaches. One potential candidate minocycline, an FDA-approved antibiotic, was assessed for its anti-influenza activity. Minocycline exerted *in vitro* and *in vivo* antiviral activity against influenza A virus. Antiviral activity was independent of interferon signaling. It targeted the MEK/ERK signaling, which is necessary for viral ribonucleoprotein export, thus interrupting the viral assembly and release. In parallel, it also represses caspase-3 dependent apoptosis triggered by IAV infection.

In addition, 27 small molecules were synthesized by a collaborating institute and assessed for anti-influenza activity. Molecular docking study revealed binding of small synthetic molecules (chalcone derivatives) to neuraminidase at an alternate binding site (430-cavity) as compared to its active sialic acid binding site (150-cavity). As these molecules bind to neuraminidase, its enzyme kinetics and mode of inhibition was studied. Enzyme kinetic study illustrated similar mode of inhibition as that of quercetin (a non-competitive inhibitor) instead of oseltamivir (a competitive inhibitor), indicating a non-competitive mode of inhibition. This reveals

minocycline as well as novel small synthetic molecules which can bind neuraminidase could be used as an adjuvant treatment alongside existing therapeutics.

Highlights of this study:

- ❖ During the study period (April'2017-March'2019) 16.5% samples from suspected cases with ILI symptoms were found to be positive for Influenza A/H1N1pdm09.
- ❖ Age groups- 5 to 20 years and above 60 years were more susceptible (19.1% and 19.1% positivity, respectively) to Influenza A/H1N1pdm09.
- ❖ There was no clear seasonal pattern, though the proportion of hospitalizations attributable to A/H1N1pdm09 infection was substantially greater throughout the summer and monsoon months.
- ❖ No gender biasness was observed with respect to Influenza A/H1N1pdm09 infection (15.4% positivity in males and 17.9% in females).
- ❖ Representative strains from Eastern India clustered with A/Human/Michigan/45/2015(H1N1) and A/Human/Brisbane/02/2018(H1N1) strains that were later included in IAV vaccines in lineage 6b.1 (in SH and NH, respectively, for the 2019–20 flu season) for HA gene suggesting that vaccine like strains have been circulating in this region prior to vaccine introduction.
- ❖ None of the isolates included in the study had the Tamiflu (Oseltamivir) resistance mutation H275Y in NA protein.
- ❖ Minocycline, a tetracycline analogue, showed potent anti-influenza virus activity both *in vitro* and *in-vivo* with an SI index of 137.1, suggesting it to be antiviral at non-toxic dose.
- ❖ Minocycline exerted its anti-influenza activity by inhibiting the shuttling of vRNPs from the nucleus to cytosol through modulation of virus-induced activation of ERK pathway.
- ❖ In addition to ERK pathway, minocycline also revealed anti-apoptotic activity, resulting in inhibition of IAV-induced late-stage apoptosis which is crucial for its dissemination.
- ❖ All the chalcone derivatives showed anti-influenza activity *in vitro* with atleast 50% CPE inhibition.
- ❖ Docking study reveals binding of these small molecules (chalcone derivatives) to an alternate binding (430-cavity) site than its active site (sialic acid binding site i.e. 150-cavity) of neuraminidase.

- ❖ Enzyme kinetics showed similar binding pattern of these small molecules as that of quercetin (non-competitive inhibitor), indicating its non-competitive form of inhibition.



Chapter 7

References

- Abdelnabi, R., and Delang, L. (2020). Antiviral strategies against arthritogenic alphaviruses. *Microorganisms* 8, 1365.
- Abdulaziz, L., Elhadi, E., Abdallah, E.A., Alnoor, F.A., and Yousef, B.A. (2022). Antiviral activity of approved antibacterial, antifungal, antiprotozoal and anthelmintic drugs: chances for drug repurposing for antiviral drug discovery. *Journal of experimental pharmacology*, 97-115.
- Acha, P.N. (2001). *Zoonoses and communicable diseases common to man and animals*. Pan American Health Org.
- Agrawal, A.S., Sarkar, M., Chakrabarti, S., Rajendran, K., Kaur, H., Mishra, A.C., Chatterjee, M.K., Naik, T.N., Chadha, M.S., and Chawla-Sarkar, M. (2009). Comparative evaluation of real-time PCR and conventional RT-PCR during a 2 year surveillance for influenza and respiratory syncytial virus among children with acute respiratory infections in Kolkata, India, reveals a distinct seasonality of infection. *Journal of medical microbiology* 58, 1616-1622.
- Agrawal, A.S., Sarkar, M., Ghosh, S., Roy, T., Chakrabarti, S., Lal, R., Mishra, A.C., Chadha, M.S., and Chawla-Sarkar, M. (2010). Genetic characterization of circulating seasonal Influenza A viruses (2005–2009) revealed introduction of oseltamivir resistant H1N1 strains during 2009 in eastern India. *Infection, Genetics and Evolution* 10, 1188-1198.
- Air, G.M. (2012). Influenza neuraminidase. *Influenza and other respiratory viruses* 6, 245.
- Air, G.M., and Laver, W.G. (1989). The neuraminidase of influenza virus. *Proteins: Structure, Function, and Bioinformatics* 6, 341-356.
- Akarsu, H., Burmeister, W.P., Petosa, C., Petit, I., Müller, C.W., Ruigrok, R.W., and Baudin, F. (2003). Crystal structure of the M1 protein-binding domain of the influenza A virus nuclear export protein (NEP/NS2). *The EMBO journal* 22, 4646-4655.
- Al Khatib, H.A., Al Thani, A.A., Gallouzi, I., and Yassine, H.M. (2019). Epidemiological and genetic characterization of pH1N1 and H3N2 influenza viruses circulated in MENA region during 2009–2017. *BMC infectious diseases* 19, 1-22.
- Ali, A., Avalos, R.T., Ponimaskin, E., and Nayak, D.P. (2000). Influenza virus assembly: effect of influenza virus glycoproteins on the membrane association of M1 protein. *Journal of virology* 74, 8709-8719.
- Altschul, S.F., Madden, T.L., Schäffer, A.A., Zhang, J., Zhang, Z., Miller, W., and Lipman, D.J. (1997). Gapped BLAST and PSI-BLAST: a new generation of protein database search programs. *Nucleic acids research* 25, 3389-3402.
- Amorim, M.J., Bruce, E.A., Read, E.K., Foeglein, A., Mahen, R., Stuart, A.D., and Digard, P. (2011). A Rab11-and microtubule-dependent mechanism for cytoplasmic transport of influenza A virus viral RNA. *Journal of virology* 85, 4143-4156.
- Ang, L.W., Tien, W.S., Lin, R.T.P., Cui, L., Cutter, J., James, L., and Goh, K.T. (2016). Characterization of Influenza activity based on virological surveillance of Influenza-like illness in tropical Singapore, 2010–2014. *Journal of medical virology* 88, 2069-2077.
- Aragón, T., De La Luna, S., Novoa, I., Carrasco, L., Ortín, J., and Nieto, A. (2000). Eukaryotic translation initiation factor 4GI is a cellular target for NS1 protein, a translational activator of influenza virus. *Molecular and cellular biology* 20, 6259-6268.
- Arora, D., and Gasse, N. (1998). Influenza virus hemagglutinin stimulates the protein kinase C activity of human polymorphonuclear leucocytes. *Archives of virology* 143, 2029-2037.
- Arzt, S., Baudin, F., Barge, A., Timmins, P., Burmeister, W.P., and Ruigrok, R.W. (2001). Combined results from solution studies on intact influenza virus M1 protein and from a new crystal form of its N-terminal domain show that M1 is an elongated monomer. *Virology* 279, 439-446.

- Ayllon, J., and García-Sastre, A. (2014). The NS1 protein: a multitasking virulence factor. *Influenza Pathogenesis and Control-Volume II*, 73-107.
- Azzeh, M., Flick, R., and Hobom, G. (2001). Functional analysis of the influenza A virus cRNA promoter and construction of an ambisense transcription system. *Virology* 289, 400-410.
- Babazadeh, A., Mohseni Afshar, Z., Javanian, M., Mohammadnia-Afrouzi, M., Karkhah, A., Masrour-Roudsari, J., Sabbagh, P., Koppolu, V., Vasigala, V.K., and Ebrahimpour, S. (2019). Influenza vaccination and Guillain–Barré syndrome: reality or fear. *Journal of translational internal medicine* 7, 137-142.
- Bagchi, P., Dutta, D., Chattopadhyay, S., Mukherjee, A., Halder, U.C., Sarkar, S., Kobayashi, N., Komoto, S., Taniguchi, K., and Chawla-Sarkar, M. (2010). Rotavirus nonstructural protein 1 suppresses virus-induced cellular apoptosis to facilitate viral growth by activating the cell survival pathways during early stages of infection. *Journal of virology* 84, 6834-6845.
- Bagheri, A., Moezzi, S.M.I., Mosaddeghi, P., Parashkouhi, S.N., Hoseini, S.M.F., Badakhshan, F., and Negahdaripour, M. (2021). Interferon-inducer antivirals: Potential candidates to combat COVID-19. *International immunopharmacology* 91, 107245.
- Balachandran, S., Roberts, P.C., Brown, L.E., Truong, H., Pattnaik, A.K., Archer, D.R., and Barber, G.N. (2000). Essential role for the dsRNA-dependent protein kinase PKR in innate immunity to viral infection. *Immunity* 13, 129-141.
- Bali, N.K., Ashraf, M., Ahmad, F., Khan, U.H., Widdowson, M.A., Lal, R.B., and Koul, P.A. (2013). Knowledge, attitude, and practices about the seasonal influenza vaccination among healthcare workers in Srinagar, India. *Influenza and other respiratory viruses* 7, 540-545.
- Barber, S.A., Bruett, L., Douglass, B.R., Herbst, D.S., Zink, M.C., and Clements, J.E. (2002). Visna virus-induced activation of MAPK is required for virus replication and correlates with virus-induced neuropathology. *Journal of virology* 76, 817-828.
- Barman, S., Adhikary, L., Chakrabarti, A.K., Bernas, C., Kawaoka, Y., and Nayak, D.P. (2004). Role of transmembrane domain and cytoplasmic tail amino acid sequences of influenza A virus neuraminidase in raft association and virus budding. *Journal of virology* 78, 5258-5269.
- Barral, P.M., Sarkar, D., Fisher, P.B., and Racaniello, V.R. (2009). RIG-I is cleaved during picornavirus infection. *Virology* 391, 171-176.
- Bawage, S.S., Tiwari, P.M., Pillai, S., Dennis, V.A., and Singh, S.R. (2019). Antibiotic minocycline prevents respiratory syncytial virus infection. *Viruses* 11, 739.
- Bayer, K., Banning, C., Bruss, V., Wiltzer-Bach, L., and Schindler, M. (2016). Hepatitis C virus is released via a noncanonical secretory route. *Journal of virology* 90, 10558-10573.
- Benn, J., Su, F., Doria, M., and Schneider, R.J. (1996). Hepatitis B virus HBx protein induces transcription factor AP-1 by activation of extracellular signal-regulated and c-Jun N-terminal mitogen-activated protein kinases. *Journal of Virology* 70, 4978-4985.
- Bergervoet, S.A., Ho, C.K., Heutink, R., Bossers, A., and Beerens, N. (2019). Spread of highly pathogenic avian influenza (HPAI) H5N5 viruses in Europe in 2016–2017 appears related to the timing of reassortment events. *Viruses* 11, 501.
- Bertram, S., Heurich, A., Lavender, H., Gierer, S., Danisch, S., Perin, P., Lucas, J.M., Nelson, P.S., Pöhlmann, S., and Soilleux, E.J. (2012). Influenza and SARS-coronavirus activating proteases TMPRSS2 and HAT are expressed at multiple sites in human respiratory and gastrointestinal tracts. *PloS one* 7, e35876.
- Bhat, N., Wright, J.G., Broder, K.R., Murray, E.L., Greenberg, M.E., Glover, M.J., Likos, A.M., Posey, D.L., Klimov, A., and Lindstrom, S.E. (2005). Influenza-associated deaths

- among children in the United States, 2003–2004. *New England Journal of Medicine* 353, 2559-2567.
- Bhowmick, R., Mukherjee, A., Patra, U., and Chawla-Sarkar, M. (2015). Rotavirus disrupts cytoplasmic P bodies during infection. *Virus research* 210, 344-354.
- Bilsel, P., Castrucci, M., and Kawaoka, Y. (1993). Mutations in the cytoplasmic tail of influenza A virus neuraminidase affect incorporation into virions. *Journal of virology* 67, 6762-6767.
- Biswas, S.K., and Nayak, D.P. (1994). Mutational analysis of the conserved motifs of influenza A virus polymerase basic protein 1. *Journal of virology* 68, 1819-1826.
- Blass, D., Patzelt, E., and Kuechler, E. (1982). Identification of the cap binding protein of influenza virus. *Nucleic acids research* 10, 4803-4812.
- Boivin, G., Goyette, N., and Bernatchez, H. (2002). Prolonged excretion of amantadine-resistant influenza A virus quasi species after cessation of antiviral therapy in an immunocompromised patient. *Clinical Infectious Diseases* 34, e23-e25.
- Bornholdt, Z.A., and Prasad, B.V. (2006). X-ray structure of influenza virus NS1 effector domain. *Nature structural & molecular biology* 13, 559-560.
- Bos, T.J., Davis, A.R., and Nayak, D.P. (1984). NH₂-terminal hydrophobic region of influenza virus neuraminidase provides the signal function in translocation. *Proceedings of the National Academy of Sciences* 81, 2327-2331.
- Böttcher-Friebertshäuser, E., Freuer, C., Sielaff, F., Schmidt, S., Eickmann, M., Uhlendorff, J., Steinmetzer, T., Klenk, H.-D., and Garten, W. (2010). Cleavage of influenza virus hemagglutinin by airway proteases TMPRSS2 and HAT differs in subcellular localization and susceptibility to protease inhibitors. *Journal of virology* 84, 5605-5614.
- Böttcher-Friebertshäuser, E., Garten, W., Matrosovich, M., and Klenk, H.D. (2014). The hemagglutinin: a determinant of pathogenicity. *Influenza Pathogenesis and Control-Volume I*, 3-34.
- Böttcher, E., Matrosovich, T., Beyerle, M., Klenk, H.-D., Garten, W., and Matrosovich, M. (2006). Proteolytic activation of influenza viruses by serine proteases TMPRSS2 and HAT from human airway epithelium. *Journal of virology* 80, 9896-9898.
- Bouloy, M., Plotch, S.J., and Krug, R.M. (1980). Both the 7-methyl and the 2'-O-methyl groups in the cap of mRNA strongly influence its ability to act as primer for influenza virus RNA transcription. *Proceedings of the National Academy of Sciences* 77, 3952-3956.
- Brankston, G., Gitterman, L., Hirji, Z., Lemieux, C., and Gardam, M. (2007). Transmission of influenza A in human beings. *The Lancet infectious diseases* 7, 257-265.
- Broor, S., Krishnan, A., Roy, D.S., Dhakad, S., Kaushik, S., Mir, M.A., Singh, Y., Moen, A., Chadha, M., and Mishra, A.C. (2012). Dynamic patterns of circulating seasonal and pandemic A (H1N1) pdm09 influenza viruses from 2007–2010 in and around Delhi, India. *PloS one* 7, e29129.
- Brun-Buisson, C., Richard, J.-C.M., Mercat, A., Thiébaud, A.C., and Brochard, L. (2011). Early corticosteroids in severe influenza A/H1N1 pneumonia and acute respiratory distress syndrome. *American journal of respiratory and critical care medicine* 183, 1200-1206.
- Brydon, E.W., Morris, S.J., and Sweet, C. (2005). Role of apoptosis and cytokines in influenza virus morbidity. *FEMS microbiology reviews* 29, 837-850.
- Bui, M., and Helenius, A. (1996). The role of nuclear import and export in influenza virus infection. *Trends in cell biology* 6, 67-71.
- Bui, M., Whittaker, G., and Helenius, A. (1996). Effect of M1 protein and low pH on nuclear transport of influenza virus ribonucleoproteins. *Journal of virology* 70, 8391-8401.
- Bullough, P.A., Hughson, F.M., Skehel, J.J., and Wiley, D.C. (1994). Structure of influenza haemagglutinin at the pH of membrane fusion. *Nature* 371, 37-43.

- Burgui, I., Aragon, T., Ortín, J., and Nieto, A. (2003). PABP1 and eIF4GI associate with influenza virus NS1 protein in viral mRNA translation initiation complexes. *Journal of General Virology* 84, 3263-3274.
- Burmeister, W., Ruigrok, R., and Cusack, S. (1992). The 2.2 Å resolution crystal structure of influenza B neuraminidase and its complex with sialic acid. *The EMBO journal* 11, 49-56.
- Burnet, F. (1948). MUCINS AND MUCOIDS IN RELATION TO INFLUENZA VIRUS ACTION V. THE DESTRUCTION OF "FRANCIS INHIBITOR" ACTIVITY IN A PURIFIED MUCOID BY VIRUS ACTION. *Australian Journal of Experimental Biology & Medical Science* 26.
- Burnet, F. (1951). Mucoproteins in relation to virus action. *Physiological reviews* 31, 131-150.
- Burnet, F., Mccrea, J., and Anderson, S. (1947). Mucin as substrate of enzyme action by viruses of the mumps influenza group. *Nature* 160, 404-405.
- Cabrera-Hernandez, A., Thepparit, C., Suksanpaisan, L., and Smith, D.R. (2007). Dengue virus entry into liver (HepG2) cells is independent of hsp90 and hsp70. *Journal of medical virology* 79, 386-392.
- Cao, S., Liu, X., Yu, M., Li, J., Jia, X., Bi, Y., Sun, L., Gao, G.F., and Liu, W. (2012). A nuclear export signal in the matrix protein of Influenza A virus is required for efficient virus replication. *Journal of virology* 86, 4883-4891.
- Carrat, F., Vergu, E., Ferguson, N.M., Lemaître, M., Cauchemez, S., Leach, S., and Valleron, A.-J. (2008). Time lines of infection and disease in human influenza: a review of volunteer challenge studies. *American journal of epidemiology* 167, 775-785.
- Caton, A.J., Brownlee, G.G., Yewdell, J.W., and Gerhard, W. (1982). The antigenic structure of the influenza virus A/PR/8/34 hemagglutinin (H1 subtype). *Cell* 31, 417-427.
- Chadha, M.S., Potdar, V.A., Saha, S., Koul, P.A., Broor, S., Dar, L., Chawla-Sarkar, M., Biswas, D., Gunasekaran, P., and Abraham, A.M. (2015). Dynamics of influenza seasonality at sub-regional levels in India and implications for vaccination timing. *PloS one* 10, e0124122.
- Chaipan, C., Kobasa, D., Bertram, S., Glowacka, I., Steffen, I., Solomon Tsegaye, T., Takeda, M., Bugge, T.H., Kim, S., and Park, Y. (2009). Proteolytic activation of the 1918 influenza virus hemagglutinin. *Journal of virology* 83, 3200-3211.
- Chen, B.J., Leser, G.P., Morita, E., and Lamb, R.A. (2007). Influenza virus hemagglutinin and neuraminidase, but not the matrix protein, are required for assembly and budding of plasmid-derived virus-like particles. *Journal of virology* 81, 7111-7123.
- Chen, C., and Zhuang, X. (2008). Epsin 1 is a cargo-specific adaptor for the clathrin-mediated endocytosis of the influenza virus. *Proceedings of the National Academy of Sciences* 105, 11790-11795.
- Chen, L.F., Dailey, N.J., Rao, A.K., Fleischauer, A.T., Greenwald, I., Deyde, V.M., Moore, Z.S., Anderson, D.J., Duffy, J., and Gubareva, L.V. (2011). Cluster of oseltamivir-resistant 2009 pandemic influenza A (H1N1) virus infections on a hospital ward among immunocompromised patients—North Carolina, 2009. *Journal of Infectious Diseases* 203, 838-846.
- Chen, W., Calvo, P.A., Malide, D., Gibbs, J., Schubert, U., Bacik, I., Basta, S., O'Neill, R., Schickli, J., and Palese, P. (2001). A novel influenza A virus mitochondrial protein that induces cell death. *Nature medicine* 7, 1306-1312.
- Chien, C.-Y., Xu, Y., Xiao, R., Aramini, J.M., Sahasrabudhe, P.V., Krug, R.M., and Montelione, G.T. (2004). Biophysical characterization of the complex between double-stranded RNA and the N-terminal domain of the NS1 protein from influenza A virus: evidence for a novel RNA-binding mode. *Biochemistry* 43, 1950-1962.

- Chien, C., Tejero, R., Huang, Y., Zimmerman, D.E., Ríos, C.B., Krug, R.M., and Montelione, G.T. (1997). A novel RNA-binding motif in influenza A virus non-structural protein 1. *Nature structural biology* 4, 891-895.
- Chintakrindi, A.S., Gohil, D.J., Kothari, S.T., Chowdhary, A.S., and Kanyalkar, M.A. (2018). Design, synthesis and evaluation of chalcones as H1N1 Neuraminidase inhibitors. *Medicinal Chemistry Research* 27, 1013-1025.
- Chlanda, P., Schraidt, O., Kummer, S., Riches, J., Oberwinkler, H., Prinz, S., Kräusslich, H.-G., and Briggs, J.A. (2015). Structural analysis of the roles of influenza A virus membrane-associated proteins in assembly and morphology. *Journal of virology* 89, 8957-8966.
- Chopra, I., and Roberts, M. (2001). Tetracycline antibiotics: mode of action, applications, molecular biology, and epidemiology of bacterial resistance. *Microbiology and molecular biology reviews* 65, 232-260.
- Chou, Y.-Y., Heaton, N.S., Gao, Q., Palese, P., Singer, R., and Lionnet, T. (2013). Colocalization of different influenza viral RNA segments in the cytoplasm before viral budding as shown by single-molecule sensitivity FISH analysis. *PLoS pathogens* 9, e1003358.
- Choudhry, A., Singh, S., Khare, S., Rai, A., Rawat, D., Aggarwal, R., and Chauhan, L. (2012). Emergence of pandemic 2009 influenza A H1N1, India. *Indian Journal of Medical Research* 135, 534-537.
- Ciampor, F., Bayley, P., Nermut, M., Hirst, E., Sugrue, R., and Hay, A. (1992). Evidence that the amantadine-induced, M2-mediated conversion of influenza A virus hemagglutinin to the low pH conformation occurs in an acidic trans Golgi compartment. *Virology* 188, 14-24.
- Clohisey, S., and Baillie, J.K. (2019). Host susceptibility to severe influenza A virus infection. *Critical care* 23, 303.
- Cohen, M., Zhang, X.-Q., Senaati, H.P., Chen, H.-W., Varki, N.M., Schooley, R.T., and Gagneux, P. (2013). Influenza A penetrates host mucus by cleaving sialic acids with neuraminidase. *Virology journal* 10, 1-13.
- Colman, P. (1994). Influenza virus neuraminidase: structure, antibodies, and inhibitors. *Protein Science* 3, 1687-1696.
- Colman, P., Varghese, J., and Laver, W. (1983). Structure of the catalytic and antigenic sites in influenza virus neuraminidase. *Nature* 303, 41-44.
- Conenello, G.M., and Palese, P. (2007). Influenza A virus PB1-F2: a small protein with a big punch. *Cell host & microbe* 2, 207-209.
- Constantinescu, S.N., Cernescu, C.D., and Popescu, L.M. (1991). Effects of protein kinase C inhibitors on viral entry and infectivity. *FEBS letters* 292, 31-33.
- Control, C.F.D., and Prevention (2009). Evaluation of rapid influenza diagnostic tests for detection of novel influenza A (H1N1) Virus--United States, 2009. *MMWR: Morbidity & Mortality Weekly Report* 58.
- Copeland, K. (2005). Modulation of HIV-1 transcription by cytokines and chemokines. *Mini reviews in medicinal chemistry* 5, 1093-1101.
- Cornberg, M., Wedemeyer, H., and Manns, M.P. (2002). Treatment of chronic hepatitis C with PEGylated interferon and ribavirin. *Current gastroenterology reports* 4, 23-30.
- Couch, R.B. (1996). Orthomyxoviruses. *Medical Microbiology*. 4th edition.
- Courageot, M.-P., Frenkiel, M.-P., Duarte Dos Santos, C., Deubel, V., and DesprèS, P. (2000). α -Glucosidase inhibitors reduce dengue virus production by affecting the initial steps of virion morphogenesis in the endoplasmic reticulum. *Journal of virology* 74, 564-572.
- Cousins, S. (2015). "Death toll from swine flu in India exceeds 2500". British Medical Journal Publishing Group).

- Cowling, B.J., Ip, D.K., Fang, V.J., Suntarattiwong, P., Olsen, S.J., Levy, J., Uyeki, T.M., Leung, G.M., Malik Peiris, J., and Chotpitayasunondh, T. (2013). Aerosol transmission is an important mode of influenza A virus spread. *Nature communications* 4, 1-6.
- Cros, J.F., García-Sastre, A., and Palese, P. (2005). An unconventional NLS is critical for the nuclear import of the influenza A virus nucleoprotein and ribonucleoprotein. *Traffic* 6, 205-213.
- Cros, J.F., and Palese, P. (2003). Trafficking of viral genomic RNA into and out of the nucleus: influenza, Thogoto and Borna disease viruses. *Virus research* 95, 3-12.
- Crow, M., Deng, T., Addley, M., and Brownlee, G.G. (2004). Mutational analysis of the influenza virus cRNA promoter and identification of nucleotides critical for replication. *Journal of virology* 78, 6263-6270.
- Cunha, A.E.S., Loureiro, R.J.S., Simões, C.J.V., and Brito, R.M.M. (2023). Unveiling New Druggable Pockets in Influenza Non-Structural Protein 1: NS1-Host Interactions as Antiviral Targets for Flu. *International Journal of Molecular Sciences* 24, 2977.
- Dai, X., Zhang, L., and Hong, T. (2011). Host cellular signaling induced by influenza virus. *Science China Life Sciences* 54, 68-74.
- Daniels, P., Jeffries, S., Yates, P., Schild, G., Rogers, G., Paulson, J., Wharton, S., Douglas, A., Skehel, J., and Wiley, D. (1987). The receptor-binding and membrane-fusion properties of influenza virus variants selected using anti-haemagglutinin monoclonal antibodies. *The EMBO journal* 6, 1459-1465.
- Daniels, R., Kurowski, B., Johnson, A.E., and Hebert, D.N. (2003). N-linked glycans direct the cotranslational folding pathway of influenza hemagglutinin. *Molecular cell* 11, 79-90.
- Daniels, R., Svedine, S., and Hebert, D.N. (2004). N-linked carbohydrates act as luminal maturation and quality control protein tags. *Cell biochemistry and biophysics* 41, 113-137.
- Dao, T.-T., Tung, B.-T., Nguyen, P.-H., Thuong, P.-T., Yoo, S.-S., Kim, E.-H., Kim, S.-K., and Oh, W.-K. (2010). C-methylated flavonoids from *Cleistocalyx operculatus* and their inhibitory effects on novel influenza A (H1N1) neuraminidase. *Journal of natural products* 73, 1636-1642.
- Dao, T.T., Nguyen, P.H., Lee, H.S., Kim, E., Park, J., Lim, S.I., and Oh, W.K. (2011). Chalcones as novel influenza A (H1N1) neuraminidase inhibitors from *Glycyrrhiza inflata*. *Bioorganic & medicinal chemistry letters* 21, 294-298.
- Darman, J., Backovic, S., Dike, S., Maragakis, N.J., Krishnan, C., Rothstein, J.D., Irani, D.N., and Kerr, D.A. (2004). Viral-induced spinal motor neuron death is non-cell-autonomous and involves glutamate excitotoxicity. *Journal of Neuroscience* 24, 7566-7575.
- Das, K., Aramini, J.M., Ma, L.-C., Krug, R.M., and Arnold, E. (2010). Structures of influenza A proteins and insights into antiviral drug targets. *Nature structural & molecular biology* 17, 530-538.
- Daum, G., Eisenmann-Tappe, I., Fries, H.-W., Troppmair, J., and Rapp, U.R. (1994). The ins and outs of Raf kinases. *Trends in biochemical sciences* 19, 474-480.
- De Castro Martin, I.F., Fournier, G., Sachse, M., Pizarro-Cerda, J., Risco, C., and Naffakh, N. (2017). Influenza virus genome reaches the plasma membrane via a modified endoplasmic reticulum and Rab11-dependent vesicles. *Nature communications* 8, 1396.
- De La Luna, S., Fortes, P., Beloso, A., and Ortín, J. (1995). Influenza virus NS1 protein enhances the rate of translation initiation of viral mRNAs. *Journal of virology* 69, 2427-2433.
- Deng, T., Vreede, F.T., and Brownlee, G.G. (2006). Different de novo initiation strategies are used by influenza virus RNA polymerase on its cRNA and viral RNA promoters during viral RNA replication. *Journal of virology* 80, 2337-2348.

- Deshaies, R.J., and Schekman, R. (1987). A yeast mutant defective at an early stage in import of secretory protein precursors into the endoplasmic reticulum. *The Journal of cell biology* 105, 633-645.
- Dias, A., Bouvier, D., Crépin, T., McCarthy, A.A., Hart, D.J., Baudin, F., Cusack, S., and Ruigrok, R.W. (2009). The cap-snatching endonuclease of influenza virus polymerase resides in the PA subunit. *Nature* 458, 914-918.
- Diaz, E., Martin-Loeches, I., Canadell, L., Vidaur, L., Suarez, D., Socias, L., Estella, A., Rueda, B.G., Guerrero, J.E., and Valverdú-Vidal, M. (2012). Corticosteroid therapy in patients with primary viral pneumonia due to pandemic (H1N1) 2009 influenza. *Journal of Infection* 64, 311-318.
- Diebold, S.S., Kaisho, T., Hemmi, H., Akira, S., and Reis E Sousa, C. (2004). Innate antiviral responses by means of TLR7-mediated recognition of single-stranded RNA. *Science* 303, 1529-1531.
- Dilantika, C., Sedyaningsih, E.R., Kasper, M.R., Agtini, M., Listiyaningsih, E., Uyeki, T.M., Burgess, T.H., Blair, P.J., and Putnam, S.D. (2010). Influenza virus infection among pediatric patients reporting diarrhea and influenza-like illness. *BMC infectious diseases* 10, 1-5.
- Domingo, E. (2010). Mechanisms of viral emergence. *Veterinary research* 41.
- Dong, G., Peng, C., Luo, J., Wang, C., Han, L., Wu, B., Ji, G., and He, H. (2015). Adamantane-resistant influenza A viruses in the world (1902–2013): frequency and distribution of M2 gene mutations. *PloS one* 10, e0119115.
- Doshi, P., Jefferson, T., and Del Mar, C. (2012). The imperative to share clinical study reports: recommendations from the Tamiflu experience. *PLoS Medicine* 9, e1001201.
- Dou, D., Da Silva, D.V., Nordholm, J., Wang, H., and Daniels, R. (2014). Type II transmembrane domain hydrophobicity dictates the cotranslational dependence for inversion. *Molecular biology of the cell* 25, 3363-3374.
- Dou, D., Hernández-Neuta, I., Wang, H., Östbye, H., Qian, X., Thiele, S., Resa-Infante, P., Kouassi, N.M., Sender, V., and Hentrich, K. (2017). Analysis of IAV replication and co-infection dynamics by a versatile RNA viral genome labeling method. *Cell reports* 20, 251-263.
- Dubois, J., Terrier, O., and Rosa-Calatrava, M. (2014). Influenza viruses and mRNA splicing: doing more with less. *MBio* 5, 10.1128/mbio.00070-00014.
- Dutta, K., Kumawat, K.L., Nazmi, A., Mishra, M.K., and Basu, A. (2010). Minocycline differentially modulates viral infection and persistence in an experimental model of Japanese encephalitis. *Journal of Neuroimmune Pharmacology* 5, 553-565.
- Ebrahimipour, S., Babazadeh, A., Sadeghi, H.Z.M., Bayani, M., Vasigala, V.K.R., and Javanian, M. (2019). Outcomes of patients with definitive diagnosis of influenza A (H1N1) virus infection admitted to affiliated hospitals of Babol University of Medical Sciences, 2015-2016. *Acta facultatis medicae Naissensis* 36, 356-364.
- Ehrhardt, C., Marjuki, H., Wolff, T., Nürnberg, B., Planz, O., Pleschka, S., and Ludwig, S. (2006). Bivalent role of the phosphatidylinositol-3-kinase (PI3K) during influenza virus infection and host cell defence. *Cellular microbiology* 8, 1336-1348.
- Ehrhardt, C., Seyer, R., Hrincius, E.R., Eierhoff, T., Wolff, T., and Ludwig, S. (2010). Interplay between influenza A virus and the innate immune signaling. *Microbes and infection* 12, 81-87.
- Ehrhardt, C., Wolff, T., Pleschka, S., Planz, O., Beermann, W., Bode, J.G., Schmolke, M., and Ludwig, S. (2007). Influenza A virus NS1 protein activates the PI3K/Akt pathway to mediate antiapoptotic signaling responses. *Journal of virology* 81, 3058-3067.

- Eisfeld, A.J., Kawakami, E., Watanabe, T., Neumann, G., and Kawaoka, Y. (2011). RAB11A is essential for transport of the influenza virus genome to the plasma membrane. *Journal of virology* 85, 6117-6126.
- Eisfeld, A.J., Neumann, G., and Kawaoka, Y. (2015). At the centre: influenza A virus ribonucleoproteins. *Nature Reviews Microbiology* 13, 28-41.
- Elleman, C., and Barclay, W. (2004). The M1 matrix protein controls the filamentous phenotype of influenza A virus. *Virology* 321, 144-153.
- Elliot, A.J., Powers, C., Thornton, A., Obi, C., Hill, C., Simms, I., Waight, P., Maguire, H., Foord, D., and Povey, E. (2009). Monitoring the emergence of community transmission of influenza A/H1N1 2009 in England: a cross sectional opportunistic survey of self sampled telephone callers to NHS Direct. *Bmj* 339.
- Elton, D., Simpson-Holley, M., Archer, K., Medcalf, L., Hallam, R., Mccauley, J., and Digard, P. (2001). Interaction of the influenza virus nucleoprotein with the cellular CRM1-mediated nuclear export pathway. *Journal of virology* 75, 408-419.
- Enami, K., Sato, T.A., Nakada, S., and Enami, M. (1994). Influenza virus NS1 protein stimulates translation of the M1 protein. *Journal of virology* 68, 1432-1437.
- Engelhardt, O.G., Smith, M., and Fodor, E. (2005). Association of the influenza A virus RNA-dependent RNA polymerase with cellular RNA polymerase II. *Journal of virology* 79, 5812-5818.
- Enose-Akahata, Y., Matsuura, E., Tanaka, Y., Oh, U., and Jacobson, S. (2012). Minocycline modulates antigen-specific CTL activity through inactivation of mononuclear phagocytes in patients with HTLV-I associated neurologic disease. *Retrovirology* 9, 1-14.
- Feigenblum, D., and Schneider, R.J. (1993). Modification of eukaryotic initiation factor 4F during infection by influenza virus. *Journal of virology* 67, 3027-3035.
- Feng, E., Shin, W.-J., Zhu, X., Li, J., Ye, D., Wang, J., Zheng, M., Zuo, J.-P., No, K.T., and Liu, X. (2013). Structure-based design and synthesis of C-1-and C-4-modified analogs of zanamivir as neuraminidase inhibitors. *Journal of Medicinal Chemistry* 56, 671-684.
- Fiore, A.E., Fry, A., Shay, D., Gubareva, L., Bresee, J.S., Uyeki, T.M., Control, C.F.D., and Prevention (2011). Antiviral agents for the treatment and chemoprophylaxis of influenza—recommendations of the Advisory Committee on Immunization Practices (ACIP). *MMWR Recomm Rep* 60, 1-24.
- Flick, R., Neumann, G., Hoffmann, E., Neumeier, E., and Hobom, G. (1996). Promoter elements in the influenza vRNA terminal structure. *Rna* 2, 1046-1057.
- Fodor, E. (2013). The RNA polymerase of influenza a virus: mechanisms of viral transcription and replication. *Acta virologica* 57, 113-122.
- Fontes, M.R., Teh, T., Jans, D., Brinkworth, R.I., and Kobe, B. (2003). Structural basis for the specificity of bipartite nuclear localization sequence binding by importin- α . *Journal of Biological Chemistry* 278, 27981-27987.
- Frabutt, D.A., and Zheng, Y.-H. (2016). Arms race between enveloped viruses and the host ERAD machinery. *Viruses* 8, 255.
- Freeman, D., and Barno, A. (1959). Deaths from Asian influenza associated with pregnancy. *American Journal of Obstetrics & Gynecology* 78, 1172-1175.
- Fukuzawa, K., Omagari, K., Nakajima, K., Nobusawa, E., and Tanaka, S. (2011). Sialic acid recognition of the pandemic influenza 2009 H1N1 virus: binding mechanism between human receptor and influenza hemagglutinin. *Protein and peptide letters* 18, 530-539.
- Gabriel, G., Klingel, K., Otte, A., Thiele, S., Hudjetz, B., Arman-Kalcek, G., Sauter, M., Schmidt, T., Rother, F., and Baumgarte, S. (2011). Differential use of importin- α isoforms governs cell tropism and host adaptation of influenza virus. *Nature communications* 2, 156.

- Gack, M.U., Albrecht, R.A., Urano, T., Inn, K.-S., Huang, I.-C., Carnero, E., Farzan, M., Inoue, S., Jung, J.U., and García-Sastre, A. (2009). Influenza A virus NS1 targets the ubiquitin ligase TRIM25 to evade recognition by the host viral RNA sensor RIG-I. *Cell host & microbe* 5, 439-449.
- Galloway, S.E., Reed, M.L., Russell, C.J., and Steinhauer, D.A. (2013). Influenza HA subtypes demonstrate divergent phenotypes for cleavage activation and pH of fusion: implications for host range and adaptation. *PLoS pathogens* 9, e1003151.
- Gambaryan, A., Tuzikov, A., Piskarev, V., Yamnikova, S., Lvov, D., Robertson, J., Bovin, N., and Matrosovich, M. (1997). Specification of receptor-binding phenotypes of influenza virus isolates from different hosts using synthetic sialylglycopolymers: non-egg-adapted human H1 and H3 influenza A and influenza B viruses share a common high binding affinity for 6'-sialyl (N-acetyl)lactosamine). *Virology* 232, 345-350.
- Gambhir, R.S., Pannu, P.R., Nanda, T., Arora, G., and Kaur, A. (2016). Knowledge and awareness regarding swine-influenza A (H1N1) virus infection among dental professionals in India-A systematic review. *Journal of Clinical and Diagnostic Research: JCDR* 10, ZE10.
- Gamblin, S.J., and Skehel, J.J. (2010). Influenza hemagglutinin and neuraminidase membrane glycoproteins. *Journal of biological chemistry* 285, 28403-28409.
- Garcia, M., Meurs, E., and Esteban, M. (2007). The dsRNA protein kinase PKR: virus and cell control. *Biochimie* 89, 799-811.
- Garner, S.E., Eady, A., Bennett, C., Newton, J.N., Thomas, K., and Popescu, C.M. (2012). Minocycline for acne vulgaris: efficacy and safety. *Cochrane Database of Systematic Reviews*.
- Garrido-Mesa, N., Zarzuelo, A., and Gálvez, J. (2013). Minocycline: far beyond an antibiotic. *British journal of pharmacology* 169, 337-352.
- Garten, R.J., Davis, C.T., Russell, C.A., Shu, B., Lindstrom, S., Balish, A., Sessions, W.M., Xu, X., Skepner, E., and Deyde, V. (2009). Antigenic and genetic characteristics of swine-origin 2009 A (H1N1) influenza viruses circulating in humans. *science* 325, 197-201.
- Gasparini, R., Amicizia, D., Lai, P.L., Bragazzi, N.L., and Panatto, D. (2014). Compounds with anti-influenza activity: present and future of strategies for the optimal treatment and management of influenza. Part I: Influenza life-cycle and currently available drugs. *Journal of preventive medicine and hygiene* 55, 69.
- Gatherer, D. (2009). On the origin of influenza A hemagglutinin. *Indian journal of microbiology* 49, 352-357.
- Gaur, P., Munjal, A., and Lal, S.K. (2011). Influenza virus and cell signaling pathways. *Medical science monitor: international medical journal of experimental and clinical research* 17, RA148.
- Gavazzi, C., Yver, M., Isel, C., Smyth, R.P., Rosa-Calatrava, M., Lina, B., Moulès, V., and Marquet, R. (2013). A functional sequence-specific interaction between influenza A virus genomic RNA segments. *Proceedings of the National Academy of Sciences* 110, 16604-16609.
- Gerl, M.J., Sampaio, J.L., Urban, S., Kalvodova, L., Verbavatz, J.-M., Binnington, B., Lindemann, D., Lingwood, C.A., Shevchenko, A., and Schroeder, C. (2012). Quantitative analysis of the lipidomes of the influenza virus envelope and MDCK cell apical membrane. *Journal of Cell Biology* 196, 213-221.
- Gerloff, N.A., Khan, S.U., Balish, A., Shanta, I.S., Simpson, N., Berman, L., Haider, N., Poh, M.K., Islam, A., and Gurley, E. (2014). Multiple reassortment events among highly pathogenic avian influenza A (H5N1) viruses detected in Bangladesh. *Virology* 450, 297-307.

- Ghoshal, A., Das, S., Ghosh, S., Mishra, M.K., Sharma, V., Koli, P., Sen, E., and Basu, A. (2007). Proinflammatory mediators released by activated microglia induces neuronal death in Japanese encephalitis. *Glia* 55, 483-496.
- Gibbs, J.S., Malide, D., Hornung, F., Bennink, J.R., and Yewdell, J.W. (2003). The influenza A virus PB1-F2 protein targets the inner mitochondrial membrane via a predicted basic amphipathic helix that disrupts mitochondrial function. *Journal of virology* 77, 7214-7224.
- Gilmore, R., Walter, P., and Blobel, G. (1982). Protein translocation across the endoplasmic reticulum. II. Isolation and characterization of the signal recognition particle receptor. *The Journal of cell biology* 95, 470-477.
- Girard, M.P., Tam, J.S., Assossou, O.M., and Kieny, M.P. (2010). The 2009 A (H1N1) influenza virus pandemic: A review. *Vaccine* 28, 4895-4902.
- Giuliani, F., Hader, W., and Yong, V.W. (2005). Minocycline attenuates T cell and microglia activity to impair cytokine production in T cell-microglia interaction. *Journal of leukocyte biology* 78, 135-143.
- Glezen, W.P. (2008). Prevention and treatment of seasonal influenza. *New England Journal of Medicine* 359, 2579-2585.
- Gonzalez, O., Fontanes, V., Raychaudhuri, S., Loo, R., Loo, J., Arumugaswami, V., Sun, R., Dasgupta, A., and French, S.W. (2009). The heat shock protein inhibitor Quercetin attenuates hepatitis C virus production. *Hepatology* 50, 1756-1764.
- González, S., and Ortín, J. (1999). Distinct regions of influenza virus PB1 polymerase subunit recognize vRNA and cRNA templates. *The EMBO journal*.
- González, S., Zürcher, T., and Ortín, J. (1996). Identification of two separate domains in the influenza virus PB1 protein involved in the interaction with the PB2 and PA subunits: a model for the viral RNA polymerase structure. *Nucleic acids research* 24, 4456-4463.
- Goodman, A.G., Smith, J.A., Balachandran, S., Perwitasari, O., Proll, S.C., Thomas, M.J., Korth, M.J., Barber, G.N., Schiff, L.A., and Katze, M.G. (2007). The cellular protein P58IPK regulates influenza virus mRNA translation and replication through a PKR-mediated mechanism. *Journal of virology* 81, 2221-2230.
- Görlich, D., Prehn, S., Hartmann, E., Kalies, K.-U., and Rapoport, T.A. (1992). A mammalian homolog of SEC61p and SECYp is associated with ribosomes and nascent polypeptides during translocation. *Cell* 71, 489-503.
- Graham, M., Liang, B., Van Domselaar, G., Bastien, N., Beaudoin, C., Tyler, S., Kaplen, B., Landry, E., Team, N.I.a.H.N.P.G.S., and Li, Y. (2011). Nationwide molecular surveillance of pandemic H1N1 influenza A virus genomes: Canada, 2009. *PLoS One* 6, e16087.
- Gravina, H., Tafuri, N., Júnior, A.S., Fietto, J., Oliveira, T., Diaz, M., and Almeida, M. (2011). In vitro assessment of the antiviral potential of trans-cinnamic acid, quercetin and morin against equid herpesvirus 1. *Research in Veterinary Science* 91, e158-e162.
- Grohskopf, L.A., Sokolow, L.Z., Olsen, S.J., Bresee, J.S., Broder, K.R., and Karron, R.A. (2015). "Prevention and control of influenza with vaccines: recommendations of the Advisory Committee on Immunization Practices, United States, 2015–16 influenza season". Elsevier).
- Guilligay, D., Tarendeau, F., Resa-Infante, P., Coloma, R., Crepin, T., Sehr, P., Lewis, J., Ruigrok, R.W., Ortin, J., and Hart, D.J. (2008). The structural basis for cap binding by influenza virus polymerase subunit PB2. *Nature structural & molecular biology* 15, 500-506.
- Guillot, L., Le Goffic, R., Bloch, S., Escriou, N., Akira, S., Chignard, M., and Si-Tahar, M. (2005). Involvement of toll-like receptor 3 in the immune response of lung epithelial

- cells to double-stranded RNA and influenza A virus. *Journal of Biological Chemistry* 280, 5571-5580.
- Gulati, U., Wu, W., Gulati, S., Kumari, K., Waner, J.L., and Air, G.M. (2005). Mismatched hemagglutinin and neuraminidase specificities in recent human H3N2 influenza viruses. *Virology* 339, 12-20.
- Guo, Z., Chen, L.-M., Zeng, H., Gomez, J.A., Plowden, J., Fujita, T., Katz, J.M., Donis, R.O., and Sambhara, S. (2007). NS1 protein of influenza A virus inhibits the function of intracytoplasmic pathogen sensor, RIG-I. *American journal of respiratory cell and molecular biology* 36, 263-269.
- Gurav, Y.K., Pawar, S.D., Chadha, M.S., Potdar, V.A., Deshpande, A.S., Koratkar, S.S., Hosmani, A.H., and Mishra, A.C. (2010). Pandemic influenza A (H1N1) 2009 outbreak in a residential school at Panchgani, Maharashtra, India. *Indian Journal of Medical Research* 132, 67-71.
- Hale, B., and Randall, R. (2007). "PI3K signalling during influenza A virus infections". Portland Press Ltd.).
- Hale, B.G., Barclay, W.S., Randall, R.E., and Russell, R.J. (2008a). Structure of an avian influenza A virus NS1 protein effector domain. *Virology* 378, 1-5.
- Hale, B.G., Jackson, D., Chen, Y.-H., Lamb, R.A., and Randall, R.E. (2006). Influenza A virus NS1 protein binds p85 β and activates phosphatidylinositol-3-kinase signaling. *Proceedings of the National Academy of Sciences* 103, 14194-14199.
- Hale, B.G., Randall, R.E., Ortín, J., and Jackson, D. (2008b). The multifunctional NS1 protein of influenza A viruses. *Journal of general virology* 89, 2359-2376.
- Hall, W.J., Douglas Jr, R.G., Zaky, D.A., Hyde, R.W., Richman, D., and Murphy, B.R. (1976). Attenuated Influenza Virus in Nonnal Adults: Role of Pulmonary Function Studies in Vaccine Trials. *Journal of Infectious Diseases* 133, 137-144.
- Hamilton, B.S., Whittaker, G.R., and Daniel, S. (2012). Influenza virus-mediated membrane fusion: determinants of hemagglutinin fusogenic activity and experimental approaches for assessing virus fusion. *Viruses* 4, 1144-1168.
- Harper, S.A., Bradley, J.S., Englund, J.A., File, T.M., Gravenstein, S., Hayden, F.G., Mcgeer, A.J., Neuzil, K.M., Pavia, A.T., and Tapper, M.L. (2009). Seasonal influenza in adults and children—diagnosis, treatment, chemoprophylaxis, and institutional outbreak management: clinical practice guidelines of the Infectious Diseases Society of America. *Clinical infectious diseases*, 1003-1032.
- Harris, C.A., and Johnson, E.M. (2001). BH3-only Bcl-2 family members are coordinately regulated by the JNK pathway and require Bax to induce apoptosis in neurons. *Journal of Biological Chemistry* 276, 37754-37760.
- Hatada, E., Hasegawa, M., Mukaigawa, J., Shimizu, K., and Fukuda, R. (1989). Control of influenza virus gene expression: quantitative analysis of each viral RNA species in infected cells. *The Journal of Biochemistry* 105, 537-546.
- Hatta, M., Gao, P., Halfmann, P., and Kawaoka, Y. (2001). Molecular basis for high virulence of Hong Kong H5N1 influenza A viruses. *Science* 293, 1840-1842.
- Hausmann, J., Kretzschmar, E., Garten, W., and Klenk, H. (1997). Biosynthesis, intracellular transport and enzymatic activity of an avian influenza A virus neuraminidase: role of unpaired cysteines and individual oligosaccharides. *Journal of general virology* 78, 3233-3245.
- Hay, A. (1992). The action of adamantanamines against influenza A viruses: inhibition of the M2 ion channel protein. *Semin Virol* 3, 21-30.
- He, J., Mao, J., Hou, L., Jin, S., Wang, X., Ding, Z., Jin, Z., Guo, H., and Dai, R. (2021). Minocycline attenuates neuronal apoptosis and improves motor function after traumatic brain injury in rats. *Experimental Animals* 70, 563-569.

- He, X., Zhou, J., Bartlam, M., Zhang, R., Ma, J., Lou, Z., Li, X., Li, J., Joachimiak, A., and Zeng, Z. (2008). Crystal structure of the polymerase PAC–PB1N complex from an avian influenza H5N1 virus. *Nature* 454, 1123-1126.
- Hebert, D.N., Zhang, J.-X., Chen, W., Foellmer, B., and Helenius, A. (1997). The number and location of glycans on influenza hemagglutinin determine folding and association with calnexin and calreticulin. *The Journal of cell biology* 139, 613-623.
- Herfst, S., Schrauwen, E.J., Linster, M., Chutinimitkul, S., De Wit, E., Munster, V.J., Sorrell, E.M., Bestebroer, T.M., Burke, D.F., and Smith, D.J. (2012). Airborne transmission of influenza A/H5N1 virus between ferrets. *science* 336, 1534-1541.
- Hilsch, M., Goldenbogen, B., Sieben, C., Höfer, C.T., Rabe, J.P., Klipp, E., Herrmann, A., and Chiantia, S. (2014). Influenza A matrix protein M1 multimerizes upon binding to lipid membranes. *Biophysical journal* 107, 912-923.
- Hirsch, A. (1883). *Handbook of geographical and historical pathology*. New Sydenham Society.
- Hirve, S., and Organization, W.H. (2015). *Seasonal influenza vaccine use in low and middle income countries in the tropics and subtropics: a systematic review*. World Health Organization.
- Holland, J., Spindler, K., Horodyski, F., Grabau, E., Nichol, S., and Vandepol, S. (1982). Rapid evolution of RNA genomes. *Science* 215, 1577-1585.
- Holsinger, L.J., and Alams, R. (1991). Influenza virus M2 integral membrane protein is a homotetramer stabilized by formation of disulfide bonds. *Virology* 183, 32-43.
- Honda, A., Mizumoto, K., and Ishihama, A. (2002). Minimum molecular architectures for transcription and replication of the influenza virus. *Proceedings of the National Academy of Sciences* 99, 13166-13171.
- Horner, G.J., and Gray Jr, F.D. (1973). Effect of uncomplicated, presumptive influenza on the diffusing capacity of the lung. *American Review of Respiratory Disease* 108, 866-869.
- Howe, M.K., Speer, B.L., Hughes, P.F., Loiselle, D.R., Vasudevan, S., and Haystead, T.A. (2016). An inducible heat shock protein 70 small molecule inhibitor demonstrates anti-dengue virus activity, validating Hsp70 as a host antiviral target. *Antiviral research* 130, 81-92.
- Hsu, J., Santesso, N., Mustafa, R., Brozek, J., Chen, Y.L., Hopkins, J.P., Cheung, A., Hovhannisyan, G., Ivanova, L., and Flottorp, S.A. (2012). Antivirals for treatment of influenza: a systematic review and meta-analysis of observational studies. *Annals of internal medicine* 156, 512-524.
- Hu, Y., Sneyd, H., Dekant, R., and Wang, J. (2017). Influenza A virus nucleoprotein: a highly conserved multi-functional viral protein as a hot antiviral drug target. *Current topics in medicinal chemistry* 17, 2271-2285.
- Huang, R.T., Rott, R., and Klenk, H.-D. (1981). Influenza viruses cause hemolysis and fusion of cells. *Virology* 110, 243-247.
- Huang, S., Chen, J., Chen, Q., Wang, H., Yao, Y., Chen, J., and Chen, Z. (2013). A second CRM1-dependent nuclear export signal in the influenza A virus NS2 protein contributes to the nuclear export of viral ribonucleoproteins. *Journal of virology* 87, 767-778.
- Huang, T., Palese, P., and Krystal, M. (1990). Determination of influenza virus proteins required for genome replication. *Journal of virology* 64, 5669-5673.
- Huet, S., Avilov, S.V., Ferbitz, L., Daigle, N., Cusack, S., and Ellenberg, J. (2010). Nuclear import and assembly of influenza A virus RNA polymerase studied in live cells by fluorescence cross-correlation spectroscopy. *Journal of virology* 84, 1254-1264.
- Hughey, P.G., Roberts, P.C., Holsinger, L.J., Zebedee, S.L., Lamb, R.A., and Compans, R.W. (1995). Effects of antibody to the influenza A virus M2 protein on M2 surface expression and virus assembly. *Virology* 212, 411-421.

- Hull, J.D., Gilmore, R., and Lamb, R.A. (1988). Integration of a small integral membrane protein, M2, of influenza virus into the endoplasmic reticulum: analysis of the internal signal-anchor domain of a protein with an ectoplasmic NH2 terminus. *The Journal of cell biology* 106, 1489-1498.
- Ilyushina, N.A., Bovin, N.V., Webster, R.G., and Govorkova, E.A. (2006). Combination chemotherapy, a potential strategy for reducing the emergence of drug-resistant influenza A variants. *Antiviral research* 70, 121-131.
- Imai, M., Watanabe, T., Hatta, M., Das, S.C., Ozawa, M., Shinya, K., Zhong, G., Hanson, A., Katsura, H., and Watanabe, S. (2012). Experimental adaptation of an influenza H5 HA confers respiratory droplet transmission to a reassortant H5 HA/H1N1 virus in ferrets. *Nature* 486, 420-428.
- Inglis, S.C., and Brown, C.M. (1981). Spliced and unspliced RNAs encoded by virion RNA segment 7 of influenza virus. *Nucleic acids research* 9, 2727-2740.
- Inoue, T., and Tsai, B. (2013). How viruses use the endoplasmic reticulum for entry, replication, and assembly. *Cold Spring Harbor perspectives in biology* 5, a013250.
- Irani, D.N., and Prow, N.A. (2007). Neuroprotective interventions targeting detrimental host immune responses protect mice from fatal alphavirus encephalitis. *Journal of Neuropathology & Experimental Neurology* 66, 533-544.
- Jagadesh, A., Krishnan, A., Nair, S., Sivadas, S., and Arunkumar, G. (2019). Genetic characterization of hemagglutinin (HA) gene of influenza A viruses circulating in Southwest India during 2017 season. *Virus Genes* 55, 458-464.
- Jarsch, I.K., Daste, F., and Gallop, J.L. (2016). Membrane curvature in cell biology: An integration of molecular mechanisms. *Journal of Cell Biology* 214, 375-387.
- Jegerlehner, A., Schmitz, N., Storni, T., and Bachmann, M.F. (2004). Influenza A vaccine based on the extracellular domain of M2: weak protection mediated via antibody-dependent NK cell activity. *The Journal of Immunology* 172, 5598-5605.
- Jeong, H.J., Ryu, Y.B., Park, S.-J., Kim, J.H., Kwon, H.-J., Kim, J.H., Park, K.H., Rho, M.-C., and Lee, W.S. (2009). Neuraminidase inhibitory activities of flavonols isolated from *Rhodiola rosea* roots and their in vitro anti-influenza viral activities. *Bioorganic & medicinal chemistry* 17, 6816-6823.
- Jin, H., Leser, G.P., and Lamb, R.A. (1994). The influenza virus hemagglutinin cytoplasmic tail is not essential for virus assembly or infectivity. *The EMBO journal* 13, 5504-5515.
- Jin, H., Leser, G.P., Zhang, J., and Lamb, R.A. (1997). Influenza virus hemagglutinin and neuraminidase cytoplasmic tails control particle shape. *The EMBO journal* 16, 1236-1247.
- Johari, J., Kianmehr, A., Mustafa, M.R., Abubakar, S., and Zandi, K. (2012). Antiviral activity of baicalein and quercetin against the Japanese encephalitis virus. *International journal of molecular sciences* 13, 16785-16795.
- Johnson, N.P., and Mueller, J. (2002). Updating the accounts: global mortality of the 1918-1920 "Spanish" influenza pandemic. *Bulletin of the History of Medicine*, 105-115.
- Jones, S., Nelson-Sathi, S., Wang, Y., Prasad, R., Rayen, S., Nandel, V., Hu, Y., Zhang, W., Nair, R., and Dharmaseelan, S. (2019). Evolutionary, genetic, structural characterization and its functional implications for the influenza A (H1N1) infection outbreak in India from 2009 to 2017. *Scientific reports* 9, 14690.
- Jorba, N., Coloma, R., and Ortín, J. (2009). Genetic trans-complementation establishes a new model for influenza virus RNA transcription and replication. *PLoS pathogens* 5, e1000462.
- Kaiser, L., Wat, C., Mills, T., Mahoney, P., Ward, P., and Hayden, F. (2003). Impact of oseltamivir treatment on influenza-related lower respiratory tract complications and hospitalizations. *Archives of internal medicine* 163, 1667-1672.

- Kajiya, T., Orihara, K., Hamasaki, S., Oba, R., Hirai, H., Nagata, K., Kumagai, T., Ishida, S., Oketani, N., and Ichiki, H. (2008). Toll-like receptor 2 expression level on monocytes in patients with viral infections: monitoring infection severity. *Journal of Infection* 57, 249-259.
- Kamps BS, Hoffmann C, Preiser W. Influenza Report 2006. © 2006 by Flying Publisher- Paris, Cagliari, Wuppertal, Sevilla. www. InfluenzaReport.com
- Kang, S.-W., Rane, N.S., Kim, S.J., Garrison, J.L., Taunton, J., and Hegde, R.S. (2006). Substrate-specific translocational attenuation during ER stress defines a pre-emptive quality control pathway. *Cell* 127, 999-1013.
- Kant, L., and Guleria, R. (2018). "Pandemic Flu, 1918: After hundred years, India is as vulnerable". Medknow).
- Kaptein, S.J., De Burghgraeve, T., Froeyen, M., Pastorino, B., Alen, M.M., Mondotte, J.A., Herdewijn, P., Jacobs, M., De Lamballerie, X., and Schols, D. (2010). A derivate of the antibiotic doxorubicin is a selective inhibitor of dengue and yellow fever virus replication in vitro. *Antimicrobial agents and chemotherapy* 54, 5269-5280.
- Karamyshev, A.L., Patrick, A.E., Karamysheva, Z.N., Griesemer, D.S., Hudson, H., Tjon-Kon-Sang, S., Nilsson, I., Otto, H., Liu, Q., and Rospert, S. (2014). Inefficient SRP interaction with a nascent chain triggers a mRNA quality control pathway. *Cell* 156, 146-157.
- Katze, M.G. (1995). Regulation of the interferon-induced PKR: can viruses cope? *Trends in microbiology* 3, 75-78.
- Katze, M.G., Decorato, D., and Krug, R.M. (1986). Cellular mRNA translation is blocked at both initiation and elongation after infection by influenza virus or adenovirus. *Journal of virology* 60, 1027-1039.
- Kawakami, E., Watanabe, T., Fujii, K., Goto, H., Watanabe, S., Noda, T., and Kawaoka, Y. (2011). Strand-specific real-time RT-PCR for distinguishing influenza vRNA, cRNA, and mRNA. *Journal of virological methods* 173, 1-6.
- Kelly, K., Sutton, T., Weathered, N., Ray, N., Caldwell, E., Plotkin, Z., and Dagher, P. (2004). Minocycline inhibits apoptosis and inflammation in a rat model of ischemic renal injury. *American Journal of Physiology-Renal Physiology* 287, F760-F766.
- Kemler, I., Whittaker, G., and Helenius, A. (1994). Nuclear import of microinjected influenza virus ribonucleoproteins. *Virology* 202, 1028-1033.
- Khan, M., Dhanwani, R., Patro, I., Rao, P., and Parida, M. (2011). Cellular IMPDH enzyme activity is a potential target for the inhibition of Chikungunya virus replication and virus induced apoptosis in cultured mammalian cells. *Antiviral research* 89, 1-8.
- Khatchikian, D., Orlich, M., and Rott, R. (1989). Increased viral pathogenicity after insertion of a 28S ribosomal RNA sequence into the haemagglutinin gene of an influenza virus. *Nature* 340, 156-157.
- Kilbourne, E.D. (2006). Influenza immunity: new insights from old studies. *The Journal of Infectious Diseases* 193, 7-8.
- Kim, C.U., Chen, X., and Mendel, D.B. (1999). Neuraminidase inhibitors as anti-influenza virus agents. *Antiviral Chemistry and Chemotherapy* 10, 141-154.
- Kim, H., Webster, R.G., and Webby, R.J. (2018). Influenza virus: dealing with a drifting and shifting pathogen. *Viral immunology* 31, 174-183.
- Kim, J.-H., Resende, R., Wennekes, T., Chen, H.-M., Bance, N., Buchini, S., Watts, A.G., Pilling, P., Streltsov, V.A., and Petric, M. (2013). Mechanism-based covalent

- neuraminidase inhibitors with broad-spectrum influenza antiviral activity. *Science* 340, 71-75.
- Kissling, E., Maurel, M., Emborg, H.-D., Whitaker, H., Mcmenamin, J., Howard, J., Trebbien, R., Watson, C., Findlay, B., and Pozo, F. (2023). Interim 2022/23 influenza vaccine effectiveness: six European studies, October 2022 to January 2023. *Eurosurveillance* 28, 2300116.
- Kistner, O., Müller, K., and Scholtissek, C. (1989). Differential phosphorylation of the nucleoprotein of influenza A viruses. *Journal of general virology* 70, 2421-2431.
- Klenk, H.-D., Rott, R., Orlich, M., and Blödmern, J. (1975). Activation of influenza A viruses by trypsin treatment. *Virology* 68, 426-439.
- Kordyukova, L.V., Serebryakova, M.V., Baratova, L.A., and Veit, M. (2008). S acylation of the hemagglutinin of influenza viruses: mass spectrometry reveals site-specific attachment of stearic acid to a transmembrane cysteine. *Journal of virology* 82, 9288-9292.
- Kotenko, S.V., Gallagher, G., Baurin, V.V., Lewis-Antes, A., Shen, M., Shah, N.K., Langer, J.A., Sheikh, F., Dickensheets, H., and Donnelly, R.P. (2003). IFN- λ s mediate antiviral protection through a distinct class II cytokine receptor complex. *Nature immunology* 4, 69-77.
- Koul, P., Khan, U., Bhat, K., Saha, S., Broor, S., Lal, R., and Chadha, M. (2013). Recrudescence wave of A/H1N1pdm09 influenza viruses in Winter 2012-2013 in Kashmir, India. *Plos Currents* 5.
- Kujime, K., Hashimoto, S., Gon, Y., Shimizu, K., and Horie, T. (2000). p38 mitogen-activated protein kinase and c-jun-NH2-terminal kinase regulate RANTES production by influenza virus-infected human bronchial epithelial cells. *The Journal of Immunology* 164, 3222-3228.
- Kulkarni, S.V., Narain, J.P., Gupta, S., Dhariwal, A.C., Singh, S.K., and Macintyre, C.R. (2019). Influenza A (H1N1) in India: Changing epidemiology and its implications. *Natl Med J India* 32, 107-108.
- Kumar, S., Tamura, K., and Nei, M. (2004). MEGA3: integrated software for molecular evolutionary genetics analysis and sequence alignment. *Briefings in bioinformatics* 5, 150-163.
- Lahaye, X., Vidy, A., Fouquet, B., and Blondel, D. (2012). Hsp70 protein positively regulates rabies virus infection. *Journal of virology* 86, 4743-4751.
- Lai, J.C., Chan, W.W., Kien, F., Nicholls, J.M., Peiris, J.M., and Garcia, J.-M. (2010). Formation of virus-like particles from human cell lines exclusively expressing influenza neuraminidase. *Journal of General Virology* 91, 2322-2330.
- Lakadamyali, M., Rust, M.J., Babcock, H.P., and Zhuang, X. (2003). Visualizing infection of individual influenza viruses. *Proceedings of the National Academy of Sciences* 100, 9280-9285.
- Lakdawala, S.S., Wu, Y., Wawrzusin, P., Kabat, J., Broadbent, A.J., Lamirande, E.W., Fodor, E., Altan-Bonnet, N., Shroff, H., and Subbarao, K. (2014). Influenza A virus assembly intermediates fuse in the cytoplasm. *PLoS pathogens* 10, e1003971.
- Lamb, R.A., Choppin, P.W., Chanock, R.M., and Lai, C.-J. (1980). Mapping of the two overlapping genes for polypeptides NS1 and NS2 on RNA segment 8 of influenza virus genome. *Proceedings of the National Academy of Sciences* 77, 1857-1861.
- Lamb, R.A., and Lai, C.-J. (1980). Sequence of interrupted and uninterrupted mRNAs and cloned DNA coding for the two overlapping nonstructural proteins of influenza virus. *Cell* 21, 475-485.
- Lamb, R.A., Lai, C.-J., and Choppin, P.W. (1981). Sequences of mRNAs derived from genome RNA segment 7 of influenza virus: colinear and interrupted mRNAs code for overlapping proteins. *Proceedings of the National Academy of Sciences* 78, 4170-4174.

- Latham, T., and Galarza, J.M. (2001). Formation of wild-type and chimeric influenza virus-like particles following simultaneous expression of only four structural proteins. *Journal of virology* 75, 6154-6165.
- Le Bon, A., and Tough, D.F. (2002). Links between innate and adaptive immunity via type I interferon. *Current opinion in immunology* 14, 432-436.
- Le Goffic, R., Pothlichet, J., Vitour, D., Fujita, T., Meurs, E., Chignard, M., and Si-Tahar, M. (2007). Cutting Edge: Influenza A virus activates TLR3-dependent inflammatory and RIG-I-dependent antiviral responses in human lung epithelial cells. *The Journal of Immunology* 178, 3368-3372.
- Lee, N., Le Sage, V., Nanni, A.V., Snyder, D.J., Cooper, V.S., and Lakdawala, S.S. (2017). Genome-wide analysis of influenza viral RNA and nucleoprotein association. *Nucleic acids research* 45, 8968-8977.
- Lee, R., White, M., and Hartshorn, K. (2006). Influenza A viruses upregulate neutrophil toll-like receptor 2 expression and function. *Scandinavian journal of immunology* 63, 81-89.
- Leela, S.L., Srisawat, C., Sreekanth, G.P., Noisakran, S., Yenchitsomanus, P.-T., and Limjindaporn, T. (2016). Drug repurposing of minocycline against dengue virus infection. *Biochemical and biophysical research communications* 478, 410-416.
- Levandowski, R.A., Gerrity, T.R., and Garrard, C.S. (1985). Modifications of lung clearance mechanisms by acute influenza A infection. *The Journal of laboratory and clinical medicine* 106, 424-427.
- Levine, H.L., Brody, R.S., and Westheimer, F. (1980). Inhibition of orotidine-5'-phosphate decarboxylase by 1-(5'-phospho-. beta.-D-ribofuranosyl) barbituric acid, 6-azauridine 5'-phosphate, and uridine 5'-phosphate. *Biochemistry* 19, 4993-4999.
- Li, Q., Qi, J., Zhang, W., Vavricka, C.J., Shi, Y., Wei, J., Feng, E., Shen, J., Chen, J., and Liu, D. (2010). The 2009 pandemic H1N1 neuraminidase N1 lacks the 150-cavity in its active site. *Nature structural & molecular biology* 17, 1266-1268.
- Li, S., Min, J.-Y., Krug, R.M., and Sen, G.C. (2006). Binding of the influenza A virus NS1 protein to PKR mediates the inhibition of its activation by either PACT or double-stranded RNA. *Virology* 349, 13-21.
- Li, S., Schulman, J., Itamura, S., and Palese, P. (1993). Glycosylation of neuraminidase determines the neurovirulence of influenza A/WSN/33 virus. *Journal of virology* 67, 6667-6673.
- Li, T.C., Chan, M.C., and Lee, N. (2015). Clinical implications of antiviral resistance in influenza. *Viruses* 7, 4929-4944.
- Lin, Y.P., Gregory, V., Collins, P., Kloess, J., Wharton, S., Cattle, N., Lackenby, A., Daniels, R., and Hay, A. (2010). Neuraminidase receptor binding variants of human influenza A (H3N2) viruses resulting from substitution of aspartic acid 151 in the catalytic site: a role in virus attachment? *Journal of virology* 84, 6769-6781.
- Lingwood, D., and Simons, K. (2010). Lipid rafts as a membrane-organizing principle. *science* 327, 46-50.
- Linko, R., Pettilä, V., Ruokonen, E., Varpula, T., Karlsson, S., Tenhunen, J., Reinikainen, M., Saarinen, K., Perttilä, J., and Parviainen, I. (2011). Corticosteroid therapy in intensive care unit patients with PCR-confirmed influenza A (H1N1) infection in Finland. *Acta anaesthesiologica scandinavica* 55, 971-979.
- Linster, M., Van Boheemen, S., De Graaf, M., Schrauwen, E.J., Lexmond, P., Mänz, B., Bestebroer, T.M., Baumann, J., Van Riel, D., and Rimmelzwaan, G.F. (2014). Identification, characterization, and natural selection of mutations driving airborne transmission of A/H5N1 virus. *Cell* 157, 329-339.

- Little, J.W., Hall, W.J., Douglas Jr, R.G., Mudholkar, G.S., Speers, D.M., and Patel, K. (1978). Airway hyperreactivity and peripheral airway dysfunction in influenza A infection. *American Review of Respiratory Disease* 118, 295-303.
- Liu, C., Eichelberger, M.C., Compans, R.W., and Air, G.M. (1995). Influenza type A virus neuraminidase does not play a role in viral entry, replication, assembly, or budding. *Journal of virology* 69, 1099-1106.
- Liu, J., Lynch, P.A., Chien, C., Montelione, G.T., Krug, R.M., and Berman, H.M. (1997). Crystal structure of the unique RNA-binding domain of the influenza virus NS1 protein. *Nature structural biology* 4, 896-899.
- Liu, S.T., Behzadi, M.A., Sun, W., Freyn, A.W., Liu, W.-C., Broecker, F., Albrecht, R.A., Bouvier, N.M., Simon, V., and Nachbagauer, R. (2018). Antigenic sites in influenza H1 hemagglutinin display species-specific immunodominance. *The Journal of clinical investigation* 128, 4992-4996.
- Lofgren, E., Fefferman, N.H., Naumov, Y.N., Gorski, J., and Naumova, E.N. (2007). Influenza seasonality: underlying causes and modeling theories. *Journal of virology* 81, 5429-5436.
- Long, J.C., and Fodor, E. (2016). The PB2 subunit of the influenza A virus RNA polymerase is imported into the mitochondrial matrix. *Journal of virology* 90, 8729-8738.
- Louie, J.K., Salibay, C.J., Kang, M., Glenn-Finer, R.E., Murray, E.L., and Jamieson, D.J. (2015). Pregnancy and severe influenza infection in the 2013–2014 influenza season. *Obstetrics & Gynecology* 125, 184-192.
- Lowy, R.J. (2003). Influenza virus induction of apoptosis by intrinsic and extrinsic mechanisms. *International reviews of immunology* 22, 425-449.
- Lu, X., Masic, A., Li, Y., Shin, Y., Liu, Q., and Zhou, Y. (2010). The PI3K/Akt pathway inhibits influenza A virus-induced Bax-mediated apoptosis by negatively regulating the JNK pathway via ASK1. *Journal of General Virology* 91, 1439-1449.
- Lu, Y., Wambach, M., Katze, M.G., and Krug, R.M. (1995). Binding of the influenza virus NS1 protein to double-stranded RNA inhibits the activation of the protein kinase that phosphorylates the eIF-2 translation initiation factor. *Virology* 214, 222-228.
- Ludwig, S., Ehrhardt, C., Neumeier, E.R., Kracht, M., Rapp, U.R., and Pleschka, S. (2001). Influenza virus-induced AP-1-dependent gene expression requires activation of the JNK signaling pathway. *Journal of Biological Chemistry* 276, 10990-10998.
- Ludwig, S., Pleschka, S., Planz, O., and Wolff, T. (2006). Ringing the alarm bells: signalling and apoptosis in influenza virus infected cells. *Cellular microbiology* 8, 375-386.
- Ludwig, S., Wolff, T., Ehrhardt, C., Wurzer, W.J., Reinhardt, J., Planz, O., and Pleschka, S. (2004). MEK inhibition impairs influenza B virus propagation without emergence of resistant variants. *FEBS letters* 561, 37-43.
- Lukarska, M., Fournier, G., Pflug, A., Resa-Infante, P., Reich, S., Naffakh, N., and Cusack, S. (2017). Structural basis of an essential interaction between influenza polymerase and Pol II CTD. *Nature* 541, 117-121.
- Lund, J.M., Alexopoulou, L., Sato, A., Karow, M., Adams, N.C., Gale, N.W., Iwasaki, A., and Flavell, R.A. (2004). Recognition of single-stranded RNA viruses by Toll-like receptor 7. *Proceedings of the National Academy of Sciences* 101, 5598-5603.
- Madak, J.T., Cuthbertson, C.R., Chen, W., Showalter, H.D., and Neamati, N. (2017). Design, synthesis, and characterization of brequinar conjugates as probes to study DHODH inhibition. *Chemistry—A European Journal* 23, 13875-13878.
- Maeda, T., Kawasaki, K., and Ohnishi, S.-L. (1981). Interaction of influenza virus hemagglutinin with target membrane lipids is a key step in virus-induced hemolysis and fusion at pH 5.2. *Proceedings of the National Academy of Sciences* 78, 4133-4137.

- Mair-Jenkins, J., Saavedra-Campos, M., Baillie, J.K., Cleary, P., Khaw, F.-M., Lim, W.S., Makki, S., Rooney, K.D., Group, C.P.S., and Nguyen-Van-Tam, J.S. (2015). The effectiveness of convalescent plasma and hyperimmune immunoglobulin for the treatment of severe acute respiratory infections of viral etiology: a systematic review and exploratory meta-analysis. *The Journal of infectious diseases* 211, 80-90.
- Majanja, J., Njoroge, R.N., Achilla, R., Wurapa, E.K., Wadegu, M., Mukunzi, S., Mwangi, J., Njiri, J., Gachara, G., and Bulimo, W. (2013). Impact of influenza A (H1N1) pdm09 virus on circulation dynamics of seasonal influenza strains in Kenya. *The American Journal of Tropical Medicine and Hygiene* 88, 940.
- Malbari, K.D., Chintakrindi, A.S., Ganji, L.R., Gohil, D.J., Kothari, S.T., Joshi, M.V., and Kanyalkar, M.A. (2019). Structure-aided drug development of potential neuraminidase inhibitors against pandemic H1N1 exploring alternate binding mechanism. *Molecular Diversity* 23, 927-951.
- Mandon, E.C., Trueman, S.F., and Gilmore, R. (2013). Protein translocation across the rough endoplasmic reticulum. *Cold Spring Harbor Perspectives in Biology* 5, a013342.
- Manzoor, R., Igarashi, M., and Takada, A. (2017). Influenza A virus M2 protein: roles from ingress to egress. *International journal of molecular sciences* 18, 2649.
- Manzoor, R., Kuroda, K., Yoshida, R., Tsuda, Y., Fujikura, D., Miyamoto, H., Kajihara, M., Kida, H., and Takada, A. (2014). Heat shock protein 70 modulates influenza A virus polymerase activity. *Journal of Biological Chemistry* 289, 7599-7614.
- Marcotrigiano, J., Gingras, A.-C., Sonenberg, N., and Burley, S.K. (1997). Cocystal structure of the messenger RNA 5' cap-binding protein (eIF4E) bound to 7-methyl-GDP. *Cell* 89, 951-961.
- Marjuki, H., Alam, M.I., Ehrhardt, C., Wagner, R., Planz, O., Klenk, H.-D., Ludwig, S., and Pleschka, S. (2006). Membrane accumulation of influenza A virus hemagglutinin triggers nuclear export of the viral genome via protein kinase C α -mediated activation of ERK signaling. *Journal of Biological Chemistry* 281, 16707-16715.
- Marjuki, H., Yen, H.-L., Franks, J., Webster, R.G., Pleschka, S., and Hoffmann, E. (2007). Higher polymerase activity of a human influenza virus enhances activation of the hemagglutinin-induced Raf/MEK/ERK signal cascade. *Virology journal* 4, 1-19.
- Martin, K., and Heleniust, A. (1991). Nuclear transport of influenza virus ribonucleoproteins: the viral matrix protein (M1) promotes export and inhibits import. *Cell* 67, 117-130.
- Martin, R. (1997). Modes of action of anthelmintic drugs. *The Veterinary Journal* 154, 11-34.
- Martínez-Alonso, M., Hengrung, N., and Fodor, E. (2016). RNA-free and ribonucleoprotein-associated influenza virus polymerases directly bind the serine-5-phosphorylated carboxyl-terminal domain of host RNA polymerase II. *Journal of virology* 90, 6014-6021.
- Maruoka, S., Hashimoto, S., Gon, Y., Nishitoh, H., Takeshita, I., Asai, Y., Mizumura, K., Shimizu, K., Ichijo, H., and Horie, T. (2003). ASK1 regulates influenza virus infection-induced apoptotic cell death. *Biochemical and Biophysical Research Communications* 307, 870-876.
- Matrosovich, M., Tuzikov, A., Bovin, N., Gambaryan, A., Klimov, A., Castrucci, M.R., Donatelli, I., and Kawaoka, Y. (2000). Early alterations of the receptor-binding properties of H1, H2, and H3 avian influenza virus hemagglutinins after their introduction into mammals. *Journal of virology* 74, 8502-8512.
- Matrosovich, M.N., Matrosovich, T.Y., Gray, T., Roberts, N.A., and Klenk, H.-D. (2004). Neuraminidase is important for the initiation of influenza virus infection in human airway epithelium. *Journal of virology* 78, 12665-12667.

- Maurer-Stroh, S., Lee, R.T.C., Eisenhaber, F., Cui, L., Phuah, S.P., and Lin, R.T. (2010). A new common mutation in the hemagglutinin of the 2009 (H1N1) influenza A virus. *PLoS Currents* 2.
- Mazur, I., Anhlán, D., Mitzner, D., Wixler, L., Schubert, U., and Ludwig, S. (2008). The proapoptotic influenza A virus protein PB1-F2 regulates viral polymerase activity by interaction with the PB1 protein. *Cellular microbiology* 10, 1140-1152.
- Mcauley, J.L., Gilbertson, B.P., Trifkovic, S., Brown, L.E., and Mckimm-Breschkin, J.L. (2019). Influenza virus neuraminidase structure and functions. *Frontiers in microbiology* 10, 432609.
- Mcauley, J.L., Hornung, F., Boyd, K.L., Smith, A.M., Mckee, R., Bennink, J., Yewdell, J.W., and McCullers, J.A. (2007). Expression of the 1918 influenza A virus PB1-F2 enhances the pathogenesis of viral and secondary bacterial pneumonia. *Cell host & microbe* 2, 240-249.
- Mcauley, J.L., Zhang, K., and McCullers, J.A. (2010). The effects of influenza A virus PB1-F2 protein on polymerase activity are strain specific and do not impact pathogenesis. *Journal of virology* 84, 558-564.
- Mcdougal, J.S., Mawle, A., Cort, S.P., Nicholson, J., Cross, G.D., Scheppeler-Campbell, J.A., Hicks, D., and Sligh, J. (1985). Cellular tropism of the human retrovirus HTLV-III/LAV. I. Role of T cell activation and expression of the T4 antigen. *Journal of immunology (Baltimore, Md.: 1950)* 135, 3151-3162.
- Mckimm-Breschkin, J.L. (2013). Influenza neuraminidase inhibitors: antiviral action and mechanisms of resistance. *Influenza and other respiratory viruses* 7, 25-36.
- Meerhoff, T.J., Simaku, A., Ulqinaku, D., Torosyan, L., Gribkova, N., Shimanovich, V., Chakhunashvili, G., Karseladze, I., Yesmagambetova, A., and Kuatbayeva, A. (2015). Surveillance for severe acute respiratory infections (SARI) in hospitals in the WHO European region-an exploratory analysis of risk factors for a severe outcome in influenza-positive SARI cases. *BMC infectious diseases* 15, 1-12.
- Merritt, T., Hope, K., Butler, M., Durrheim, D., Gupta, L., Najjar, Z., Conaty, S., Boonwatt, L., and Fletcher, S. (2016). Effect of antiviral prophylaxis on influenza outbreaks in aged care facilities in three local health districts in New South Wales, Australia, 2014. *Western Pacific surveillance and response journal: WPSAR* 7, 14.
- Mibayashi, M., MartíNez-Sobrido, L., Loo, Y.-M., Cárdenas, W.B., Gale Jr, M., and García-Sastre, A. (2007). Inhibition of retinoic acid-inducible gene I-mediated induction of beta interferon by the NS1 protein of influenza A virus. *Journal of virology* 81, 514-524.
- Michaelis, M., Kleinschmidt, M.C., Doerr, H.W., and Cinatl Jr, J. (2007). Minocycline inhibits West Nile virus replication and apoptosis in human neuronal cells. *Journal of Antimicrobial Chemotherapy* 60, 981-986.
- Min, J.-Y., and Krug, R.M. (2006). The primary function of RNA binding by the influenza A virus NS1 protein in infected cells: Inhibiting the 2'-5' oligo (A) synthetase/RNase L pathway. *Proceedings of the National Academy of Sciences* 103, 7100-7105.
- Min, J.-Y., Li, S., Sen, G.C., and Krug, R.M. (2007). A site on the influenza A virus NS1 protein mediates both inhibition of PKR activation and temporal regulation of viral RNA synthesis. *Virology* 363, 236-243.
- Mir, M.A., Lal, R.B., Sullender, W., Singh, Y., Garten, R., Krishnan, A., and Broor, S. (2012). Genetic diversity of HA1 domain of hemagglutinin gene of pandemic influenza H1N1pdm09 viruses in New Delhi, India. *Journal of medical virology* 84, 386-393.
- Mishra, B. (2015). 2015 resurgence of influenza a (H1N1) 09: Smoldering pandemic in India? *Journal of global infectious diseases* 7, 56-59.

- Mishra, M.K., and Basu, A. (2008). Minocycline neuroprotects, reduces microglial activation, inhibits caspase 3 induction, and viral replication following Japanese encephalitis. *Journal of neurochemistry* 105, 1582-1595.
- Mitzner, D., Dudek, S.E., Studtrucker, N., Anhlán, D., Mazur, I., Wissing, J., Jänsch, L., Wixler, L., Bruns, K., and Sharma, A. (2009). Phosphorylation of the influenza A virus protein PB1-F2 by PKC is crucial for apoptosis promoting functions in monocytes. *Cellular microbiology* 11, 1502-1516.
- Mochalova, L., Kurova, V., Shtyrya, Y., Korchagina, E., Gambaryan, A., Belyanchikov, I., and Bovin, N. (2007). Oligosaccharide specificity of influenza H1N1 virus neuraminidases. *Archives of virology* 152, 2047-2057.
- Moghadami, M., Moattari, A., Tabatabaee, H.R., Mirahmadizadeh, A., Rezaianzadeh, A., Hasanzadeh, J., Ebrahimi, M., Zamiri, N., Alborzi, A., and Bagheri Lankarani, K. (2010). High titers of hemagglutination inhibition antibodies against 2009 H1N1 influenza virus in Southern Iran. *Iran J Immunol* 7, 39-48.
- Mohd Ropidi, M.I., Khazali, A.S., Nor Rashid, N., and Yusof, R. (2020). Endoplasmic reticulum: a focal point of Zika virus infection. *Journal of biomedical science* 27, 1-13.
- Molineux, D. (1694). Dr. Molineux's Historical Account of the Late General Coughs and Colds; with Some Observations on Other Epidemick Distempers. *Philosophical Transactions (1683-1775)*, 105-111.
- Momose, F., Sekimoto, T., Ohkura, T., Jo, S., Kawaguchi, A., Nagata, K., and Morikawa, Y. (2011). Apical transport of influenza A virus ribonucleoprotein requires Rab11-positive recycling endosome. *PloS one* 6, e21123.
- Mondal, A., Potts, G.K., Dawson, A.R., Coon, J.J., and Mehle, A. (2015). Phosphorylation at the homotypic interface regulates nucleoprotein oligomerization and assembly of the influenza virus replication machinery. *PLoS pathogens* 11, e1004826.
- Mor, A., White, A., Zhang, K., Thompson, M., Esparza, M., Muñoz-Moreno, R., Koide, K., Lynch, K.W., García-Sastre, A., and Fontoura, B. (2016). Influenza virus mRNA trafficking through host nuclear speckles. *Nature microbiology* 1, 1-13.
- Moreira, É.A., Weber, A., Bolte, H., Kolesnikova, L., Giese, S., Lakdawala, S., Beer, M., Zimmer, G., García-Sastre, A., and Schwemmler, M. (2016). A conserved influenza A virus nucleoprotein code controls specific viral genome packaging. *Nature Communications* 7, 12861.
- Morens, D.M., and Taubenberger, J.K. (2019). Making universal influenza vaccines: lessons from the 1918 pandemic. *The Journal of infectious diseases* 219, S5-S13.
- Mori, I., Komatsu, T., Takeuchi, K., Nakakuki, K., Sudo, M., and Kimura, Y. (1995). In vivo induction of apoptosis by influenza virus. *Journal of general virology* 76, 2869-2873.
- Mosnier, A., Caini, S., Daviaud, I., Nauleau, E., Bui, T.T., Debost, E., Bedouret, B., Agius, G., Van Der Werf, S., and Lina, B. (2015). Clinical characteristics are similar across type A and B influenza virus infections. *PLoS One* 10, e0136186.
- Mudhigeti, N., Racherla, R.G., Mahalakshmi, P.A., Pamireddy, M.L., Nallapireddy, U., Kante, M., and Kalawat, U. (2018). A study of influenza 2017–2018 outbreak in Andhra Pradesh, India. *Indian Journal of Medical Microbiology* 36, 526-531.
- Mukherjee, A., Nayak, M.K., Dutta, S., Panda, S., Satpathi, B.R., and Chawla-Sarkar, M. (2016). Genetic characterization of circulating 2015 A (H1N1) pdm09 influenza viruses from Eastern India. *PLoS One* 11, e0168464.
- Mukherjee, A., Roy, T., Agrawal, A.S., Sarkar, M., Lal, R., Chakrabarti, S., and Chawla-Sarkar, M. (2010). Prevalence and epidemiology of pandemic H1N1 strains in hospitals of Eastern India. *Journal of Public Health and Epidemiology* 2, 171-174.
- Mukherjee, T.R., Agrawal, A.S., Chakrabarti, S., and Chawla-Sarkar, M. (2012). Full genomic analysis of an influenza A (H1N2) virus identified during 2009 pandemic in Eastern

- India: evidence of reassortment event between co-circulating A (H1N1) pdm09 and A/Brisbane/10/2007-like H3N2 strains. *Virology journal* 9, 1-10.
- Murhekar, M., and Mehendale, S. (2016). The 2015 influenza A (H1N1) pdm09 outbreak in India. *Indian Journal of Medical Research* 143, 821-823.
- Muthuri, S.G., Venkatesan, S., Myles, P.R., Leonardi-Bee, J., Al Khuwaitir, T.S., Al Mamun, A., Anovadiya, A.P., Azziz-Baumgartner, E., Báez, C., and Bassetti, M. (2014). Effectiveness of neuraminidase inhibitors in reducing mortality in patients admitted to hospital with influenza A H1N1pdm09 virus infection: a meta-analysis of individual participant data. *The lancet Respiratory medicine* 2, 395-404.
- Nakagawa, H., Noma, H., Kotake, O., Motohashi, R., Yasuda, K., and Shimura, M. (2017). Optic neuritis and acute anterior uveitis associated with influenza A infection: a case report. *International medical case reports journal*, 1-5.
- Nakagawa, Y., Kimura, N., Toyoda, T., Mizumoto, K., Ishihama, A., Oda, K., and Nakada, S. (1995). The RNA polymerase PB2 subunit is not required for replication of the influenza virus genome but is involved in capped mRNA synthesis. *Journal of virology* 69, 728-733.
- Nayak, D. (2014). Influenza virus infections. *Reference Module in Biomedical Sciences*.
- Nayak, D.P., Hui, E.K.-W., and Barman, S. (2004). Assembly and budding of influenza virus. *Virus research* 106, 147-165.
- Nemeroff, M.E., Barabino, S.M., Li, Y., Keller, W., and Krug, R.M. (1998). Influenza virus NS1 protein interacts with the cellular 30 kDa subunit of CPSF and inhibits 3' end formation of cellular pre-mRNAs. *Molecular cell* 1, 991-1000.
- Nemeroff, M.E., Qian, X.-Y., and Krug, R.M. (1995). The influenza virus NS1 protein forms multimers in vitro and in vivo. *Virology* 212, 422-428.
- Neumann, G., Hughes, M.T., and Kawaoka, Y. (2000). Influenza A virus NS2 protein mediates vRNP nuclear export through NES-independent interaction with hCRM1. *The EMBO journal*.
- Newcomb, L.L., Kuo, R.-L., Ye, Q., Jiang, Y., Tao, Y.J., and Krug, R.M. (2009). Interaction of the influenza A virus nucleocapsid protein with the viral RNA polymerase potentiates unprimed viral RNA replication. *Journal of virology* 83, 29-36.
- Nguyen, H.K., Nguyen, P.T., Nguyen, T.C., Hoang, P.V., Le, T.T., Vuong, C.D., Nguyen, A.P., Tran, L.T., Nguyen, B.G., and Lê, M.Q. (2015). Virological characterization of influenza H1N1pdm09 in Vietnam, 2010-2013. *Influenza and other respiratory viruses* 9, 216-224.
- Nguyen, T.N.A., Dao, T.T., Tung, B.T., Choi, H., Kim, E., Park, J., Lim, S.-I., and Oh, W.K. (2011). Influenza A (H1N1) neuraminidase inhibitors from *Vitis amurensis*. *Food chemistry* 124, 437-443.
- Nieto, A., De La Luna, S., Bárcena, J., Portela, A., and Ortin, J. (1994). Complex structure of the nuclear translocation signal of influenza virus polymerase PA subunit. *Journal of general virology* 75, 29-36.
- Nikodemova, M., Duncan, I.D., and Watters, J.J. (2006). Minocycline exerts inhibitory effects on multiple mitogen-activated protein kinases and I κ B α degradation in a stimulus-specific manner in microglia. *Journal of neurochemistry* 96, 314-323.
- Nishiura, H. (2010). Case fatality ratio of pandemic influenza. *The Lancet infectious diseases* 10, 443-444.
- Nobusawa, E., Aoyama, T., Kato, H., Suzuki, Y., Tateno, Y., and Nakajima, K. (1991). Comparison of complete amino acid sequences and receptor-binding properties among 13 serotypes of hemagglutinins of influenza A viruses. *Virology* 182, 475-485.

- Nordholm, J., Da Silva, D.V., Damjanovic, J., Dou, D., and Daniels, R. (2013). Polar residues and their positional context dictate the transmembrane domain interactions of influenza A neuraminidases. *Journal of Biological Chemistry* 288, 10652-10660.
- Nordholm, J., Petitou, J., Östbye, H., Da Silva, D.V., Dou, D., Wang, H., and Daniels, R. (2017). Translational regulation of viral secretory proteins by the 5' coding regions and a viral RNA-binding protein. *Journal of Cell Biology* 216, 2283-2293.
- Noton, S.L., Medcalf, E., Fisher, D., Mullin, A.E., Elton, D., and Digard, P. (2007). Identification of the domains of the influenza A virus M1 matrix protein required for NP binding, oligomerization and incorporation into virions. *Journal of General Virology* 88, 2280-2290.
- O'Neill, R.E., Jaskunas, R., Blobel, G., Palese, P., and Moroianu, J. (1995). Nuclear Import of Influenza Virus RNA Can Be Mediated by Viral Nucleoprotein and Transport Factors Required for Protein Import (*). *Journal of Biological Chemistry* 270, 22701-22704.
- O'Neill, R.E., Talon, J., and Palese, P. (1998). The influenza virus NEP (NS2 protein) mediates the nuclear export of viral ribonucleoproteins. *The EMBO journal*.
- Obayashi, E., Yoshida, H., Kawai, F., Shibayama, N., Kawaguchi, A., Nagata, K., Tame, J.R., and Park, S.-Y. (2008). The structural basis for an essential subunit interaction in influenza virus RNA polymerase. *Nature* 454, 1127-1131.
- Ohmit, S.E., Petrie, J.G., Malosh, R.E., Fry, A.M., Thompson, M.G., and Monto, A.S. (2015). Influenza vaccine effectiveness in households with children during the 2012–2013 season: assessments of prior vaccination and serologic susceptibility. *The Journal of infectious diseases* 211, 1519-1528.
- Opitz, B., Rejaibi, A., Dauber, B., Eckhard, J., Vinzing, M., Schmeck, B., Hippenstiel, S., Suttorp, N., and Wolff, T. (2007). IFN β induction by influenza A virus is mediated by RIG-I which is regulated by the viral NS1 protein. *Cellular microbiology* 9, 930-938.
- Organization, W.H. (2008). Recommended composition of influenza virus vaccines for use in the 2009 Southern Hemisphere influenza season. *Weekly Epidemiological Record= Relevé épidémiologique hebdomadaire* 83, 366-372.
- Palache, A., Abelin, A., Hollingsworth, R., Cracknell, W., Jacobs, C., Tsai, T., and Barbosa, P. (2017). Survey of distribution of seasonal influenza vaccine doses in 201 countries (2004–2015): the 2003 World Health Assembly resolution on seasonal influenza vaccination coverage and the 2009 influenza pandemic have had very little impact on improving influenza control and pandemic preparedness. *Vaccine* 35, 4681-4686.
- Palazzo, A.F., Springer, M., Shibata, Y., Lee, C.-S., Dias, A.P., and Rapoport, T.A. (2007). The signal sequence coding region promotes nuclear export of mRNA. *PLoS biology* 5, e322.
- Palese, P., and Compans, R. (1976). Inhibition of influenza virus replication in tissue culture by 2-deoxy-2, 3-dehydro-N-trifluoroacetylneuraminic acid (FANA): mechanism of action. *Journal of General Virology* 33, 159-163.
- Palese, P., and Shaw, M. (2007). Fields virology. *Orthomyxoviridae: The Viruses and Their Replication, 5th edn*, Philadelphia, PA: Lippincott Williams & Wilkins, Wolters Kluwer Business, 1647-1689.
- Palese, P., Tobita, K., Ueda, M., and Compans, R.W. (1974). Characterization of temperature sensitive influenza virus mutants defective in neuraminidase. *Virology* 61, 397-410.
- Pandey, S., Sahu, M., Potdar, V., and Barde, P. (2018). Molecular analysis of influenza A H1N1pdm09 virus circulating in Madhya Pradesh, India in the year 2017. *Virusdisease* 29, 380-384.
- Panthu, B., Terrier, O., Carron, C., Traversier, A., Corbin, A., Balvay, L., Lina, B., Rosa-Calatrava, M., and Ohlmann, T. (2017). The NS1 protein from influenza virus

- stimulates translation initiation by enhancing ribosome recruitment to mRNAs. *Journal of Molecular Biology* 429, 3334-3352.
- Park, Y.W., and Katze, M.G. (1995). Translational control by influenza virus: Identification of cis-acting sequences and trans-acting factors which may regulate selective viral mRNA translation. *Journal of Biological Chemistry* 270, 28433-28439.
- Patel, M.C., Shirey, K.A., Pletneva, L.M., Boukhvalova, M.S., Garzino-Demo, A., Vogel, S.N., and Blanco, J.C. (2014). Novel drugs targeting Toll-like receptors for antiviral therapy. *Future virology* 9, 811-829.
- Paterson, R.G., and Lamb, R.A. (1990). Conversion of a class II integral membrane protein into a soluble and efficiently secreted protein: multiple intracellular and extracellular oligomeric and conformational forms. *The Journal of cell biology* 110, 999-1011.
- Patient, A. (2009). Swine influenza A (H1N1) infection in two children—Southern California, March–April 2009. *Morbidity and Mortality Weekly Report* 58, 400-402.
- Patrick, G. (2013). Drug design: Optimizing target interactions. *An Introduction to Medicinal Chemistry, 5th ed.; Oxford University Press: Oxford, UK*, 215-226.
- Pflug, A., Lukarska, M., Resa-Infante, P., Reich, S., and Cusack, S. (2017). Structural insights into RNA synthesis by the influenza virus transcription-replication machine. *Virus research* 234, 103-117.
- Pinto, L.H., Holsinger, L.J., and Lamb, R.A. (1992). Influenza virus M2 protein has ion channel activity. *cell* 69, 517-528.
- Pinto, L.H., and Lamb, R.A. (2006). The M2 proton channels of influenza A and B viruses. *Journal of Biological Chemistry* 281, 8997-9000.
- Planz, O., Pleschka, S., and Ludwig, S. (2001). MEK-specific inhibitor U0126 blocks spread of Borna disease virus in cultured cells. *Journal of Virology* 75, 4871-4877.
- Pleschka, S., Wolff, T., Ehrhardt, C., Hobom, G., Planz, O., Rapp, U.R., and Ludwig, S. (2001). Influenza virus propagation is impaired by inhibition of the Raf/MEK/ERK signalling cascade. *Nature cell biology* 3, 301-305.
- Plotch, S.J., Bouloy, M., Ulmanen, I., and Krug, R.M. (1981). A unique cap (m7GpppXm)-dependent influenza virion endonuclease cleaves capped RNAs to generate the primers that initiate viral RNA transcription. *Cell* 23, 847-858.
- Poole, E., Elton, D., Medcalf, L., and Digard, P. (2004). Functional domains of the influenza A virus PB2 protein: identification of NP- and PB1-binding sites. *Virology* 321, 120-133.
- Poon, L.L., Pritlove, D.C., Fodor, E., and Brownlee, G.G. (1999). Direct evidence that the poly (A) tail of influenza A virus mRNA is synthesized by reiterative copying of a U track in the virion RNA template. *Journal of virology* 73, 3473-3476.
- Popovic, N., Schubart, A., Goetz, B.D., Zhang, S.C., Linington, C., and Duncan, I.D. (2002). Inhibition of autoimmune encephalomyelitis by a tetracycline. *Annals of Neurology: Official Journal of the American Neurological Association and the Child Neurology Society* 51, 215-223.
- Rambaut, A., Pybus, O.G., Nelson, M.I., Viboud, C., Taubenberger, J.K., and Holmes, E.C. (2008). The genomic and epidemiological dynamics of human influenza A virus. *Nature* 453, 615-619.
- Ramos, E.L., Mitcham, J.L., Koller, T.D., Bonavia, A., Usner, D.W., Balaratnam, G., Fredlund, P., and Swiderek, K.M. (2015). Efficacy and safety of treatment with an anti-m2e monoclonal antibody in experimental human influenza. *The Journal of infectious diseases* 211, 1038-1044.
- Rathore, A.P., Haystead, T., Das, P.K., Merits, A., Ng, M.-L., and Vasudevan, S.G. (2014). Chikungunya virus nsP3 & nsP4 interacts with HSP-90 to promote virus replication: HSP-90 inhibitors reduce CHIKV infection and inflammation in vivo. *Antiviral research* 103, 7-16.

- Ravindran, M.S., Bagchi, P., Cunningham, C.N., and Tsai, B. (2016). Opportunistic intruders: how viruses orchestrate ER functions to infect cells. *Nature Reviews Microbiology* 14, 407-420.
- Raymonda, M.H., Ciesla, J., Monaghan, M., Leach, J., Asantewaa, G., Smorodintsev-Schiller, L., Lutz Iv, M., Schafer, X., Takimoto, T., and Dewhurst, S. (2022). Pharmacologic profiling reveals lapatinib as a novel antiviral against SARS-CoV-2 in vitro. *Virology* 566, 60-68.
- Reich, S., Guilligay, D., Pflug, A., Malet, H., Berger, I., Crépin, T., Hart, D., Lunardi, T., Nanao, M., and Ruigrok, R.W. (2014). Structural insight into cap-snatching and RNA synthesis by influenza polymerase. *Nature* 516, 361-366.
- Rialdi, A., Hultquist, J., Jimenez-Morales, D., Peralta, Z., Campisi, L., Fenouil, R., Moshkina, N., Wang, Z.Z., Laffleur, B., and Kaake, R.M. (2017). The RNA exosome syncs IAV-RNAPII transcription to promote viral ribogenesis and infectivity. *Cell* 169, 679-692. e614.
- Richardson-Burns, S.M., and Tyler, K.L. (2005). Minocycline delays disease onset and mortality in reovirus encephalitis. *Experimental neurology* 192, 331-339.
- Richardson, J., and Akkina, R. (1991). NS 2 protein of influenza virus is found in purified virus and phosphorylated in infected cells. *Archives of virology* 116, 69-80.
- Robb, N.C., and Fodor, E. (2012). The accumulation of influenza A virus segment 7 spliced mRNAs is regulated by the NS1 protein. *Journal of general virology* 93, 113-118.
- Robb, N.C., Te Velhuis, A.J., Wieneke, R., Tampé, R., Cordes, T., Fodor, E., and Kapanidis, A.N. (2016). Single-molecule FRET reveals the pre-initiation and initiation conformations of influenza virus promoter RNA. *Nucleic acids research* 44, 10304-10315.
- Robertson, J.S., Schubert, M., and Lazzarini, R.A. (1981). Polyadenylation sites for influenza virus mRNA. *Journal of virology* 38, 157-163.
- Robinson, M.J., and Cobb, M.H. (1997). Mitogen-activated protein kinase pathways. *Current opinion in cell biology* 9, 180-186.
- Rodems, S.M., and Spector, D.H. (1998). Extracellular signal-regulated kinase activity is sustained early during human cytomegalovirus infection. *Journal of Virology* 72, 9173-9180.
- Rodrigo, C., Leonardi-Bee, J., Nguyen-Van-Tam, J.S., and Lim, W.S. (2015). Effect of corticosteroid therapy on influenza-related mortality: a systematic review and meta-analysis. *The Journal of infectious diseases* 212, 183-194.
- Rogers, G.N., and Paulson, J.C. (1983). Receptor determinants of human and animal influenza virus isolates: differences in receptor specificity of the H3 hemagglutinin based on species of origin. *Virology* 127, 361-373.
- Rojas, Á., Del Campo, J.A., Clement, S., Lemasson, M., García-Valdecasas, M., Gil-Gómez, A., Ranchal, I., Bartosch, B., Bautista, J.D., and Rosenberg, A.R. (2016). Effect of quercetin on hepatitis C virus life cycle: from viral to host targets. *Scientific Reports* 6, 31777.
- Rossmann, J.S., Jing, X., Leser, G.P., and Lamb, R.A. (2010). Influenza virus M2 protein mediates ESCRT-independent membrane scission. *Cell* 142, 902-913.
- Rossmann, J.S., and Lamb, R.A. (2013). Viral membrane scission. *Annual review of cell and developmental biology* 29, 551-569.
- Roy, A.-M.M., Parker, J.S., Parrish, C.R., and Whittaker, G.R. (2000). Early stages of influenza virus entry into Mv-1 lung cells: involvement of dynamin. *Virology* 267, 17-28.
- Ruigrok, R.W., Barge, A., Durrer, P., Brunner, J., Ma, K., and Whittaker, G.R. (2000). Membrane interaction of influenza virus M1 protein. *Virology* 267, 289-298.

- Rust, M.J., Lakadamyali, M., Zhang, F., and Zhuang, X. (2004). Assembly of endocytic machinery around individual influenza viruses during viral entry. *Nature structural & molecular biology* 11, 567-573.
- Ryu, Y.B., Kim, J.H., Park, S.-J., Chang, J.S., Rho, M.-C., Bae, K.-H., Park, K.H., and Lee, W.S. (2010). Inhibition of neuraminidase activity by polyphenol compounds isolated from the roots of *Glycyrrhiza uralensis*. *Bioorganic & medicinal chemistry letters* 20, 971-974.
- S Chintakrindi, A., Af Martis, E., J Gohil, D., T Kothari, S., S Chowdhary, A., C Coutinho, E., and A Kanyalkar, M. (2016). A computational model for docking of noncompetitive neuraminidase inhibitors and probing their binding interactions with neuraminidase of influenza virus H5N1. *Current Computer-Aided Drug Design* 12, 272-281.
- Saitou, N., and Nei, M. (1987). The neighbor-joining method: a new method for reconstructing phylogenetic trees. *Molecular biology and evolution* 4, 406-425.
- Sakai, T., Nishimura, S.I., Naito, T., and Saito, M. (2017). Influenza A virus hemagglutinin and neuraminidase act as novel motile machinery. *Scientific reports* 7, 45043.
- Samuel, C.E. (2001). Antiviral actions of interferons. *Clinical microbiology reviews* 14, 778-809.
- Sanz-Ezquerro, J.J., Zürcher, T., De La Luna, S., Ortín, J., and Nieto, A. (1996). The amino-terminal one-third of the influenza virus PA protein is responsible for the induction of proteolysis. *Journal of virology* 70, 1905-1911.
- Sarkar, M., Agrawal, A.S., Sharma Dey, R., Chattopadhyay, S., Mullick, R., De, P., Chakrabarti, S., and Chawla-Sarkar, M. (2011). Molecular characterization and comparative analysis of pandemic H1N1/2009 strains with co-circulating seasonal H1N1/2009 strains from eastern India. *Archives of virology* 156, 207-217.
- Satterly, N., Tsai, P.-L., Van Deursen, J., Nussenzweig, D.R., Wang, Y., Faria, P.A., Levay, A., Levy, D.E., and Fontoura, B.M. (2007). Influenza virus targets the mRNA export machinery and the nuclear pore complex. *Proceedings of the National Academy of Sciences* 104, 1853-1858.
- Schalken, J.A., Roebroek, A., Oomen, P., Wagenaar, S.S., Debruyne, F., Bloemers, H., and Van De Ven, W. (1987). *fur* gene expression as a discriminating marker for small cell and nonsmall cell lung carcinomas. *The Journal of clinical investigation* 80, 1545-1549.
- Schmitt, A.P., and Lamb, R.A. (2005). Influenza virus assembly and budding at the viral budding zone. *Advances in virus research* 64, 383-416.
- Schotsaert, M., De Filette, M., Fiers, W., and Saelens, X. (2009). Universal M2 ectodomain-based influenza A vaccines: preclinical and clinical developments. *Expert review of vaccines* 8, 499-508.
- Shanmuganatham, K., Feeroz, M.M., Jones-Engel, L., Walker, D., Alam, S., Hasan, M., McKenzie, P., Krauss, S., Webby, R.J., and Webster, R.G. (2014). Genesis of avian influenza H9N2 in Bangladesh. *Emerging microbes & infections* 3, 1-17.
- Shapiro, G., Gurney Jr, T., and Krug, R. (1987). Influenza virus gene expression: control mechanisms at early and late times of infection and nuclear-cytoplasmic transport of virus-specific RNAs. *Journal of virology* 61, 764-773.
- Shaw, M., and Palese, P. (2007). Orthomyxoviridae: The viruses and their replication. *Fields Virology*, 1647-1689.
- Shen, Z., Lou, K., and Wang, W. (2015). New small-molecule drug design strategies for fighting resistant influenza A. *Acta Pharmaceutica Sinica B* 5, 419-430.
- Sheng, Z.-M., Chertow, D.S., Ambroggio, X., McCall, S., Przygodzki, R.M., Cunningham, R.E., Maximova, O.A., Kash, J.C., Morens, D.M., and Taubenberger, J.K. (2011). Autopsy series of 68 cases dying before and during the 1918 influenza pandemic peak. *Proceedings of the National Academy of Sciences* 108, 16416-16421.

- Shi, L., Summers, D.F., Peng, Q., and Galarza, J.M. (1995). Influenza A virus RNA polymerase subunit PB2 is the endonuclease which cleaves host cell mRNA and functions only as the trimeric enzyme. *Virology* 208, 38-47.
- Shimizu, T., Takizawa, N., Watanabe, K., Nagata, K., and Kobayashi, N. (2011). Crucial role of the influenza virus NS2 (NEP) C-terminal domain in M1 binding and nuclear export of vRNP. *FEBS letters* 585, 41-46.
- Shin, Y.-K., Li, Y., Liu, Q., Anderson, D.H., Babiuk, L.A., and Zhou, Y. (2007a). SH3 binding motif 1 in influenza A virus NS1 protein is essential for PI3K/Akt signaling pathway activation. *Journal of virology* 81, 12730-12739.
- Shin, Y.-K., Liu, Q., Tikoo, S.K., Babiuk, L.A., and Zhou, Y. (2007b). Influenza A virus NS1 protein activates the phosphatidylinositol 3-kinase (PI3K)/Akt pathway by direct interaction with the p85 subunit of PI3K. *Journal of General Virology* 88, 13-18.
- Shtykova, E.V., Dadinova, L.A., Fedorova, N.V., Golanikov, A.E., Bogacheva, E.N., Ksenofontov, A.L., Baratova, L.A., Shilova, L.A., Tashkin, V.Y., and Galimzyanov, T.R. (2017). Influenza virus Matrix Protein M1 preserves its conformation with pH, changing multimerization state at the priming stage due to electrostatics. *Scientific reports* 7, 16793.
- Shutter, M., and Akhondi, H. (2023). Tetracycline.[Updated 2023 Jun 5]. *StatPearls [Internet]. Treasure Island (FL): StatPearls Publishing.*
- Siston, A.M., Rasmussen, S.A., Honein, M.A., Fry, A.M., Seib, K., Callaghan, W.M., Louie, J., Doyle, T.J., Crockett, M., and Lynfield, R. (2010). Pandemic 2009 influenza A (H1N1) virus illness among pregnant women in the United States. *Jama* 303, 1517-1525.
- Skehel, J., Bayley, P., Brown, E., Martin, S., Waterfield, M., White, J., Wilson, I., and Wiley, D. (1982). Changes in the conformation of influenza virus hemagglutinin at the pH optimum of virus-mediated membrane fusion. *Proceedings of the National Academy of Sciences* 79, 968-972.
- Skehel, J.J., and Wiley, D.C. (2000). Receptor binding and membrane fusion in virus entry: the influenza hemagglutinin. *Annual review of biochemistry* 69, 531-569.
- Song, Y., Wei, E.-Q., Zhang, W.-P., Zhang, L., Liu, J.-R., and Chen, Z. (2004). Minocycline protects PC12 cells from ischemic-like injury and inhibits 5-lipoxygenase activation. *Neuroreport* 15, 2181-2184.
- Sreekanth, G.P., Chuncharunee, A., Sirimontaporn, A., Panaampon, J., Srisawat, C., Morchang, A., Malakar, S., Thuwajit, P., Kooptiwut, S., and Suttitheptumrong, A. (2014). Role of ERK1/2 signaling in dengue virus-induced liver injury. *Virus research* 188, 15-26.
- Stankavichyus, A., Stankavichene, L., Sapragonene, M., Korobchenko, L., Boreko, E., and Vladyko, G. (1988). Synthesis and antiviral activity of cinnamic acid derivatives. *Pharmaceutical Chemistry Journal* 22, 896-900.
- Staudt, L.M., and Gerhard, W. (1983). Generation of antibody diversity in the immune response of BALB/c mice to influenza virus hemagglutinin. I. Significant variation in repertoire expression between individual mice. *The Journal of experimental medicine* 157, 687-704.
- Steinhauer, D.A., and Holland, J. (1987). Rapid evolution of RNA viruses. *Annual Reviews in Microbiology* 41, 409-431.
- Steinhauer, D.A., Wharton, S.A., Skehel, J.J., Wiley, D.C., and Hay, A.J. (1991). Amantadine selection of a mutant influenza virus containing an acid-stable hemagglutinin glycoprotein: evidence for virus-specific regulation of the pH of glycoprotein transport vesicles. *Proceedings of the National Academy of Sciences* 88, 11525-11529.
- Stetson, D.B., and Medzhitov, R. (2006). Antiviral defense: interferons and beyond. *The Journal of experimental medicine* 203, 1837-1841.

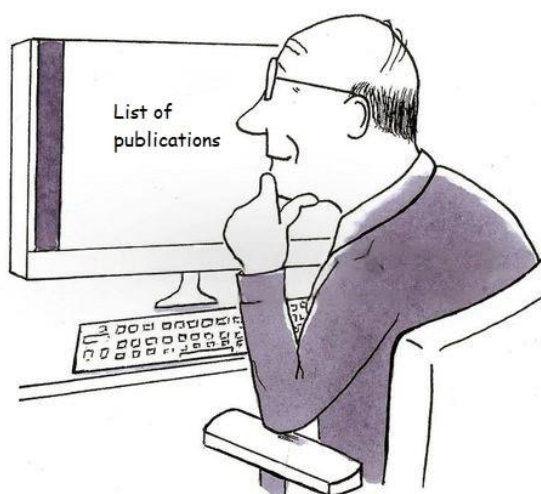
- Stewart, S.M., and Pekosz, A. (2011). Mutations in the membrane-proximal region of the influenza A virus M2 protein cytoplasmic tail have modest effects on virus replication. *Journal of virology* 85, 12179-12187.
- Stieneke-Gröber, A., Vey, M., Angliker, H., Shaw, E., Thomas, G., Roberts, C., Klenk, H., and Garten, W. (1992). Influenza virus hemagglutinin with multibasic cleavage site is activated by furin, a subtilisin-like endoprotease. *The EMBO journal* 11, 2407-2414.
- Sugiyama, K., Obayashi, E., Kawaguchi, A., Suzuki, Y., Tame, J.R., Nagata, K., and Park, S.Y. (2009a). Structural insight into the essential PB1–PB2 subunit contact of the influenza virus RNA polymerase. *The EMBO journal* 28, 1803-1811.
- Sugiyama, K., Obayashi, E., Kawaguchi, A., Suzuki, Y., Tame, J.R.H., Nagata, K., and Park, S.Y. (2009b). Structural insight into the essential PB1–PB2 subunit contact of the influenza virus RNA polymerase. *The EMBO Journal* 28, 1803-1811.
- Szeto, G.L., Brice, A.K., Yang, H.-C., Barber, S.A., Siliciano, R.F., and Clements, J.E. (2010). Minocycline attenuates HIV infection and reactivation by suppressing cellular activation in human CD4+ T cells. *The Journal of infectious diseases* 201, 1132-1140.
- Szyfres, B. (2001). Zoonoses and communicable diseases common to man and animals.
- Taguwa, S., Maringer, K., Li, X., Bernal-Rubio, D., Rauch, J.N., Gestwicki, J.E., Andino, R., Fernandez-Sesma, A., and Frydman, J. (2015). Defining Hsp70 subnetworks in dengue virus replication reveals key vulnerability in flavivirus infection. *Cell* 163, 1108-1123.
- Takatsuki, A., and Tamura, G. (1971). Tunicamycin, a new antibiotic. II some biological properties of the antiviral activity of tunicamycin. *The Journal of Antibiotics* 24, 224-231.
- Takeda, M., Leser, G.P., Russell, C.J., and Lamb, R.A. (2003). Influenza virus hemagglutinin concentrates in lipid raft microdomains for efficient viral fusion. *Proceedings of the National Academy of Sciences* 100, 14610-14617.
- Takeuchi, K., and Lamb, R.A. (1994). Influenza virus M2 protein ion channel activity stabilizes the native form of fowl plague virus hemagglutinin during intracellular transport. *Journal of virology* 68, 911-919.
- Takeuchi, O., and Akira, S. (2008). MDA5/RIG-I and virus recognition. *Current opinion in immunology* 20, 17-22.
- Talon, J., Horvath, C.M., Polley, R., Basler, C.F., Muster, T., Palese, P., and García-Sastre, A. (2000). Activation of interferon regulatory factor 3 is inhibited by the influenza A virus NS1 protein. *Journal of virology* 74, 7989-7996.
- Tamma, P.D., Aitken, S.L., Bonomo, R.A., Mathers, A.J., Van Duin, D., and Clancy, C.J. (2022). Infectious Diseases Society of America guidance on the treatment of AmpC β -lactamase-producing Enterobacterales, carbapenem-resistant *Acinetobacter baumannii*, and *Stenotrophomonas maltophilia* infections. *Clinical Infectious Diseases* 74, 2089-2114.
- Tarendeau, F., Crepin, T., Guilligay, D., Ruigrok, R.W., Cusack, S., and Hart, D.J. (2008). Host determinant residue lysine 627 lies on the surface of a discrete, folded domain of influenza virus polymerase PB2 subunit. *PLoS pathogens* 4, e1000136.
- Terstegen, L., Gatsios, P., Ludwig, S., Pleschka, S., Jahnen-Dechent, W., Heinrich, P.C., and Graeve, L. (2001). The vesicular stomatitis virus matrix protein inhibits glycoprotein 130-dependent STAT activation. *The Journal of Immunology* 167, 5209-5216.
- Thakre, R., and Patil, P. (2019). Influenza vaccine paradox. *Indian Paediatrics* 56, 80.
- Tian, C., Gao, P.F., Pinto, L.H., Lamb, R.A., and Cross, T.A. (2003). Initial structural and dynamic characterization of the M2 protein transmembrane and amphipathic helices in lipid bilayers. *Protein Science* 12, 2597-2605.

- Toyoda, T., Adyshev, D.M., Kobayashi, M., Iwata, A., and Ishihama, A. (1996). Molecular assembly of the influenza virus RNA polymerase: determination of the subunit-subunit contact sites. *Journal of General Virology* 77, 2149-2157.
- Trapp, S., Soubieux, D., Lidove, A., Esnault, E., Lion, A., Guillory, V., Wacquiez, A., Kut, E., Quéré, P., and Larcher, T. (2018). Major contribution of the RNA-binding domain of NS1 in the pathogenicity and replication potential of an avian H7N1 influenza virus in chickens. *Virology journal* 15, 1-12.
- Treanor, J.J. (2015). Prospects for broadly protective influenza vaccines. *Vaccine* 33, D39-D45.
- Treisman, R. (1996). Regulation of transcription by MAP kinase cascades. *Current opinion in cell biology* 8, 205-215.
- Trucchi, C., Paganino, C., Orsi, A., Amicizia, D., Tisa, V., Piazza, M.F., Gallo, D., Simonetti, S., Buonopane, B., and Icardi, G. (2019). Hospital and economic burden of influenza-like illness and lower respiratory tract infection in adults ≥ 50 years-old. *BMC health services research* 19, 1-11.
- Tsitoura, D.C., Blumenthal, R.L., Berry, G., Dekruyff, R.H., and Umetsu, D.T. (2000). Mechanisms preventing allergen-induced airways hyperreactivity: role of tolerance and immune deviation. *Journal of allergy and clinical immunology* 106, 239-246.
- Tumpey, T.M., Maines, T.R., Van Hoeven, N., Glaser, L., SolóRzano, A., Pappas, C., Cox, N.J., Swayne, D.E., Palese, P., and Katz, J.M. (2007). A two-amino acid change in the hemagglutinin of the 1918 influenza virus abolishes transmission. *Science* 315, 655-659.
- Valcárcel, J., Portela, A., and Ortín, J. (1991). Regulated M1 mRNA splicing in influenza virus-infected cells. *Journal of general virology* 72, 1301-1308.
- Varghese, J., and Colman, P. (1991). Three-dimensional structure of the neuraminidase of influenza virus A/Tokyo/3/67 at 2.2 Å resolution. *Journal of molecular biology* 221, 473-486.
- Varghese, J., Laver, W., and Colman, P.M. (1983). Structure of the influenza virus glycoprotein antigen neuraminidase at 2.9 Å resolution. *Nature* 303, 35-40.
- Vester, D., Lagoda, A., Hoffmann, D., Seitz, C., Heldt, S., Bettenbrock, K., Genzel, Y., and Reichl, U. (2010). Real-time RT-qPCR assay for the analysis of human influenza A virus transcription and replication dynamics. *Journal of virological methods* 168, 63-71.
- Viegas-Junior, C., Danuello, A., Da Silva Bolzani, V., Barreiro, E.J., and Fraga, C.a.M. (2007). Molecular hybridization: a useful tool in the design of new drug prototypes. *Current medicinal chemistry* 14, 1829-1852.
- Wagner, R., Herwig, A., Azzouz, N., and Klenk, H.D. (2005). Acylation-mediated membrane anchoring of avian influenza virus hemagglutinin is essential for fusion pore formation and virus infectivity. *Journal of virology* 79, 6449-6458.
- Wang, N., Glidden, E.J., Murphy, S.R., Pearse, B.R., and Hebert, D.N. (2008). The cotranslational maturation program for the type II membrane glycoprotein influenza neuraminidase. *Journal of biological chemistry* 283, 33826-33837.
- Wang, P., Palese, P., and O'Neill, R.E. (1997). The NPI-1/NPI-3 (karyopherin alpha) binding site on the influenza A virus nucleoprotein NP is a nonconventional nuclear localization signal. *Journal of virology* 71, 1850-1856.
- Wang, W., Riedel, K., Lynch, P., Chien, C.-Y., Montelione, G.T., and Krug, R.M. (1999). RNA binding by the novel helical domain of the influenza virus NS1 protein requires its dimer structure and a small number of specific basic amino acids. *Rna* 5, 195-205.
- Wang, X., Basler, C.F., Williams, B.R., Silverman, R.H., Palese, P., and García-Sastre, A. (2002). Functional replacement of the carboxy-terminal two-thirds of the influenza A

- virus NS1 protein with short heterologous dimerization domains. *Journal of virology* 76, 12951-12962.
- Wang, X., Zhu, S., Drozda, M., Zhang, W., Stavrovskaya, I.G., Cattaneo, E., Ferrante, R.J., Kristal, B.S., and Friedlander, R.M. (2003). Minocycline inhibits caspase-independent and-dependent mitochondrial cell death pathways in models of Huntington's disease. *Proceedings of the National Academy of Sciences* 100, 10483-10487.
- Ward, A.C., Castelli, L.A., Lucantoni, A.C., White, J.F., Azad, A.A., and Macreadie, I.G. (1995). Expression and analysis of the NS 2 protein of influenza A virus. *Archives of virology* 140, 2067-2073.
- Watanabe, Y., Bowden, T.A., Wilson, I.A., and Crispin, M. (2019). Exploitation of glycosylation in enveloped virus pathobiology. *Biochimica et Biophysica Acta (BBA)-General Subjects* 1863, 1480-1497.
- Webster, R., Kendal, A., and Gerhard, W. (1979). Analysis of antigenic drift in recently isolated influenza A (H1N1) viruses using monoclonal antibody preparations. *Virology* 96, 258-264.
- Webster, R., and Laver, W. (1967). Preparation and properties of antibody directed specifically against the neuraminidase of influenza virus. *The Journal of Immunology* 99, 49-55.
- Webster, R.G., Bean, W.J., Gorman, O.T., Chambers, T.M., and Kawaoka, Y. (1992). Evolution and ecology of influenza A viruses. *Microbiological reviews* 56, 152-179.
- Weinstein, R.A., Bridges, C.B., Kuehnert, M.J., and Hall, C.B. (2003). Transmission of influenza: implications for control in health care settings. *Clinical infectious diseases* 37, 1094-1101.
- Weis, W., Brown, J., Cusack, S., Paulson, J., Skehel, J., and Wiley, D. (1988). Structure of the influenza virus haemagglutinin complexed with its receptor, sialic acid. *Nature* 333, 426-431.
- White, J., Helenius, A., and Gething, M.-J. (1982). Haemagglutinin of influenza virus expressed from a cloned gene promotes membrane fusion. *Nature* 300, 658-659.
- Whitfield, J., Neame, S.J., Paquet, L., Bernard, O., and Ham, J. (2001). Dominant-negative c-Jun promotes neuronal survival by reducing BIM expression and inhibiting mitochondrial cytochrome c release. *Neuron* 29, 629-643.
- Williams, G.D., Townsend, D., Wylie, K.M., Kim, P.J., Amarasinghe, G.K., Kutluay, S.B., and Boon, A.C. (2018). Nucleotide resolution mapping of influenza A virus nucleoprotein-RNA interactions reveals RNA features required for replication. *Nature communications* 9, 465.
- Wilson, I.A., Skehel, J.J., and Wiley, D. (1981). Structure of the haemagglutinin membrane glycoprotein of influenza virus at 3 Å resolution. *Nature* 289, 366-373.
- Winkvist, E.B., Abdurahman, S., Tranell, A., Lindström, S., Tingsborg, S., and Schwartz, S. (2012). Inefficient splicing of segment 7 and 8 mRNAs is an inherent property of influenza virus A/Brevig Mission/1918/1 (H1N1) that causes elevated expression of NS1 protein. *Virology* 422, 46-58.
- Winter, G., and Fields, S. (1981). The structure of the gene encoding the nucleoprotein of human influenza virus A/PR/8/34. *Virology* 114, 423-428.
- Wu, W.W., Weaver, L.L., and Panté, N. (2007). Ultrastructural analysis of the nuclear localization sequences on influenza A ribonucleoprotein complexes. *Journal of molecular biology* 374, 910-916.
- Xie, Y., Xu, D., Huang, B., Ma, X., Qi, W., Shi, F., Liu, X., Zhang, Y., and Xu, W. (2014). Discovery of N-substituted oseltamivir derivatives as potent and selective inhibitors of H5N1 influenza neuraminidase. *Journal of medicinal chemistry* 57, 8445-8458.
- Yamanaka, K., Nagata, K., and Ishihama, A. (1991). Temporal control for translation of influenza virus mRNAs. *Archives of virology* 120, 33-42.

- Yang, Q., Hughes, T.A., Kelkar, A., Yu, X., Cheng, K., Park, S., Huang, W.-C., Lovell, J.F., and Neelamegham, S. (2020). Inhibition of SARS-CoV-2 viral entry upon blocking N-and O-glycan elaboration. *elife* 9, e61552.
- Yang, X., Steukers, L., Forier, K., Xiong, R., Braeckmans, K., Van Reeth, K., and Nauwynck, H. (2014). A beneficiary role for neuraminidase in influenza virus penetration through the respiratory mucus. *PloS one* 9, e110026.
- Yao, X., Ye, F., Zhang, M., Cui, C., Huang, B., Niu, P., Liu, X., Zhao, L., Dong, E., and Song, C. (2020). In vitro antiviral activity and projection of optimized dosing design of hydroxychloroquine for the treatment of severe acute respiratory syndrome coronavirus 2 (SARS-CoV-2). *Clinical infectious diseases* 71, 732-739.
- Yen, H.-L. (2016). Current and novel antiviral strategies for influenza infection. *Current opinion in virology* 18, 126-134.
- Yen, H.-L., Hoffmann, E., Taylor, G., Scholtissek, C., Monto, A.S., Webster, R.G., and Govorkova, E.A. (2006). Importance of neuraminidase active-site residues to the neuraminidase inhibitor resistance of influenza viruses. *Journal of virology* 80, 8787-8795.
- Yin, C., Khan, J.A., Swapna, G., Ertekin, A., Krug, R.M., Tong, L., and Montelione, G.T. (2007). Conserved surface features form the double-stranded RNA binding site of non-structural protein 1 (NS1) from influenza A and B viruses. *Journal of Biological Chemistry* 282, 20584-20592.
- Yondola, M.A., Fernandes, F., Belicha-Villanueva, A., Uccellini, M., Gao, Q., Carter, C., and Palese, P. (2011). Budding capability of the influenza virus neuraminidase can be modulated by tetherin. *Journal of virology* 85, 2480-2491.
- Yoneyama, M., and Fujita, T. (2007). Function of RIG-I-like receptors in antiviral innate immunity. *Journal of Biological Chemistry* 282, 15315-15318.
- York, A., and Fodor, E. (2013). Biogenesis, assembly, and export of viral messenger ribonucleoproteins in the influenza A virus infected cell. *RNA biology* 10, 1274-1282.
- Yoshimura, A., and Ohnishi, S. (1984). Uncoating of influenza virus in endosomes. *Journal of virology* 51, 497-504.
- Yuan, P., Bartlam, M., Lou, Z., Chen, S., Zhou, J., He, X., Lv, Z., Ge, R., Li, X., and Deng, T. (2009). Crystal structure of an avian influenza polymerase PAN reveals an endonuclease active site. *Nature* 458, 909-913.
- Zamarin, D., García-Sastre, A., Xiao, X., Wang, R., and Palese, P. (2005). Influenza virus PB1-F2 protein induces cell death through mitochondrial ANT3 and VDAC1. *PLoS pathogens* 1, e4.
- Zanin, M., Marathe, B., Wong, S.-S., Yoon, S.-W., Collin, E., Oshansky, C., Jones, J., Hause, B., and Webby, R. (2015). Pandemic swine H1N1 influenza viruses with almost undetectable neuraminidase activity are not transmitted via aerosols in ferrets and are inhibited by human mucus but not swine mucus. *Journal of virology* 89, 5935-5948.
- Zebedee, S.L., and Lamb, R.A. (1988). Influenza A virus M2 protein: monoclonal antibody restriction of virus growth and detection of M2 in virions. *Journal of virology* 62, 2762-2772.
- Zhang, J., and Lamb, R.A. (1996). Characterization of the membrane association of the influenza virus matrix protein in living cells. *Virology* 225, 255-266.
- Zhang, J., Pekosz, A., and Lamb, R.A. (2000). Influenza virus assembly and lipid raft microdomains: a role for the cytoplasmic tails of the spike glycoproteins. *Journal of virology* 74, 4634-4644.
- Zhang, L., Huang, P., Chen, H., Tan, W., Lu, J., Liu, W., Wang, J., Zhang, S., Zhu, W., and Cao, J. (2017). The inhibitory effect of minocycline on radiation-induced neuronal apoptosis via AMPK α 1 signaling-mediated autophagy. *Scientific Reports* 7, 16373.

- Zhang, Q., Gong, R., Qu, J., Zhou, Y., Liu, W., Chen, M., Liu, Y., Zhu, Y., and Wu, J. (2012). Activation of the Ras/Raf/MEK pathway facilitates hepatitis C virus replication via attenuation of the interferon-JAK-STAT pathway. *Journal of virology* 86, 1544-1554.
- Zhang, S., Wang, J., Wang, Q., and Toyoda, T. (2010). Internal initiation of influenza virus replication of viral RNA and complementary RNA in vitro. *Journal of biological chemistry* 285, 41194-41201.
- Zhirnov, O.P., Ikizler, M.R., and Wright, P.F. (2002). Cleavage of influenza A virus hemagglutinin in human respiratory epithelium is cell associated and sensitive to exogenous antiproteases. *Journal of virology* 76, 8682-8689.
- Zhu, X., McBride, R., Nycholat, C.M., Yu, W., Paulson, J.C., and Wilson, I.A. (2012). Influenza virus neuraminidases with reduced enzymatic activity that avidly bind sialic acid receptors. *Journal of virology* 86, 13371-13383.
- Zurcher, T., Luo, G., and Palese, P. (1994). Mutations at palmitoylation sites of the influenza virus hemagglutinin affect virus formation. *Journal of virology* 68, 5748-5754.
- 天野稜大 (2019). Cinnamic acid derivatives inhibit hepatitis C virus replication via the induction of oxidative stress.

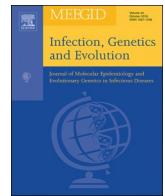


Publications

- **Saha P**, Biswas M, Gupta R, Majumdar A, Mitra S, Banerjee A, Mukherjee A, Dutta S, Chawla-Sarkar M. Molecular characterization of Influenza A pandemic H1N1 viruses circulating in eastern India during 2017–19: Antigenic diversity in comparison to the vaccine strains. **Infection, Genetics and Evolution**. 2020 Jul 1;81:104270. [IF 4.4]
- **Saha P**, Saha R, Chaudhuri RD, Sarkar R, Sarkar M, Koley H, Chawla-Sarkar M. Unveiling the Antiviral Potential of Minocycline: Modulation of Nuclear Export of Viral Ribonuclear Proteins During Influenza Virus Infection. (**Manuscript under communication**).
- Malbari K, **Saha P**, Chawla-Sarkar M, Dutta S, Rai S, Joshi M, Kanyalkar M. In quest of small-molecules as potent non-competitive inhibitors against influenza. **Bioorganic Chemistry**. 2021 Sep 1;114:105139. [IF 5.1]
- Chandra P, Lo M, Mitra S, Banerjee A, **Saha P**, Okamoto K, Deb AK, Ghosh SK, Manna A, Dutta S, Chawla-Sarkar M. Genetic characterization and phylogenetic variations of human adenovirus-F strains circulating in eastern India during 2017–2020. **Journal of medical virology**. 2021 Nov;93(11):6180-90. [IF 12.7]
- Sarkar R, Mitra S, Chandra P, **Saha P**, Banerjee A, Dutta S, Chawla-Sarkar M. Comprehensive analysis of genomic diversity of SARS-CoV-2 in different geographic regions of India: an endeavour to classify Indian SARS-CoV-2 strains on the basis of co-existing mutations. **Archives of virology**. 2021 Mar;166:801-12. [IF 2.7]
- Mukhopadhyay U, Patra U, Chandra P, **Saha P**, Gope A, Dutta M, Chawla-Sarkar M. Rotavirus activates MLKL-mediated host cellular necroptosis concomitantly with apoptosis to facilitate dissemination of viral progeny. **Molecular Microbiology**. 2022 Apr;117(4):818-36. [IF 3.6]
- Chandra P, Banerjee S, **Saha P**, Chawla-Sarkar M, Patra U. Sneaking into the viral safe-houses: Implications of host components in regulating integrity and dynamics of rotaviral replication factories. **Frontiers in Cellular and Infection Microbiology**. 2022 Sep 14;12:977799. [IF 4.6]

Abstracts, Posters, Presentation

- **Saha P**, Malbari K, Chawla-Sarkar M, Ganji L, Rai S, Joshi M, Kanyalkar M. Design, synthesis and biological evaluation of bio-organics against influenza. 91st Annual Meeting of the Society of Biological Chemists (India). West Bengal, India, December 2022.
- **Saha P**, Malbari K, Chawla-Sarkar M, Ganji L, Rai S, Joshi M, Kanyalkar M. Evaluation of Small-Molecules as Potent Non-Competitive Inhibitors Against pH1N1 Influenza. 1st World Society For Virology 2021 Conference, Virtual meeting, June 2021.
- **Saha P**, Malbari K, Chawla-Sarkar M, Ganji L, Rai S, Joshi M, Kanyalkar M. Evaluation of synthetic Small-Molecules as Potent Non-Competitive Inhibitors Against H1N1 Influenza. 19th International Congress on Infectious Diseases. Kuala Lumpur, Malaysia, February 2020.



Research Paper

Molecular characterization of Influenza A pandemic H1N1 viruses circulating in eastern India during 2017–19: Antigenic diversity in comparison to the vaccine strains

Priyanka Saha^a, Madhumonti Biswas^b, Rudrak Gupta^b, Agniva Majumdar^b, Suvroto Mitra^a, Anindita Banerjee^a, Anupam Mukherjee^c, Shanta Dutta^b, Mamta Chawla-Sarkar^{a,*}

^a Division of Virology, ICMR-National Institute of Cholera and Enteric Diseases, Kolkata, India

^b Regional Virus Research and Diagnostic Lab, ICMR-National Institute of Cholera and Enteric Diseases, Kolkata, India

^c National AIDS Research Institute, Pune, India

ARTICLE INFO

Keywords:

A/H1N1pdm09
Antigenic variation
Vaccine strains
Outbreak
Nucleotide homology

ABSTRACT

In the endemic settings of India, high CFR (3.6–7.02%) was observed in the consecutive 2009, 2015 and 2017 A/H1N1pdm09 outbreaks, though in eastern India CFR varied between 0 and 5.5% during same period. Recurrent outbreaks of pandemic Influenza A/H1N1pdm09, fragmented nationwide incidence data, lack of national policy for Influenza vaccination in India underscores the necessity for generating regional level data. Thus, during 2017–19, 4106 referred samples from patients hospitalized with severe acute respiratory illness (SARI) in eastern India were tested for A/H1N1pdm09 infection. Among which 16.5% ($n = 677/4106$) were found A/H1N1pdm09 positive. Individuals < 20 years and middle-aged persons (40–60 years) were most susceptible to A/H1N1pdm09 infection. The vaccine strain (A/human/California/07/2009) which was globally used before 2017, clustered in a different lineage away from the representative eastern Indian strains in the phylogenetic dendrogram. The vaccine strain (A/human/Michigan/45/2015) used in India during the study period and the WHO recommended strain (A/human/Brisbane/02/2018) for 2019–20 flu season for the northern hemisphere, clustered with the circulating isolates in the same lineage-6b. Dissimilarities in the amino acids encompassing the antigenic epitopes were seen to be highest with the vaccine strain- A/human/California/07/2009. The significant amino acid variations in the circulating strains with the current WHO recommended vaccine strain, implies the exigency of continuous pandemic A/H1N1pdm09 surveillance studies in this epidemiological setting. The absence of any Oseltamivir resistant mutation (H275Y) in the neuraminidase gene of the current isolates suggests continuing use of Tamiflu® as an antiviral therapy in suspected subjects in this region.

1. Introduction

Viruses causing respiratory tract infections bring on widespread mortality and morbidity among infants, elderly and immunocompromised individuals worldwide (Trucchi et al., 2019). Among the predominant respiratory viruses, Influenza A virus (IAV) infects humans worldwide with nearly 650,000 death tolls annually (<http://www.who.int/mediacentre/news/releases/2017/seasonal-flu>). Besides human, IAV also infects other mammalian and avian species. The associated symptoms include sudden onset of fever, general dry cough, headache, sore throat, running nose, acute malaise along with muscle and joint pain (Dool et al., 2008). IAV, belonging to the family of *Orthomyxoviridae* comprises of a single stranded segmented negative

sense RNA genome. The two surface proteins, i.e., hemagglutinin (HA) and neuraminidase (NA) are responsible for generating a high degree of genetic diversity among the co-circulating IAV strains. Co-infection of multiple strains could lead to rapid evolution of IAV due to aggregation of point mutations in the antibody-binding sites, along with gene-segment reassortments (different combination of HA and/or NA types) (Webster et al., 1992; Rambaut et al., 2008; Domingo, 2010). This eventually provokes antigenic drift resulting in the emergence of novel subtypes, which cannot be effectively neutralized by antibodies prevailing against the previous IAV strains (Treanor, 2004).

The novel 2009 A/H1N1 pandemic strain, emerged in Mexico (Veracruz) and USA (California) and was responsible for 18,449 deaths worldwide, of which 3.6% ($n = 981/27,236$) were reported solely from

* Corresponding author at: ICMR-National Institute of Cholera and Enteric Diseases, P-33, C.I.T. Road, Scheme-XM, Beliaghata, Kolkata 700010, West Bengal, India.
E-mail address: chawlasarkar.m@icmr.gov.in (M. Chawla-Sarkar).

<https://doi.org/10.1016/j.meegid.2020.104270>

Received 19 November 2019; Received in revised form 8 February 2020; Accepted 2 March 2020

Available online 03 March 2020

1567-1348/© 2020 Published by Elsevier B.V.

India (Girard et al., 2010; World Health Organization, 2020; Influenza A, 2020). Since 2009, the proportion of pre-pandemic seasonal Influenza A/H1N1, A/H3N2 and Influenza B viruses have been eventually replaced by the antigenically unique triple reassortant pandemic A/H1N1pdm09 viruses infecting nearly 24% of the population across the globe (Broor et al., 2012; Broor et al., 2011; Majanja et al., 2013; Mishra, 2015; Mudhigeti et al., 2018). Indian states like Maharashtra, Delhi, Rajasthan, Gujarat, Tamil Nadu, Madhya Pradesh, Karnataka, Haryana, Kerala and Andhra Pradesh were significantly affected in the 2009 pandemic (Gurav et al., 2010; Choudhry et al., 2012; Mudhigeti et al., 2018). Though the annual proportion of A/H1N1pdm09 declined during the subsequent years in India (< 5000 cases yearly), however in the 2015 and 2017 outbreaks, 42,592 and 38,811 cases were reported with 7.02% ($n = 2990/42,592$) and 5.8% ($n = 2266/38,811$) deaths, respectively (State/UT - wise, 2020; Kulkarni et al., 2019). Worldwide, the 2017–18 flu season had significantly higher incidence of influenza-like illness and increased hospitalization-rates compared to 2009–10 (CDC, 2019). In India, the proportion of lab confirmed A/H1N1pdm09 related deaths during 2017–18 was around 5.6% ($n = 4511/81,115$), though this may be an underestimation due to limited testing capacity (State/UT - wise, 2020; Kulkarni et al., 2019). Any genetic mutation in the surface antigens which might lead to these consecutive A/H1N1pdm09 epidemics in India remains unclear to date.

Depending on the circulating IAV subtypes, World Health Organization (WHO) recommends vaccine strains for optimal regional efficacy across the northern (NH) and southern (SH) hemispheres (World Health Organization, 2018a, 2018b). Though both NH and SH influenza vaccines are available in India, WHO has categorized India in the southern hemisphere (SH) tropical Asia vaccination zone (Thakre and Patil, 2019). During 2010–2016, A/California/07/2009 (H1N1) pdm09-like virus strain was a part of the IAV vaccine, which was replaced by A/human/Michigan/45/2015 (H1N1) pdm09 strain during 2017–2019 in both the hemispheres. In 2019, A/human/Michigan/45/2015 (H1N1) pdm09-like strain was substituted by A/human/Brisbane/02/2018 (H1N1) pdm09-like virus only for the northern hemisphere, though for 2020 A/human/Brisbane/02/2018 (H1N1) pdm09 has been recommended for both hemispheres (World Health Organization, 2015a, 2015b, 2016a, 2016b, 2017a, 2017b, 2018a, 2018b, 2019a, 2019b). In addition, Sanofi Pasteur also launched their first quadrivalent influenza vaccine (FluQuadri) in 2018 in India, which has been shown to provide large-scale protection against IAV to individuals above 3 years. It comprises of A/human/Michigan/45/2015 (H1N1) pdm09, A/Switzerland/8060/2017 (H3N2), B/Colorado/06/2017 (B/Victoria/2/87 lineage) and B/Phuket/3073/2013 (B/Yamagata/16/88 lineage)-like virus strains. In spite of availability of both live attenuated and recombinant vaccines in India, it has not been included in the national immunization program. The Ministry of Health and Family welfare (MOHF&W) has recommended Influenza vaccine for elderly (> 65 years), children (0.5–8 years), pregnant women and health care workers (Kant and Guleria, 2018; Dang and Sharma, 2020). In addition, Indian Academy of Paediatrics has also recommended Influenza vaccine for all infants in 2018–19. But overall, the Influenza vaccination coverage in the low and middle income countries of Africa and Asia is very low ($\approx 1\%$) (Hirve, 2015; Palache et al., 2017).

In India during 2009–2017, the yearly case fatality ratio (CFR) estimates of A/H1N1pdm09 (3.6–7.02%) surpasses the magnitudes reported from several other countries, worldwide underscoring the disease severity among the population (Nishiura, 2010). Small scale IAV epidemiological data is available from few regions in India (Agrawal et al., 2010; Agrawal et al., 2009; Sarkar et al., 2011; Mukherjee et al., 2016; Mukherjee et al., 2012; Mukherjee et al., 2010; Pandey et al., 2018; Jagadesh et al., 2019; Jones et al., 2019). This study was conducted to assess the proportion of Influenza A/H1N1pdm09 among patients requiring hospitalization due to severe acute respiratory illness (SARI), affected age group, antiviral resistance and phylodynamics of circulating strains. Continuous monitoring of the circulating IAV

subtypes and emergence of novel reassortant strains are the keys to effective control set of future epidemics. The relevant dataset generated by comparison of the antigenic epitopes of the circulating A/H1N1pdm09 strains with the recommended vaccine strains may help to estimate the effectiveness of vaccine in the region.

2. Materials and method

2.1. Clinical sample collection

The Regional Virus Research & Diagnostic Laboratory (VRDL) in Indian Council of Medical research- National Institute of Cholera and Enteric Diseases (ICMR-NICED) is a Government designated referral laboratory for providing laboratory diagnosis for Influenza A/H1N1pdm09 in eastern zone. Nasopharyngeal and/or throat swab samples ($n = 4106$) from patients hospitalized with severe acute respiratory illness (SARI) in eastern India were referred for diagnosis during April 2017 through March 2019. The test reports were provided for initiating treatment and quarantine measures.

2.2. Identification of Influenza A/H1N1pdm09-like viruses

Extraction of viral RNAs from the clinical isolates was performed using the QIAamp® viral RNA mini kit (Qiagen, Germany). The RNAs were tested for A/H1N1pdm09 by Quantitative real-time reverse-transcription polymerase chain reaction (qRT-PCR) (StepOnePlus Real-Time PCR System) using U.S. Centres for Disease Control and Prevention (CDC) primer-probes and following their protocol (WHO, 2009).

2.3. Amplification of HA and NA genes and DNA sequencing

All the positive samples ($n = 677$) were cultured in Madin-Darby Canine Kidney (MDCK) cell-line with Minimum Essential Medium (MEM, Gibco, by Life Technologies), among which nearly 20% culture-positives ($n = 135$) were chosen for amplification of HA and NA genes by RT-PCR (GeneAmp® PCR System 9700) using Superscript III RT-PCR system (Invitrogen Corporation, CA, USA) and gene specific primer sets (Supplementary Table S1). Each of the segments were amplified in 3 (for HA gene) or 2 (for NA gene) fragments of 500–700 bp each with 200 bp overlap to obtain the complete sequence. The amplified products were run on 1.5% agarose gel and visualized in a gel doc. Purification of the amplicons were done using QIAquick PCR purification kit (Qiagen GmbH, Hilden, Germany) prior to processing for DNA sequencing in an ABI Prism 3730 Genetic Analyzer using ABI Prism BigDye Terminator Cycle Ready Reaction Kit v3.1 (Applied Biosystems, Foster City, California, USA). The nucleotide sequences were analyzed through BLAST (Basic Local Alignment Search Tool) in National Centre for Biotechnology Information (NCBI, National Institutes of Health, Bethesda, MD) server on GenBank database release 143.0 (Schaffer, 2001). The sequences obtained were submitted to NCBI GenBank under accession numbers MN508837 to MN508844, MN508971 to MN508995, MN508849 to MN508863, MN508846 and MN508847.

2.4. Phylogenetic analyses

The nucleotide sequences of the HA and NA genes of 25 representative samples were converted to amino acids (aa) sequences using TRANSEQ (Transeq Nucleotide to Protein Sequence Conversion Tool, EMBL-EBI, Cambridgeshire, UK) and the multiple aa sequences were aligned through MUSCLE tool. All the phylogenetic trees were constructed on the basis of aa sequences using MEGA (Molecular Evolutionary Genetics Analysis) program, version X, using maximum-likelihood statistical method with JTT + G + F (JTT = Jones-Taylor-Thornton, G = Gamma distribution, F = Frequency) model and at 1000 Bootstrap replicates (Kumar et al., 2018). The best fit model for each

HA and NA protein was chosen by the model testing tool of MEGA X software. Sequences of the H1N1 strains circulating worldwide and the vaccine strains obtained from NCBI GenBank and Global Initiative on Sharing Avian Influenza Database (GISAID) were used to construct the phylogenetic dendrograms so that the clustering pattern and lineage distribution of the representative strains could be deciphered.

2.5. Statistical analysis

Statistical parameters (Chi-square and *p*-values) were obtained through Epi Info software. *P*-values < .05 were considered statistically significant.

3. Results

3.1. Epidemiology of A/H1N1pdm09 strains

Among the 4106 nasopharyngeal and/or throat swab samples, 16.5% (*n* = 677/4106) were found to be positive for A/H1N1pdm09. The positivity rates in age groups < 5, 5–20 and 40–60 years was observed almost similar (19.1%, 18.9% and 19.1%, respectively) but the higher age group (> 60 years) had significantly lower positivity rate i.e. 12.7% (Chi-square value = 24.35, *p*-value < .0001) (Fig. 1). As per referring hospital records, the vaccine coverage among the patients admitted with SARI was ≤ 1%. Proportion of hospitalizations attributed to A/H1N1pdm09 infection were relatively higher during the summer and monsoon months (April–July and June–October during 2017 and 2018, respectively), though no distinct pattern of seasonality was evident (Fig. 2). 15.4% (*n* = 347/2260) of the males and 17.9% (*n* = 330/1846) of the females were found positive for A/H1N1pdm09 virus.

3.2. Phylogenetic analyses of eastern Indian A/H1N1pdm09 strains

Phylogenetic dendrogram based on the aa sequences of the HA and NA gene of circulating A/H1N1pdm09 strains were analyzed with respect to the other circulating IAV H1N1 and H3N2 (outgroup) strains. The representative eastern Indian A/H1N1pdm09 strains which were included in the dendrogram were chosen on the basis of aa sequence homology among themselves. One representative strain from each subset of similar strains (with greater than 98% DNA sequence homology) was selected.

3.2.1. HA gene

Analysis of the dendrogram revealed that the representative A/H1N1pdm09 strains (*n* = 25) from eastern India formed a separate cluster among themselves within lineage-6b.1 (98.4–99.4% DNA homology). These strains were close to the strains from USA (California,

Wisconsin, Arizona, Washington- 98.1%); Africa (Nigeria, Ghana- 98.7%) and previously reported Indian strains (A/human/India/1706/2017, A/human/India/3196/2018; 98.6%) of lineage-6b.1. Previously reported A/H1N1pdm09 strains from the 2015 outbreak from the same region [A/human/India/Kol-3846/3959/3828/2015(H1N1)] clustered at a distance belonging to a different sub-lineage 6b.2 within the same lineage (94.8–95.8% DNA sequence homology). The strain A/Human/California/07/2009(H1N1) which was implemented both in NH and SH as the vaccine strain during 2010–16, was seen to cluster within lineage-1, far away from the representative strains of the current study (96.1–96.9% nucleotide identity). A/Human/Michigan/45/2015(H1N1) and A/Human/Brisbane/02/2018(H1N1) strains later incorporated in IAV vaccine (in SH and NH respectively for the 2019–20 flu season) clustered along with our representative strains in lineage-6b.1, revealing > 98% DNA homology. The IAV seasonal H1N1 strains formed a separate clade and clustered at a maximum distance from the representative A/H1N1pdm09 strains of this study in the phylogenetic dendrogram (Fig. 3).

3.2.2. NA gene

The phylogenetic analyses revealed that the eastern Indian strains formed a distinct cluster among themselves (99.6% DNA homology) within lineage-6b, with strains from Africa (Nigeria, Ghana- 99%), USA (California, Arizona, and Texas- 97.4%), Asia (India, Nepal, Pakistan, Sri Lanka, Indonesia- 98.5%). A/H1N1pdm09 strains from the 2015 outbreak in eastern Indian [A/human/India/Kol-3846/3959/3828/2015(H1N1)] clustered at a distance from the current strains within the same lineage 6b (97.7–98.4% DNA homology). The vaccine strain [A/Human/California/07/2009(H1N1)] of 2010–16, recommended both for NH and SH, clustered far away in lineage-I (96.8–97.5% homology). A/Human/Michigan/45/2015(H1N1) (98.4–99.2% homology) clustered at a distance within the same lineage, while A/Human/Brisbane/02/2018(H1N1) (99.2–99.8% identity) clustered with the representative eastern Indian strains in the dendrogram. The seasonal IAV H1N1 strains formed a separate clade and clustered far away from the representative A/H1N1pdm09 strains (Fig. 4).

3.3. Analyses of the amino acid sequence variation among the antigenic epitopes of HA and NA proteins

Antigenic epitopes of the HA and NA protein of the representative eastern Indian A/H1N1pdm09 strains were compared to that of the IAV H1N1 vaccine strains [A/Human/California/07/2009(H1N1), A/Human/Michigan/45/2015(H1N1) and A/Human/Brisbane/02/2018(H1N1)], to identify any variability which might exist among them.

3.3.1. HA protein

49 aa residues in the highly conserved antigenic epitopes of HA protein are responsible for antibody recognition (Cb, Ca2, Sa, Ca1 and Sb domains) (Caton et al., 1982; Liu et al., 2018). The representative eastern Indian strains clustered into one broad group (group A), except for 3 strains [A/human/India/Kol-7346/2018(H1N1), A/human/India/Kol-7339/2018(H1N1) and A/human/India/Kol-6247/2017(H1N1)]. These 3 strains were distinctly different at same aa positions. For group A strains, 6 mismatches existed with A/Human/California/07/2009(H1N1) [1, 0, 3, 1, 1 in domain Cb, Ca2, Sa, Ca1 and Sb, respectively]. With respect to A/Human/Michigan/45/2015(H1N1), 3 mismatches were seen [1, 0, 1, 1, 0 in domain Cb, Ca2, Sa, Ca1 and Sb, respectively], while only 1 aa change was observed with A/Human/Brisbane/02/2018(H1N1) [0, 0, 1, 0, 0 in domain Cb, Ca2, Sa, Ca1 and Sb, respectively] (Table 1).

Other than the antigenic epitopes, change in any of the highly conserved residues (Y108, W167, 197H, 209Y) which form the base of the receptor binding pocket was not observed in any of the representative strains of this study (Mir et al., 2012). Substitution I233T

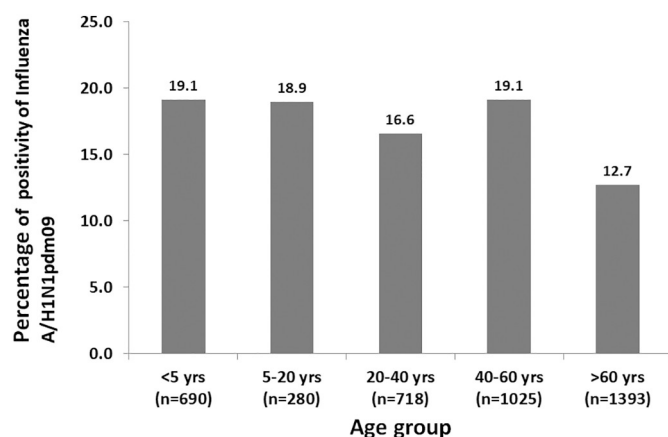


Fig. 1. Age-wise distribution of Influenza A/H1N1pdm09 positivity in eastern India during April' 2017- March' 2019.

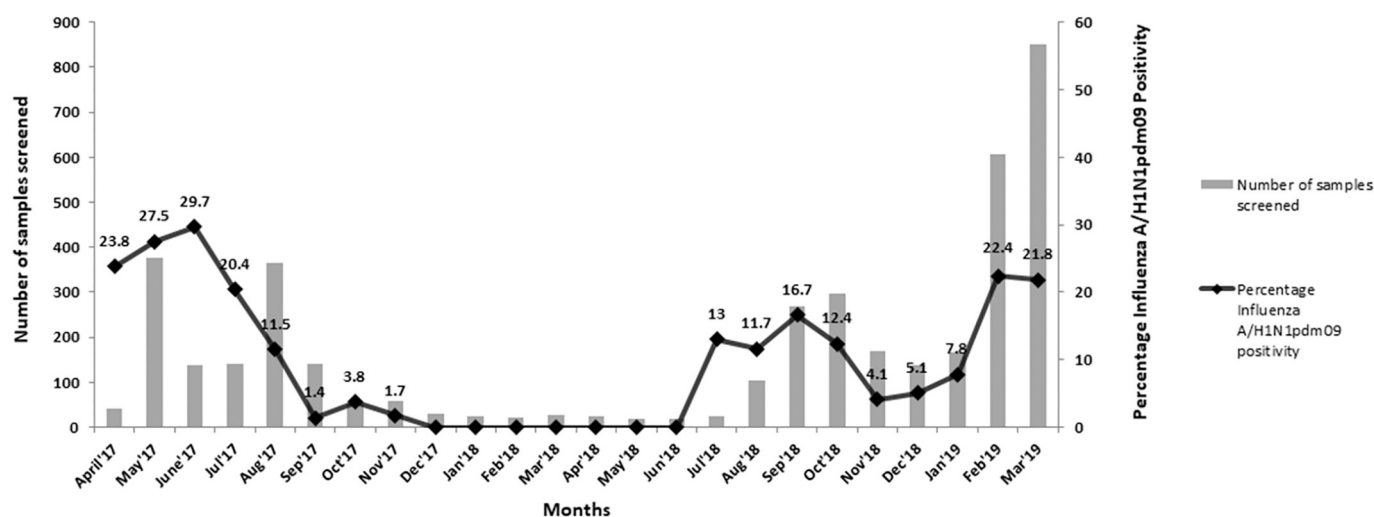


Fig. 2. Seasonal distribution of Influenza A/H1N1pdm09 positivity in eastern India during April' 2017- March'2019.

at the receptor binding site was a common feature in all the isolates of the study. S202T and T214A aa changes in the 190-helix region were observed while all the aa of the 130-loop and 220-loop of the receptor binding site in all the current isolates were found to be highly conserved (Fukuzawa et al., 2011). Some additional substitutions were also observed in all the isolates (as shown in Supplementary Table S2).

3.3.2. NA protein

The changes in the aa residues encircling the antigenic sites (83–143, 156–190, 252–303, 330, 332, 340–345, 368, 370, 387–395, 400, 431–435 and 448–468) of the representative strains were compared to the Influenza A H1N1 vaccine strains [A/Human/California/07/2009(H1N1), A/Human/Michigan/45/2015(H1N1) and A/Human/Brisbane/02/2018(H1N1)] along with previously reported strains from eastern India (Maurer-Stroh et al., 2010; Graham et al., 2011). Majority of the representative eastern Indian strains clustered into three groups viz. group A, B and C; except for 9 strains [A/human/India/Kol-5546/2017(H1N1), A/human/India/Kol-625/2017(H1N1), A/human/India/Kol-5733/2017(H1N1), A/human/India/Kol-5943/2017(H1N1), A/human/India/Kol-6247/2017(H1N1), A/human/India/Kol-7341/2017(H1N1), A/human/India/Kol-7346/2017(H1N1), A/human/India/Kol-731/2017(H1N1) and A/human/India/Kol-7367/2017(H1N1)] which did not cluster under any of the 3 groups due to unique aa changes. The group A strains had 4, 1 and 0 mismatches with the vaccine strains A/Human/California/07/2009(H1N1), A/Human/Michigan/45/2015(H1N1) and A/Human/Brisbane/02/2018(H1N1), respectively. The group B strains had 5, 2 and 1 aa variations with A/Human/California/07/2009(H1N1), A/Human/Michigan/45/2015(H1N1) and A/Human/Brisbane/02/2018(H1N1), respectively; while the strains of group C revealed 5, 3 and 1 changes with A/Human/California/07/2009(H1N1), A/Human/Michigan/45/2015(H1N1) and A/Human/Brisbane/02/2018(H1N1), respectively (Table 2).

The Tamiflu (Oseltamivir) resistant mutation H275Y was not observed in any of the isolates of the study. All the catalytic sites (118R, 119E, 151D, 152R, 179W, 223I, 225R, 277E, 368R and 402Y) and the framework residues supporting the catalytic sites (156R, 180S, 228E, 247S, 278E and 295N) of NA protein were found to be conserved in the isolates of this study (data not shown). Some additional mutations were observed in the non-antigenic domains in the study isolates (shown in Supplementary Table S3).

4. Discussion

The 2015 A/H1N1pdm09 epidemic was far more widespread as compared to the 2009 pandemic, affecting 22 Indian states with nearly 10% increase in the infected cases (Cousins, 2015; Murhekar and

Mehendale, 2016). The period between the two peaks had low level of viral activity among the Indian population (2011–14). Positivity rate in eastern India during 2017–19 was low (16.5%) as compared to the 2015 outbreak in eastern India (23.3%) and 2017–18 outbreak in Andhra Pradesh (27.68%) (Mukherjee et al., 2016; Mudhigeti et al., 2018).

Upsurge of Influenza A activity has been frequently associated with lowering of ambient temperature, but bi-modal seasonality patterns have been reported from Vietnam and England in case of both seasonal as well as pandemic strains (a summer peak and the other one during the winter months) (Lofgren et al., 2007; Elliot et al., 2009; Nguyen et al., 2015). A report from China also revealed two peaks- a seasonal influenza peak in July and a pandemic A/H1N1pdm09 peak in November (Lin et al., 2013). India, with its wide range of climatic conditions, reveals year-round influenza activity (Chadha et al., 2015). Two resurgent seasonal waves of infection have been observed- a monsoon peak in the tropical regions whereas a winter peak among the temperate northern parts of the country (Koul et al., 2013; Chadha et al., 2015; Mudhigeti et al., 2018; Jagadesh et al., 2019). The present study revealed no fixed seasonality pattern of A/H1N1pdm09, while the increase in viral activity during the summer and monsoon months in this tropical setting was in concordance with the previous reports (Agrawal et al., 2009; Mukherjee et al., 2010; Chadha et al., 2015; Mudhigeti et al., 2018). The inconsistent seasonality pattern revealed in this study might be due to the inclusion of only referred samples from hospitals rather than being a systemic surveillance.

In a report from northern Manitoba and Italy, 0–12 months' infants were most vulnerable to infection, while in Mexico, people around 20–59 years were mostly affected followed by 5–19 years during the 2009 pandemic (Charu et al., 2011; Pollock et al., 2012; Costantino et al., 2019). Earlier studies from India as well as USA, revealed that children below 5 years were more vulnerable to A/H1N1pdm09 infection; while people > 60 years were less susceptible (Siddharth et al., 2012; Mukherjee et al., 2016; Mudhigeti et al., 2018). In the current study the most vulnerable age group belonged to the younger and middle-aged persons (< 5, 5–20 and 40–60 years) which is consistent with the previous reports from various parts of India (Mukherjee et al., 2016; Mukherjee et al., 2010; Malhotra et al., 2016; Kulkarni et al., 2019; <http://www.acvip.org/iap-immunization.php>; National Immunization Schedule, 2020). Low influenza vaccination coverage ($1 \pm 0.5\%$) as per records from the referring hospitals could be due to both lack of awareness in the community as well as high cost of vaccine. This is consistent with the report on overall low coverage (< 1%) of vaccine in Africa and Asia (Hirve, 2015). Of all the vaccine doses distributed in 201 countries in 2015, 95% of vaccine doses were consumed by Americas, Europe and western pacific WHO regions and only 5%

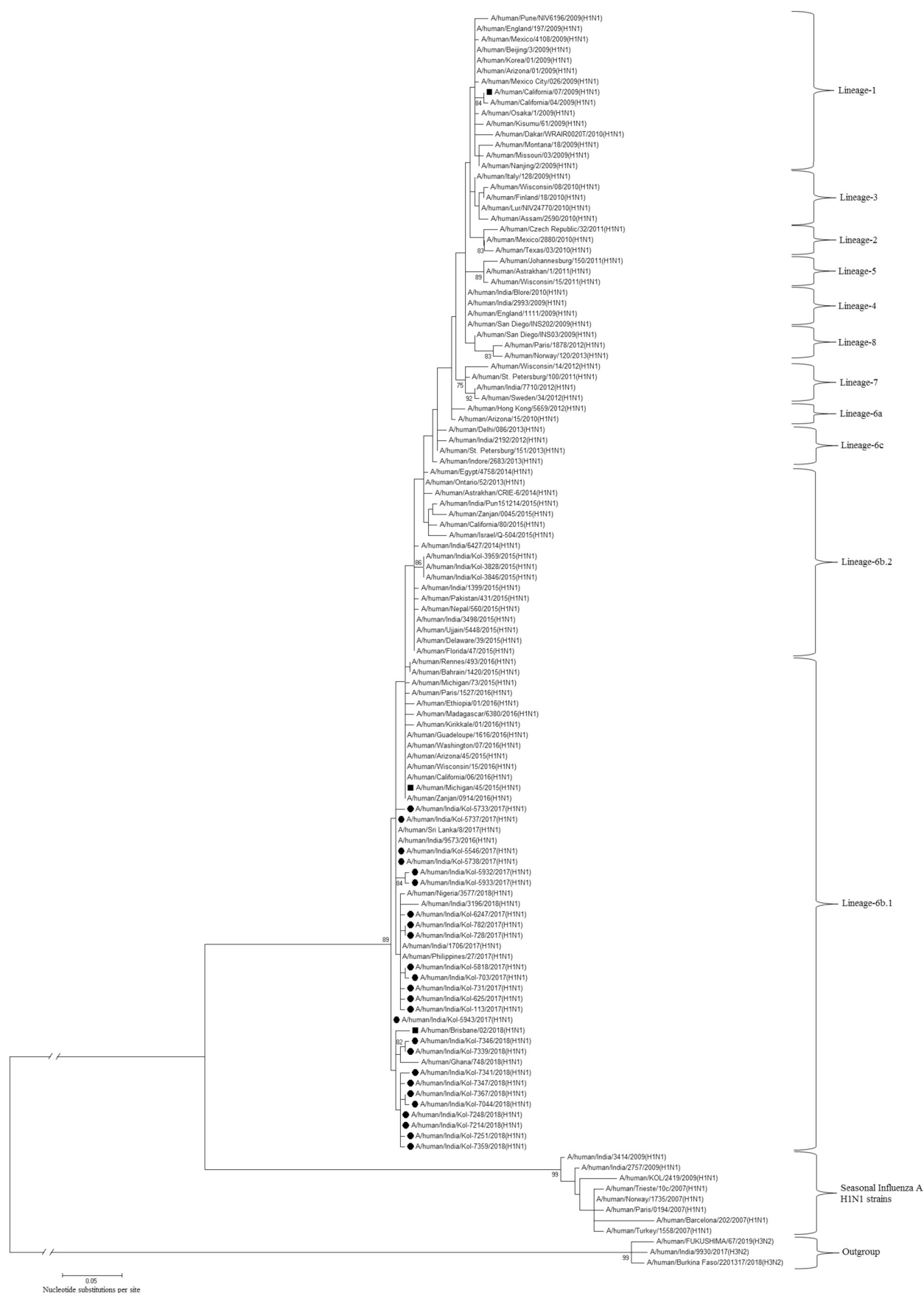


Fig. 3. Phylogenetic dendrogram based on amino acid sequences of HA protein of eastern Indian A/H1N1pdm09 isolates (marked with ●) from April' 2017- March' 2019. Scale bar: 0.05 nucleotide substitutions per site. Bootstrap values < 70% are not shown. The vaccine strains have been marked with ■. The outgroup (H3N2) and seasonal H1N1 strains have been denoted.

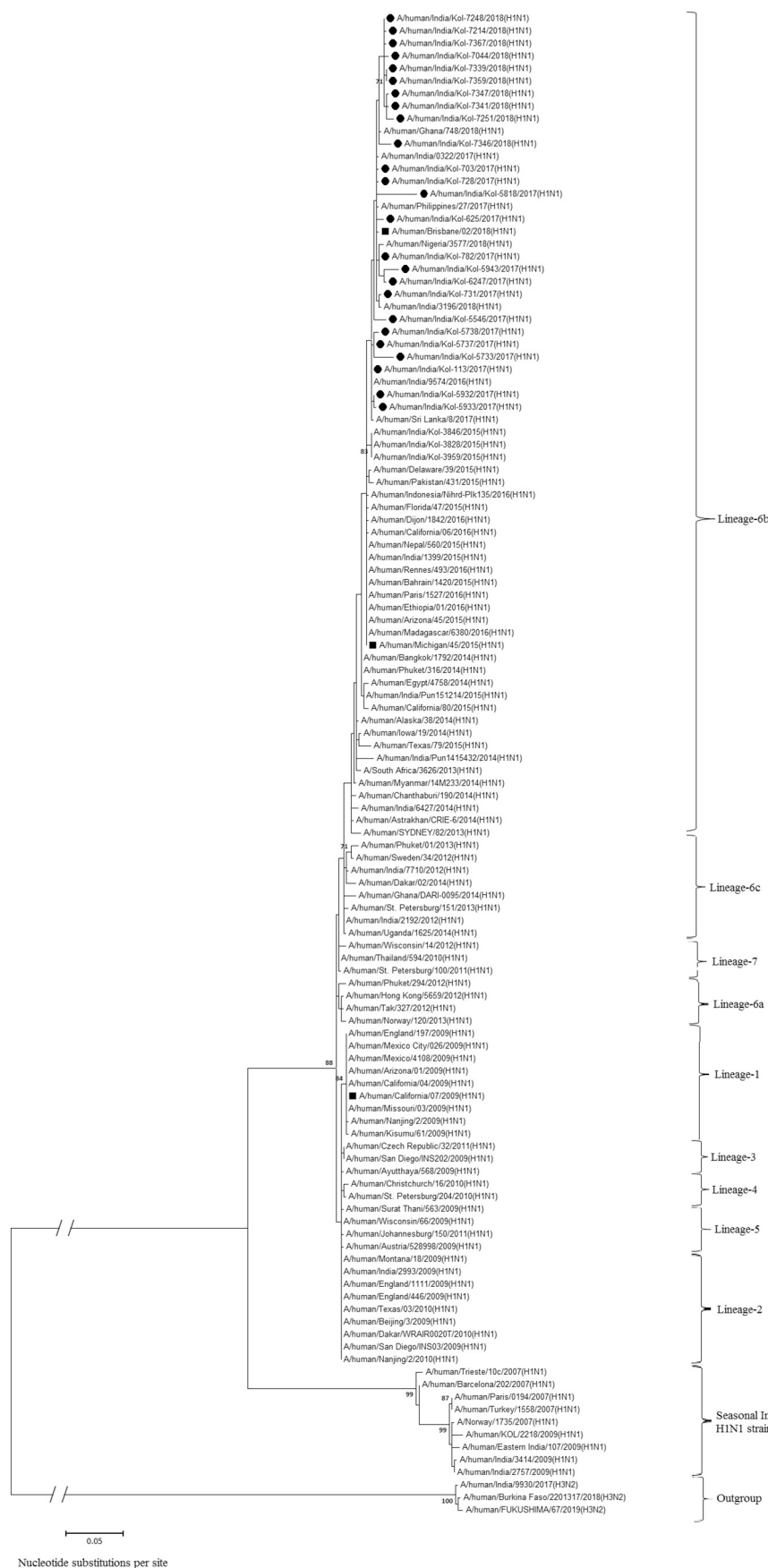


Fig. 4. Phylogenetic dendrogram based on amino acid sequences of NA protein of eastern Indian A/H1N1pdm09 isolates (marked with ●) from April' 2017- March' 2019. Scale bar: 0.05 nucleotide substitutions per site. The bootstrap values ($n = 1000$) are shown at the branch nodes (values < 70% not shown). The vaccine strains have been marked with ■. The outgroup (H3N2) and seasonal H1N1 strains have been denoted.

Table 1

Domains		Cb domain			Sa domain			Ca2 domain			Sa domain					
Amino acid positions	87	88	89	90	91	92	142	143	154	155	156	157	158	159	170	171
A/human/California/07/2009(H1N1)	L	S	T	A	S	S	P	N	P	H	A	G	A	K	K	K
A/human/Michigan/45/2015(H1N1)	L	S	T	A	S	S	P	N	P	H	A	G	A	K	K	K
A/human/Brisbane/02/2018(H1N1)	L	S	T	A	R	S	P	N	P	H	A	G	A	K	K	K
A/human/KOL/2419/2009	L	I	S	K	E	S	N	H	S	H	N	G	E	R	G	K
A/human/India/Kol-3959/2015	L	S	T	A	S	S	N	H	P	H	A	G	A	K	K	K
Group A	L	S	T	A	R	S	P	N	P	H	A	G	A	K	K	K
A/human/India/Kol-7346/2018(H1N1)	L	S	T	A	R	S	P	N	P	H	A	G	A	K	K	K
A/human/India/Kol-7339/2018(H1N1)	L	S	T	A	R	S	P	N	P	H	A	G	A	K	K	K
A/human/India/Kol-6247/2017(H1N1)	L	S	T	A	R	S	P	N	P	H	A	G	A	K	K	K

Domains		Sa domain			Ca1 domain			Sb domain									
Amino acid positions	172	173	174	176	177	178	179	180	181	183	184	185	186	187	201	202	203
A/human/California/07/2009(H1N1)	G	N	S	P	K	L	S	K	S	I	N	D	K	G	T	S	A
A/human/Michigan/45/2015(H1N1)	G	N	S	P	K	L	N	Q	S	I	N	D	K	G	T	T	A
A/human/Brisbane/02/2018(H1N1)	G	N	S	P	K	L	N	Q	T	I	N	D	K	G	T	T	A
A/human/KOL/2419/2009	N	G	L	P	N	L	S	K	S	A	N	N	K	E	S	I	S
A/human/India/Kol-3959/2015	G	N	S	P	K	L	S	Q	S	I	N	D	K	G	T	T	A
Group A	G	N	S	P	K	L	N	Q	T/S	I	N	D	K	G	T	T	A
A/human/India/Kol-7346/2018(H1N1)	G	N	S	P	K	L	N	Q	T	I	N	D	K	G	T	I	A
A/human/India/Kol-7339/2018(H1N1)	G	N	S	P	K	L	N	Q	T	I	N	D	K	G	T	I	A
A/human/India/Kol-6247/2017(H1N1)	G	N	S	P	K	L	N	Q	T	I	N	D	K	G	T	T	A

Domains	Cb do-main	Sb domain			Ca1 domain											
Amino acid positions	92	204	205	206	207	208	209	210	211	212	220	221	222	252	253	254
A/human/California/07/2009(H1N1)	S	D	Q	Q	S	L	Y	Q	N	A	S	S	R	E	P	G

(continued on next page)

Table 1 (continued)

Domains	Cb do-main	Sb domain										Ca1 domain									
		204	205	206	207	208	209	210	211	212		220	221	222	252	253	254				
Amino acid positions	92																				
A/human/Michigan/45/2015(H1N1)	S	D	Q	Q	S	L	Y	Q	N	A		T	S	R	E	P	G				
A/human/Brisbane/02/2018(H1N1)	S	D	Q	Q	S	L	Y	Q	N	A		T	S	R	E	P	G				
A/human/KOL/2419/2009	S	D	Q	K	T	L	Y	H	T	E		S	S	H	E	P	G				
A/human/India/Kol-3959/2015	S	D	Q	Q	S	L	Y	Q	N	A		T	S	R	E	P	G				
Group A	S	D	Q	Q	S	L	Y	Q	N	A		T	S	R	E	P	G				
A/human/India/Kol-7346/2018(H1N1)	S	D	Q	Q	S	L	Y	Q	N	A		T	S	R	E	P	G				
A/human/India/Kol-7339/2018(H1N1)	S	D	Q	Q	S	L	Y	Q	N	A		T	S	R	E	P	G				
A/human/India/Kol-6247/2017(H1N1)	S	D	Q	Q	S	L	Y	Q	N	A		T	S	R	K	P	G				

Group A represents strains with accession number MN508837, MN508838, MN508839, MN508840, MN508841, MN508842, MN508843, MN508844, MN508849, MN508850, MN508851, MN508853, MN508854, MN508855, MN508856, MN508857, MN508858, MN508859, MN508860, MN508861, MN508862, MN508863.

were available for Africa, South-east Asia, Africa and east Mediterranean regions (Palache et al., 2017). Studies among health care professionals in India also highlighted low coverage ($\approx 5\%$) inspite of their awareness and affordability status. The key reasons for non-acceptability varied from skepticism regarding efficacy, fear of side effects, lack of time and perception of not being at risk (Bali et al., 2013; Gambhir et al., 2016; Kant and Guleria, 2018). There are contrasting reports regarding gender specificity of the IAV infection (Shukla et al., 2010; Dee and Jayathissa, 2010). However, consistent to the previous observation from western and eastern parts of India, no gender specific difference was observed in our study population (51.3% males and 48.7% females being infected) (Mukherjee et al., 2016; Mukherjee et al., 2010; Arbat et al., 2017).

Since the emergence of A/H1N1pdm09 in 2009, wide genetic diversity has been observed through the subsequent outbreaks (Nguyen et al., 2015). The evolution of the HA genes due to antigenic drift might have contributed to the successive epidemics of A/H1N1pdm09 (Mukherjee et al., 2016). Though the current isolates had 95–96% nucleotide identity with the 2015 outbreak strains of eastern India, nevertheless, in case of HA dendrogram they grouped under two different sub-lineages (6b.1 and 6b.2). On the contrary, strains circulating in central and south-western India during 2015–17 flu seasons clubbed in lineage-6b.1 (Parida et al., 2016; Barde et al., 2017; Jagadeesh et al., 2019; Jones et al., 2019). In the context of NA gene, though the 2015 outbreak strains and the current isolates clustered under the same lineage (6b) with 97–98% DNA homology, but they were distant apart from each other. These observations denote that over time a marked accumulation of genetic diversity within the HA and NA proteins might lead to antigenic drift causing evolution of A/H1N1pdm09 strains in a particular endemic setting.

HA being the chief surface antigen remains to be the most important component of vaccines (Ekiert et al., 2009; Treanor, 2015; Petrova and Russell, 2018). Among its highly conserved antigenic sites (namely Ca1/2, Cb, Sa and Sb), several mutations which were observed in this study isolates are responsible for antibody recognition and might lead to rapid molecular evolution of the circulating strains. The HA amino acids (180, 202 and 239) which were positively selected in the A/H1N1pdm09 Indian lineage may have increased the fitness of the viruses, eventually becoming fixed in host population (Luo et al., 2018; Adam et al., 2019). The site (position 239) was different from the pattern seen in other South Asian nations. The K180Q mutation modifies the antigenicity of the viruses; whereas the S202T aa change which enhances receptor binding avidity remains conserved (Matos-Patrón et al., 2015; Yasuhara et al., 2017). However with the available data, it cannot be concluded whether these positively selected sites were one of the drivers of consecutive A/H1N1pdm09 epidemics, because none of these were endemic to India.

The T214A change in the HA protein which decreases the receptor binding avidity was found during 2009 pandemic, 2015 outbreak and continued to persist thereafter, as evident in our isolates (de Vries et al., 2013; Jones et al., 2019). Substitutions like S101N, S179N and I233T were observed in all the isolates which are usual characteristics of lineage-6b.1 (Korsun et al., 2017). The two unique mutations in 2017 A/H1N1pdm09 Indian strains (S181T: responsible for decoupling a β -sheet in HA protein and I312V: disrupting a small hydrophobic knot close to the N293 glycosylation site) were also evident in these isolates (Jones et al., 2019). The I233T aa change reduces the pH stability of HA protein rearranging the glycan binding loop constituted by aa 230–242 (Jones et al., 2019). The phosphorylation site at T358 was highly conserved while mutations like S101N, D114N, K180Q and A13T in the signal peptide reported back in 2015 from eastern India were conserved during 2017–19 (Hutchinson et al., 2012; Mukherjee et al., 2016). Several potential glycosylation sites reported from strains of Middle East and North Africa (aa positions 28, 40, 104, 304, 498 and 557) were also conserved in these strains (Al Khatib et al., 2019). The substitution S179N (at the head of the HA protein) generating a novel glycosylation

Table 2

Amino acid substitutions in the antigenic epitopes in the NA gene among the N1 subtypes of Influenza A(H1N1)pdm09 isolates in comparison to vaccine strains A/human/California/07/2009(H1N1), A/human/Michigan/45/2015(H1N1), A/human/Brisbane/02/2018(H1N1) and previously reported eastern Indian strains. Single amino acid change has been underlined while more than one change has been represented in boldface.

Amino acid positions	93	117	143	188	264	267	270	292	294	301	389	394	432	451	452	455	458	460
A/human/California/07/2009(H1N1)	P	I	K	I	V	V	N	C	D	R	I	V	K	D	T	W	P	G
A/human/Michigan/45/2015(H1N1)	P	I	K	I	I	V	K	C	D	R	I	V	E	D	T	W	P	G
A/human/Brisbane/02/2018(H1N1)	P	I	K	T	I	V	K	C	D	R	I	V	E	D	T	W	P	G
A/human/India/Kol-3959/2015	P	I	K	I	I	V	K	C	D	R	I	V	E	D	T	W	P	G
Group A	P	I	K	T	I	V	K	C	D	R	I	V	E	D	T	W	P	G
Group B	P	<u>M</u>	K	T	I	V	<u>K</u>	C	D	R	I	V	<u>E</u>	D	T	W	P	G
Group C	P	I	<u>R</u>	T	I	V	<u>K</u>	C	D	R	I	V	<u>E</u>	D	T	W	P	G
A/human/India/Kol-5546/2017(H1N1)	P	I	K	T	I	I	<u>K</u>	C	D	P	I	V	<u>E</u>	D	T	W	P	G
A/human/India/Kol-625/2017(H1N1)	P	I	K	T	I	V	<u>K</u>	W	E	R	I	V	<u>E</u>	D	T	W	P	G
A/human/India/Kol-5733/2017(H1N1)	P	I	K	T	I	V	<u>K</u>	C	D	R	M	V	<u>E</u>	D	T	W	R	D
A/human/India/Kol-5943/2017(H1N1)	P	I	K	T	I	V	<u>K</u>	C	D	R	I	G	<u>E</u>	D	T	<u>C</u>	P	<u>A</u>
A/human/India/Kol-6247/2017(H1N1)	H	I	K	T	I	V	<u>K</u>	C	D	R	I	V	<u>E</u>	A	T	<u>C</u>	P	<u>A</u>
A/human/India/Kol-7341/2017(H1N1)	P	I	K	T	I	V	<u>E</u>	C	D	R	I	V	<u>E</u>	D	T	W	P	G
A/human/India/Kol-7346/2017(H1N1)	P	I	K	T	I	V	<u>K</u>	C	D	R	I	I	<u>E</u>	D	I	W	P	G
A/human/India/Kol-731/2017(H1N1)	P	I	K	I	V	V	<u>K</u>	C	D	R	I	V	<u>E</u>	D	T	W	P	G
A/human/India/Kol-7367/2017(H1N1)	P	I	K	T	I	V	<u>K</u>	C	D	R	I	V	<u>G</u>	D	T	W	P	G

Group A represents strains with accession numbers MN508971, MN508972, MN508974, MN508977, MN508979, MN508981, MN508982, MN508983, MN508984, MN508985, MN508989, MN508990, MN508991, MN508993.

Group B represents strains with accession numbers MN508975, MN508976.

Group C represents strains with accession numbers MN508994, MN508995.

site since 2015 was prominent among the strains analyzed in this study (Mukherjee et al., 2016; Al Khatib et al., 2019).

The aa responsible for enzymatic activity of NA were found to be conserved among the circulating strains (aa positions 19, 232, 248 and 436) (Zanin et al., 2017). Few changes like V13I, I34V, N200S, V241I, N248D, I314M, N369K and N386K which prevailed in eastern India during the 2015 outbreak, persisted during this period too (Mukherjee et al., 2016). Loss of the glycosylation site at aa position 386 was reported in all the current isolates. Amino acids I223, H275, Q313, I427 responsible for binding to neuraminidase inhibitors were consistent and mutation N295S which caused multidrug resistance was not detected in the circulating strains (McKimm-Breschkin, 2013). The neuraminidase inhibitor resistant marker (H275Y) which was observed in the seasonal H1N1 strains during 2009, was absent in all the present pandemic strains (Agrawal et al., 2010), suggesting that Tamiflu can be used as an antiviral therapy for high risk patients in this region. Mutation K432E which promotes salt bridge formation in the vicinity of the active site with R371 residue was found in maximum strains (96%). This would result in loss of a prime electrostatic pharmacophore feature for the neuraminidase inhibitors like Zanamivir and Oseltamivir, impairing the effectiveness of these inhibitors (Jones et al., 2019).

Evolution of A/H1N1pdm09 viruses continuously pose a threat to the effectiveness of vaccines in a particular epidemiological setting. Phylogenetic analyses and comparison of the antigenic epitopes between the current circulating eastern Indian A/H1N1pdm09 strains and the WHO recommended vaccine strains highlight the distinct changes among them. DNA homology of the current isolates (circulating during 2017–19) was higher with the vaccine strain A/human/Michigan/45/2015 (98.8%) and A/human/Brisbane/02/2018 (99%) than with A/human/California/07/2009 (96.9%). Recurrent outbreaks of A/H1N1pdm09, high CFR rates and low awareness among population regarding benefits of vaccine in India highlight the urgent need to formulate a national policy for influenza vaccination specially for the high risk persons.

The major limitation of this study is that it is not an active surveillance (community or hospital based), thus the disease burden of Influenza A/H1N1 in the population cannot be estimated as the denominator remains unknown. The study only focuses on estimating proportion of Influenza A/H1N1pdm09 among the severe acute respiratory hospitalized cases and phylogenetic analysis of circulating strains in a small region of India. Moreover, as the virus lab receives

samples from hospitals for diagnostics, information regarding vaccination history, co-morbidity and outcome is lacking.

5. Conclusion

Large scale surveillance study of the IAV pandemic A/H1N1pdm09 strains across India is warranted to deduce the burden of disease, mortality rates, economic burden on health care system and efficacy of current vaccines in this endemic region. Such information will pave the way to advocate for formulating a national policy to vaccinate the high risk groups with seasonal flu vaccines. In addition, it may raise awareness about Influenza and dispel misapprehensions about flu vaccines among the community and healthcare workers.

Supplementary data to this article can be found online at <https://doi.org/10.1016/j.meegid.2020.104270>.

Declaration of Competing Interest

The authors declare that they have no conflict of interest.

Acknowledgement

This study was financially supported by Indian Council of Medical Research (ICMR) and Department of Health Research (DHR), Ministry of Health and Family Welfare (MOHFW), Govt. of India. The authors acknowledge Dr. Byomkesh Manna for his assistance in statistical analysis.

References

- Adam, D.C., Scotch, M., MacIntyre, C.R., 2019. Phylodynamics of Influenza A/H1N1pdm09 in India reveals circulation patterns and increased selection for clade 6b residues and other high mortality mutants. *Viruses* 11 (9), 791. <https://doi.org/10.3390/v11090791>.
- Agrawal, A.S., Sarkar, M., Chakrabarti, S., Rajendran, K., Kaur, H., Mishra, A.C., Chatterjee, M.K., Naik, T.N., Chadha, M.S., Chawla-Sarkar, M., 2009. Comparative evaluation of real-time PCR and conventional RT-PCR during a 2-year surveillance for influenza and respiratory syncytial virus among children with acute respiratory infections in Kolkata, India, reveals a distinct seasonality of infection. *J. Med. Microbiol.* 58 (12), 1616–1622. <https://doi.org/10.1099/jmm.0.011304-0>.
- Agrawal, A.S., Sarkar, M., Ghosh, S., Roy, T., Chakrabarti, S., Lal, R., Mishra, A.C., Chadha, M.S., Chawla-Sarkar, M., 2010. Genetic characterization of circulating seasonal Influenza A viruses (2005–2009) revealed introduction of oseltamivir resistant H1N1 strains during 2009 in eastern India. *Infect. Genet. Evol.* 10 (8), 1188–1198.

- <https://doi.org/10.1016/j.jmeegid.2010.07.019>.
- Al Khatib, H.A., Al Thani, A.A., Gallouzi, I., Yassine, H.M., 2019. Epidemiological and genetic characterization of pH1N1 and H3N2 influenza viruses circulated in MENA region during 2009–2017. *BMC Infect. Dis.* 19 (1), 314. <https://doi.org/10.1186/s12879-019-3930-6>.
- Arbat, S., Dave, M., Niranjan, V., Rahman, I., Arbat, A., 2017. Analyzing the clinical profile of swine flu/influenza A H1N1 infection in Central India: a retrospective study. *Virus Dis.* 28 (1), 33–38. <https://doi.org/10.1007/s13337-017-0363-y>.
- Bali, N.K., Ashraf, M., Ahmad, F., 2013. Knowledge, attitude and practices about the seasonal influenza vaccination among healthcare workers in Srinagar, India. *Influenza Other Respir. Viruses* 7 (4), 540–545.
- Barde, P.V., Sahu, M., Shukla, M.K., Bharti, P.K., Sharma, R.K., Sahare, L.K., Ukey, M.J., Singh, N., 2017. The high frequency of non-aspartic acid residues at HA222 in influenza A(H1N1) 2009 pandemic viruses is associated with mortality during the upsurge of 2015: a molecular and epidemiological study from Central India. *Epidemiol. Infect.* 145 (13), 2656–2665. <https://doi.org/10.1017/S0950268817001595>.
- Broor, S., Gupta, S., Mohapatra, S., Kaushik, S., Mir, M.A., Jain, P., Dar, L., Lal, R.B., 2011. Emergence of 2009A/H1N1 cases in a tertiary care hospital in New Delhi, India. *Influenza Other Respir. Viruses* 5 (6), e552–e557. <https://doi.org/10.1111/j.1750-2659.2011.00274.x>.
- Broor, S., Krishnan, A., Roy, D.S., Dhakad, S., Kaushik, S., Mir, M.A., Singh, Y., Moen, A., Chadha, M., Mishra, A.C., Lal, R.B., 2012. Dynamic patterns of circulating seasonal and pandemic A(H1N1)pdm09 influenza viruses from 2007–2010 in and around Delhi, India. *PLoS One* 7, e29129. <https://doi.org/10.1371/journal.pone.0029129>.
- Caton, A.J., Brownlee, G.G., Yewdell, J.W., Gerhard, W., 1982. The antigenic structure of the influenza virus A/PR/8/34 hemagglutinin (H1 subtype). *Cell* 31 (2 Pt 1), 417–427. [https://doi.org/10.1016/0092-8674\(82\)90135-0](https://doi.org/10.1016/0092-8674(82)90135-0).
- Chadha, M.S., Potdar, V.A., Saha, S., Koul, P.A., Broor, S., Dar, L., Chawla-Sarkar, M., Biswas, D., Gunasekaran, P., Abraham, A.M., Shrikhande, S., 2015. Dynamics of influenza seasonality at sub-regional levels in India and implications for vaccination timing. *PLoS One* 10 (5), e0124122. <https://doi.org/10.1371/journal.pone.0124122>.
- Charu, V., Chowell, G., Palacio Mejia, L.S., Echevarria-Zuno, S., Borja-Aburto, V.H., Simonsen, L., Miller, M.A., Viboud, C., 2011. Mortality burden of the A/H1N1 pandemic in Mexico: a comparison of deaths and years of life lost to seasonal influenza. *Clin. Infect. Dis.* 53 (10), 985–993. <https://doi.org/10.1093/cid/cir644>.
- Choudhry, A., Singh, S., Khare, S., Rai, A., Rawat, D.S., Aggarwal, R.K., Chauhan, L.S., 2012. Emergence of pandemic 2009 influenza A H1N1, India. *Indian J. Med. Res.* 135 (4), 534.
- Costantino, C., Restivo, V., Amodio, E., Colomba, G.M.E., Vitale, F., Tramuto, F., 2019. A mid-term estimate of 2018/2019 vaccine effectiveness to prevent laboratory confirmed A (H1N1) pdm09 and A (H3N2) influenza cases in Sicily (Italy). *Vaccine* 37 (39), 5812–5816. <https://doi.org/10.1016/j.vaccine.2019.08.014>.
- Cousins, S., 2015. Death toll from swine flu in India exceeds 2500. *BMJ*. 351, h4966. <https://doi.org/10.1136/bmj.h4966>.
- Dang, A., Sharma, J., 2020. Assessing the low Influenza vaccination coverage rate among healthcare personnel in India: a review of obstacles, beliefs, and strategies. *Sci. Direct*. 21 (C), 100–104.
- de Vries, R.P., de Vries, E., Martinez-Romero, C., McBride, R., van Kuppeveld, F.J., Rottier, P.J.M., Garcia-Sastre, A., Paulson, J.C., de Haan, C.A.M., 2013. Evolution of the hemagglutinin protein of the new pandemic H1N1 influenza virus: maintaining optimal receptor binding by compensatory substitutions. *J. Virol.* 87 (24), 13868–13877. <https://doi.org/10.1128/jvi.01955-13>.
- Dee, S., Jayathissa, S., 2010. Clinical and epidemiological characteristics of the hospitalised patients due to pandemic H1N1 2009 viral infection: experience at Hutt hospital, New Zealand. *N. Z. Med. J.* 123 (1312), 45–53.
- Domingo, E., 2010. Mechanisms of viral emergence. *Vet. Res.* 41 (6), 38. <https://doi.org/10.1051/vetres/2010010>.
- Dool, C.V.D., Hak, E., Wallinga, J., Loon, A.M.V., Lammers, J.W.J., Bonten, M.J.M., 2008. Symptoms of Influenza virus infection in hospitalized patients. In: *Infection Control and Hospital Epidemiology*. The University of Chicago Press on behalf of The Society for Healthcare Epidemiology of America Stable. 29, pp. 314–319.
- Ekiert, D.C., Bhabha, G., Elsliger, M.A., Friesen, R.H.E., Jongeneelen, M., Throsby, M., Goudsmit, J., Wilson, I.A., 2009. Antibody recognition of a highly conserved influenza virus epitope. *Science* 324 (5924), 246–251. <https://doi.org/10.1126/science.1171491>.
- Elliot, A.J., Powers, C., Thornton, A., Obi, C., Hill, C., Simms, I., Waight, P., Maguire, H., Foord, D., Povey, E., Wreghitt, T., 2009. Monitoring the emergence of community transmission of influenza A/H1N1 2009 in England: a cross sectional opportunistic survey of self sampled telephone callers to NHS direct. *Bmj*. 339, b3403. <https://doi.org/10.1136/bmj.b3403>.
- Fukuzawa, K., Omagari, K., Nakajima, K., Nobusawa, E., Tanaka, S., 2011. Sialic acid recognition of the pandemic Influenza 2009 H1N1 virus: binding mechanism between human receptor and Influenza hemagglutinin. *Protein Pept. Lett.* 18 (5), 530–539. <https://doi.org/10.2174/092986611794927893>.
- Gambhir, R.S., Pannu, P.R., Nanda, T., 2016. Knowledge and awareness regarding swine influenza A(H1N1) virus infection among dental professional in India-a systematic review. *J. Clin. Diagn. Res.* 10 (9), ZE10–ZE13.
- Girard, M.P., Tam, J.S., Assossou, O.M., Kiény, M.P., 2010. The 2009 A (H1N1) influenza virus pandemic: a review. *Vaccine*. 28, 4895–4902. <https://doi.org/10.1016/j.vaccine.2010.05.031>.
- Graham, M., Liang, B., van Domselaar, G., Bastien, N., Beaudoin, C., Tyler, S., Kaplen, B., Landry, E., Li, Y., 2011. Nationwide molecular surveillance of pandemic H1N1 influenza A virus genomes. *Canada*, 2009. *PLoS One* 6 (1), e16087. <https://doi.org/10.1371/journal.pone.0016087>.
- Guirav, Y.K., Pawar, S.D., Chadha, M.S., Potdar, V.A., Deshpande, A.S., Koratkar, S.S., Hosmani, A.H., Mishra, A.C., 2010. Pandemic influenza A(H1N1) 2009 outbreak in a residential school at Panchgani, Maharashtra, India. *Indian J. Med. Res.* 132, 67–71. <http://icmr.nic.in/ijmr/2010/july/0711.pdf>.
- Hirve, S., 2015. *Seasonal Influenza Vaccine Use in Low and Middle Income Countries in the Tropics and Subtropics: A Systematic Review*. World Health Organization.
- Hutchinson, E.C., Denham, E.M., Thomas, B., Trudgian, D.C., Hester, S.S., Ridlova, G., York, A., Turell, L., Fodor, E., 2012. Mapping the Phosphoproteome of Influenza A and B viruses by mass spectrometry. *PLoS Pathog.* 8 (11), e1002993. <https://doi.org/10.1371/journal.ppat.1002993>.
- Influenza A, 2020. H1N1 (Swine Flu) – State/UT- wise, Year- wise from 2009–2015. Ministry of Health and Family Welfare. Last accessed - February 24, 2015. <https://pib.gov.in/newsite/PrintRelease.aspx?relid=115710>.
- Jagadeesh, A., Krishnan, A., Nair, S., Sivadas, S., Arunkumar, G., 2019. Genetic characterization of hemagglutinin (HA) gene of influenza A viruses circulating in Southwest India during 2017 season. *Virus Genes* 1–7. <https://doi.org/10.1007/s11262-019-01675-x>.
- Jones, S., Nelson-Sathi, S., Wang, Y., Prasad, R., Rayen, S., Nandel, V., Hu, Y., Zhang, W., Nair, R., Dharmaseelan, S., Chirundodh, D.V., 2019. Evolutionary, genetic, structural characterization and its functional implications for the influenza A (H1N1) infection outbreak in India from 2009 to 2017. *Sci. Rep.* 9 (1). <https://doi.org/10.1038/s41598-019-51097-w>. 1–0.
- Kant, L., Guleria, R., 2018. Pandemic flu, 1918: after hundred years, India is as vulnerable. *IJMR*. 147 (3), 221–224. https://doi.org/10.4103/ijmr.IJMR_407_18.
- Korsun, N., Angelova, S., Gregory, V., Daniels, R., Georgieva, I., McCauley, J., 2017. Antigenic and genetic characterization of influenza viruses circulating in Bulgaria during the 2015/2016 season. *Infect. Genet. Evol.* 49, 241–250. <https://doi.org/10.1016/j.jmeegid.2017.01.027>.
- Koul, P., Khan, U., Bhat, K., Saha, S., Broor, S., Lal, R., Chadha, M., 2013. Recrudescence wave of A/H1N1pdm09 Influenza viruses in winter 2012–2013 in Kashmir, India. *PLoS Curr.* 26, 5. <https://doi.org/10.1371/currents.outbreaks.fl241c3a2625fc7a81bf25ea81f66e6>.
- Kulkarni, S., Narain, J., Gupta, S., Dhariwal, A., Singh, S., Macintyre, Cr., 2019. Influenza A (H1N1) in India: changing epidemiology and its implications. *Natl Med. J. India*. <https://doi.org/10.4103/0970-258x.253355>.
- Kumar, S., Stecher, G., Li, M., Knyaz, C., Tamura, K., 2018. MEGA X: molecular evolutionary genetics analysis across computing platforms. *Mol. Biol. Evol.* 35 (6), 1547–1549. <https://doi.org/10.1093/molbev/msy096>.
- Lin, J., Kang, M., Zhong, H., Zhang, X., Yang, F., Ni, H., Huang, P., Hong, T., Ke, C., He, J., 2013. Influenza seasonality and predominant subtypes of influenza virus in Guangdong, China, 2004–2012. *J. Thorac Dis* 5 (Suppl. 2), S109–S117. <https://doi.org/10.3978/j.issn.2072-1439.2013.08.09>.
- Liu, S.T.H., Behzadi, M.A., Sun, W., Freyn, A.W., Liu, W.C., Broecker, F., Albrecht, R.A., Bouvier, N.M., Simon, V., Nachbagauer, R., Krammer, F., Palese, P., 2018. Antigenic sites in influenza H1 hemagglutinin display species-specific immunodominance. *J. Clin. Invest.* 8. <https://doi.org/10.1172/JCI122895>. 128(11).
- Lofgren, E., Fefferman, N.H., Naumov, Y.N., Gorski, J., Naumova, E.N., 2007. Influenza seasonality: underlying causes and modeling theories. *J. Virol.* 81 (11), 5429–5436. <https://doi.org/10.1128/jvi.01680-06>.
- Luo, T., Liu, L., Shen, X., Irwin, D.M., Liao, M., Shen, Y., 2018. The evolutionary dynamics of H1N1/pdm2009 in India. *Infect. Genet. Evol.* 65, 276–282. <https://doi.org/10.1016/j.jmeegid.2018.08.009>.
- Majanja, J., Njorge, R.N., Achilla, R., Wurapa, E.K., Wadegu, M., Mukunzi, S., Mwangi, J., Njiri, J., Gachara, G., Bulimo, W., 2013. Impact of influenza A(H1N1)pdm09 virus on circulation dynamics of seasonal influenza strains in Kenya. *Am. J. Trop. Med. Hyg.* 88 (5), 940–945. <https://doi.org/10.4269/ajtmh.12-0147>.
- Malhotra, B., Singh, R., Sharma, P., Meena, D., Gupta, J., Atreya, A., Meena, B.R., 2016. Epidemiological & clinical profile of influenza A (H1N1) 2009 virus infections during 2015 epidemic in Rajasthan. *Indian J. Med. Res.* 144 (6), 918. https://doi.org/10.4103/ijmr.IJMR_1183_15.
- Matos-Patón, A., Byrd-Leotis, L., Steinhauer, D.A., Barclay, W.S., Ayora-Talavera, G., 2015. Amino acid substitution D222N from fatal influenza infection affects receptor-binding properties of the influenza A(H1N1)pdm09 virus. *Virology* 484, 15–21. <https://doi.org/10.1016/j.virol.2015.05.012>.
- Maurer-Stroh, S., Lee, R.T.C., Eisenhaber, F., Cui, L., Phuah, S.P., Lin, R.T.P., 2010. A new common mutation in the hemagglutinin of the 2009 (H1N1) influenza A virus. *PLoS Curr.* 2, RRN1162. <https://doi.org/10.1371/currents.RRN1162>.
- McKimm-Breschkin, J.L., 2013. Influenza neuraminidase inhibitors: antiviral action and mechanisms of resistance. *Influenza Other Respir. Viruses* 7, 25–36.
- Mir, M.A., Lal, R.B., Sullender, W., Singh, Y., Garten, R., Krishnan, A., Broor, S., 2012. Genetic diversity of HA1 domain of hemagglutinin gene of pandemic influenza H1N1pdm09 viruses in New Delhi, India. *J. Med. Virol.* 84 (3), 386–393. <https://doi.org/10.1002/jmv.23205>.
- Mishra, B., 2015. 2015 resurgence of influenza A (H1N1) 09: smoldering pandemic in India? *J. Glob 7* (2), 56–59. *Infect. Dis. Ther.* <https://doi.org/10.4103/0974-777X.157236>.
- Mudhigeti, N., Racherla, R., Mahalakshmi, P., Pamireddy, M., Nallapireddy, U., Kante, M., Kalawat, U., 2018. A study of influenza 2017–2018 outbreak in Andhra Pradesh, India. *Indian J. Med. Microbiol.* 36 (4), 526–531. https://doi.org/10.4103/ijmm.IJMM_18_272.
- Mukherjee, A., Roy, T., Agrawal, A.S., Sarkar, M., Lal, R., Chakrabarti, S., Chawla-Sarkar, M., 2010. Prevalence and epidemiology of pandemic H1N1 strains in hospitals of eastern India. *J. Public Heal. Epidemiol.* 2 (7), 171–174.
- Mukherjee, T.R., Agrawal, A.S., Chakrabarti, S., Chawla-Sarkar, M., 2012. Full genomic analysis of an influenza A (H1N2) virus identified during 2009 pandemic in eastern India: evidence of reassortment event between co-circulating A(H1N1)pdm09 and A/Brisbane/10/2007-like H3N2 strains. *Virol. J.* 9, 233. <https://doi.org/10.1186/1743-422X-9-233>.

- Mukherjee, A., Nayak, M.K., Dutta, S., Panda, S., Satpathi, B.R., Chawla-Sarkar, M., 2016. Genetic characterization of circulating 2015 A(H1N1)pdm09 influenza viruses from eastern India. *PLoS One* 11 (12), e0168464. <https://doi.org/10.1371/journal.pone.0168464>.
- Murhekar, M., Mehendale, S., 2016. The 2015 influenza A (H1N1) pdm09 outbreak in India. *Indian J. Med. Res.* 143 (6), 821–823. <https://doi.org/10.4103/0971-5916.192077>.
- National Immunization Schedule, 2020. https://nhm.gov.in/New_Updates_2018/NHM_Components/Immunization/report/National_Immunization_Schedule.pdf.
- Nguyen, H.K.L., Nguyen, P.T.K., Nguyen, T.C., Hoang, P.V.M., Le, T.T., Vuong, C.D., Nguyen, A.P., Tran, L.T.T., Nguyen, B.G., Lê, M.Q., 2015. Virological characterization of influenza H1N1pdm09 in Vietnam, 2010–2013. *Influenza Other Respir. Viruses* 9 (4), 216–224. <https://doi.org/10.1111/irv.12323>.
- Nishiura, H., 2010. Case fatality ratio of pandemic influenza. *Lancet Infect. Dis.* 10 (7), 443–444. [https://doi.org/10.1016/S1473-3099\(10\)70120-1](https://doi.org/10.1016/S1473-3099(10)70120-1).
- Palache, A., Abelin, A., Hollingsworth, R., Cracknell, W., Jacobs, C., Tsai, T., 2017. Survey of distribution of seasonal influenza vaccine doses in 201 countries (2004–2015): the 2003 world health assembly resolution on seasonal influenza vaccination coverage and the 2009 influenza pandemic have had very little impact on improving influenza control and pandemic preparedness. *Vaccine* 35, 4681–4686.
- Pandey, S., Sahu, M., Potdar, V., Barde, P., 2018. Molecular analysis of influenza A H1N1pdm09 virus circulating in Madhya Pradesh, India in the year 2017. *VirusDisease*. 29 (3), 380–384. <https://doi.org/10.1007/s13337-018-0474-0>.
- Parida, M., Dash, P.K., Kumar, J.S., Joshi, G., Tandel, K., Sharma, S., Srivastava, A., Agarwal, A., Saha, A., Saraswat, S., Karothia, D., Malviya, V., 2016. Emergence of influenza A(H1N1)pdm09 genogroup 6B and drug resistant virus, India, January to may 2015. *Eurosurveillance*. 21 (5), 6–11. <https://doi.org/10.2807/1560-7917.ES.2016.21.5.30124>.
- Petrova, V.N., Russell, C.A., 2018. The evolution of seasonal influenza viruses. *Nat. Rev. Microbiol.* 16 (1), 47–60. <https://doi.org/10.1038/nrmicro.2017.118>.
- Pollock, S.L., Sagan, M., Oakley, L., Fontaine, J., Poffenroth, L., 2012. Investigation of a pandemic H1N1 influenza outbreak in a remote first nations community in northern Manitoba, 2009. *Can. J. Public Heal.* 103 (2), 90–93. <https://doi.org/10.1007/bf03404209>.
- Rambaut, A., Pybus, O.G., Nelson, M.I., Viboud, C., Taubenberger, J.K., Holmes, E.C., 2008. The genomic and epidemiological dynamics of human influenza A virus. *Nature*. 453 (7195), 615–619. <https://doi.org/10.1038/nature06945>.
- Sarkar, M., Agrawal, A.S., Dey, R.S., Chattopadhyay, S., Mullick, R., De, P., Chakrabarti, S., Chawla-Sarkar, M., 2011. Molecular characterization and comparative analysis of pandemic H1N1/2009 strains with co-circulating seasonal H1N1/2009 strains from eastern India. *Arch. Virol.* 156 (2), 207–217. <https://doi.org/10.1007/s00705-010-0842-6>.
- Schaffer, A.A., 2001. Improving the accuracy of PSI-BLAST protein database searches with composition-based statistics and other refinements. *Nucleic Acids Res.* 29 (14), 2994–3005. <https://doi.org/10.1093/nar/29.14.2994>.
- Shukla, D., Patel, S., Panchal, S., Shah, N., Sridharan, S., Patel, P., 2010. Awareness regarding swine flu amongst patients attending swine flu OPD in a tertiary Care Centre in South Gujarat. *Natl. J. Community Med.* 1, 103–105.
- Siddharth, V., Goyal, V., Koushal, V., 2012. Clinical-epidemiological profile of influenza A H1N1 cases at a tertiary care institute of India. *Indian J. Community Med.* 37 (4), 232–235. <https://doi.org/10.4103/0970-0218.103471>.
- State/UT - wise, 2020. Year-Wise Number Of Cases and Deaths from 2012–2019. Ministry of Health and Family Welfare Last accessed- November 4, 2019. <https://ncdc.gov.in/showfile.php?lid=280>.
- Thakre, R., Patil, P.S., 2019. Influenza vaccine paradox. *Indian Pediatr.* 56 (1), 80.
- Treanor, J., 2004. Influenza vaccine - outmaneuvering antigenic shift and drift. *N. Engl. J. Med.* 350 (3), 218–220. <https://doi.org/10.1056/NEJMp038238>.
- Treanor, J., 2015. Prospects for broadly protective influenza vaccines. *Vaccine* 33, D39–D45. <https://doi.org/10.1016/j.vaccine.2015.08.053>.
- Trucchi, C., Paganino, C., Orsi, A., Amicizia, D., Tisa, V., Piazza, M.F., Gallo, D., Simonetti, S., Buonopane, B., Icardi, G., Ansaldi, F., 2019. Hospital and economic burden of influenza-like illness and lower respiratory tract infection in adults ≥ 50 years-old. *BMC Health Serv. Res.* 19 (1), 585. <https://doi.org/10.1186/s12913-019-4412-7>.
- US Centers for Disease Control and Prevention (CDC), 2019. Summary of the 2017–2018 Influenza Season. September 5. <https://www.cdc.gov/flu/about/season/flu-season-2017-2018.htm>.
- Webster, R.G., Bean, W.J., Gorman, O.T., Chambers, T.M., Kawaoka, Y., 1992. Evolution and ecology of influenza a viruses. *Microbiol. Mol. Biol. Rev.* 56 (1), 152–179.
- World Health Organization, 2009. CDC protocol of real-time RT-PCR for influenza A (H1N1). 28 April, 2009. https://www.who.int/csr/resources/publications/swineflu/CDCrealtimeRTPCRprotocol_20090428.pdf.
- World Health Organization, 2015a. Recommended composition of influenza virus vaccines for use in the 2015–16 northern hemisphere influenza season. 26 February, 2015. https://www.who.int/influenza/vaccines/virus/recommendations/2015_16_north/en/.
- World Health Organization, 2015b. Recommended composition of influenza virus vaccines for use in the 2016 southern hemisphere influenza season. 24 September, 2015. https://www.who.int/influenza/vaccines/virus/recommendations/2015_16_south/en/.
- World Health Organization, 2016a. Recommended composition of influenza virus vaccines for use in the 2016–17 northern hemisphere influenza season. 25 February 2016. https://www.who.int/influenza/vaccines/virus/recommendations/2016_17_north/en/.
- World Health Organization, 2016b. Recommended composition of influenza virus vaccines for use in the 2017 southern hemisphere influenza season. 29 September 2016. https://www.who.int/influenza/vaccines/virus/recommendations/2017_south/en/.
- World Health Organization, 2017a. Recommended composition of influenza virus vaccines for use in the 2018 southern hemisphere influenza season. September 27, 2017. https://www.who.int/influenza/vaccines/virus/recommendations/201709_recommendation.pdf?ua=1.
- World Health Organization, 2017b. Up to 650 000 people die of respiratory diseases linked to seasonal flu each year. December 19, 2017. <http://www.who.int/mediacentre/news/releases/2017/seasonal-flu>.
- World Health Organization, 2018a. Recommended composition of influenza virus vaccines for use in the 2018–19 northern hemisphere influenza season. 22 February, 2018. https://www.who.int/influenza/vaccines/virus/recommendations/2018_19_north/en/.
- World Health Organization, 2018b. Recommended composition of influenza virus vaccines for use in the 2019 southern hemisphere influenza season. 27 September 2018. https://www.who.int/influenza/vaccines/virus/recommendations/2019_south/en/.
- World Health Organization, 2019a. Recommended composition of influenza virus vaccines for use in the 2019–2020 northern hemisphere influenza season. 21 February 2019. updated 21 March, 2019. https://www.who.int/influenza/vaccines/virus/recommendations/2019_20_north/en/.
- World Health Organization, 2019b. Recommended composition of influenza virus vaccines for use in the 2020 southern hemisphere influenza season. 27 September 2019.
- World Health Organization, 2020. Pandemic (H1N1) 2009 - Update 112. 6 August 2010. https://www.who.int/csr/don/2010_08_06/en/.
- Yasuhara, A., Yamayoshi, S., Soni, P., Takenaga, T., Kawakami, C., Takashita, E., Sakai-Tagawa, Y., Uraki, R., Ito, M., Iwatsuki-Horimoto, K., Sasaki, T., Ikuta, K., Yamada, S., Kawaoka, Y., 2017. Diversity of antigenic mutants of influenza A(H1N1)pdm09 virus escaped from human monoclonal antibodies. *Sci. Rep.* 7 (1), 17735. <https://doi.org/10.1038/s41598-017-17986-8>.
- Zanin, M., Duan, S., Wong, S.S., Kumar, G., Baviskar, P., Collin, E., Russell, C., Barman, S., Hause, B., Webby, R., 2017. An amino acid in the stalk domain of N1 neuraminidase is critical for enzymatic activity. *J. Virol.* 91 (2). <https://doi.org/10.1128/jvi.00868-16>.



In quest of small-molecules as potent non-competitive inhibitors against influenza

Khushboo Malbari^a, Priyanka Saha^b, Mamta Chawla-Sarkar^b, Shanta Dutta^b, Swita Rai^a, Mamata Joshi^c, Meena Kanyalkar^{a,*}

^a Department of Pharmaceutical Chemistry, Prin K M Kundnani College of Pharmacy, Cuffe Parade, Mumbai 400005, India

^b Division of Virology, ICMR-National Institute of Cholera and Enteric Diseases (ICMR-NICED), Belehata, Kolkata 700010, India

^c National Facility for High Field NMR, Tata Institute of Fundamental Research (TIFR), Colaba, Mumbai 400005, India

ARTICLE INFO

Keywords:

430-cavity
Neuraminidase
Non-competitive inhibition
Pandemic H1N1
Influenza

ABSTRACT

A series of scaffolds namely aurones, 3-indolinones, 4-quinolones and cinnamic acid-piperazine hybrids, was designed, synthesized and investigated *in vitro* against influenza A/H1N1pdm09 virus. Designed molecules adopted different binding mode i.e., in 430-cavity of neuraminidase, unlike sialic acid and oseltamivir in molecular docking studies. All molecules reduced the viral titer and exhibited non-cytotoxicity along with cryo-protective property towards MDCK cells. Molecules (Z)-2-(3'-Chloro-benzylidene)-1,2-dihydro-indol-3-one (**2f**), (Z)-2-(4'-Chloro-benzylidene)-1,2-dihydro-indol-3-one (**2g**) and 2-(2'-Methoxy-phenyl)-1H-quinolin-4-one (**3a**) were the most interesting molecules identified in this research, endowed with robust potencies showing low-nanomolar EC₅₀ values of 4.0 nM, 6.7 nM and 4.9 nM, respectively, compared to reference competitive and non-competitive inhibitors: oseltamivir (EC₅₀ = 12.7 nM) and quercetin (EC₅₀ = 0.56 μM), respectively. Besides, **2f**, **2g** and **3a** exhibited good neuraminidase inhibitory activity in sub-micromolar range (IC₅₀ = 0.52 μM, 3.5 μM, 1.3 μM respectively). Moreover, these molecules were determined as non-competitive inhibitors similar to reference non-competitive inhibitor quercetin unlike reference competitive inhibitor oseltamivir in kinetics studies.

1. Introduction

Influenza A/H1N1pdm09, despite being a mild pandemic, remains a critical challenge to public health in terms of mortality and morbidity. In addition, one cannot rule out further inter genotypic reassortment events with currently circulating high pathogenic avian influenza strains such as H5N1 and H9N2 [1–3]. The influenza life cycle depends on an accurate balance between the functionality of two viral surface glycoproteins viz. Hemagglutinin (HA) and Neuraminidase (NA). HA being a fusion protein, facilitates the fusion of endocytosed virus particle with the host cell endosomal membrane after binding to the surface receptors containing sialic acid (SA). This brings about the viral internalization. NA being an exosialidase, cleaves the α-ketosidic linkage between SA

and adjacent sugar residue [4,5]. The virulence and replication of a pandemic H1N1 strain has been reported to be greater than that for a seasonal H1N1 strain, and this difference increases the severity of the disease [6,7].

The anti-influenza drugs currently used as treatment, such as oseltamivir (OMV) and zanamivir (ZMV), have the structural similarity to SA and consequently similar binding pattern to the NA enzyme. But, mutations in NA gene limits their use as competitive inhibitors due to resistance [8,9]. This reinforces the requirement of an alternate approach in design and synthesis of new molecules to be developed as potential anti-influenza agents. This could be achieved by discovery of newer scaffolds that are structurally dissimilar to OMV/ZMV and have different binding pattern in the enzyme cavity. The resistance problem

Abbreviations: CAPI, Cinnamic acid-piperazine; CC, Cell control; CV, Crystal violet; CPE, Cytopathic effect; DCM, Dichloromethane; DMF, Dimethyl formamide; DMSO, Dimethylsulfoxide; FBS, Foetal Bovine Serum; HA, Hemagglutinin; HA titer, Hemagglutination titer; HAI, Hemagglutination inhibition; LR, Laboratory Reagent; MDCK, Madin-Darby Canine Kidney cells; MEM, Minimum Essential Medium; NA, Neuraminidase; OMVC, Oseltamivir Carboxylate; OMVP, Oseltamivir Phosphate; PDB, Protein Data Bank; QR, Quercetin; SA, Sialic Acid; VC, VirusControl.

* Corresponding author at: Department of Pharmaceutical Chemistry, Prin. K. M. Kundnani College of Pharmacy, Plot 23, Jote Joy Building, Rambhau Salgaonkar Marg, Cuffe Parade, Mumbai 400005, India.

E-mail address: ma.kanyalkar@kmcpc.edu.in (M. Kanyalkar).

<https://doi.org/10.1016/j.bioorg.2021.105139>

Received 18 November 2020; Received in revised form 14 May 2021; Accepted 28 June 2021

Available online 1 July 2021

0045-2068/© 2021 Elsevier Inc. All rights reserved.

towards competitive inhibitors of NA i.e., OMV and ZMV, due to mutations could be avoided by developing non-competitive inhibitors which inhibit the enzyme by binding allosterically to the target enzyme. There are two cavities present adjacent to SA/OMV binding site in NA viz., 150-cavity and 430-cavity. These two cavities could be considered as the potential alternate binding sites in NA.

There are reported molecules that bind to 150-cavity and 430-cavity demonstrating potent inhibition of various NA subtypes [10,11]. In fact, in recent years, discovery of various molecules, by our lab team, probing 150-cavity and 430-cavity led us to a series of chalcones showing non-competitive inhibition mechanism towards H1N1-NA and H5N1-NA along with certain other scaffolds, showing anti-influenza activities against H1N1-NA [12–15]. Among several reported antiviral phytoconstituents and our lab team's findings, we have selected chalcones that is characterized by α , β -unsaturated carbonyl functional groups. Nonetheless, chalcones show weaker anti-influenza activity along with cytotoxicity [16–19]. This scaffold can be modified to various cyclized derivatives such as aurones, flavones, 3-indolinones and 4-quinolones, for cyclized rigidification has been proven to improve the activity of a lead molecule [20]. Chalcones, the chosen parent scaffold, can correspondingly be compared with other α , β -unsaturated carbonyl functional group containing phytoconstituent showing antiviral activity such as cinnamic acid derivatives [21–23]. Further, piperazine moiety, having wide variety of activity [24,25], is a commonly used scaffold in various drugs, and thus had been selected and linked with cinnamic acid scaffold by molecular hybridization approach [26]. Therefore, considering the above facts and modifications, we report here the design, synthesis and evaluation of a series of four scaffolds, namely aurones, 3-indolinones, 4-quinolones and cinnamic acid-piperazine (CAPI) hybrids against influenza A/H1N1pdm09 virus. The above-mentioned selected scaffolds are structurally dissimilar to the transition state of sialo-glycoconjugate being hydrolysed by viral NA, the substrate for NA. They were designed with introducing substituents with varied functional groups attributing electronic, steric and volume effect to the molecules.

Cytopathic effect (CPE) inhibition and hemagglutination inhibition (HAI) assays were executed on the molecules that were selected based on docking results and cytotoxicity, to screen them for further extensive evaluation studies on the basis of % CPE inhibition and % HA titer reduction of virus with candidate molecules. All the screened molecules were subjected to cell-based assay to determine their EC_{50} values followed by enzyme-based assay to determine their IC_{50} values. Additionally, mechanism of inhibition of the molecules was determined by enzyme kinetics studies which showed non-competitive inhibition when compared with competitive inhibitor viz. OMV. This strengthens our idea of developing potential anti-influenza agents and propose better therapeutic and prophylactic upshots than what current anti-influenza drugs can offer us.

Also, there has been studies conducted to suggest the correlation between influenza and SARS-CoV-2 [27]. It was demonstrated that influenza caused increase in the SARS-CoV-2 transmission along with enabling the spread of COVID-19 in Europe during early 2020. More generally, taking into account the resistance issue of influenza, it is imperative to develop agents with alternate mechanism of action that this current work is all about that can combat this very contributing factor of influenza to the spread of COVID-19.

2. Results and discussion

2.1. Computational studies demonstrating alternate binding mode in NA enzyme

The active site of N1-NA was classified into three cavities for suitability: (i) the SA catalytic cavity (R118, E119, N146, D151, R152, Y178, I222, E227, E276, E277, R292, N294, N347, R371, and Y406); (ii) the 150-cavity (N146-R152) and (iii) the 430-cavity (N325, P326, G348, S369, S370, W403, I427, G429, R430-T439) [13,28]. Interestingly, the

crystal structure of NA from the pandemic 2009 influenza A/H1N1pdm09 strain indicated that it lacks the 150-loop in its active site (akin to closed conformation in contrast to the open conformation observed in seasonal H1N1-NA influenza attributed to the presence of 150-loop) [29–33]. The initial docking validation studies could acceptably replicate (RMSD 0.32 Å) the binding pose of the co-crystallized ligand viz. oseltamivir carboxylate (OMVC) in the influenza A/H1N1pdm09-NA X-ray crystal structure (PDB ID: 3TI6). The cleavage of α -ketosidic linkages between SA and adjacent sugar residue occurs during NA catalyses [8,34]. Thus, to understand the interaction pattern and critical residues involved in SA binding, we docked sialic acid in SA catalytic cavity of NA (Fig. 1a). It was observed that the carbonyl of *N*-acetamido group formed H-bond with R152 while the deoxy formed H-bond with E277. The terminal hydroxyl groups of glycerol sidechain formed H-bond with R118, E119, and Y406. The carboxylate group formed H-bond with the sidechain of R292 along with a bi-dentate interaction with R371. The hydroxyl group formed H-bond with R151.

To ensure about the unbiased search of binding site of our designed molecules, we explored all the putative binding pockets for docking in NA enzyme. This strategy is often applied when prior knowledge of the binding mode of the molecule is unknown [35,36]. Initially, we docked quercetin, active natural non-competitive anti-influenza agent [37] in NA to gain insight into its non-competitive inhibition behaviour. As anticipated from its non-competitive nature, quercetin did not bind to SA cavity, rather its binding was confined to 430-cavity within the active site than other putative binding pockets. Moreover, to ensure whether quercetin occupy distinctly different region than SA binding site or not, we have docked it into the active site of NA already complexed with OMVC/SA. It was observed that it still bound the same way as observed in absence of OMVC/SA. This confirmed that quercetin occupied a very distinct site and did not overlap with the SA binding site that further signified existence of an alternate binding region for quercetin within the catalytic site discrete from available drugs and SA (Fig. 1b). The two hydroxyl groups of flavone ring of quercetin formed H-bond with N347 and K432 along with π -alkyl interaction with R371 and P431. The hydroxyl of phenyl ring formed H-bond with I427 and phenyl ring had π -alkyl interaction with R371, I427, P431 and K432.

Additionally, non-bonded interaction energies were calculated for quercetin with the catalytic site residues. Fig. 2 demonstrates that quercetin has favourable non-bonded interactions with the catalytic site residues that included R118, I149, R152, N294, N347, S370, R371, W403, Y406, R430, P431, L432, T436, I437 and W438. The previously reported site-directed mutagenesis studies highlighted the importance of N146, R152, W178, E276, E277, S370, R371, W403, Y406 in the catalytic activity of NA [9,38], out of which quercetin showed non-bonded interactions with R152, S370, R371, W403 and Y406. Moreover, it was observed that R152 is involved in the binding of SA to active site of NA (*vide supra*) in molecular docking studies. Therefore, it could be presumed from the above outcomes that on account of H-bonding and non-bonded interactions, quercetin cause hinderance in the catalytic activity of NA thereby inhibiting it, nonetheless, with an alternate binding mode in the NA enzyme.

The designed molecules were then docked in influenza A/H1N1pdm09-NA enzyme to have knowledge of how substituting various functional groups at different positions and having the scaffold changed affect their binding mode in NA enzyme. The introduction of substituents may improve the pharmacokinetic and pharmacodynamic properties of the molecule by virtue of imparting electronic and lipophilic characters [39].

The comprehensive analysis of molecular docking studies highlighted that the binding affinity of our designed molecules was confined to the 430-cavity similar to quercetin, which was considered as the standard for non-competitive inhibition, unlike SA and OMVC as shown in Fig. 3. In the series of aurones, the benzofuranone ring of all molecules occupied the hydrophobic cavity (W403, I427, P431, K432). Molecules

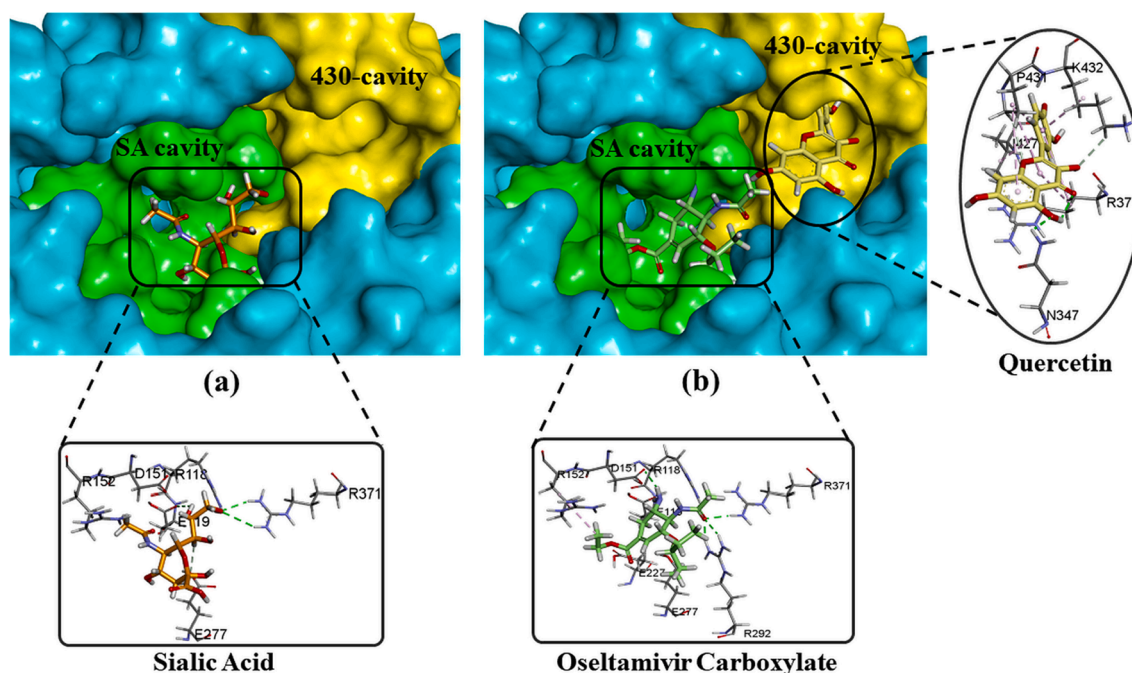


Fig.1. Docked poses of (a) sialic acid (orange colour) in SA cavity and (b) oseltamivir carboxylate (green colour) in SA cavity and quercetin (yellow colour) in 430-cavity of H1N1-NA enzyme. The SA cavity is represented in green colour and 430-cavity is represented in yellow colour in the surface model. The figure was prepared using Discovery Studio visualizer tool. (For interpretation of the references to colour in this figure legend, the reader is referred to the web version of this article.)

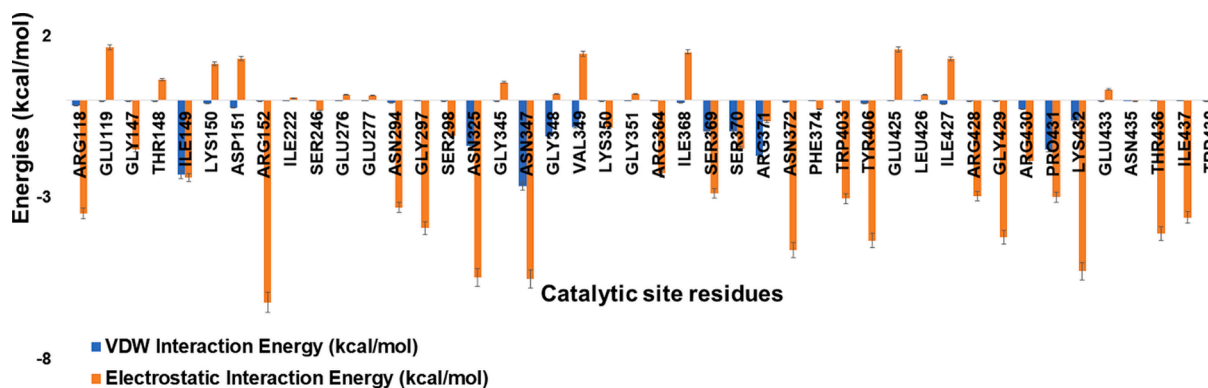


Fig.2. Histogram of interaction energies (van der Waal i.e., vdW and Electrostatic) of quercetin with the catalytic site residues.

1a-1c showed H-bonding with K432. **1d** showed H-bond interactions with R371 and N347; while **1e** had electrostatic interaction with W403 and salt bridge with D283. The docked conformations of 3-indolinone molecules **2a-2e**, **2g** and **2h** revealed that the 3-indolinone ring of these molecules had hydrophobic interactions with I427, P431 and K432 along with hydrogen bond and hydrophobic interactions with R371; while the phenyl ring interacted hydrophobically with P326. However, molecule **2f** had reverse orientation in which the phenyl ring showed hydrophobic interactions with I427, P431 and K432 along with interaction of its *m*-chloro group with R371 and W403; while the 3-indolinone ring had hydrogen bond and hydrophobic interaction with R371, which could be responsible for its higher activity. The molecules **3a**, **3c-3f**, **3h** and **3i** were docked such that commonly the 4-quinolone ring of these molecules had hydrophobic interactions with R371, I427, P431 and K432 along with hydrogen bond and hydrophobic interaction with R371; while phenyl ring showed interaction with N347. **3b** and **3g** were docked in a different orientation than others having their phenyl ring interacting hydrophobically with I427, P431 and K432 and with R371 as well showing hydrogen bond and hydrophobic interaction; while the 4-quinolone ring showed hydrogen bond interactions with R118 and I149.

The molecules **4a-4e** were docked with their phenyl ring interacting hydrophobically with I427, P431 and K432 along with hydrogen bond and hydrophobic interaction with R371. The piperazine ring of CAPI hybrid molecules had hydrogen bond interactions with N347 and S369. It is evident that additionally, all the designed molecules have either H-bonding or hydrophobic interaction with backbone and sidechain of R371. Detailed analysis of binding interactions of the molecules with NA enzyme is depicted in Table 1.

The observations from computational studies recommended that the molecules might bind tight to the NA enzyme attributed to their additional interactions, consequently leading to better anti-influenza activity.

The pharmacological activity and the performance of a drug candidate can be predicted to some extent by determining their ADME properties. Accurate prediction of *in vivo* pharmacological activity of a potential drug molecule is the ultimate aim of *in-silico* ADME studies [40]. Various descriptors were evaluated for ADME properties of candidate molecules. None of the designed molecules violated Lipinski's rule of five indicating towards their drug-likeness. All the molecules' molecular weight was in the range values of 130–725, donor HB

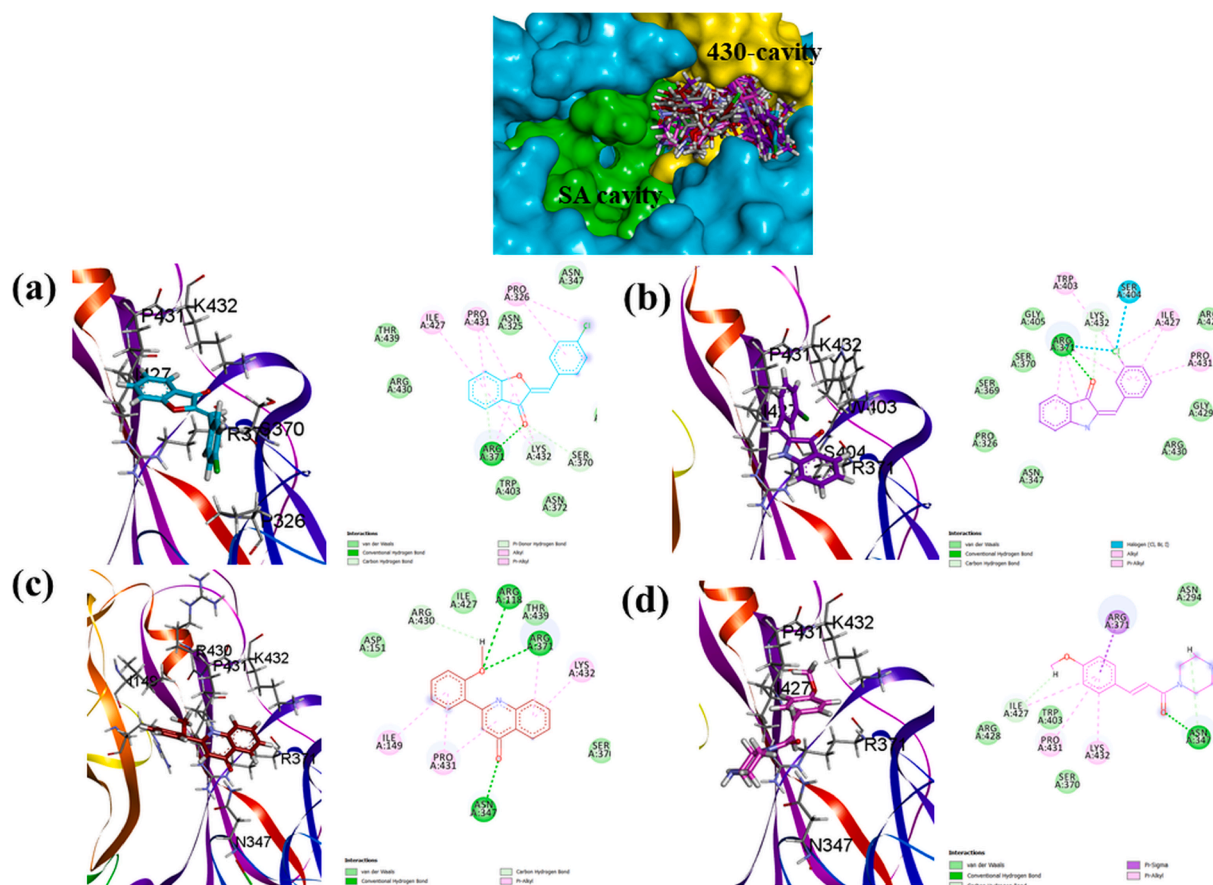


Fig. 3. Docked poses of designed molecules in 430-cavity (top) in surface model of H1N1-NA enzyme. 3D docking model and corresponding 2D schematic diagram of docking model of representative (a) aurone, (b) 3-indolinone, (c) 4-quinolone and (d) cinnamic acid-piperazine hybrid.

(hydrogen bond) and acceptor HB were in the range of 0–6 and 2–20 respectively. Solvent accessible surface area (SASA) is an indication of the partition coefficient and aqueous solubility which was found to be in the range of 300–1000 for all the designed molecules [41]. The bioavailability of a molecule is considerably determined by QPlogPo/w which was found to be favourable in the range of –2 to 6.5. The ionization potential parameter is indicative of distribution of molecule that affects the molecule's availability for further physical, chemical or biological reactions. The solute ionization potential (eV) was found to be in the range of 7.9–10.5 for all the molecules. It is indicated that the designed molecules possess favourable pharmacokinetic properties evident from the overall *in-silico* ADME results.

2.2. Chemistry

Based on the outcomes of computational studies of newly designed four scaffolds; with respect to their interactions with the enzyme, their binding poses and affinity; twenty-seven molecules corresponding to four scaffolds were synthesized *viz.* five aurones (1a–1e), eight 3-indolinones (2a–2h), nine 4-quinolones (3a–3i), and five CAPI hybrids (4a–4e). The target molecules were synthesized as shown in Scheme 1 and Scheme 2. The IR spectra demonstrated expected absorption bands for the functional groups of the synthesized molecules. All the aurone molecules showed cyclic C–O stretching near 1300 cm^{-1} . The absorption band for NH stretching in 3-indolinone molecules was observed near $3450\text{--}3100\text{ cm}^{-1}$, while that for 4-quinolones was observed near $3232\text{--}3080\text{ cm}^{-1}$ and that for CAPI hybrids was observed near 3130 cm^{-1} . The IR band for carbonyl C=O stretch in aurones and 3-indolinones was around 1650 cm^{-1} , while that in 4-quinolones was around 1715 cm^{-1} . Carbonyl C=O stretch for CAPI hybrids was observed near

$1640\text{--}1645\text{ cm}^{-1}$. The exocyclic C=C in aurones and 3-indolinones was characterized by a band near $1660\text{--}1667\text{ cm}^{-1}$, whereas the endocyclic C=C in 4-quinolones was near $1600\text{--}1620\text{ cm}^{-1}$. The C=C stretch in CAPI hybrids was around $1600\text{--}1615\text{ cm}^{-1}$. ^1H and ^{13}C NMR spectra of molecules represented predictable delta values for all aliphatic and aromatic protons and carbons, respectively. In ^1H NMR spectra of synthesized molecules, the vinylic proton of aurones and 3-indolinones (H-10) appeared in the range of $\delta\ 6.90\text{--}7.11$ and $\delta\ 6.63\text{--}7.20$, respectively as singlet, while the pyridone ring proton (H-3) in 4-quinolones showed chemical shift value in the range of $\delta\ 6.02\text{--}7.28$ as singlet. The downfield appearance of vinylic proton (H-10) of 3-indolinones is the characteristics of Z isomer. We interpret this to be due to the H-10 proton being deshielded by the neighbouring carbonyl at C-3 position [42–45]. The NH of 3-indolinones and 4-quinolones appeared downfield around $\delta\ 10\text{--}12$, while the piperazine NH appeared around $\delta\ 1.5\text{--}1.6$. The chemical shift value of vinylic carbon (C-10) of aurones were in the range of $\delta\ 108.38\text{--}113.76$ [46] represented in ^{13}C NMR which is the characteristics of thermodynamically more stable Z isomer. Mass spectra of representative synthesized molecules gave the predicted m/z peak corresponding to their estimated molecular weight. The HPLC purity of molecules was > 95%. Therefore, it was confirmed that the anticipated structures of the synthesized molecules are correct and are pure (Spectra in Supplementary data).

2.3. Anti-influenza evaluation

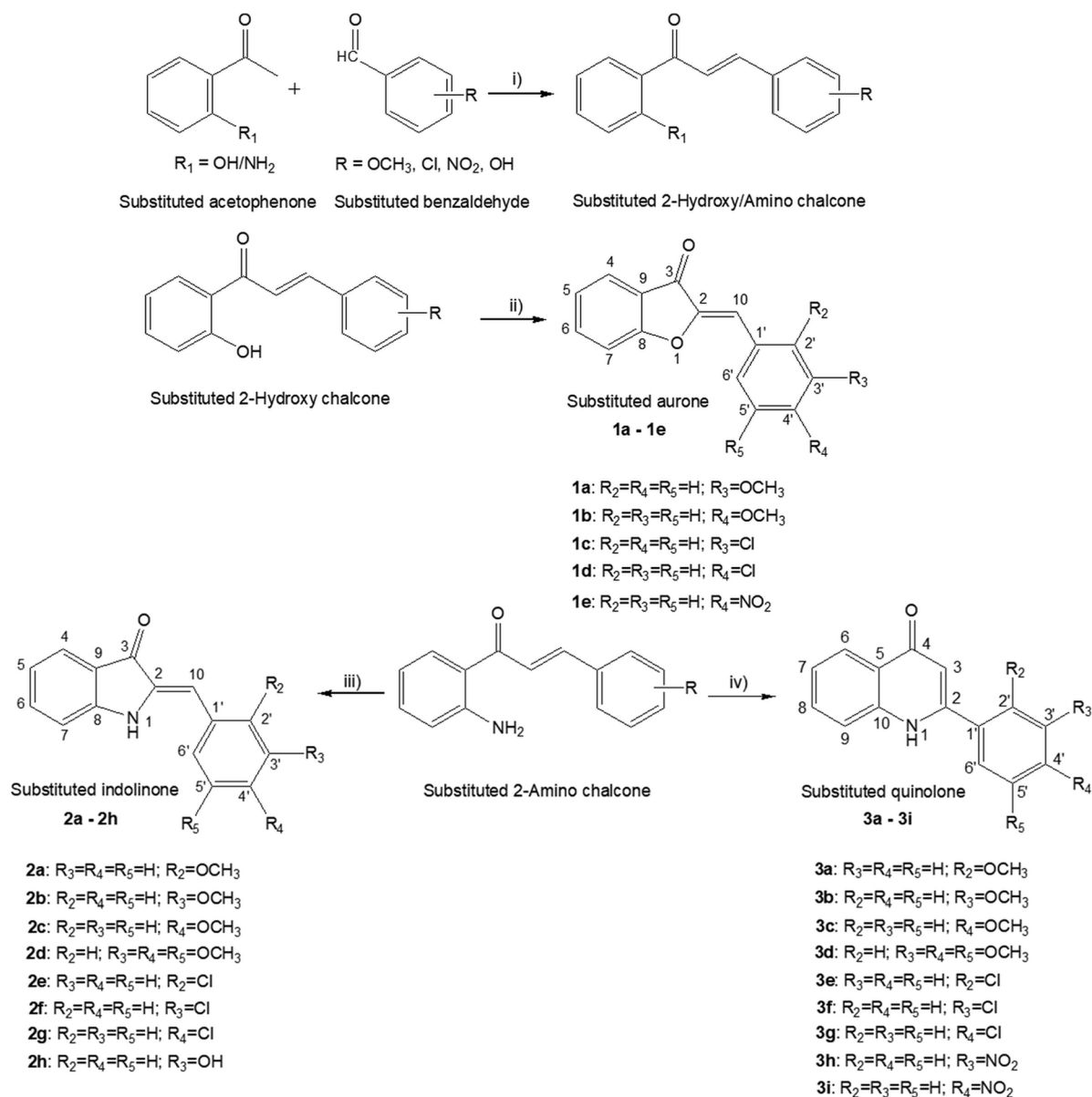
Oseltamivir phosphate (OMVP) was considered as standard for cellular assays, *viz.* MTT, CPE, HAI and CV assays, as the esterase enzyme present in cells convert it to its active metabolite i.e., oseltamivir carboxylate (OMVC) [47,48], while oseltamivir carboxylate was

Table 1

Detailed analysis of binding interactions of docked molecules with amino acid residues of H1N1-NA.

Residues	R118*	E119*	I149	D151*	R152*	R224*	R292*	P326	N347	S369	S370	R371*	W403	I427	R430	P431	K432	E433
Molecules																		
1a	H	–	–	–	–	–	–	–	H	–	–	H	–	–	–	–	H, π -a	–
1b	–	–	–	–	–	–	–	–	H	–	–	H	–	–	–	–	H	–
1c	H	–	–	–	–	–	–	–	H	–	–	H	π - π	–	–	–	H	–
1d	–	–	–	–	–	–	–	π -a (2)	H	–	–	H (2), π -a	–	π -a	–	π -a (2)	H, π -a (2)	–
1e	–	–	–	–	–	–	–	–	H	–	–	H	π -a, π - π	–	–	–	H	–
2a	H (2)	–	–	–	–	–	–	H (2), π -a	H	–	H	H, π -a (2)	–	π -a	–	π -a (2)	π -a (2)	–
2b	–	–	–	–	–	–	–	π -a	–	H	–	H, π -a, π - σ	–	π -a	–	π -a (2)	π -a (2)	–
2c	–	–	–	–	–	–	–	π -a	–	–	H	H, π -a, π - σ	–	π -a	–	π -a (2)	π - π , π -a (2)	–
2d	–	–	–	–	–	–	–	–	–	–	–	π -a, π - σ	–	π -a	–	π -a (3)	π -a (2)	–
2e	–	–	–	–	–	–	–	π -a (2)	–	–	H	H, π -a, π - σ (2)	–	π -a	–	π -a (2)	π -a (2)	–
2f	–	–	–	–	–	–	–	–	–	–	–	H, π -a (3), halogen	π -a	π -a (2)	–	π -a	H, π -a	–
2g	–	–	–	–	–	–	–	π -a (2)	H	–	–	H, π -a, π - σ	–	π -a	–	π -a (2)	H, π -a (2)	–
2h	–	–	–	–	–	–	–	π -a	–	–	H	H, π -a, π - σ	–	π -a	–	π -a (2)	π -a (2)	–
3a	H	–	π -a	–	–	–	–	–	H	–	–	H, π -a	–	–	H	π -a (2)	π -a	–
3b	H	–	–	–	–	–	–	–	–	–	H	H, π -a	–	π -a (2)	–	π -a (3)	H (2), π -a	–
3c	–	–	–	–	–	–	–	–	H	–	H	H, π -a, π - σ	–	π -a	–	π -a (2)	H, π -a (2)	–
3d	H	–	–	H	π -a	H, π -a	H	–	–	–	–	H	–	–	–	–	–	–
3e	–	–	–	–	–	–	–	–	π - π	–	H	H, π -a, π - σ (2)	–	π -a	–	π -a (3)	H, π -a (2)	–
3f	–	–	π -a	–	–	–	–	–	–	–	–	π -a	π -a	π -a (2)	H	π -a (2)	π -a (2)	–
3g	H	–	π -a	–	–	–	–	–	–	–	–	π -a, π - σ	π -a	π -a	–	π -a (3)	H, π -a	–
3h	–	–	–	–	–	–	H	–	H	–	H	H (2), π -a, π - σ	–	π -a	–	π -a (2)	H, π -a (2)	–
3i	–	–	–	–	–	–	–	π - σ	H	–	–	H, π -a, π - σ	–	π -a (2)	–	π -a (2)	π -a (2)	–
4a	–	–	–	–	–	–	–	–	–	–	H	H, π - σ	–	π - σ	–	π - σ	π - σ	–
4b	–	–	–	–	–	–	–	–	H (2)	–	–	H, π -a	–	π -a	H	π -a	π -a	–
4c	–	–	–	–	–	–	–	–	H (2)	–	–	π - σ	–	H, π -a	–	π -a	π -a	–
4d	–	–	–	H	–	–	–	–	–	–	–	H, π -a, π - σ	H	H, π -a	–	π -a	π -a	–
4e	–	–	–	–	–	–	–	–	–	H (2)	–	π -a	π -a	π -a	–	π -a	π -a (2)	Halogen

H: Hydrogen bond; π - π : pi- pi interaction (hydrophobic); π -a: pi-alkyl interaction (hydrophobic); π - σ : pi-sigma interaction (hydrophobic); *Catalytic site residues interacting with SA. Figures in brackets indicate number of bonds.



Scheme 1. Synthesis of aurone (**1a-1e**) from 2-hydroxychalcone; 3-indolinone (**2a-2h**) and 4-quinolone (**3a-3i**) from 2-aminochalcone. Reagents and conditions used: (i) 20% NaOH, absolute ethanol, 10 °C, 4–5 h; (ii) Hg(OAc)₂, pyridine, 110 °C, 1–2 h; (iii) acetic acid, 10% w/w Amberlyst-15, 80 °C, 2–5 h; (iv) DMSO, iodine crystal, reflux, 30 min.

directly used as standard for enzymatic assays viz. NA inhibition assay and enzyme kinetics studies. **OMVP/OMVC** and quercetin (**QR**, the reported natural non-competitive inhibitor[37]) were used as standards for representing the competitive and non-competitive inhibition, respectively.

2.3.1. Cytotoxicity studies of all the synthesized molecules

Cytotoxicity studies determined the concentration of synthesized molecules responsible for 50% reduction in cell viability (CC₅₀). The results of MTT-Formazan assay for cytotoxicity study of twenty-seven synthesized molecules indicated that they had no serious effect on MDCK cells except for molecule **4d** having CC₅₀ of 40 μM (Table 2). The anti-influenza activity of these non-cytotoxic molecules was further evaluated for decrease in cytopathic effect (CPE) of influenza A/H1N1pdm09 strain in MDCK cells in presence of the molecules.

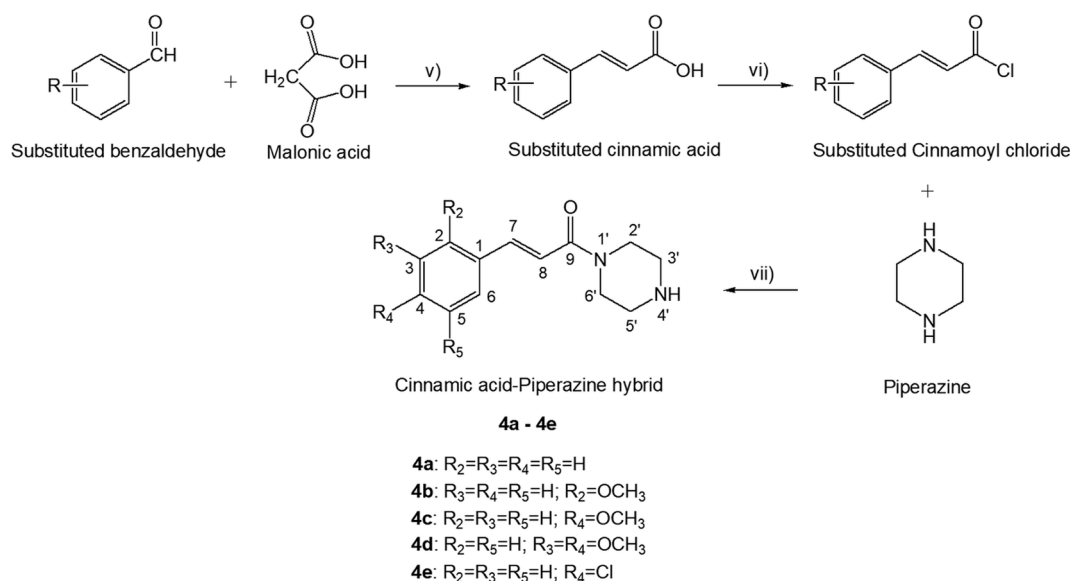
2.3.2. Cytopathic effect (CPE) inhibition of all the molecules

CPE inhibition assay of all twenty-seven synthesized molecules was

carried out as qualitative evaluation study to assess the degree of viral inhibitory activity of the molecules after comparison with **OMVP** as standard drug. Interestingly, CPEs in the form of loss of cell adhesion that is the characteristics of influenza A/H1N1pdm09 virus infection were found to be considerably reduced in our synthesized molecule-treated infected cells, further asserting a robust cyto-protective and anti-influenza property of these molecules. The degree of inhibition of viral CPE by all the evaluated molecules is depicted in [supplementary table, Table S1](#). All the molecules showed at least 50% CPE inhibition suggestive of the substantial ability of molecules to reduce the viral load. Subsequently, they were carried forward for further assays.

2.3.3. Hemagglutination inhibition (HAI) to determine viral titer reduction by molecules

The CPE inhibition was further assessed by comparing the HA titer of virus in virus control well with the HA titer of virus in molecule-treated wells. Relative viral load viz. the HA titer of molecule-treated infected cells was represented as ‘% HA titer reduction’ considering the



Scheme 2. Synthesis of cinnamic acid-piperazine hybrid (**4a-4e**). Reagents and conditions: (v) pyridine/piperidine, 100 °C, 2 h; (vi) DCM, thionyl chloride, DMF, reflux, 24 h; (vii) DCM, TEA, 0 °C till reaction completed monitored by TLC.

infectivity, in terms of HA titer, of the vehicle-treated infected control as 100% in each replicate of triplicate experiments. OMVP and QR were used as standards, and %HA viral titer reduction data for all the molecules are summarized in Table 3. As evident from data, most of the molecules caused robust and persistent reduction in the viral titer at least by 50%, as shown in Fig. 4. The results of HAI assay illustrated that our molecules efficiently suppress the viral titer showing weak-to-moderate-to-high potencies compared to standards (OMVP = $85 \pm 4\%$ and QR = $79 \pm 4\%$, at 100 μM) further directing towards the anti-influenza activity of the molecules. The structure–activity relationship was tough to draw, attributed to the vague outline between these molecules and reduction rates of %HA titer. Next, the molecules were carried further for quantitative evaluation of their anti-influenza activity.

2.3.4. Cell-based crystal violet (CV) assay to quantify the effective concentration of molecules

CV assay determined quantitatively the effective concentration of tested molecules that resulted in 50% cell survival (EC_{50}). Consistent with the marked attenuated viral HA titer, the tested molecules notably showed significant degrees of cell survival in CV assay (Table 2). Molecules **2f** (3-indolinone with *m*-chloro group on benzyl ring), **2g** (3-indolinone with *p*-chloro group on benzyl ring) and **3a** (4-quinolone with *o*-methoxy group on phenyl ring) having EC_{50} of 4.0 ± 0.1 nM, 6.7 ± 0.1 nM and 4.9 ± 0.1 nM, respectively, had highest activity with their EC_{50} values better than commercial drug i.e., OMVP ($EC_{50} = 12.7 \pm 0.3$ nM) as well as QR ($EC_{50} = 0.56 \pm 0.01$ μM). Molecules **1d** (aurone with *p*-chloro group on benzyl ring) and **2b** (3-indolinone with *m*-methoxy group on benzyl ring) with $EC_{50} = 39 \pm 2$ nM and 25 ± 1 nM, respectively, however were slightly less active than OMVP, but better than QR, still could be believed to have remarkable anti-influenza property. The effects of representative potent molecules along with standards on % cell survival infected with pdmH1N1 virus are shown in Fig. 5. These results suggested that these molecules could hamper overall replication of virus in MDCK cells. The high selectivity index values of these compounds indicated that they decreased the virus replication without adverse effect on the living host cells.

2.3.5. Enzyme-based NA inhibition to determine inhibitory concentration of molecules

H1N1-NA inhibition by twenty-five molecules, based on CV assay, was determined by calculating the concentration required to inhibit

50% of the enzyme activity (IC_{50}). Dose response curves depicting the effect of our molecules on H1N1-NA enzyme are shown in Fig. 6.

The IC_{50} values of the evaluated molecules ranged from 0.52 ± 0.01 μM to 24.6 ± 1.3 μM . OMVC and QR, the standards chosen in enzyme-based assay, has IC_{50} value of 1.9 ± 0.1 nM and 8.7 ± 0.1 μM , respectively (Table 2). Though the potent molecules discussed in CV assay had their IC_{50} values lower than OMVC, they certainly tend to exhibit excellent activity with their IC_{50} values at low-micromolar level, intriguingly, better than QR. The trend of efficacy of molecules seen in CV assay is followed in NA inhibition assay as well, the potent molecules **2f** ($IC_{50} = 0.52 \pm 0.01$ μM), **2g** ($IC_{50} = 3.5 \pm 0.1$ μM) and **3a** ($IC_{50} = 1.3 \pm 0.2$ μM) possessed lowest IC_{50} values than other molecules of the series. Interestingly, the combined results of CV assay and NA inhibition studies suggested that the evaluated molecules suppress overall viral replication than inhibiting the NA enzyme *per se*. These results pointed towards the fact that there might be an accompanying mechanism by which our evaluated molecules control virus replication indicated by their potency *in vitro*.

2.3.6. Enzyme kinetics studies to ascertain mechanism of inhibition of molecules

Enzyme kinetics study was performed on eleven most active molecules (based on CV and NA inhibition assay) to validate the non-competitive inhibition of designed molecules as exhibited by docking studies. In this study, OMVC and QR were used as standards for competitive and non-competitive inhibition, respectively. Unsurprisingly, OMVC being structurally similar and transition state analogue of SA, showed competitive inhibition evident from the plots exhibited in Fig. 7 which shows Lineweaver-Burk plot of $1/V$ versus $1/[S]$. The plots were obtained by considering absence of inhibitor molecule (i.e., at 0 nM concentration) and at two concentrations bracketing the IC_{50} value of the inhibitor molecule. Increasing concentrations of OMVC ($K_i = 2.8 \times 10^{-4}$ μM) resulted in collection of lines with increased K_m while the V_{max} remained unaffected i.e., they have equivalent y-axis intercept but with higher value of x-axis intercept. This indicated its competitive inhibition. However, increasing concentrations of QR ($K_i = 5.1$ μM) resulted in collections of lines wherein the K_m remained unaffected while V_{max} showed reduction i.e., they have equivalent x-axis intercepts along with increase in the y-axis intercept values. This demonstrated its anticipated non-competitive inhibition as reported in literature.

Interestingly, in case of our evaluated molecules, the Lineweaver-

Table 2*In-vitro* evaluation of tested molecules.

Sr. No.	Molecules	CC ₅₀ (μM)	EC ₅₀ (μM)	SI	IC ₅₀ (μM)	Ki (μM)
1	1a	193 ± 1	>100	–	Not tested	Not tested
2	1b	171 ± 1	1.5 ± 0.9	117	9.3 ± 0.1	10.5 ± 0.7
3	1c	120 ± 1	1.0 ± 0.1	118	14.9 ± 1.2	Not tested
4	1d	113 ± 1	(39 ± 2) × 10 ³	2.9 × 10 ³	1.8 ± 0.1	11.2 ± 2.8
5	1e	111 ± 1	>100	–	Not tested	Not tested
6	2a	263 ± 1	5.1 ± 0.9	52	20.9 ± 1.3	Not tested
7	2b	292 ± 1	(25 ± 1) × 10 ³	1.2 × 10 ⁴	22.4 ± 1.3	2.6 ± 0.1
8	2c	287 ± 1	11.9 ± 1.3	24	10.5 ± 1.2	Not tested
9	2d	128 ± 1	0.17 ± 0.05	752	19.8 ± 1.3	Not tested
10	2e	269 ± 1	3.1 ± 0.1	88	19.4 ± 1.2	Not tested
11	2f	272 ± 1	(4.0 ± 0.1) × 10 ³	6.8 × 10 ⁴	0.52 ± 0.01	2.8 ± 0.2
12	2g	192 ± 1	(6.7 ± 0.1) × 10 ³	2.8 × 10 ⁴	3.5 ± 0.1	2.0 ± 0.003
13	2h	115 ± 1	0.25 ± 0.01	462	15.7 ± 1.2	33.7 ± 2.3
14	3a	286 ± 1	(4.9 ± 0.1) × 10 ³	5.8 × 10 ⁴	1.3 ± 0.2	2.1 ± 0.2
15	3b	235 ± 1	>100	–	24.3 ± 1.3	Not tested
16	3c	277 ± 1	>100	–	3.8 ± 0.1	53.6 ± 9
17	3d	200 ± 1	>100	–	12.2 ± 1	2.8 ± 1
18	3e	181 ± 1	>100	–	18.4 ± 1.2	Not tested
19	3f	163 ± 1	>100	–	16.9 ± 1.4	Not tested
20	3g	163 ± 1	0.22 ± 0.01	742	8.7 ± 0.1	7.1 ± 0.2
21	3h	117 ± 1	78 ± 1	2	6.4 ± 0.1	8.4 ± 0.1
22	3i	118 ± 1	>100	–	16.7 ± 1.2	Not tested
23	4a	155 ± 1	3.6 ± 0.2	43	15 ± 2	Not tested
24	4b	106 ± 1	5.1 ± 0.1	21	24.6 ± 1.3	Not tested
25	4c	137 ± 1	7.8 ± 0.1	18	18.4 ± 1.2	Not tested
26	4d	40 ± 1	>100	–	12 ± 2	Not tested
27	4e	189 ± 1	6.7 ± 0.9	28	11.2 ± 1.7	Not tested
28	QR	254 ± 1	0.56 ± 0.01	453	8.72 ± 0.1	5.1 ± 0.1
29	OMV	713 ± 1	(12.7 ± 0.3) × 10 ³	5.6 × 10 ⁴	(1.9 ± 0.1) × 10 ³	(2.8 ± 0.3) × 10 ⁴

MTT assay and crystal violet experiments performed in triplicates to give CC₅₀ and EC₅₀ values respectively, NA-inhibition and enzyme kinetics experiments performed in duplicates to give IC₅₀ and Ki values respectively; CC₅₀ (mean ± std dev) values represent the concentration of molecules that showed 50% cytotoxicity; EC₅₀ (mean ± std dev) values represent the concentration that resulted in 50% cell survival after infection in presence of inhibitor; SI = Selectivity Index was generated by the ratio of CC₅₀ and EC₅₀; IC₅₀ (mean ± std dev) values of molecules represent the concentration that caused 50% enzyme activity loss; Ki represents the enzyme inhibitor constant.

Burk plot of 1/V versus 1/[S] resulted in group of lines as observed in **QR**, signifying their mechanism of enzyme inhibition to be non-competitive. Fig. 7 displays the plot for the representative potent molecules.

Table 3

Reductions of %HA titer of pdmH1N1 virus by aurone (**1a–1e**), 3-indolinone (**2a–2h**), 4-quinolone (**3a–3i**), CAPI hybrids (**4a–4e**); and standard competitive and non-competitive inhibitors oseltamivir phosphate and quercetin, respectively.

Molecules	HA titer Reduction (%) ^a	Molecules	HA titer Reduction (%) ^a
1a	31 ± 2%	3c	17 ± 1%
1b	82 ± 5%	3d	20 ± 2%
1c	64 ± 3%	3e	19 ± 2%
1d	81 ± 4%	3f	30 ± 3%
1e	12 ± 2%	3g	82 ± 5%
2a	75 ± 4%	3h	20 ± 2%
2b	70 ± 3%	3i	54 ± 2%
2c	70 ± 3%	4a	52 ± 2%
2d	60 ± 2%	4b	58 ± 3%
2e	63 ± 4%	4c	41 ± 2%
2f	89 ± 4%	4d	54 ± 2%
2g	65 ± 3%	4e	42 ± 3%
2h	72 ± 4%	OMVP	85 ± 4%
3a	84 ± 4%	QR	79 ± 4%
3b	50 ± 2%		

^a Reduction of %HA titer of pdmH1N1 virus (mean ± std dev of three experiments) in presence of 100 μM of inhibitors, measured by hemagglutination inhibition assay.

2.4. Induced fit docking (IFD)

IFD is an accurate and robust docking technique that takes into account the ligand and protein flexibility. Validation of IFD process was done by superimposing the docked oseltamivir structure over the oseltamivir obtained from crystal structure of NA enzyme (PDB 3TI6). RMSD value for all the heavy atoms was obtained as 0.17 Å. Furthermore, the receptor binding of oseltamivir was found similar to that in the crystal structure. The interactions formed by both crystal structure and docked oseltamivir are: amide functional group of oseltamivir forming H-bond with R152; amino group forming salt bridges with E119, D151 and E277 and H-bond with E119 and E227; carboxylate moiety forming H-bonds with R118, R292 and R371 as shown in Fig. 1b (*vide supra*). IFD was executed on five most potent molecules to have an insight towards the accurate binding of these molecules when the enzyme is in its optimal conformation. IFD scores were found to be consistent with experimental CV assay results as shown in Table 4.

2.5. Structure-activity relationship (SAR)

All the designed scaffolds fitted well in the 430-cavity which was believed to be the alternate binding region within the catalytic active site. However, the scaffolds exhibited varied degree of anti-influenza activity. The prototype scaffold selected i.e., chalcone, having uncyclized α, β-unsaturated carbonyl system, showed weaker anti-influenza activity as evident from literature. Comprehensive examination of the anti-influenza evaluation of our designed scaffolds suggested that cyclization of chalcone not only reduced cytotoxicity but also caused the improvement in activity. It was observed that 5-exo cyclocondensation of 2-amino chalcone to yield 3-indolinone enhanced the activity than 6-endo cyclocondensation to yield 4-quinolone. 3-indolinones were found to be even more active than the oxidative cyclized product of 2-hydroxy chalcone viz. aurone. Thus, it can be said that the isosteric replacement of nitrogen in 3-indolinone to oxygen in aurone reduced the activity. Incorporation/presence of phenyl rings provides hydrophobic sites for interaction between inhibitor molecule and the enzyme. The higher activity of 3-indolinones, 4-quinolones and aurones may be attributed to the presence of another phenyl ring that imparted more hydrophobicity to the molecules indicating towards their prominent interactions with the hydrophobic 430-cavity in docking studies. At the same time, when cinnamic acid (scaffold similar to chalcone having α, β-unsaturated carbonyl system) was linked to piperazine moiety, it improved the activity than cinnamic acid itself. This may be attributed to decrease in the

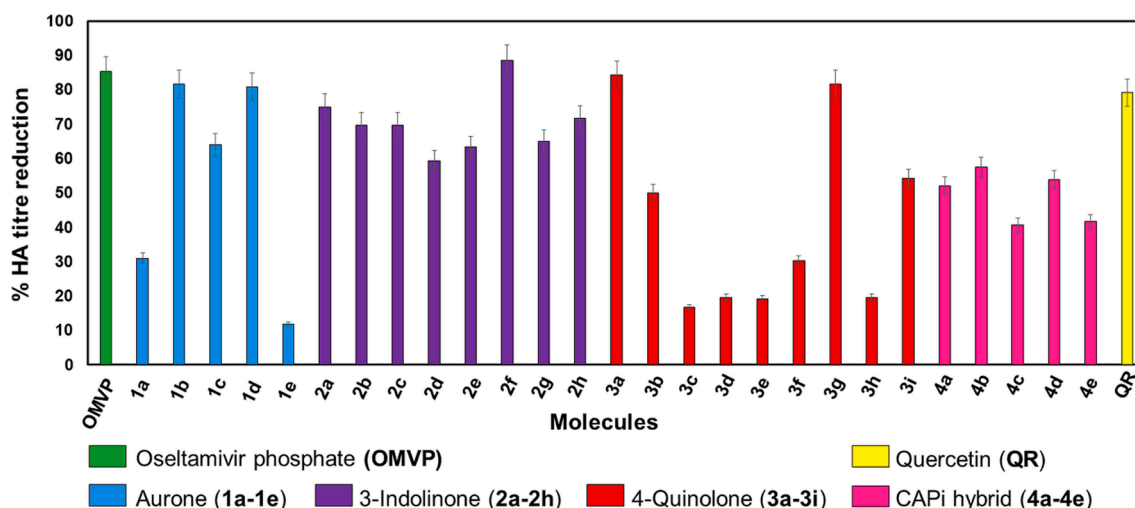


Fig. 4. Histogram of % HA titer reduction of virus treated with candidate molecules showing the effect of oseltamivir phosphate (OMVP, green colour), quercetin (QR, yellow colour) and evaluated molecules on pdmH1N1 virus yield. (For interpretation of the references to colour in this figure legend, the reader is referred to the web version of this article.)

acidity of the molecule. The scaffolds were designed by substitution of various electron-withdrawing and electron-donating groups. Among tested molecules, substituting the benzyl ring with chloro group enhanced activity, out of which *meta* and *para* substituted chloro group containing 3-indolinones, **2f** and **2g** respectively, showed potency better than oseltamivir. While for 4-quinolones, electron-donating methoxy group at *ortho* position (**3a**) showed better activity than oseltamivir.

Hence, it can be said that for 5-exo cyclocondensation of chalcones, chloro group substitution at benzyl ring enhanced the activity while for 6-endo cyclocondensation, methoxy group substitution at phenyl ring showed better activity than the standard drug. Overall SAR studies pointed towards a better understanding of effect of presence of phenyl ring at 1–2 carbon lengths, 5-exo cyclocondensation, chloro substitution along with decreased acidity of the designed molecules towards their anti-influenza activity against influenza A/H1N1pdm09 virus.

Interesting to note here is that the active site of NA comprises of 430-cavity where our designed molecules bound. This binding region is distinctly different from oseltamivir and sialic acid binding site. Therefore, the molecules displayed non-competitive nature of inhibition. Since, this binding region of the molecules is adjacent to catalytic site and is present within the same active site, these molecules could correspondingly be called “mutually non-competitive” agents.

3. Conclusion

In current backdrop of COVID pandemic, our research is focused on another pandemic virus viz. swine flu – pandemic H1N1, which created havoc in 2009. Although, the current floating strains are not virulent and vaccine is available for its defense but the lesson learnt from COVID crisis is not to underestimate the strength of the virus. The impulsiveness of a potential influenza A pandemic outbreak and rapid unpredictable emergence of influenza A virus resistance to current anti-influenza drugs are urging the researchers and scientists to come up with newer strategies to overcome resistance and develop better options in terms of treatment than what current drugs can offer us. Based on the results obtained in the present study, we can say that subset of the drug molecules showed substantial antiviral activity against influenza A/H1N1pdm09 virus. Computational studies identified the molecules as binders of 430-cavity, an alternate binding region within the active site, similar to quercetin which was the standard for non-competitive inhibition, but distinct from OMV in SA binding site which was the standard for competitive inhibition. The non-cytotoxic molecules efficiently reduced the viral titer and remarkably restricted viral replication more

actively than inhibiting the NA enzyme alone. Among the tested molecules, **2f**, **2g** and **3a** were found to be most potent anti-influenza agents having low-nanomolar EC_{50} values 4.02 nM, 6.72 nM and 4.96 nM, respectively, that were better compared to reference competitive and non-competitive inhibitors: oseltamivir (EC_{50} = 12.7 nM) and quercetin (EC_{50} = 0.56 μ M). **2f**, **2g** and **3a** also exhibited good NA inhibitory activity in sub-micromolar range (IC_{50} = 0.52 μ M, 3.46 μ M, 1.31 μ M respectively). In addition, enzyme kinetics studies suggested that the mechanism of inhibition of our designed molecules is non-competitive that was highlighted by *in-silico* studies as well wherein the molecules bound to the alternate binding site. Owing to the fact that current commercial drugs work like charm in wild-type influenza, the potent molecules of present study can therefore be certainly used as an adjunct therapy in combination with oseltamivir or zanamivir for improved antiviral efficiency. This further strengthens our idea of developing potential anti-influenza agents in future which can be used as an alternative in wake of oseltamivir resistance owing to their non-competitive inhibition mechanism.

Thus, it can be concluded that the current work has generated few potential anti-influenza molecules especially for influenza A/H1N1pdm09 strain. The approach used here is completely different than the currently available marketed drugs. The potent molecules can be subsequently developed to be used either alone or in combination with current NA inhibitors for better management and eradication of influenza virus.

4. Experimental section

4.1. Materials

The chemicals, reagents and catalyst Amberlyst-15 employed for synthesis were purchased from SD Fine chem Ltd. and Sigma Aldrich Chemicals Pvt Ltd. All the solvents used for synthesis were of LR grade. Oseltamivir phosphate (OMVP) was obtained as a gift sample from Cipla Ltd, India. Oseltamivir carboxylate (OMVC) and quercetin (QR) was purchased from Clearysynth Labs, Ltd and Sigma Aldrich Chemicals Pvt Ltd, respectively. The strain of A(H1N1)pdm09 virus Kolkata isolate [A/human/India/Kol-7251/2018(H1N1); accession number: MN508979] was obtained from ICMR-National Institute of Cholera and Enteric Diseases (ICMR-NICED), Kolkata, India. Madin-Darby Canine Kidney (MDCK) cells were obtained from National Institute of Virology (NIV), Pune, India.

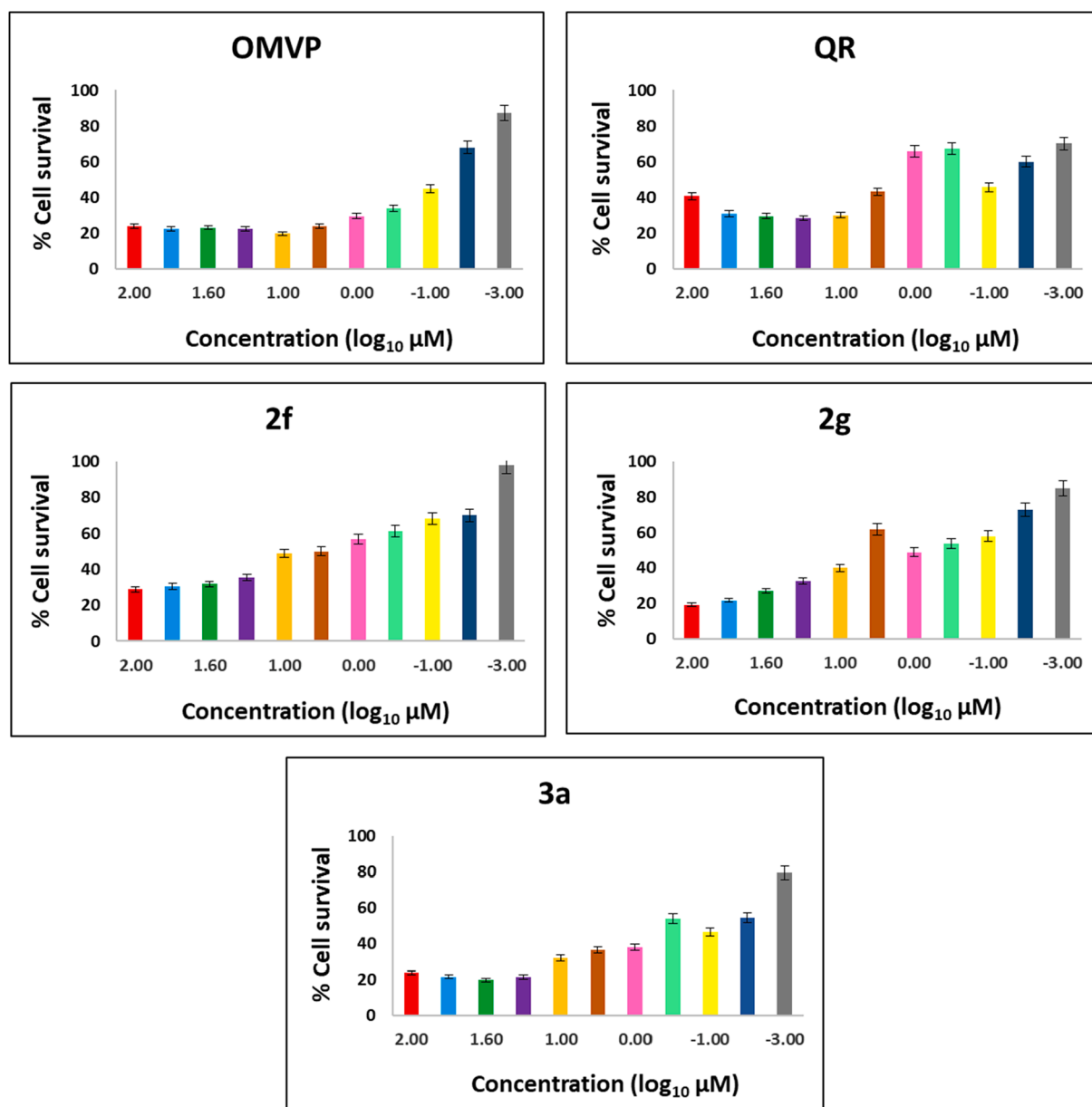


Fig.5. Effects of oseltamivir phosphate (OMVP), quercetin (QR) and representative potent molecules 2f, 2g and 3a on % cell survival infected with H1N1 virus.

4.2. Methods

4.2.1. Modelling and system preparation for modelling

The X-ray crystal structure of OMV-complexed pandemic H1N1-NA enzyme was imported from RCSB protein data bank (PDB ID: 3TI6), with a resolution of 1.69 Å [32]. Since NA is a homotetramer, monomer unit of the enzyme (3TI6) was considered for docking calculations in computational studies. Protein Preparation Wizard module of Maestro 11.5, Schrödinger LLC, New York, USA [49] was employed to optimize the geometry of the enzyme. The crystallographic waters were removed, hydrogen atoms were added to the enzyme structure consistent with a pH of 6.5, which is the optimum pH for NA enzymatic activity [50]. N- and C-termini were capped. Ca^{2+} is reported to be crucial for enzyme activity and stability, therefore, two Ca^{2+} ions were retained: one whose binding site is close to the active site which helps in holding the active site in appropriate conformation for substrate binding; while the other whose binding site was found in 1918 N1 and 2009 swine-origin N1 structures [50,51]. The terminal rotamer states were set automatically for Asn, Gln and His, as well as tautomeric and protonation states of His

to optimize the hydrogen-bonding network in the complex using ProTAssign program in Maestro. Minimization was implemented using OPLS3e forcefield.

SiteMap [36,52] tool was applied to explore the potential binding sites and characterize them. Different molecules were designed with introducing substituents with varied functional groups attributing electronic, steric and volume effect to the scaffolds. All the designed molecules were built using the 2D sketcher available with Maestro 11.5 (Schrödinger LLC NY 2016) and their geometries were optimised using LigPrep v3 module [53] with OPLS3e forcefield and docked in the putative binding sites using Glide XP [35,54]. Best docking scores were for the molecules showing binding in the 430-cavity of influenza A/H1N1pdm09-NA enzyme than other putative binding pockets. Additionally, induced fit docking (IFD) [55] of the best molecules was executed in this binding pocket since the receptor may not be in an optimal conformation to bind the inhibitor molecules. The validation of docking protocol was done by replicating the binding pose and interactions of co-crystallized ligand i.e., oseltamivir in the X-ray crystal structure.

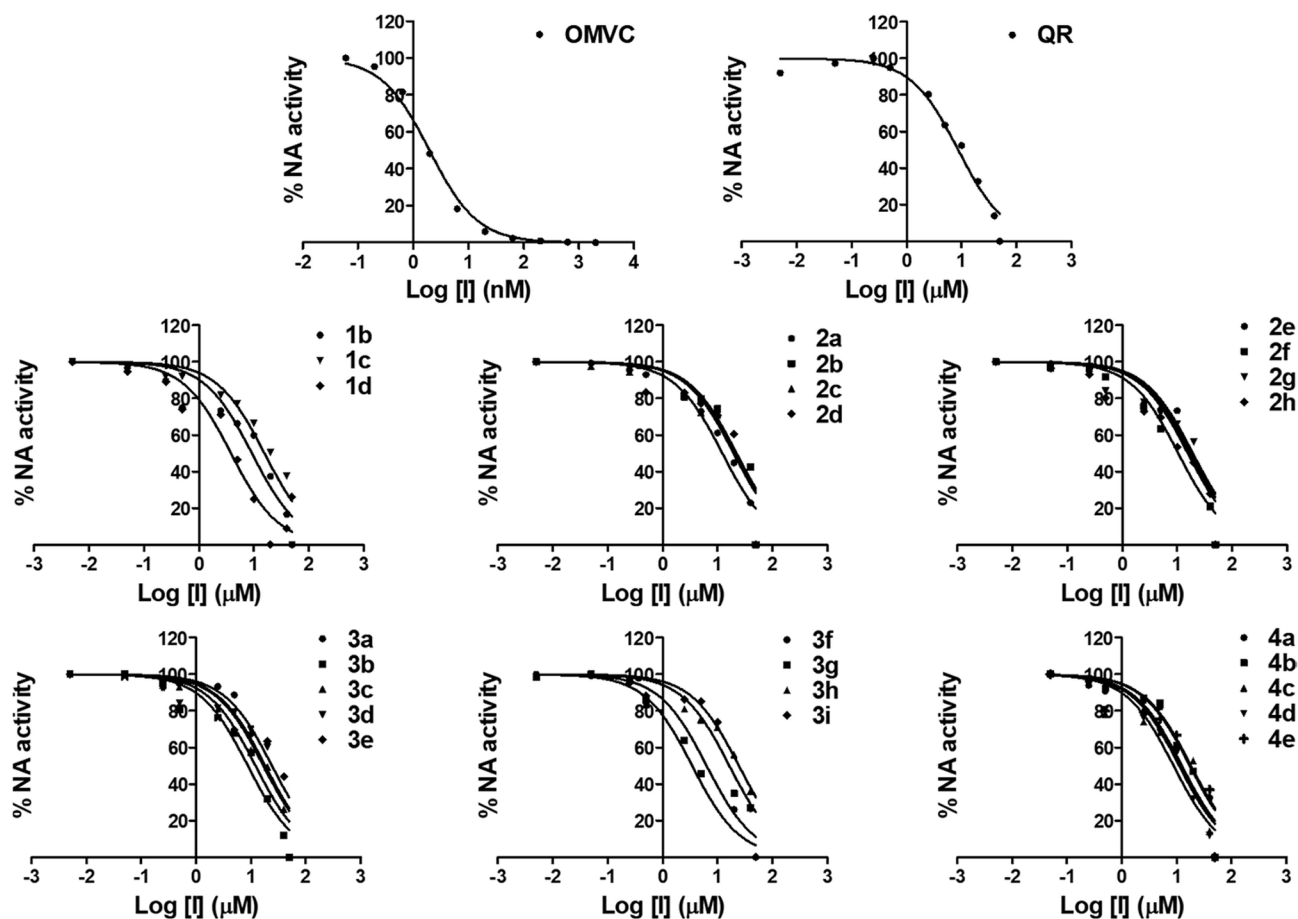


Fig.6. Effects of oseltamivir carboxylate (OMVC), quercetin (QR) and evaluated molecules on H1N1-NA for the hydrolysis of substrate.

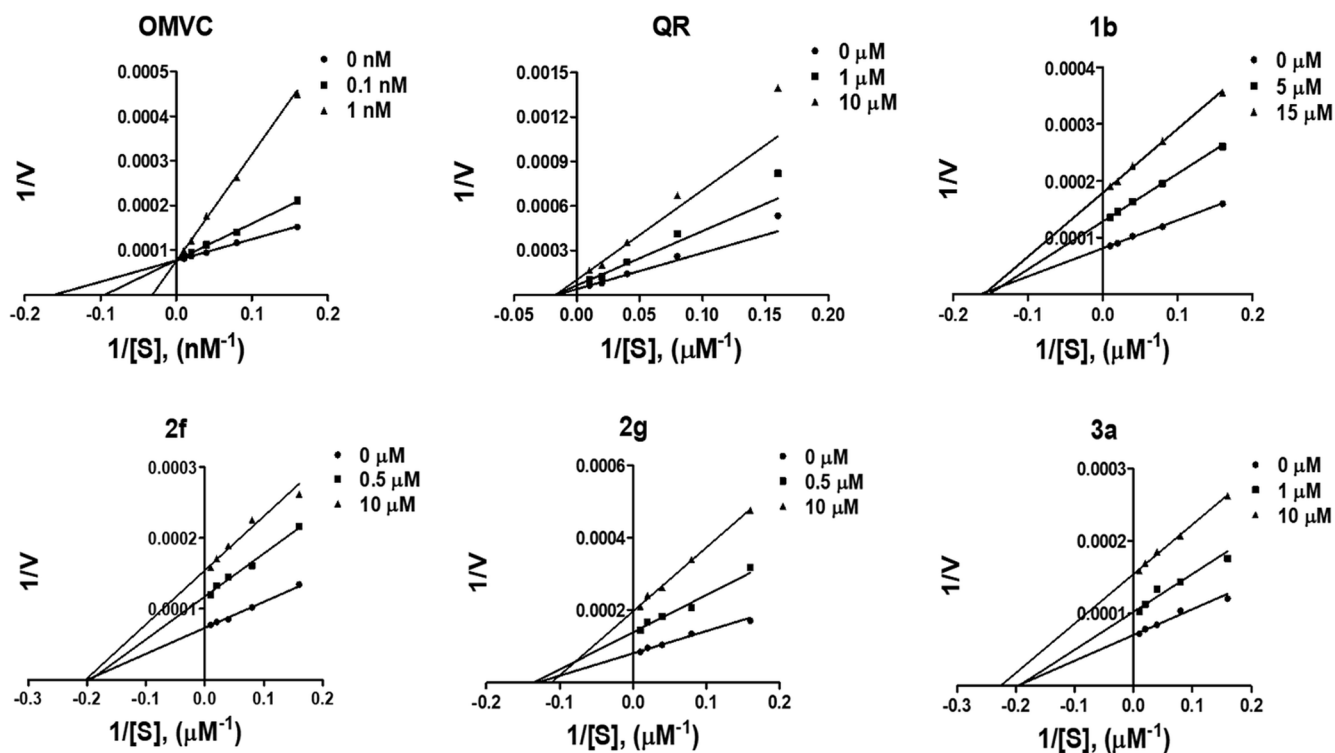


Fig.7. Lineweaver–Burk plots for the inhibition of oseltamivir carboxylate (OMVC), quercetin (QR) and representative evaluated molecules on H1N1-NA for the hydrolysis of substrate in the presence of increasing concentrations of tested molecules (two conc. bracketing IC_{50}) for lines from bottom to top.

Table 4IFD scores, EC₅₀ and IC₅₀ values of potent inhibitor molecules.

Molecules	EC ₅₀ (μM)	IC ₅₀ (μM)	IFD scores
2f	(4.0 ± 0.1) × 10 ³	0.52 ± 0.01	−861.6
2g	(6.7 ± 0.1) × 10 ³	3.5 ± 0.1	−858.9
3a	(4.9 ± 0.1) × 10 ³	1.3 ± 0.2	−860.5
QR	0.56 ± 0.01	8.7 ± 0.1	−857.7
OMV	(12.7 ± 0.3) × 10 ³	(1.9 ± 0.1) × 10 ³	−858.0

The physicochemical properties, viz. absorption, distribution, metabolism and elimination (ADME), of the designed molecules were predicted *in-silico* by QikProp 3.3 (Schrödinger LLC, New York, USA) [56]. The out file of LigPrep, employed to optimize the designed molecules, was employed as the input for QikProp to predict the molecular descriptors as well as properties of the molecules that are physically significant and pharmaceutically relevant. Comparison between properties of the designed molecules with those of 95% of overall known drugs was done using the range values of each molecular descriptor provided by QikProp.

4.2.2. Chemistry

The starting materials and solvents utilized for synthesis were assessed for their purity by determining their physical constants (viz. melting and boiling point) and by thin-layer chromatography (TLC) on Merck silica gel F₂₅₄ plates. We report here the synthesis of four scaffolds namely aurones, 3-indolinones, 4-quinolones and CAPI hybrids (Scheme 1 and Scheme 2). Synthesis was carried out in Carousel 6-reaction station parallel synthesizer by Radleys. TLC was employed to monitor the synthetic reaction progress. Physical constants (melting point) of the reaction products were determined by Analab melting point apparatus μThermoCal10. Infrared spectroscopy (IR), ¹H NMR and ¹³C NMR were employed for structural characterization of the synthesized molecules. Mass spectra (MS) and HPLC purity of the synthesized molecules were measured as well. IR experiments were recorded on an inhouse Bruker Alpha-T spectrometer with 44 scans, and data were processed by OPUS software. NMR experiments were recorded on 800 MHz Bruker Avance spectrometer and 600 MHz Varian spectrometer using DMSO-*d*₆ and CDCl₃ solvent, and the data were processed using Bruker Topspin 2.1 and Varian software. 64 scans were recorded for 1D proton NMR (in 600 MHz NMR spectrometer), while for carbon NMR, 2064 scans (in 150 MHz NMR spectrometer) and 500 scans (in 200 MHz NMR spectrometer) were recorded. LC-MS/MS were recorded on Water make Mass Spectrometry LCMS: water alliance quadrupole mass. HPLC was performed on Agilent 1200 series HPLC system.

4.2.2.1. General procedure for synthesis of aurones (1a–1e). 2-Hydroxychalcones were primarily synthesized followed by their oxidative cyclization to obtain aurones (Scheme 1). 2-Hydroxychalcones and mercuric acetate [Hg(OAc)₂] were dissolved in pyridine (15–20 mL) in equimolar (0.002 mol) quantities at 27 °C. The reaction mixture was kept on stirring at 110 °C for 1–2 h. Completion of reaction was monitored by TLC (Hexane:Ethyl acetate; 3:2). The cooled reaction mixture was poured into ice-cold water and acidified with dil. HCl (10% aqueous solution). The precipitated solid was extracted with dichloromethane or ethyl acetate, the extracts were dried over sodium sulphate bed and the solvent was evaporated to give a solid which was recrystallized from absolute ethanol.

(Z)-2-(3'-Methoxy-benzylidene)-benzofuran-3-one (1a). Yellow solid, yield (64%), m.p. 117–120 °C. ¹H NMR (DMSO-*d*₆, 600 MHz, 25 °C, TMS) δ ppm 7.81–7.78 (d, t, 2H, H-4, H-5), 7.59–7.55 (d, s, 3H, H-6', H-7, H-2'), 7.43–7.40 (t, 1H, H-5'), 7.33–7.30 (t, 1H, H-6), 7.04–7.03 (d, 1H, H-4'), 6.90 (s, 1H, H-10), 3.81 (s, 3H, OCH₃); ¹³C NMR (DMSO-*d*₆, 200 MHz, 25 °C, TMS) δ ppm 184.15 (C=O, C-3), 165.96 (C, C-3'), 159.92 (C, C-8), 146.86 (C, C-2), 138.21 (C, C-1'), 133.58 (CH, C-6), 130.55 (CH, C-4), 124.80 (CH, C-5'), 121.28 (C, C-9), 117.12 (CH, C-

5), 116.29 (CH, C-4'), 113.76 (CH, C-10), 112.63 (CH, C-2'), 55.66 (OCH₃). MS: calcd for C₁₆H₁₂O₃ *m/z* = 252, found 253.1. HPLC peak purity: 99.6%.

(Z)-2-(4'-Methoxy-benzylidene)-benzofuran-3-one (1b). Yellow solid, yield (52%), m.p. 137–139 °C. ¹H NMR (DMSO-*d*₆, 600 MHz, 25 °C, TMS) δ ppm 7.96–7.94 (d, 2H, H-2', H-6'), 7.78–7.75 (d, t, 2H, H-4, H-5), 7.53–7.52 (d, 1H, H-7), 7.31–7.28 (t, 1H, H-6), 7.08–7.06 (d, 2H, H-3', H-5'), 6.91 (s, 1H, H-10), 3.82 (s, 3H, OCH₃); ¹³C NMR (DMSO-*d*₆, 200 MHz, 25 °C, TMS) δ ppm 183.74 (C=O, C-3), 165.61 (C, C-4'), 161.34 (C, C-8), 145.63 (C, C-2), 137.79 (CH, C-6), 133.89 (CH, C-4), 124.90 (CH, C-2', C-6'), 124.64 (C, C-1'), 124.28 (CH, C-9), 121.62 (CH, C-5), 115.195 (CH, C-7), 113.65 (CH, C-10), 113.23 (CH, C-3', C-5'), 55.88 (OCH₃). MS: calcd for C₁₆H₁₂O₃ *m/z* = 252, found 253.1. HPLC peak purity: 97.3%.

(Z)-2-(3'-Chloro-benzylidene)-benzofuran-3-one (1c). Yellow solid, yield (53%), m.p. 165–168 °C. ¹H NMR (DMSO-*d*₆, 600 MHz, 25 °C, TMS) δ ppm 8.02 (s, 1H, H-2'), 7.95–7.94 (d, 1H, H-6'), 7.82–7.78 (d, t, 2H, H-4, H-5), 7.58–7.56 (d, 1H, H-7), 7.54–7.50 (d, t, 2H, H-4', H-5'), 7.34–7.31 (t, 1H, H-6), 6.93 (s, 1H, H-10). MS: calcd for C₁₅H₉O₂Cl *m/z* = 256.5, found 257.0. HPLC peak purity: 98.7%.

(Z)-2-(4'-Chloro-benzylidene)-benzofuran-3-one (1d). Yellow solid, yield (62%), m.p. 154–160 °C. ¹H NMR (DMSO-*d*₆, 600 MHz, 25 °C, TMS) δ ppm 8.00–7.99 (d, 2H, H-2', H-6'), 7.81–7.79 (d, t, 2H, H-4, H-5), 7.57–7.53 (d, d, 3H, H-3', H-5', H-7), 7.33–7.30 (t, 1H, H-6), 6.94 (s, 1H, H-10); ¹³C NMR (DMSO-*d*₆, 150 MHz, 25 °C, TMS) δ ppm 183.59 (C=O, C-3), 165.44 (C, C-8), 146.47 (C, C-2), 137.87 (CH, C-6), 134.65 (C, C-4'), 132.97 (C, C-1'), 130.86 (C, C-4), 129.21 (CH, C-3', C-5'), 124.44 (CH, C-2', C-6'), 124.19 (C, C-9), 120.74 (CH, C-5), 113.31 (CH, C-7), 111.04 (CH, C-10). MS: calcd for C₁₅H₉O₂Cl *m/z* = 256.5, found 257.1. HPLC peak purity: 97.4%.

(Z)-2-(4'-Nitro-benzylidene)-benzofuran-3-one (1e). Yellow solid, yield (48%), m.p. 211–215 °C. ¹H NMR (DMSO-*d*₆, 600 MHz, 25 °C, TMS) δ ppm 8.40–8.38 (d, 2H, H-3', H-5'), 8.26–8.25 (d, 2H, H-2', H-6'), 7.82–7.79 (d, t, 2H, H-4, H-5), 7.58–7.56 (d, 1H, H-7), 7.36–7.33 (t, 1H, H-6), 7.11 (s, 1H, H-10). MS: calcd for C₁₅H₉NO₄ *m/z* = 267, found 268.0.

4.2.2.2. General procedure for synthesis of 3-indolinones (2a–2h). The scheme is based on 5-exo cyclic condensation of 2-amino chalcone in presence of Amberlyst-15 as a catalyst [57] as shown in Scheme 1. 0.075 mol of 2-amino chalcone derivatives were dissolved in 3–5 mL of acetic acid. To this solution 10% w/w Amberlyst-15 was added. The mixture was stirred at 80 °C for 2–5 h until starting material was not detected by TLC (Hexane:Ethyl acetate; 3:2). The product was filtered and recrystallized from absolute ethanol. The catalyst was obtained back by washing with methanol, which could be reused.

(Z)-2-(2'-Methoxy-benzylidene)-1,2-dihydro-indol-3-one (2a). Pale yellow solid, yield (52%), m.p. 173–175 °C. ¹H NMR (DMSO-*d*₆, 600 MHz, 25 °C, TMS) δ ppm 11.24 (s, 1H, NH), 7.93 (d, 1H, H-4), 7.67 (d, 1H, H-6'), 7.60 (d, 1H, H-7), 7.52 (t, 1H, H-6), 7.35 (t, 1H, H-4'), 7.00–6.90 (m, 4H, H-3', H-5, H-5', H-10), 3.69 (s, 3H, OCH₃); ¹³C NMR (DMSO-*d*₆, 200 MHz, 25 °C, TMS) δ ppm 186.30 (C=O, C-3), 157.49 (C, C-2'), 144.97 (C, C-2), 135.61 (CH, C-6), 135.21 (C, C-8), 133.53 (CH, C-4'), 128.25 (CH, C-6'), 124.01 (CH, C-4), 123.01 (CH, C-5'), 122.57 (C, C-1'), 121.41 (C, C-9), 119.61 (CH, C-5), 112.81 (CH, C-7), 111.91 (CH, C-3'), 108.38 (C-10), 54.53 (OCH₃). MS: calcd for C₁₆H₁₃NO₂ *m/z* = 251, found 250.96. HPLC peak purity: 99.7%.

(Z)-2-(3'-Methoxy-benzylidene)-1,2-dihydro-indol-3-one (2b). Pale yellow solid, yield (64%), m.p. 117–120 °C. ¹H NMR (DMSO-*d*₆, 600 MHz, 25 °C, TMS) δ ppm 11.26 (s, 1H, NH), 7.94 (d, 1H, H-4), 7.62 (d, 1H, H-7), 7.53 (t, 1H, H-6'), 7.24–7.19 (m, 3H, H-2', H-5', 6'), 6.96 (t, 1H, H-5), 6.86 (d, 1H, H-4'), 6.65 (s, 1H, H-10), 3.65 (s, 3H, OCH₃); ¹³C NMR (DMSO-*d*₆, 200 MHz, 25 °C, TMS) δ ppm 188.23 (C=O, C-3), 159.72 (C, C-3'), 144.37 (C, C-2), 137.06 (C, C-8), 136.67 (C, C-1'), 135.61 (CH, C-6), 126.61 (CH, C-5'), 125.01 (CH, C-6'), 124.01 (CH, C-

4), 121.24 (C, C-9), 119.61 (CH, C-5), 114.79 (CH, C-4'), 114.65 (CH, C-2'), 112.81 (CH, C-7), 110.41 (CH, C-10), 55.25 (OCH₃). MS: calcd for C₁₆H₁₃NO₂ *m/z* = 251, found 253.98. HPLC peak purity: 99.5%.

(Z)-2-(4'-Methoxy-benzylidene)-1,2-dihydro-indol-3-one (2c). Pale yellow solid, yield (52%), m.p. 137–140 °C. ¹H NMR (DMSO-*d*₆, 600 MHz, 25 °C, TMS) δ ppm 11.25 (s, 1H, NH), 7.94 (d, 1H, H-4), 7.62 (d, 1H, H-7), 7.55–7.49 (t, d, 3H, H-6, H-2', H-6'), 6.97–6.95 (d, 3H, H-5, H-3', H-5'), 6.64 (s, 1H, H-10), 3.70 (s, 3H, OCH₃); ¹³C NMR (DMSO-*d*₆, 150 MHz, 25 °C, TMS) δ ppm 188.23 (C=O, C-3), 159.85 (C, C-4'), 145.34 (C, C-2), 137.06 (C, C-8), 135.61 (CH, C-6), 130.22 (CH, C-2', C-6'), 129.72 (C, C-1'), 124.01 (CH, C-4), 121.24 (C, C-9), 119.61 (CH, C-5), 113.98 (CH, C-3', C-5'), 112.81 (CH, C-7), 110.56 (CH, C-10), 55.35 (OCH₃). MS: calcd for C₁₆H₁₃NO₂ *m/z* = 251, found 254.30. HPLC peak purity: 99.2%.

(Z)-2-(3', 4', 5'-Trimethoxy-benzylidene)-1,2-dihydro-indol-3-one (2d). Pale yellow solid (56%), m.p. 138–141 °C. ¹H NMR (DMSO-*d*₆, 600 MHz, 25 °C, TMS) δ ppm 11.25 (s, 1H, NH), 7.93 (d, 1H, H-4), 7.62 (d, 1H, H-7), 7.52 (t, 1H, H-6), 6.95 (t, 1H, H-5), 6.84 (s, 2H, H-2', H-6'), 6.64 (s, 1H, H-10), 3.73–3.64 (d, 9H, OCH₃); ¹³C NMR (DMSO-*d*₆, 150 MHz, 25 °C, TMS) δ ppm 188.23 (C=O, C-3), 154.24 (C, C-3', C-5'), 144.29 (C, C-2), 143.34 (C, C-4'), 137.06 (C, C-8), 135.61 (CH, C-6), 131.95 (C, C-1'), 124.01 (CH, C-4), 121.24 (C, C-9), 119.61 (CH, C-5), 112.81 (CH, C-7), 110.06 (CH, C-10), 107.52 (CH, C-2', C-6'), 60.68–56.20 (OCH₃). MS: calcd for C₁₈H₁₇NO₄ *m/z* = 311, found 311.92. HPLC peak purity: 99.4%.

(Z)-2-(2'-Chloro-benzylidene)-1,2-dihydro-indol-3-one (2e). Pale yellow solid, yield (58%), m.p. 136–138 °C. ¹H NMR (DMSO-*d*₆, 600 MHz, 25 °C, TMS) δ ppm 10.91 (s, 1H, NH), 8.21 (d, 1H, H-4), 7.49 (d, 2H, H-3', H-6'), 7.36–7.30 (m, 2H, H-6, H-4'), 7.24 (t, 1H, H-5), 7.20–7.16 (t, s, 2H, H-5', H-10), 6.98 (d, 1H, H-7); ¹³C NMR (DMSO-*d*₆, 150 MHz, 25 °C, TMS) δ ppm 181.92 (C=O, C-3), 148.98 (C, C-8), 138.01 (C, C-2'), 134.65 (C, C-1'), 133.47 (CH, C-6'), 129.59 (CH, C-4'), 129.47 (CH, C-6), 128.98 (CH, C-3'), 126.64 (C, C-2), 126.43 (CH, C-5'), 122.76 (CH, C-4), 121.10 (CH, C-5), 118.34 (C, C-9), 112.91 (CH, C-7), 104.28 (CH, C-10). MS: calcd for C₁₅H₁₀NOCl *m/z* = 255.5, found 255.92. HPLC peak purity: 94.5%.

(Z)-2-(3'-Chloro-benzylidene)-1,2-dihydro-indol-3-one (2f). Pale yellow solid, yield (53%), m.p. 101–103 °C. ¹H NMR (DMSO-*d*₆, 600 MHz, 25 °C, TMS) δ ppm 10.65 (s, 1H, NH), 8.11 (d, 1H, H-4), 7.79 (d, 1H, H-6'), 7.60 (s, 1H, H-2'), 7.33–7.30 (t, 2H, H-4', H-5'), 7.18 (t, 1H, H-5), 7.09 (t, 1H, H-6) 6.88–6.86 (d, 2H, H-7, H-10); ¹³C NMR (DMSO-*d*₆, 200 MHz, 25 °C, TMS) δ ppm 180.04 (C=O, C-3), 148.95 (C, C-8), 135.11 (C, C-1'), 133.52 (C, C-3'), 133.21 (CH, C-2'), 131.13 (CH, C-6'), 130.65 (CH, C-4'), 129.47 (CH, C-6), 128.48 (CH, C-5'), 127.78 (C, C-2), 122.76 (CH, C-4), 121.10 (CH, C-5), 118.31 (C, C-9), 112.91 (CH, C-7), 107.98 (CH, C-10). MS: calcd for C₁₅H₁₀NOCl *m/z* = 255.5, found 255.92. HPLC peak purity: 99.9%.

(Z)-2-(4'-Chloro-benzylidene)-1,2-dihydro-indol-3-one (2g). Pale yellow solid, yield (62%), m.p. 156–160 °C. ¹H NMR (DMSO-*d*₆, 600 MHz, 25 °C, TMS) δ ppm 10.67 (s, 1H, NH), 8.11 (d, 1H, H-4), 7.73 (d, 2H, H-2', H-6'), 7.43 (d, 2H, H-3', H-5'), 7.25 (t, 1H, H-6), 7.04 (t, 1H, H-5), 6.88–6.85 (d, 2H, H-7, H-10); ¹³C NMR (DMSO-*d*₆, 200 MHz, 25 °C, TMS) δ ppm 180.02 (C=O, C-3), 148.95 (C, C-8), 135.41 (C, C-1'), 134.48 (CH, C-3', C-5'), 132.16 (C, C-4'), 129.47 (CH, C-6), 129.22 (CH, C-2', C-6'), 127.07 (CH, C-4), 122.76 (CH, C-5), 121.10 (C, C-9), 118.31 (CH, C-7), 112.91 (C, C-2), 107.68 (CH, C-10). MS: calcd for C₁₅H₁₀NOCl *m/z* = 255.5, found 255.92. HPLC peak purity: 99.3%.

(Z)-2-(3'-Hydroxy-benzylidene)-1,2-dihydro-indol-3-one (2h). Pale yellow solid, yield (56%), m.p. 130–132 °C. ¹H NMR (DMSO-*d*₆, 600 MHz, 25 °C, TMS) δ ppm 11.26 (s, 1H, NH), 9.87 (s, 1H, OH), 7.94 (d, 1H, H-4), 7.62 (d, 1H, H-7), 7.53 (t, 1H, H-6), 7.14 (t, 1H, H-5'), 7.07 (d, 1H, H-6'), 6.96 (t, 1H, H-5), 6.65–6.63 (d, 3H, H-2', H-4', H-10); ¹³C NMR (DMSO-*d*₆, 200 MHz, 25 °C, TMS) δ ppm 188.23 (C=O, C-3), 156.32 (C, C-3'), 144.37 (C, C-2), 137.06 (CH, C-8), 136.74 (C, C-1'), 135.61 (CH, C-6), 130.04 (CH, C-5'), 124.85 (CH, C-6'), 124.01 (CH, C-4), 121.24 (C, C-9), 119.69 (CH, C-2'), 119.61 (CH, C-5), 116.55 (CH, C-

4'), 112.81 (CH, C-7), 110.41 (CH, C-10). MS: calcd for C₁₅H₁₁NO₂ *m/z* = 237, found 237.99.

4.2.2.3. General procedure for synthesis of 4-quinolones (3a–3i). 4-quinolones were obtained by 6-endo cyclocondensation of 2-amino chalcone derivatives using iodine and dimethylsulfoxide (DMSO) as shown in Scheme 1. 2-Amino chalcone derivatives were suspended in DMSO (10 mL) and a crystal of iodine was added to it. The reaction mixture was refluxed for 30 min and then diluted with water. The solid obtained was filtered off, washed with 20% sodium thiosulphate and recrystallized from absolute ethanol.

2-(2'-Methoxy-phenyl)-1H-quinolin-4-one (3a). White solid, yield (57%), m.p. 102–104 °C. ¹H NMR (DMSO-*d*₆, 600 MHz, 25 °C, TMS) δ ppm 11.50 (s, 1H, NH), 7.98 (d, 1H, H-6), 7.65 (d, 1H, H-9), 7.59–7.51 (t, t, 2H, H-7, H-8), 7.37 (d, 1H, H-6'), 7.28 (t, 1H, H-4'), 7.00 (d, 1H, H-3'), 6.94–6.88 (t, 1H, H-5'), 6.02 (s, 1H, H-3), 3.74 (s, 3H, OCH₃); ¹³C NMR (DMSO-*d*₆, 200 MHz, 25 °C, TMS) δ ppm 182.44 (C=O, C-4), 155.01 (C, C-2'), 141.08 (C, C-10), 140.71 (C, C-2), 137.01 (CH, C-4'), 133.43 (CH, C-8), 130.32 (CH, C-6'), 125.01 (CH, C-6), 124.21 (C, C-1'), 123.83 (C, C-5), 123.31 (CH, C-7), 122.88 (CH, C-5'), 119.07 (CH, C-9), 110.53 (CH, C-3'), 106.19 (CH, C-3), 55.20 (OCH₃). MS: calcd for C₁₆H₁₃NO₂ *m/z* = 251, found 251.99. HPLC peak purity: 99.9%.

2-(3'-Methoxy-phenyl)-1H-quinolin-4-one (3b). White solid, yield (64%), m.p. 130–134 °C. ¹H NMR (DMSO-*d*₆, 600 MHz, 25 °C, TMS) δ ppm 11.65 (s, 1H, NH), 8.09 (d, 1H, H-6), 7.76 (d, 1H, H-9), 7.71–7.63 (t, t, 2H, H-7, H-8), 7.45 (t, 1H, H-5'), 7.36 (d, 1H, H-6'), 7.27 (s, 1H, H-2'), 7.09 (d, 1H, H-4'), 6.31 (s, 1H, H-3), 3.75 (s, 3H, OCH₃); ¹³C NMR (DMSO-*d*₆, 150 MHz, 25 °C, TMS) δ ppm 182.44 (C=O, C-4), 161.82 (C, C-3'), 156.61 (C, C-2), 141.64 (C, C-10), 138.82 (C, C-1'), 133.43 (CH, C-8), 125.01 (CH, C-6), 123.31 (CH, C-7), 122.56 (CH, C-4'), 122.41 (C, C-5), 119.61 (CH, C-6'), 118.41 (CH, C-2'), 115.36 (CH, C-9), 108.21 (CH, C-5'), 105.71 (CH, C-3), 55.50 (OCH₃). MS: calcd for C₁₆H₁₃NO₂ *m/z* = 251, found 251.97. HPLC peak purity: 97.6%.

2-(4'-Methoxy-phenyl)-1H-quinolin-4-one (3c). White solid, yield (64%), m.p. 156–159 °C. ¹H NMR (DMSO-*d*₆, 600 MHz, 25 °C, TMS) δ ppm 11.66 (s, 1H, NH), 8.09 (d, 1H, H-6), 7.84–7.80 (d, 2H, H-3', H-5'), 7.76 (d, 1H, H-9), 7.71–7.63 (t, t, 2H, H-7, H-8), 7.13–7.12 (d, 2H, H-2', H-6'), 6.32 (s, 1H, H-3), 3.75 (s, 3H, OCH₃); ¹³C NMR (DMSO-*d*₆, 150 MHz, 25 °C, TMS) δ ppm 182.44 (C=O, C-4), 158.80 (C, C-4'), 151.79 (C, C-2), 141.66 (C, C-10), 133.43 (CH, C-8), 128.79 (CH, C-2', C-6'), 128.29 (C, C-1'), 125.01 (CH, C-6), 123.31 (CH, C-7), 122.41 (C, C-5), 115.36 (CH, C-9), 114.33 (CH, C-3', C-5'), 105.65 (CH, C-3), 55.35 (OCH₃). MS: calcd for C₁₆H₁₃NO₂ *m/z* = 251, found 251.97. HPLC peak purity: 96.7%.

2-(3', 4', 5'-Trimethoxy-phenyl)-1H-quinolin-4-one (3d). White solid, yield (75%), m.p. 162–164 °C. ¹H NMR (DMSO-*d*₆, 600 MHz, 25 °C, TMS) δ ppm 11.65 (s, 1H, NH), 8.09 (d, 1H, H-6), 7.77 (d, 1H, H-9), 7.71–7.63 (t, t, 2H, H-7, H-8), 6.92 (s, 2H, H-2', H-6'), 6.31 (s, 1H, H-3), 3.84–3.75 (d, 9H, OCH₃); ¹³C NMR (DMSO-*d*₆, 150 MHz, 25 °C, TMS) δ ppm 182.44 (C=O, C-4), 153.72 (C, C-3'), 152.86 (C, C-2, 5'), 141.68 (C, C-10, C-4'), 141.64 (CH, C, C-8, C-1'), 133.43 (CH, C-6), 125.01 (CH, C-7), 123.31 (C, C-5), 122.41 (CH, C-9), 115.36 (CH, C-3), 104.99 (CH, C-2'), 104.08 (CH, C-6'), 60.68–56.26 (OCH₃). MS: calcd for C₁₈H₁₇NO₄ *m/z* = 311, found 311.91. HPLC peak purity: 99.8%.

2-(2'-Chloro-phenyl)-1H-quinolin-4-one (3e). Off-white solid, yield (56%), m.p. 116–119 °C. ¹H NMR (DMSO-*d*₆, 600 MHz, 25 °C, TMS) δ ppm 11.62 (s, 1H, NH), 8.09 (d, 1H, H-6), 7.76 (d, 1H, H-9), 7.70 (t, 1H, H-8), 7.64 (t, 1H, H-7), 7.59 (d, 1H, H-3'), 7.49 (t, 1H, H-4'), 7.42 (d, 1H, H-6'), 7.24 (t, 1H, H-5'), 6.14 (s, 1H, H-3); ¹³C NMR (DMSO-*d*₆, 150 MHz, 25 °C, TMS) δ ppm 182.44 (C=O, C-4), 141.08 (C, C-10), 140.53 (C, C-2), 136.39 (C, C-1'), 133.43 (C, C-2'), 133.29 (CH, C-8), 130.79 (CH, CC-4'), 129.90 (CH, C-3'), 129.40 (CH, C-6'), 126.00 (CH, C-5'), 125.01 (CH, C-6), 123.83 (C, C-5), 123.31 (CH, C-7), 119.07 (CH, C-9), 113.95 (CH, C-3). MS: calcd for C₁₅H₁₀NOCl *m/z* = 255.5, found 258.90. HPLC peak purity: 96.7%.

2-(3'-Chloro-phenyl)-1H-quinolin-4-one (3f). Off-white solid, yield (53%), m.p. 109–110 °C. ^1H NMR (DMSO- d_6 , 600 MHz, 25 °C, TMS) δ ppm 11.55 (s, 1H, NH), 7.99 (d, 1H, H-6), 7.66 (d, 1H, H-9), 7.61–7.53 (t, t, 2H, H-7, H-8), 7.46 (d, 1H, H-6'), 7.3–7.2 (m, 3H, H-2', H-4', H-5'), 6.21 (s, 1H, H-3); ^{13}C NMR (DMSO- d_6 , 150 MHz, 25 °C, TMS) δ ppm 182.44 (C=O, C-4), 156.61 (C, C-2), 141.64 (C, C-10), 138.36 (CH, C-1'), 134.03 (C, C-3'), 133.43 (CH, C-8), 130.39 (CH, C-4'), 129.51 (CH, C-5'), 128.68 (CH, C-2'), 125.20 (CH, C-6'), 125.01 (CH, C-6), 123.31 (CH, C-7), 122.41 (C, C-5), 115.36 (CH, C-9), 105.71 (CH, C-3). MS: calcd for $\text{C}_{15}\text{H}_{10}\text{NOCl}$ m/z = 255.5, found 255.28. HPLC peak purity: 85.5%.

2-(4'-Chloro-phenyl)-1H-quinolin-4-one (3g). Off-white solid, yield (59%), m.p. 170–179 °C. ^1H NMR (DMSO- d_6 , 600 MHz, 25 °C, TMS) δ ppm 11.66 (s, 1H, NH), 8.09 (d, 1H, H-6), 7.84–7.83 (d, 2H, H-3', H-5'), 7.76 (d, 1H, H-9), 7.71–7.63 (t, t, 2H, H-7, H-8), 6.92–6.91 (d, 2H, H-2', H-6'), 6.32 (s, 1H, H-3); ^{13}C NMR (DMSO- d_6 , 200 MHz, 25 °C, TMS) δ ppm 182.44 (C=O, C-4), 151.79 (C, C-2), 141.66 (C, C-10), 135.80 (C, C-1'), 134.23 (C, C-4'), 133.43 (CH, C-8), 129.41 (CH, C-3', C-5'), 129.22 (CH, C-2', C-6'), 125.01 (CH, C-6), 123.31 (CH, C-7), 122.41 (C, C-5), 115.36 (CH, C-9), 105.65 (CH, C-3). MS: calcd for $\text{C}_{15}\text{H}_{10}\text{NOCl}$ m/z = 255.5, found 255.91. HPLC peak purity: 99.3%.

2-(3'-Nitro-phenyl)-1H-quinolin-4-one (3h). Pale yellow solid, yield (49%), m.p. 195–196 °C. ^1H NMR (DMSO- d_6 , 600 MHz, 25 °C, TMS) δ ppm 11.53 (s, 1H, NH), 8.02–7.9 (m, 3H, H-6, H-4', H-6'), 7.73 (s, 1H, H-2'), 7.65 (d, 1H, H-9), 7.60–7.52 (t, t, 2H, H-7, H-8), 7.45 (t, 1H, H-5'), 6.21 (s, 1H, H-3); ^{13}C NMR (DMSO- d_6 , 200 MHz, 25 °C, TMS) δ ppm 182.44 (C=O, C-4), 156.61 (C, C-2), 147.93 (C, C-3'), 141.64 (C, C-10), 138.46 (C, C-1'), 133.82 (CH, C-5'), 133.43 (CH, C-8), 128.82 (CH, C-6'), 125.21 (CH, C-4'), 125.01 (CH, C-6), 123.47 (CH, C-2'), 123.31 (CH, C-7), 122.41 (C, C-5), 115.36 (CH, C-9), 105.71 (CH, C-3). MS: calcd for $\text{C}_{15}\text{H}_{10}\text{N}_2\text{O}_3$ m/z = 266, found 266.93. HPLC peak purity: 98.3%.

2-(4'-Nitro-phenyl)-1H-quinolin-4-one (3i). Pale yellow solid, yield (45%), m.p. 195–196 °C. ^1H NMR (DMSO- d_6 , 600 MHz, 25 °C, TMS) δ ppm 11.56 (s, 1H, NH), 8.22–8.21 (d, 2H, H-3', H-5'), 8.00 (d, 1H, H-6), 7.79–7.77 (d, 2H, H-2', H-6'), 7.67 (d, 1H, H-9), 7.62–7.54 (t, t, 2H, H-7, H-8), 6.32 (s, 1H, H-3); ^{13}C NMR (DMSO- d_6 , 150 MHz, 25 °C, TMS) δ ppm 182.44 (C=O, C-4), 151.79 (C, C-2), 151.79 (C, C-4'), 147.79 (C, C-1'), 142.32 (C, C-10), 141.66 (CH, C-8), 133.43 (CH, C-2'), 128.76 (CH, C-6'), 125.01 (CH, C-6), 124.31 (CH, C-3'), 124.21 (CH, C-5'), 123.31 (CH, C-7), 122.41 (C, C-5), 115.36 (CH, C-9), 105.65 (CH, C-3).

4.2.2.4. General procedure for synthesis of cinnamic acid-piperazine hybrids (4a – 4e). Synthetic scheme is shown in Scheme 2. Substituted cinnamic acid (1 mol) was taken in organic solvent (dichloromethane, DCM) and thionyl chloride (1.2 mol) was added followed by addition of catalytic amount of dimethylformamide (DMF). The reaction mixture was refluxed for 24 h. Completion of reaction was monitored by TLC (Hexane:Ethyl acetate:methanol; 3:2:0.5). After completion of reaction, solvent was evaporated to remove excess of thionyl chloride and to get cinnamoyl chloride in the form of an amorphous powder. Unsubstituted piperazine (3 mol) was dissolved in DCM and triethylamine (TEA) (3 equivalent) was added to it and stirred at 0 °C. Substituted cinnamoyl chloride (1 mol) was dissolved in DCM and added dropwise to above stirred solution at 0 °C. Completion of reaction was monitored by TLC (Hexane : Ethyl acetate : methanol; 3:2:0.5). After completion, the precipitate obtained was filtered and washed with water. The resulting solid product was suspended in 5% sodium bicarbonate solution to remove any acid impurity. The final product was recrystallized from absolute alcohol.

3-Phenyl-1-piperazin-1-yl-propenone (4a). White solid, yield (61.85%), m.p. 264–265 °C. ^1H NMR (CDCl_3 , 600 MHz, 25 °C, TMS) δ ppm 7.7 (d, 1H, H-7), 7.5 (d, 2H, H-2, H-6), 7.3 (m, 3H, H-3, H-4, H-5), 6.8 (d, 1H, H-8), 3.8 (bd, 6H, H-2', H-3', H-5', H-6'), 1.6 (s, 1H, NH); ^{13}C NMR (CDCl_3 200 MHz, 25 °C, TMS) δ ppm 165.74 (C=O, C-9), 143.7 (CH, C-7), 135 (C, C-1), 129.9 (CH, C-4), 128.8 (CH, C-3, C-5), 127.8

(CH, C-2, C-6), 116.40 (CH, C-8), 45.9 (CH_2 , C-2', C-6'), 42.2 (CH_2 , C-3', C-5'). MS: calcd for $\text{C}_{13}\text{H}_{16}\text{N}_2\text{O}$ m/z = 216, found 216.99. HPLC peak purity: 93.2%.

3-(2-Methoxy-phenyl)-1-piperazin-1-yl-propenone (4b). White solid, yield (57%), m.p. 224–225 °C. ^1H NMR (CDCl_3 , 600 MHz, 25 °C, TMS) δ ppm 7.94 (d, 1H, H-7), 7.5 (d, 1H, H-6), 7.33 (t, 1H, H-5), 6.96 (d, t, d, 3H, H-3, H-4, H-8), 3.8 (s, 1H, H-2), 3.7 (bd, 6H, H-2', H-3', H-5', H-6'), 1.6 (s, 1H, NH); ^{13}C NMR (CDCl_3 200 MHz, 25 °C, TMS) δ ppm 166.4 (C=O, C-9), 158.2 (C, C-2), 139.1 (CH, C-7), 130.9 (CH, C-4), 129.2 (CH, C-6), 124.0 (C, C-1), 120.6 (CH, C-5), 117.4 (CH, C-8), 111.1 (CH, C-3), 55.5 (OCH_3), 45.6 (CH_2 , C-2', C-6'), 42.1 (CH_2 , C-3', C-5'). MS: calcd for $\text{C}_{14}\text{H}_{18}\text{N}_2\text{O}_2$ m/z = 246, found 246.16. HPLC peak purity: 99.8%.

3-(4-Methoxy-phenyl)-1-piperazin-1-yl-propenone (4c). White solid, yield (66%), m.p. 240–242 °C. ^1H NMR (CDCl_3 , 600 MHz, 25 °C, TMS) δ ppm 7.6 (d, 1H, H-7), 7.4 (d, 2H, H-2, H-6), 6.9 (d, 2H, H-3, H-5), 6.7 (d, 1H, H-8), 3.8 (s, 1H, H-4), 3.7 (bd, 6H, H-2', H-3', H-5', H-6'), 1.57 (s, 1H, NH); ^{13}C NMR (CDCl_3 200 MHz, 25 °C, TMS) δ ppm 166.0 (C=O, C-9), 161.0 (C, C-4), 143.3 (CH, C-7), 129.4 (CH, C-2, C-6), 127.7 (C, C-1), 114.2 (CH, C-3, C-5), 113.8 (CH, C-8), 55.3 (OCH_3), 45.5 (CH_2 , C-2', C-6'), 42.1 (CH_2 , C-3', C-5'). MS: calcd for $\text{C}_{14}\text{H}_{18}\text{N}_2\text{O}_2$ m/z = 246, found 246.17. HPLC peak purity: 99.9%.

3-(3,4-Dimethoxy-phenyl)-1-piperazin-1-yl-propenone (4d). White solid, yield (70%), m.p. 241–242 °C. ^1H NMR (CDCl_3 , 600 MHz, 25 °C, TMS) δ ppm 7.6 (d, 1H, H-7), 7.1 (d, 1H, H-6), 7.0 (s, 1H, H-2), 6.8 (d, 1H, H-5), 6.7 (d, 1H, H-8), 3.93 (s, 1H, H-4), 3.91 (s, 1H, H-3), 3.8 (bd, 6H, H-2', H-3', H-5', H-6'), 1.58 (s, 1H, NH); ^{13}C NMR (CDCl_3 200 MHz, 25 °C, TMS) δ ppm 165.90 (C=O, C-9), 150.8 (C, C-3), 149.1 (C, C-4), 143.7 (CH, C-7), 127.9 (C, C-1), 122.0 (CH, C-8), 114.0 (CH, C-6), 111.1 (CH, C-5), 109.9 (CH, C-2), 55.9 (OCH_3), 45.6 (CH_2 , C-2', C-6'), 42.1 (CH_2 , C-3', C-5'). MS: calcd for $\text{C}_{15}\text{H}_{20}\text{N}_2\text{O}_3$ m/z = 276, found 276.28. HPLC peak purity: 99.9%.

3-(4-Chloro-phenyl)-1-piperazin-1-yl-propenone (4e). Off-white solid, yield (76%), m.p. 275–276 °C. ^1H NMR (CDCl_3 , 600 MHz, 25 °C, TMS) δ ppm 7.6 (d, 1H, H-7), 7.4 (d, 2H, H-3, H-5), 7.3 (d, 2H, H-2, H-6), 6.8 (d, 1H, H-8), 3.76 (bd, 6H, H-2', H-3', H-5', H-6'), 1.57 (s, 1H, NH).

4.2.3. In vitro evaluation

4.2.3.1. Cells and virus

4.2.3.1.1. Maintenance of MDCK cells. Madin-Darby canine kidney (MDCK) cells were grown in minimum essential medium (MEM, Gibco, by Life Technologies) complemented with 10% foetal bovine serum (FBS, Gibco, by Life Technologies) and 1% Antibiotic (10,000 U/mL penicillin and 0.5 mg/mL streptomycin) (Gibco, by Life Technologies).

4.2.3.1.2. Preparation of virus stock. The influenza A(H1N1)pdm09 virus was propagated in MDCK cells in the presence of 2 $\mu\text{g/mL}$ tosyl phenylalanyl chloromethyl ketone (TPCK)-trypsin. The stock of virus was obtained by adding 500 μL of A(H1N1)pdm09 virus to 85–90% confluent MDCK cells after removing the medium from flask and incubated for 1 h at 37 °C with 5% CO_2 to maximize the viral adsorption to the cells. Subsequently, 4.5 mL of viral growth medium (2 $\mu\text{g/mL}$ TPCK-trypsin + MEM) was added and incubated at above mentioned conditions for 5–7 days. Supernatant was then collected based on cytopathic effect of the virus and stored at –80 °C. These were repeated several times for adequate virus stock.

4.2.3.2. Cytotoxicity studies. Cytotoxicity studies of the synthesized molecules and standard drug viz. oseltamivir phosphate (OMVP) were carried out by MTT-Formazan assay [58]. MDCK cells were inoculated into 96-well plates and incubated at 37 °C with 5% CO_2 for 24 h until grown to 90% confluency. The media was then replaced with serum-free DMEM (Dulbecco's Modified Eagle Medium, without phenol red) containing serially diluted molecules (1000, 500, 250, 200, 125, 100, 40,

10, 1, 0.1 μM corresponding to 10-folds, 5-folds and 2-folds dilutions). After 16 h of incubation, the media was removed and 100 μL of a 0.5 mg/mL MTT (3-(4,5-Dimethylthiazol-2-yl)-3,5-diphenyl tetrazolium bromide, Sigma-Aldrich) solution was added to each well and incubated at 37 °C for 4 h. After removal of supernatant, 100 μL of dimethylsulfoxide (DMSO, Sigma-Aldrich) was added to each well so that the formed formazan crystals get dissolved. Absorbance was measured at 540 nm in a microplate reader. Data were normalized following the equation: Cell viability (%) = (sample value - blank control)/(cell control - blank control) \times 100. The cytotoxic concentration 50% (CC_{50}) was calculated as the concentration at which 50% cells remain viable. It was calculated in GraphPad Prism 5 from a dose response curve obtained using a non-linear regression (curve fit).

4.2.3.3. Cytopathic effect (CPE) inhibition assay. The virus (100 μL) was inoculated onto near confluent MDCK cell monolayers for 1 h to allow for viral adsorption in 24-well plates after removing the media at 37 °C under 5% CO_2 atmosphere. 2 mL of molecules prepared at different concentrations (500, 250, 200, 125, 100, 10, 1, 0.1 μM) in MEM containing 2 $\mu\text{g/mL}$ TPCK-trypsin was added in the allotted wells. The cultures were incubated for 3–4 days at 37 °C under 5% CO_2 atmosphere to develop CPE if any, checked every day. Controls were set consisting of only cells (i.e. no virus, no drug), referred as Cell Control (CC); and cells with virus only (i.e. virus but no drug), referred as Virus Control (VC). The candidate molecule was said to have antiviral activity if there was absence of viral CPE. The antiviral effect of the molecules was determined by grading system developed by Kudi and Myint mentioned in our previous work [59]. After 3–4 days, when VC showed 95–100% CPE, the supernatant from each well was removed and tested for hemagglutination (HA) titer of virus. The reduction of HA titer of virus in molecule treated wells was compared to HA titer of virus in VC well. The HA titer was determined by means of hemagglutination inhibition (HAI) assay.

4.2.3.4. Hemagglutination inhibition (HAI) assay. Serial two-fold dilutions of supernatant of infected cells (100 μL) were prepared using 1X PBS in a 96-well U-bottom plate. A 50 μL of 1% chicken red blood cells was added to each well. After 30 min incubation at 22 °C, hemagglutination (reddish mesh across entire well) and precipitation of red blood cells (red dot in the centre of well) was noted. The highest dilution factor that caused hemagglutination is the HA titer of the virus. [60]. HA titer of the VC and molecule treated wells was compared to ascertain the reduction in %HA viral titer treated by molecules.

4.2.3.5. Cell-based screening of hit molecules using crystal violet (CV) assay. CV assay was executed by reported method [61,62], with few modifications. MDCK cells were seeded in 48-well tissue culture plates and incubated for 24 h at 37 °C under 5% CO_2 atmosphere. The media was aspirated. Controls were set i.e., CC and VC (as discussed above) along with DC (Drug control i.e., only drugs and cells). 30 μL of virus dilution (256 HA units/mL) was added in each well except for CC and DC. The plates were incubated for 1 h for maximum adsorption of virus. The dilutions of candidate molecules at different concentrations (100 μM to 0.001 μM) were then added in the treatment cells while serum free media was added in CC, DC and VC. The plates were kept for incubation at 37 °C under 5% CO_2 atmosphere for 24–36 h till the CPE was observed. Further, the media was aspirated from all wells and washings were given twice with 1X PBS. Plates were inverted on filter paper and tapped to remove remaining fluid. 100 μL of crystal violet (0.5%) was added to each well and incubated for 20 min at room temperature (RT) on a bench rocker with frequency of 20 oscillations/min. The plates were washed with tap water to remove the unbound dye. Plates were inverted on filter paper and tapped to remove remaining fluid. The plates were air dried at RT without the lid on. 300 μL of absolute methanol was added to each well and incubated with lid on for 20 min at RT on bench rocker with a frequency of 20 oscillations/min. Optical

density (OD) was measured at 570 nm. The percentage cell survival in wells treated with molecules was calculated in reference to the uninfected untreated control i.e., CC and plotted against the molecule's concentration. EC_{50} was calculated using a linear regression analysis tool. The experiment was performed in triplicate for each candidate molecule.

4.2.3.6. Enzyme-based NA inhibition assay. NA inhibitory activity was determined using the NA-Star® influenza neuraminidase inhibitor resistance detection kit (Applied Biosystem) as per previously reported method [13]. Succinctly, 25 μL of candidate molecules (conc. ranging from 100 μM to 0.001 μM) or quercetin (QR, conc. ranging from 100 μM to 0.001 μM) or oseltamivir carboxylate (OMVC, conc. ranging from 1000 nM to 1 nM) at two times the desired concentration was added in duplicate to a 96-well microtiter plate. H1N1 virus was diluted 5-fold with the assay buffer. To the plate, 25 μL of the diluted virus was mixed with the molecules and incubated at 37 °C for 20 min. The substrate was diluted at 1:1000 in assay buffer immediately before use. Then 10 μL of the diluted substrate were added to each well. The reaction mixtures were kept for incubation at RT for 15 min and then activated by adding 60 μL of accelerator. The chemiluminescent signal was quantified immediately by microplate reader [63]. A 50% inhibitory concentration (IC_{50}), relative to the activity in positive control i.e., the reaction mixture well containing virus but no test molecule, was determined to measure inhibitory activity of test molecules using GraphPad Prism 5.

4.2.3.7. Enzyme kinetics assay. The mechanism of NA inhibition was determined by kinetics assay with previously reported method [13]. To 96-well microtiter plate, 25 μL of OMVC or QR or candidate molecules (two conc. bracketing IC_{50} , along with I_0) was pre-incubated with 25 μL diluted H1N1 virus at 37 °C for 20 min. This was followed by addition of substrate (6.25, 12.5, 25, 50, 100 μM). Kinetic characterization for the hydrolysis of substrate catalysed by H1N1-NA was carried out by measuring the chemiluminescent signal of hydrolysis product. The parallel control experiment was implemented without molecules in the mixture. K_m and V_{max} values were obtained from GraphPad Prism 5.

4.2.4. Statistical analyses

Mean \pm standard deviation (std dev, SD) of at least three independent biological replicates ($n \geq 3$) was considered for analyses. For antiviral assays, $p < 0.05$ (Mann-Whitney U test and Student's t test) was believed to be statistically significant. All the statistical analyses were performed using GraphPad Prism 5 and the R statistical environment.

Funding sources

The biological evaluation was funded by Indian Council of Medical Research (ICMR), New Delhi, India (58/36/2013-BMS).

Declaration of Competing Interest

The authors declare that they have no known competing financial interests or personal relationships that could have appeared to influence the work reported in this paper.

Acknowledgements

K. Malbari and M. Kanyalkar are grateful to ICMR (58/27/2007-BMS) for funding computational facility at Department of Pharmaceutical Chemistry, Prin K M Kundnani College of Pharmacy. K. Malbari is indebted to ICMR for Senior Research Fellowship (58/36/2013-BMS) and acknowledges Schrödinger Inc. for the trial license with OPLS3e forcefield. Authors also acknowledge the infrastructure funding provided by Department of Science and Technology's Fund for

Improvement of S&T Infrastructure in Higher Educational Institutions (DST-FIST), New Delhi (SR/FST/College-264/2015(C)) at Prin KM Kundnani College of Pharmacy, Mumbai, India. K. Malbari and M. Joshi acknowledge National NMR Facility provided by Tata Institute of Fundamental Research (TIFR), Colaba, Mumbai, India.

Appendix A. Supplementary material

Supplementary data to this article can be found online at <https://doi.org/10.1016/j.bioorg.2021.105139>.

References

- [1] S.A. Bergervoet, C.K.Y. Ho, R. Heutink, A. Bossers, N. Beerens, Spread of Highly Pathogenic Avian Influenza (HPAI) H5N5 viruses in Europe in 2016–2017 appears related to the timing of reassortment events, *Viruses* 11 (2019) 501, <https://doi.org/10.3390/v11060501>.
- [2] N.A. Gerloff, S.U. Khan, A. Balish, I.S. Shanta, N. Simpson, L. Berman, N. Haider, M.K. Poh, A. Islam, E. Gurley, M.A. Hasnat, T. Dey, B. Shu, S. Emery, S. Lindstrom, A. Haque, A. Klimov, J. Villanueva, M. Rahman, E. Azziz-Baumgartner, M. Ziaur Rahman, S.P. Luby, N. Zeidner, R.O. Donis, K. Sturm-Ramirez, C.T. Davis, Multiple reassortment events among highly pathogenic avian influenza A(H5N1) viruses detected in Bangladesh, *Virology* 450–451 (2014) 297–307, <https://doi.org/10.1016/j.virol.2013.12.023>.
- [3] K. Shanmuganatham, M.M. Feeroz, L. Jones-Engel, D. Walker, Smr. Alam, Mk. Hasan, P. McKenzie, S. Krauss, R.J. Webby, R.G. Webster, Genesis of avian influenza H9N2 in Bangladesh, *Emerg. Microbes Infect.* 3 (2014) e88–e88. DOI: 10.1038/emi.2014.84.
- [4] C. Liu, M.C. Eichelberger, R.W. Compans, G.M. Air, Influenza type A virus neuraminidase does not play a role in viral entry, replication, assembly, or budding, *J. Virol.* 69 (1995) 1099–1106.
- [5] Z.-M. Sheng, D.S. Chertow, X. Ambroggio, S. McCall, R.M. Przygodzki, R. E. Cunningham, O.A. Maximova, J.C. Kash, D.M. Morens, J.K. Taubenberger, Autopsy series of 68 cases dying before and during the 1918 influenza pandemic peak, *Proc. Natl. Acad. Sci. U. S. A.* 108 (2011) 16416–16421, <https://doi.org/10.1073/pnas.1111179108>.
- [6] N.M. Bouvier, A.C. Lowen, Animal Models for Influenza Virus Pathogenesis and Transmission, *Viruses* 2 (2010) 1530–1563, <https://doi.org/10.3390/v20801530>.
- [7] J.K. Taubenberger, D.M. Morens, Influenza: the mother of all pandemics, *Emerg. Infect. Dis.* 12 (2006) 15–22, <https://doi.org/10.3201/eid1201.050979>.
- [8] C.U. Kim, X. Chen, D.B. Mendel, Neuraminidase inhibitors as anti-influenza virus agents, *Antivir. Chem. Chemother.* 10 (1999) 141–154, <https://doi.org/10.1177/095632029901000401>.
- [9] H.-L. Yen, E. Hoffmann, G. Taylor, C. Scholtissek, A.S. Monto, R.G. Webster, E. A. Govorkova, Importance of neuraminidase active-site residues to the neuraminidase inhibitor resistance of influenza viruses, *J. Virol.* 80 (2006) 8787–8795, <https://doi.org/10.1128/JVI.00477-06>.
- [10] Y. Xie, D. Xu, B. Huang, X. Ma, W. Qi, F. Shi, X. Liu, Y. Zhang, W. Xu, Discovery of N-substituted oseltamivir derivatives as potent and selective inhibitors of H5N1 influenza neuraminidase, *J. Med. Chem.* 57 (2014) 8445–8458, <https://doi.org/10.1021/jm500892k>.
- [11] E. Feng, W.-J. Shin, X. Zhu, J. Li, D. Ye, J. Wang, M. Zheng, J.-P. Zuo, K.T. No, X. Liu, W. Zhu, W. Tang, B.-L. Seong, H. Jiang, H. Liu, Structure-based design and synthesis of C-1- and C-4-modified analogs of zanamivir as neuraminidase inhibitors, *J. Med. Chem.* 56 (2013) 671–684, <https://doi.org/10.1021/jm3009713>.
- [12] A.S. Chintakrindi, E.A.F. Martis, D.J. Gohil, S.T. Kothari, A.S. Chowdhary, E. C. Coutinho, M.A. Kanyalkar, A computational model for docking of noncompetitive neuraminidase inhibitors and probing their binding interactions with neuraminidase of influenza virus H5N1, *Curr. Comput. Aided. Drug Des.* 12 (2016) 272–281.
- [13] A.S. Chintakrindi, D.J. Gohil, S.T. Kothari, A.S. Chowdhary, M.A. Kanyalkar, Design, synthesis and evaluation of chalcones as H1N1 Neuraminidase inhibitors, *Med. Chem. Res.* 27 (2018) 1013–1025, <https://doi.org/10.1007/s00044-017-2124-2>.
- [14] K.D. Malbari, A.S. Chintakrindi, L.R. Ganji, D.J. Gohil, S.T. Kothari, M.V. Joshi, M. A. Kanyalkar, Structure-aided drug development of potential neuraminidase inhibitors against pandemic H1N1 exploring alternate binding mechanism, *Mol. Divers.* (2019), <https://doi.org/10.1007/s11030-019-09919-6>.
- [15] K.M.P. Suruse, K. Malbari, A. Chintakrindi, D. Gohil, S. Srivastava, S. Kothari, A. Chowdhary, Virucidal activity of newly synthesized chalcone derivatives against H1N1 virus supported by molecular docking and membrane interaction studies, *J. Antivir. Antiretrovir.* 8 (2016) 79–89. DOI: 10.4172/jaa.1000139.
- [16] T.T. Dao, P.H. Nguyen, H.S. Lee, E. Kim, J. Park, S. Il Lim, W.K. Oh, Chalcones as novel influenza A (H1N1) neuraminidase inhibitors from Glycyrrhiza inflata, *Bioorg. Med. Chem. Lett.* 21 (2011) 294–298, <https://doi.org/10.1016/j.bmcl.2010.11.016>.
- [17] T.-T. Dao, B.-T. Tung, P.-H. Nguyen, P.-T. Thuong, S.-S. Yoo, E.-H. Kim, S.-K. Kim, W.-K. Oh, C-Methylated Flavonoids from Cleistocalyx operculatus and Their Inhibitory Effects on Novel Influenza A (H1N1) Neuraminidase, *J. Nat. Prod.* 73 (2010) 1636–1642, <https://doi.org/10.1021/np1002753>.
- [18] Y.B. Ryu, J.H. Kim, S.-J. Park, J.S. Chang, M.-C. Rho, K.-H. Bae, K.H. Park, W. S. Lee, Inhibition of neuraminidase activity by polyphenol compounds isolated from the roots of Glycyrrhiza uralensis, *Bioorg. Med. Chem. Lett.* 20 (2010) 971–974, <https://doi.org/10.1016/j.bmcl.2009.12.106>.
- [19] T.N.A. Nguyen, T.T. Dao, B.T. Tung, H. Choi, E. Kim, J. Park, S.I. Lim, W.K. Oh, Influenza A (H1N1) neuraminidase inhibitors from Vitis amurensis., *Food Chem.* 124 (2010) 437–443. doi: 10.1016/j.foodchem.2010.06.049.
- [20] G. Patrick, Drug design: optimizing target interactions, in: G. Patrick, An Introd. to Med. Chem. Oxford, Oxford Univ. Press, 2013: pp. 215–247.
- [21] H.D. Gravina, N.F. Tafuri, A. Silva Júnior, J.L.R. Fietto, T.T. Oliveira, M.A.N. Diaz, M.R. Almeida, In vitro assessment of the antiviral potential of trans-cinnamic acid, quercetin and morin against equid herpesvirus 1, *Res. Vet. Sci.* 91 (2011) e158–e162, <https://doi.org/10.1016/j.rvsc.2010.11.010>.
- [22] A.P. Stankavichyus, L.M.M. Stankavichene, M.S. Sapragonene, L. V. Korobchenko, E.I. Boreko, G.V. Vladkyo, Synthesis and antiviral activity of cinnamic acid derivatives, *Pharm. Chem. J.* 22 (1988) 896–900, <https://doi.org/10.1007/BF00771641>.
- [23] R. Amano, A. Yamashita, H. Kasai, T. Hori, S. Miyasato, S. Saito, H. Yokoe, K. Takahashi, T. Tanaka, T. Ootoguro, S. Maekawa, N. Enomoto, M. Tsubuki, K. Moriishi, Cinnamic acid derivatives inhibit hepatitis C virus replication via the induction of oxidative stress, *Antiviral Res.* 145 (2017) 123–130, <https://doi.org/10.1016/j.antiviral.2017.07.018>.
- [24] R.J. Martin, Modes of action of anthelmintic drugs, *Vet. J.* 154 (1997) 11–34, [https://doi.org/10.1016/S1090-0233\(05\)80005-X](https://doi.org/10.1016/S1090-0233(05)80005-X).
- [25] WHO, Helminths: Intestinal nematode infection: Piperazine; WHO Model Prescribing Information: Drugs Used in Parasitic Diseases, 2nd ed., n.d.
- [26] C. Viegas-Junior, A. Danuello, V. da Silva Bolzani, E.J. Barreiro, C.A.M. Fraga, Molecular hybridization: a useful tool in the design of new drug prototypes, *Curr. Med. Chem.* 14 (2007) 1829–1852, <https://doi.org/10.2174/09298670771058805>.
- [27] M. Domenech de Celles, J.-S. Casalegno, B. Lina, L. Opatowski, Influenza may facilitate the spread of SARS-CoV-2, *MedRxiv.* (2020) 2020.09.07.20189779. DOI: 10.1101/2020.09.07.20189779.
- [28] J.L. McAuley, B.P. Gilbertson, S. Trifkovic, L.E. Brown, J.L. McKimm-Breschkin, Influenza virus neuraminidase structure and functions, *Front. Microbiol.* 10 (2019) 26–32, <https://doi.org/10.3389/fmicb.2019.00039>.
- [29] M. von Itzstein, R. Thomson, Anti-influenza drugs: the development of sialidase inhibitors BT - antiviral strategies, in: H.-G. Kräusslich, R. Bartschlagler (Eds.), Springer Berlin Heidelberg, Berlin, Heidelberg, 2009: pp. 111–154. DOI: 10.1007/978-3-540-79086-0_5.
- [30] A. Chintakrindi, C.D. and M. Kanyalkar, Rational development of neuraminidase inhibitor as novel anti-flu drug, *Mini-Reviews, Med. Chem.* 12 (2012) 1273–1281, <https://doi.org/10.2174/138955712802761997>.
- [31] Q. Li, J. Qi, W. Zhang, C.J. Vavricka, Y. Shi, J. Wei, E. Feng, J. Shen, J. Chen, D. Liu, J. He, J. Yan, H. Liu, H. Jiang, M. Teng, X. Li, G.F. Gao, The 2009 pandemic H1N1 neuraminidase N1 lacks the 150-cavity in its active site, *Nat. Struct. & Mol. Biol.* 17 (2010) 1266. <https://doi.org/10.1038/nsmb.1909>.
- [32] C.J. Vavricka, Q. Li, Y. Wu, J. Qi, M. Wang, Y. Liu, F. Gao, J. Liu, E. Feng, J. He, J. Wang, H. Liu, H. Jiang, G.F. Gao, Structural and functional analysis of laninamivir and its octanoate prodrug reveals group specific mechanisms for influenza NA inhibition, *PLoS Pathog.* 7 (2011), e1002249, <https://doi.org/10.1371/journal.ppat.1002249>.
- [33] X. Xu, X. Zhu, R.A. Dwek, J. Stevens, I.A. Wilson, Structural characterization of the 1918 influenza virus H1N1 neuraminidase, *J. Virol.* 82 (2008) 10493–10501. DOI: 10.1128/JVI.00959-08.
- [34] M.C. Zambon, The pathogenesis of influenza in humans, *Rev. Med. Virol.* 11 (2001) 267–241, <https://doi.org/10.1002/rmv.319>.
- [35] I. Tubert-Brohman, W. Sherman, M. Repasky, T. Beuming, Improved Docking of Polypeptides with Glide, *J. Chem. Inf. Model.* 53 (2013) 1689–1699, <https://doi.org/10.1021/ci400128m>.
- [36] T.A. Halgren, Identifying and characterizing binding sites and assessing druggability, *J. Chem. Inf. Model.* 49 (2009) 377–389.
- [37] H.J. Jeong, Y.B. Ryu, S.J. Park, J.H. Kim, H.J. Kwon, J.H. Kim, K.H. Park, M. C. Rho, W.S. Lee, Neuraminidase inhibitory activities of flavonols isolated from Rhodiola rosea roots and their in vitro anti-influenza viral activities, *Bioorganic Med. Chem.* 17 (2009) 6816–6823, <https://doi.org/10.1016/j.bmc.2009.08.036>.
- [38] M.R. Lentz, R.G. Webster, G.M. Air, Site-directed mutation of the active site of influenza neuraminidase and implications for the catalytic mechanism, *Biochemistry* 26 (1987) 5351–5358, <https://doi.org/10.1021/bi00391a020>.
- [39] C. D'Souza, M. Kanyalkar, M. Joshi, E. Coutinho, S. Srivastava, Search for novel neuraminidase inhibitors: Design, synthesis and interaction of oseltamivir derivatives with model membrane using docking, NMR and DSC methods, *Biochim. Biophys. Acta - Biomembr.* 1788 (2009) 1740–1751, <https://doi.org/10.1016/j.bbmem.2009.04.014>.
- [40] M.P. Gleeson, A. Hersey, S. Hannongbua, In-silico ADME models: a general assessment of their utility in drug discovery applications, *Curr. Top. Med. Chem.* 11 (2011) 358–381.
- [41] W.J. Dunn, M.G. Koehler, S. Grigoras, The role of solvent-accessible surface area in determining partition coefficients, *J. Med. Chem.* 30 (1987) 1121–1126, <https://doi.org/10.1021/jm00390a002>.
- [42] W. Chu, D. Zhou, V. Gaba, J. Liu, S. Li, X. Peng, J. Xu, D. Dhavale, D.P. Bagchi, A. d'Avignon, N.B. Shakerdige, B.J. Bacska, Z. Tu, P.T. Kotzbauer, R.H. Mach, Design, synthesis, and characterization of 3-(benzylidene)indolin-2-one derivatives as ligands for α -synuclein fibrils, *J. Med. Chem.* 58 (2015) 6002–6017, <https://doi.org/10.1021/acs.jmedchem.5b00571>.

- [43] L. Sun, N. Tran, F. Tang, H. App, P. Hirth, G. McMahon, C. Tang, Synthesis and biological evaluations of 3-substituted indolin-2-ones: A novel class of tyrosine kinase inhibitors that exhibit selectivity toward particular receptor tyrosine kinases, *J. Med. Chem.* 41 (1998) 2588–2603, <https://doi.org/10.1021/jm980123i>.
- [44] A. Andreani, M. Rambaldi, A. Locatelli, A. Bongini, R. Bossa, I. Galatulas, M. Ninci, Synthesis and cardiotonic activity of pyridylmethylene-2-indolinones, *Eur. J. Med. Chem.* 27 (1992) 167–170.
- [45] C. Klöck, X. Jin, K. Choi, C. Khosla, P.B. Madrid, A. Spencer, B.C. Raimundo, P. Boardman, G. Lanza, J.H. Griffin, Acylideneoxindoles: a new class of reversible inhibitors of human transglutaminase 2, *Bioorg. Med. Chem. Lett.* 21 (2011) 2692–2696, <https://doi.org/10.1016/j.bmcl.2010.12.037>.
- [46] A. Pelter, R.S. Ward, H.G. Heller, Carbon-13 nuclear magnetic resonance spectra of (Z)- and (E)-aurones, *J. Chem. Soc. Perkin Trans. 1* (1979) 328–329.
- [47] B.E. Davies, Pharmacokinetics of oseltamivir: an oral antiviral for the treatment and prophylaxis of influenza in diverse populations, *J. Antimicrob. Chemother.* 65 Suppl 2 (2010) ii5–ii10. DOI: 10.1093/jac/dkq015.
- [48] P.C. Wagaman, H.A. Spence, R.J. O'Callaghan, Detection of influenza C virus by using an in situ esterase assay, *J. Clin. Microbiol.* 27 (1989) 832–836, <https://pubmed.ncbi.nlm.nih.gov/2745694>.
- [49] G.M. Sastry, M. Adzhigirey, T. Day, R. Annabhimoju, W. Sherman, Protein and ligand preparation: parameters, protocols, and influence on virtual screening enrichments, *J. Comput. Aided. Mol. Des.* 27 (2013) 221–234, <https://doi.org/10.1007/s10822-013-9644-8>.
- [50] A. Gaymard, N. Le Briand, E. Frobert, B. Lina, V. Escuret, Functional balance between neuraminidase and haemagglutinin in influenza viruses, *Clin. Microbiol. Infect.* 22 (2016) 975–983, <https://doi.org/10.1016/j.cmi.2016.07.007>.
- [51] J.N. Varghese, P.M. Colman, Three-dimensional structure of the neuraminidase of influenza virus A/Tokyo/3/67 at 2.2 Å resolution, *J. Mol. Biol.* 221 (1991) 473–486. DOI: 10.1016/0022-2836(91)80068-6.
- [52] T. Halgren, New method for fast and accurate binding-site identification and analysis, *Chem. Biol. Drug Des.* 69 (2007) 146–148, <https://doi.org/10.1111/j.1747-0285.2007.00483.x>.
- [53] LigPrep, Schrödinger, LLC, New York, NY, 2019, (n.d.).
- [54] R.A. Friesner, J.L. Banks, R.B. Murphy, T.A. Halgren, J.J. Klicic, D.T. Mainz, P. S. Shenkin, Glide, A new approach for rapid, accurate docking and scoring. 1. Method and assessment of docking accuracy, *J. Med. Chem.* (2004).
- [55] W. Sherman, T. Day, M.P. Jacobson, R.A. Friesner, R. Farid, Novel procedure for modeling ligand/receptor induced fit effects, *J. Med. Chem.* 49 (2006) 534–553.
- [56] QikProp, Schrödinger, LLC, New York, NY, 2019, (n.d.).
- [57] R. Abonia, P. Cuervo, J. Castillo, B. Insuasty, J. Quiroga, M. Nogueras, J. Cobo, Unexpected intramolecular cyclization of some 2'-aminochalcones to indolin-3-ones mediated by Amberlyst®-15, *Tetrahedron Lett.* 49 (2008) 5028–5031.
- [58] T. Mosmann, Rapid colorimetric assay for cellular growth and survival: application to proliferation and cytotoxicity assays, *J. Immunol. Methods.* 65 (1983) 55–63.
- [59] A.C. Kudi, S.H. Myint, Antiviral activity of some Nigerian medicinal plant extracts, *J. Ethnopharmacol.* 68 (1999) 289–294.
- [60] S.M. Hosseini, E. Amini, M. Tavassoti Kheiri, P. Mehrbod, M. Shahidi, E. Zabihi, Anti-influenza Activity of a Novel Polyoxometalate Derivative (POM-4960), *Int. J. Mol. Cell. Med.* 1 (2012) 21–29, <https://www.ncbi.nlm.nih.gov/pubmed/24551755>.
- [61] M. Feoktistova, P. Geserick, M. Leverkus, Crystal violet assay for determining viability of cultured cells, *Cold Spring Harb. Protoc.* 2016 (2016) pdb.prot087379. DOI: 10.1101/pdb.prot087379.
- [62] J.N. Makau, K. Watanabe, T. Ishikawa, S. Mizuta, T. Hamada, N. Kobayashi, Identification of small molecule inhibitors for influenza A virus using in silico and in vitro approaches, *PLoS One.* 12 (2017) e0173582.
- [63] J. An, D.C.W. Lee, A.H.Y. Law, C.L.H. Yang, L.L.M. Poon, A.S.Y. Lau, S.J.M. Jones, A novel small-molecule inhibitor of the avian influenza H5N1 virus determined through computational screening against the neuraminidase, *J. Med. Chem.* 52 (2009) 2667–2672, <https://doi.org/10.1021/jm800455g>.



Comprehensive analysis of genomic diversity of SARS-CoV-2 in different geographic regions of India: an endeavour to classify Indian SARS-CoV-2 strains on the basis of co-existing mutations

Rakesh Sarkar¹ · Suvroto Mitra¹ · Pritam Chandra¹ · Priyanka Saha¹ · Anindita Banerjee¹ · Shanta Dutta¹ · Mamta Chawla-Sarkar¹

Received: 22 July 2020 / Accepted: 21 October 2020 / Published online: 19 January 2021
© The Author(s), under exclusive licence to Springer-Verlag GmbH, AT part of Springer Nature 2021

Abstract

Accumulation of mutations within the genome is the primary driving force in viral evolution within an endemic setting. This inherent feature often leads to altered virulence, infectivity and transmissibility, and antigenic shifts to escape host immunity, which might compromise the efficacy of vaccines and antiviral drugs. Therefore, we carried out a genome-wide analysis of circulating SARS-CoV-2 strains to detect the emergence of novel co-existing mutations and trace their geographical distribution within India. Comprehensive analysis of whole genome sequences of 837 Indian SARS-CoV-2 strains revealed the occurrence of 33 different mutations, 18 of which were unique to India. Novel mutations were observed in the S glycoprotein (6/33), NSP3 (5/33), RdRp/NSP12 (4/33), NSP2 (2/33), and N (1/33). Non-synonymous mutations were found to be 3.07 times more prevalent than synonymous mutations. We classified the Indian isolates into 22 groups based on their co-existing mutations. Phylogenetic analysis revealed that the representative strains of each group were divided into various sub-clades within their respective clades, based on the presence of unique co-existing mutations. The A2a clade was found to be dominant in India (71.34%), followed by A3 (23.29%) and B (5.36%), but a heterogeneous distribution was observed among various geographical regions. The A2a clade was highly predominant in East India, Western India, and Central India, whereas the A2a and A3 clades were nearly equal in prevalence in South and North India. This study highlights the divergent evolution of SARS-CoV-2 strains and co-circulation of multiple clades in India. Monitoring of the emerging mutations will pave the way for vaccine formulation and the design of antiviral drugs.

Introduction

When a virus adapts to a new host within an endemic setting, it needs to exploit the host's cellular machinery for successful entry, establishing its replication, and evading the host's immune responses [1]. To achieve this, viruses modify antigenic epitopes on their proteins by continuously

mutating their genomes. If the virus evolves in a stable environment with minimal selection, transition mutations are more frequent than the transversions [2]. Accumulation of deleterious mutations, which may include insertion, deletion, or substitution mutations, are filtered out through natural selection, either by reverting back to the ancestral state or by getting fixed with compensatory mutations that offset the effects of deleterious mutations while advantageous mutations persist [2–5]. Hence, digging deep into the type of mutations that occur may help in understanding how selection pressure might be acting on a novel virus [6].

In pursuit of the origin of severe acute respiratory syndrome coronavirus 2 (SARS-CoV-2), researchers found traces of its zoonotic transmission, as a number of the initial cases were reported in people visiting the Wuhan Seafood Market [7–9]. The transmission dynamics of this virus were a major focus of research in the early period of the pandemic, where there were numerous controversies and questions. Phylogenetic analysis of the virus isolated from infected

Handling Editor: Zhenhai Chen.

Supplementary Information The online version contains supplementary material available at <https://doi.org/10.1007/s00705-020-04911-0>.


✉ Mamta Chawla-Sarkar
chawlam70@gmail.com; chawlasarkar.m@icmr.gov.in

¹ Division of Virology, National Institute of Cholera and Enteric Diseases, P-33, C.I.T. Road, Scheme-XM, Beliaghata, Kolkata, West Bengal 700010, India

RESEARCH ARTICLE

WILEY

Rotavirus activates MLKL-mediated host cellular necroptosis concomitantly with apoptosis to facilitate dissemination of viral progeny

Urbi Mukhopadhyay¹ | Upayan Patra¹ | Pritam Chandra¹ | Priyanka Saha¹ | Animesh Gope² | Moumita Dutta³ | Mamta Chawla-Sarkar¹ 

¹Division of Virology, ICMR-National Institute of Cholera and Enteric Diseases, Kolkata, India

²ICMR-National Institute of Cholera and Enteric Diseases, Kolkata, India

³Division of Electron Microscopy, ICMR-National Institute of Cholera and Enteric Diseases, Kolkata, India

Correspondence

Mamta Chawla-Sarkar, Division of Virology, ICMR-National Institute of Cholera and Enteric Diseases, P-33, C.I.T. Road, Scheme-XM, Beliaghata, Kolkata 700010, West Bengal, India.
Emails: chawlasarkar.m@icmr.gov.in, chawlam70@gmail.com

Funding information

Department of Biotechnology-National Women Bioscientist Grant, Ministry of Science and Technology, India, Grant/Award Number: BT/HRD/NWBA/36/01/2013-14; Indian Council of Medical Research

Abstract

Reprogramming the host cellular environment is an obligatory facet of viral pathogens to foster their replication and perpetuation. One of such reprogramming events is the dynamic cross-talk between viruses and host cellular death signaling pathways. Rotaviruses (RVs) have been reported to develop multiple mechanisms to induce apoptotic programmed cell death for maximizing viral spread and pathogenicity. However, the importance of non-apoptotic programmed death events has remained elusive in context of RV infection. Here, we report that RV-induced apoptosis accompanies another non-apoptotic mode of programmed cell death pathway called necroptosis to promote host cellular demise at late phase of infection. Phosphorylation of mixed lineage kinase domain-like (MLKL) protein indicative of necroptosis was observed to concur with caspase-cleavage (apoptotic marker) beyond 6 hr of RV infection. Subsequent studies demonstrated phosphorylated-MLKL to oligomerize and to translocate to plasma membrane in RV infected cells, resulting in loss of plasma membrane integrity and release of alarmin molecules e.g., high mobility group box protein 1 (HMGB1) in the extracellular media. Moreover, inhibiting caspase-cleavage and apoptosis could not fully rescue virus-induced cell death but rather potentiated the necroptotic trigger. Interestingly, preventing both apoptosis and necroptosis by small molecules significantly rescued virus-induced host cytopathy by inhibiting viral dissemination.

KEYWORDS

apoptosis, high mobility group box protein 1, mixed lineage kinase domain-like protein, necroptosis, non-apoptotic cell death, rotavirus, viral spread


1 | INTRODUCTION

Induction of host cellular death in response to viral pathogens represents a powerful component of the host antiviral defense machinery by which infected cells are cleared through programmed self-destruction (Danthi, 2016). Apoptosis, the earliest described mechanism of programmed cell death, has been shown to be involved in clearance of virus-infected cells in many cases of viral infection (Kerr et al., 1972; Roulston et al., 1999).

During apoptosis, multiple upstream signaling cascades can activate caspases, a family of cysteine dependent aspartate specific proteases, which then function as executioners of the apoptotic program by systematically dismantling the infected cells and collapsing them from inside into discrete packages for eventual recycling (Nicholson, 1999; Taylor et al., 2008). Not surprisingly, therefore, inhibition of caspases, by either virus-encoded inhibitory proteins or pharmacological means, should nullify virus-induced host cellular death. However, rather paradoxically,

RESEARCH ARTICLE

Genetic characterization and phylogenetic variations of human adenovirus-F strains circulating in eastern India during 2017–2020

Pritam Chandra¹ | Mahadeb Lo¹ | Suvroto Mitra¹ | Anindita Banerjee¹ |
Priyanka Saha¹ | Keinosuke Okamoto² | Alok Kumar Deb³ |
Sanat Kumar Ghosh⁴ | Asis Manna⁵ | Shanta Dutta⁶ | Mamta Chawla-Sarkar¹ 

¹Division of Virology, National Institute of Cholera and Enteric Diseases, Beliaghata, Kolkata, West Bengal, India

²Collaborative Research Centre of Okayama University for Infectious Disease at Indian ICMR-National Institute of Cholera and Enteric Diseases, Beliaghata, Kolkata, West Bengal, India

³Division of Epidemiology, ICMR-National Institute of Cholera and Enteric Diseases, Beliaghata, Kolkata, West Bengal, India

⁴Dr. B.C. Roy Post Graduate Institute of Pediatric Sciences, Kolkata, West Bengal, India

⁵Infectious diseases and Beliaghata General (ID & BG) Hospital, Beliaghata, Kolkata, West Bengal, India

⁶Regional Virus Research and Diagnostic Laboratory, ICMR-National Institute of Cholera and Enteric Diseases, Beliaghata, Kolkata, West Bengal, India

Correspondence

Mamta Chawla-Sarkar, Division of Virology, National Institute of Cholera and Enteric Diseases, P-33, C.I.T. Rd, Scheme-XM, Beliaghata, Kolkata, West Bengal 700010, India.
Email: chawlam70@gmail.com and chawlasarkar.m@icmr.gov.in

Funding information

Indian Council of Medical Research, Grant/Award Number: Sanction No. 5/8-1(47) 2013-14-ECD-II; Okayama University Project through the Japan Initiative for Global Research Network on Infectious Diseases (J-GRID) of the Agency for Medical Research and Development (AMED), Grant/Award Number: JP21wm0125004

Abstract

Human adenovirus-F (HAdV-F) (genotype 40/41) is the second-most leading cause of pediatric gastroenteritis after rotavirus, worldwide, accounting for 2.8%–11.8% of infantile diarrheal cases. Earlier studies across eastern India revealed a shift in the predominance of genotypes from HAdV41 in 2007–09 to HAdV40 in 2013–14. Thus, the surveillance for HAdV-F genotypes in this geographical setting was undertaken over 2017–2020 to analyze the viral evolutionary dynamics. A total of 3882 stool samples collected from children (≤ 5 years) were screened for HAdV-F positivity by conventional PCR. The hypervariable regions of the hexon and the partial shaft region of long fiber genes were amplified, sequenced, and phylogenetically analyzed with respect to the prototype strains. A marginal decrease in enteric HAdV prevalence was observed (9.04%, $n = 351/3882$) compared to the previous report (11.8%) in this endemic setting. Children < 2 years were found most vulnerable to enteric HAdV infection. Reduction in adenovirus-rotavirus co-infection was evident compared to the sole adenovirus infection. HAdV-F genotypes 40 and 41 were found to co-circulate, but HAdV41 was predominant. HAdV40 strains were genetically conserved, whereas HAdV41 strains accumulated new mutations. On the basis of a different set of mutations in their genome, HAdV41 strains segregated into 2 genome type clusters (GTCs). Circulating HAdV41 strains clustered with GTC1 of the fiber gene, for the first time during this study period. This study will provide much-needed baseline data on the emergence and circulation of HAdV40/41 strains for future vaccine development.

KEYWORDS

genome type cluster (GTC), human adenovirus (HAdV), mutation, phylogenetic analysis, rotavirus vaccine



OPEN ACCESS

EDITED BY
Rameez Raja,
Cleveland Clinic, United States

REVIEWED BY
Aravinthkumar Jayabalan,
Johns Hopkins University,
United States
Sathya Neelatur Sriramareddy,
Moffitt Cancer Center, United States
Muhammad Bilal Latif,
Emory University, United States

*CORRESPONDENCE
Mamta Chawla-Sarkar
chawlam70@gmail.com;
chawlasarkar.m@icmr.gov.in
Upayan Patra
patra@med.uni-frankfurt.de

[†]These authors have contributed
equally to this work

SPECIALTY SECTION
This article was submitted to
Virus and Host,
a section of the journal
Frontiers in Cellular and
Infection Microbiology

RECEIVED 24 June 2022
ACCEPTED 18 August 2022
PUBLISHED 14 September 2022

CITATION
Chandra P, Banerjee S, Saha P,
Chawla-Sarkar M and Patra U (2022)
Sneaking Into the Viral Safe-Houses:
Implications of Host Components in
Regulating Integrity and Dynamics of
Rotaviral Replication Factories.
Front. Cell. Infect. Microbiol. 12:977799.
doi: 10.3389/fcimb.2022.977799

COPYRIGHT
© 2022 Chandra, Banerjee, Saha,
Chawla-Sarkar and Patra. This is an
open-access article distributed under
the terms of the [Creative Commons
Attribution License \(CC BY\)](#). The use,
distribution or reproduction in other
forums is permitted, provided the
original author(s) and the copyright
owner(s) are credited and that the
original publication in this journal is
cited, in accordance with accepted
academic practice. No use,
distribution or reproduction is
permitted which does not comply with
these terms.

Sneaking into the viral safe-houses: Implications of host components in regulating integrity and dynamics of rotaviral replication factories

Pritam Chandra^{1†}, Shreya Banerjee^{1†}, Priyanka Saha¹,
Mamta Chawla-Sarkar^{1*} and Upayan Patra^{2*}

¹Division of Virology, Indian Council of Medical Research National Institute of Cholera and Enteric Diseases, Kolkata, India, ²Institute of Biochemistry II, Faculty of Medicine, Goethe University, Frankfurt, Germany

The biology of the viral life cycle essentially includes two structural and functional entities—the viral genome and protein machinery constituting the viral arsenal and an array of host cellular components which the virus closely associates with—to ensure successful perpetuation. The obligatory requirements of the virus to selectively evade specific host cellular factors while exploiting certain others have been immensely important to provide the platform for designing host-directed antiviral therapeutics. Although the spectrum of host-virus interaction is multifaceted, host factors that particularly influence viral replication have immense therapeutic importance. During lytic proliferation, viruses usually form replication factories which are specialized subcellular structures made up of viral proteins and replicating nucleic acids. These viral niches remain distinct from the rest of the cellular milieu, but they effectively allow spatial proximity to selective host determinants. Here, we will focus on the interaction between the replication compartments of a double stranded RNA virus rotavirus (RV) and the host cellular determinants of infection. RV, a diarrheagenic virus infecting young animals and children, forms replication bodies termed viroplasms within the host cell cytoplasm. Importantly, viroplasms also serve as the site for transcription and early morphogenesis of RVs and are very dynamic in nature. Despite advances in the understanding of RV components that constitute the viroplasmic architecture, knowledge of the contribution of host determinants to viroplasm dynamicity has remained limited. Emerging evidence suggests that selective host determinants are sequestered inside or translocated adjacent to the RV viroplasms. Functional implications of such host cellular reprogramming are also ramifying—disarming the antiviral host determinants and usurping the pro-viral components to facilitate specific stages of the viral life cycle. Here, we will provide a critical update on the wide variety of host cellular pathways that have been reported to regulate the spatial and temporal dynamicity of RV viroplasms. We will also discuss the methods used so far to study the host-viroplasm interactions and emphasize